

N° Ordre : 3096

THÈSE

Présentée

DEVANT L'UNIVERSITÉ DE RENNES 1

Pour obtenir

Le grade de **DOCTEUR DE L'UNIVERSITÉ DE RENNES 1**

Mention **INFORMATIQUE**

Par

Jad NASREDDINE

Équipe d'accueil : Département Réseaux et Services Multimédia,
ENST de Bretagne, Campus de Rennes
École Doctorale : Mathématiques, Télécommunications,
Informatique, Signal, Systèmes et Électronique
Composante Universitaire: ENST de Bretagne

TITRE DE LA THÈSE

*Allocation de ressources radios dans les systèmes UMTS
à duplexage temporel*

SOUTENUE LE : 30 mars 2005 devant la commission d'Examen

COMPOSITION DU JURY :

MM.

Ghaïs El Zein

Président

Ramón Agusti

Rapporteurs

Philippe Godlewski

Bruno Jechoux

Examineurs

Bruno Tuffin

Xavier Lagrange

Directeur de thèse

A mes parents

Progress lies not in enhancing what is, but in advancing toward what will be.

Kahlil Gibran, "A Handful of Sand on the Shore"

Remerciements

Mes premiers remerciements vont à mon directeur de thèse, Professeur Xavier Lagrange pour exprimer ma profonde gratitude envers lui. Je tiens à le remercier pour la confiance et la liberté qu'il m'a accordées tout au long des années de ma thèse. Ses conseils et ses critiques m'ont permis d'avoir une première expérience dans le domaine de recherche. Je lui suis reconnaissant pour sa patience, ses efforts et tout le temps qu'il m'a accordé afin d'éclaircir un chemin si mystique, le chemin d'une thèse.

Je tiens à remercier Professeur Ramón Agusti et Professeur Philippe Godlewski pour avoir consacré de leur temps pour rapporter sur ma thèse et pour leurs commentaires et leurs remarques constructives. Mes remerciements vont également aux examinateurs Professeur Ghais El Zein, Mr. Bruno Jechoux et Dr. Bruno Tuffin pour leur participation à ma soutenance et leurs commentaires pertinents.

J'aimerais par ailleurs exprimer mes profondes gratitudes aux membres du département RSM pour l'ambiance amicale et encourageante qu'ils ont créée. Je remercie particulièrement Loufi Nuaymi pour ses conseils et son soutien pendant les années de ma thèse.

Cette thèse n'aurait jamais pris fin sans le soutien moral et l'encouragement des étudiants du département RSM, qui ont rendu mon séjour à Rennes un séjour inoubliable. Je pense particulièrement à Patrick pour son humour et les parties sympathiques de ping-pong. Je remercie aussi Elizabeth, Joel, Kamal, Rachid et Youssef pour tous les moments qu'on a passés ensemble. Je remercie aussi mon collègue de bureau Lucian pour son calme et son soutien surtout pendant les derniers mois de ma thèse.

Je ne peux pas oublier de dédier un remerciement du fond de mon cœur à mes amis à Rennes. Chacun d'eux a contribué à l'évolution de mon moral, de ma personnalité et de mes rêves. Une pensée particulière est dédiée à Samer et Chadi pour leur amitié que je ne peux décrire avec les mots. Je tiens aussi à remercier mes amis à Paris et Toulouse qui étaient toujours à mes côtés dans les moments les plus durs de ma thèse et qui ont rendu ma vie plus agréable. Je ne peux jamais oublier l'été de 2001 à Paris avec Assaad et Bassem.

Loin de mon pays, j'ai eu une autre famille grâce à l'amour et le soutien de Hassan, Rima et Wael pendant tout mon séjour en France. Aucun mot ne peut exprimer mon gratitude envers eux.

Finalement, je dédie cette thèse à mes parents et mes frères. Ces anges gardiens qui veillent sur moi de si loin par la force de leur amour indescriptible.

Contents

Abbreviations and Acronyms	xi
Index Notations	xiii
Résumé	xvii
Abstract	xxxix
1 Introduction	1
1.1 Universal Mobile Telecommunications System	2
1.1.1 Major Features of UMTS	2
1.1.2 UMTS Network	4
1.1.3 Radio Interface Protocol Architecture	5
1.2 UTRA TDD	7
1.2.1 Physical Layer	8
1.2.2 Benefits	11
1.2.3 Drawbacks	11
1.3 Context of the Thesis	11
1.4 Thesis Scope and Outline	12
2 Radio Resource Management	15
2.1 Interference in TDMA-CDMA/TDD Systems	15
2.1.1 Index Notations	16
2.1.2 Normalized Pathgain	17
2.1.3 Power Budget	18
2.1.4 Interference Profile	18
2.2 Power Control	22
2.3 Channel Allocation	23
2.4 Performance Evaluation	26
2.4.1 Types of Simulations	26
2.4.2 Performance Measures	27
2.5 Summary	29
3 Centralized Optimum Power Control	31
3.1 Problem Formulation	32
3.1.1 Generic Equation of the CIR in Pure CDMA Systems	32
3.1.2 Optimization Problem Formulation	35
3.2 Optimum Power Control in Pure CDMA Systems	37

3.2.1	Centralized Unconstrained Optimum Power Control	37
3.2.2	Centralized Constrained Optimum Power Control	40
3.3	Simplified Generic Optimum Power Control	41
3.3.1	Unconstrained Power Control in Noiseless Systems	42
3.3.2	Performance Analysis using Simplified Generic Optimum Power Control	48
3.4	User Removal Algorithms	52
3.4.1	Stepwise Removal Algorithms for Pure Downlink and Uplink Slots	52
3.4.2	Generic Mobile-based Stepwise Removal Algorithm	55
3.5	Lower-Bounded Constrained Power Control	57
3.5.1	Problem Formulation	58
3.5.2	Optimization Problem Solution	59
3.6	Concluding Remarks	60
4	Iterative Power Control	63
4.1	Iterative Power Control Algorithms	63
4.1.1	Iterative Optimum Power Control Algorithms	63
4.1.2	Iterative Algorithms in Noisy Systems	65
4.1.3	Other Power Control Algorithms	67
4.2	Standardized Power Control	67
4.2.1	3GPP Power Control Algorithms	68
4.2.2	Problem Formulation	69
4.2.3	Modified Adaptive Power Control	71
4.2.4	Simulation Model	73
4.2.5	Simulation Results	74
4.3	Concluding Remarks	80
5	Slot Allocation Techniques	81
5.1	Problem Formulation	81
5.1.1	System Model	81
5.1.2	Optimization Problem Definition	82
5.2	Optimal Slot Allocation Algorithms	86
5.2.1	Heuristic Methods for Partition Search	87
5.2.2	Stepwise Allocation Algorithm	90
5.3	Channel Re-allocation Algorithms	91
5.3.1	Simulated Annealing	91
5.3.2	Re-Allocation Meta-heuristic Algorithm	92
5.4	Simulations and Results	95
5.4.1	System Model	95
5.4.2	Noiseless System	96
5.4.3	Noisy Systems	98
5.5	Summary	104
6	Interference Avoidance Techniques	105
6.1	Problem Formulation	105
6.1.1	Different Time Slot Allocation Based on Region Division	105
6.1.2	Disjoint Base Station Sets Method	106
6.2	Slot Allocation Method Based on Mobile-to-Base Station Pathgains	106
6.2.1	Main Idea	108

6.2.2	SAP Behavior in Hexagonal Networks	108
6.3	Slot Allocation Method Based on Mobile-to-Base Station Normalized Pathgains . . .	109
6.3.1	Main Idea	109
6.3.2	SANP Behavior in Hexagonal Networks	109
6.4	Guideline for Implementation	109
6.5	Interference Avoidance Techniques Analysis	110
6.5.1	System Model	111
6.5.2	Simulations and Results	115
6.6	Summary	118
7	Conclusions and Perspectives	119
7.1	Conclusions	119
7.2	Perspectives	121
A	Useful Propositions for Constrained Power Control Algorithms	123
B	Number of all Possible Partitions in a CDMA/TDMA System	127
B.1	\mathcal{N} as a function of \mathcal{N}_j	127
B.2	Computation of \mathcal{N}_j	128
B.2.1	All possible Partitions	128
B.2.2	Partitions with only Fair Element Distributions to Subsets	129
C	Publications	131

List of Figures

1	La structure du canal physique dans une trame TDMA-CDMA	xix
2	Interférence commune de deux modes de duplexage FDD et TDD	xxii
3	Interférence commune de deux modes de duplexage FDD et TDD	xxii
4	La différence entre le C/I maximum atteint dans les slots croisés et le C/I maximum atteint dans les slots montants	xxiv
5	La distribution du CDF de niveau de performance pour un systèmes avec 7 cellules, 7 slots 5 mobiles/cellule/slot	xxviii
1.1	UMTS coverage	2
1.2	UMTS architecture	5
1.3	Radio interface protocol architecture	6
1.4	Resource distribution in FDD mode and in TDD mode	8
1.5	UTRA TDD islands in the global UTRA FDD system	9
1.6	Different possible switching point configurations in TDD frames	10
1.7	Burst structure for UTRA TDD HCR	10
2.1	Mobile and base station notations	16
2.2	An example of mobile and base station indices	17
2.3	Power notations in uplink and downlink during slot n	17
2.4	Different-entity interference	20
2.5	Same-entity interference	21
2.6	Example of slot configuration using the common switching point technique.	25
2.7	Example of slot configuration using the diversified switching point technique	25
2.8	Uplink and downlink search for available channel using the movable boundary technique	26
2.9	Frame configuration with multiple switching points using the SSP technique	26
3.1	Three types of mobile distribution	49
3.2	The pdf of the maximum achievable CIR for uplink and crossed slots	50
3.3	Slot capacity for $\gamma_0 = -10$ dB	50
3.4	The mean difference between the maximum achievable CIR in crossed and uplink slots	51
3.5	CIR-balancing and user removal algorithm	53
3.6	The average outage probability of the GMSR and the quasi-optimal algorithms as a function of the cell load	57
3.7	The average difference between the outage probability of the quasi-optimal algorithm and the outage probability of the proposed algorithm with confidence interval	58
4.1	Uplink inner-loop power control algorithm steps (UTRA TDD)	68

4.2	Downlink inner-loop power control algorithm steps	69
4.3	A comparison between fixed-step and adaptive-step power control convergence	70
4.4	Solving the oscillation problem by using either a CIR margin or a stabilization zone	71
4.5	MAPC algorithm steps in mobiles	73
4.6	MAPC steps in base stations	73
4.7	The mean frame-outage probability percentage for different values of the margin	75
4.8	The mean frame-outage probability percentage as a function of Φ for different values of M and with a cell load of 26 mobiles/cell.	76
4.9	The mean frame-outage probability percentage for different cell loads and a fixed mobile configuration.	77
4.10	The mean total transmitted power as a function of the cell load	78
4.11	Convergence rate of power control algorithms when 26 mobiles/cell/slot are active simultaneously	78
4.12	The mean frame-outage probability percentage as function of cell load with TPC errors	79
4.13	The TPC BER impact on the mean-frame outage probability for a cell load of 26 mobiles/cell	79
5.1	Three partition examples in a TDMA-CDMA/TDD system	82
5.2	Comparison between the VMMs with fair mobile partitions and all mobile partitions in the same cell	89
5.3	Example of a partition using the variance minimization method	89
5.4	Example of a partition using the normalized pathloss sorting method	90
5.5	A convergence example of the RAMA when using either WMM or BMM strategies in a system of 7 cells, 7 slots and 5 mobiles/cell/slot	94
5.6	The CDF of the performance-indices given by the exhaustive method, the NSM, the VMM and the random method in a noiseless system with 2 cells, 2 slots and 16 mobiles without shadowing	97
5.7	The CDF of the performance-indices given by the exhaustive method, the NSM, the VMM and the random method in a noiseless system with 2 cells, 2 slots and 16 mobiles with shadowing	98
5.8	The CDF of the performance-indices given by the exhaustive method, the NSM, the VMM and the random method in a noisy system with 2 cells, 2 slots and 16 mobiles without shadowing	99
5.9	The CDF of the performance-indices given by the random method, the RAMA, the SAA, the exhaustive method and the VMM in a noisy system of 16 mobiles without shadowing	99
5.10	the CDF of the performance-indices given by the exhaustive method, the NSM, the VMM and the random method in a noisy system with 2 cells, 2 slots and 16 mobiles with shadowing	101
5.11	The CDF of the performance-indices given by the random method, the RAMA, the SAA, the exhaustive method and the VMM in a noisy system of 16 mobiles with shadowing	102
5.12	The CDF of the performance-indices given by the random method, the RAMA, the SAA and the exhaustive method in a noisy system of 36 mobiles with shadowing	102
5.13	The CDF of the performance-indices given by the random method, the RAMA, the SAA and the exhaustive method in a noisy system of 245 mobiles with shadowing	103
6.1	Crossed time slot in a system with two cells	106

6.2	The inner zone and the outer zone of the DARD method	107
6.3	The set of the 2 strongest base stations for 3 mobiles (DBS method)	107
6.4	Forbidden zone in cell j when the slot allocation method based on mobile-to-base station pathgains (SAP) is used	108
6.5	Forbidden zone in cell j when the slot allocation method based on normalized mobile-to-base station pathgains (SANP) is used	110
6.6	Base station-to-base station interference in crossed slot and base station-to-mobile interference	111
6.7	Forbidden cells for three mobiles when an interference avoidance method is used	112
6.8	The diversified and common switching point techniques	113
6.9	Traffic distribution over cells	113
6.10	The percentage of unsatisfied, bad-quality and blocked codes as a function of ϑ_{SANP} for a normalized cell load of 0.65	116
6.11	The percentage of unsatisfied codes as a function of the normalized cell load	117
6.12	The percentage of bad-quality codes as a function of the normalized cell load.	117
6.13	The percentage of blocked codes as a function of the normalized cell load.	118

List of Tables

1.1	UMTS service classes	3
1.2	Main parameters of UTRA	9
2.1	A summary of the interference characteristics in downlink and uplink	19
3.1	The characteristics of different user removal algorithms	55
3.2	Propagation model constants	57
4.1	Power limits and receiver thermal noise power	74
4.2	Power control parameters	74
5.1	Simulation parameters	95
5.2	Propagation model and simulated annealing parameters	95
5.3	Comparison between the performance-indices given by the exhaustive method, the NSM, the VMM and the random method in a noiseless system with 2 cells, 2 slots and 16 mobiles without shadowing	96
5.4	Comparison between the performance-indices given by the exhaustive method, the NSM, the VMM and the random method in a noiseless system with 2 cells, 2 slots and 16 mobiles with shadowing	97
5.5	Comparison between the performance-indices given by the exhaustive method, the NSM, the VMM and the random method in a noisy system with 2 cells, 2 slots and 16 mobiles without shadowing	100
5.6	Comparison between the performance-indices given by the random method, the RAMA and the BMM, the RAMA and the WMM, the SAA, the exhaustive method and in a noisy system of 16 mobiles without shadowing	100
5.7	Comparison between the performance-indices given by the exhaustive method, the random method, the NSM and the VMM in a noisy system with 2 cells, 2 slots and 16 mobiles with shadowing	101
5.8	Comparison between the performance-indices given by the random method, the RAMA and the BMM, the RAMA and the WMM, the SAA and the exhaustive method in a noisy system of 16 mobiles with shadowing	103
5.9	Comparison between the performance-indices given by the random method, the RAMA and the BMM, the RAMA and the WMM and the SAA in a noisy system of 245 mobiles with shadowing	104
5.10	Iteration number in a noisy system of 245 mobiles with shadowing	104
6.1	Simulation parameters	114
6.2	Propagation model constants	114

Abbreviations and Acronyms

3GPP	Third Generation Partnership Project
16-QAM	16 Quadrature Amplitude Modulation
ARQ	Automatic Repeat reQuest
ASPC	Adaptive-Step Power Control
BDPC	Balanced Distributed Power Control algorithm
BCH	Broadcast Channel
BER	Bit Error Rate
BFA	Brute Force Algorithm
BLER	Block Error Rate
BMC	Broadcast/Multicast Control
CIR	Carrier-to-Interference Ratio
CN	Core Network
C-plane	Control-plane
CRC	Cyclic Redundancy Check
DB	Distributed Balanced power control algorithm
DCA	Dynamic Channel Allocation
DCPC	Distributed Constrained Power Control algorithm
DPC	Distributed Power Control algorithm
EDGE	Enhanced Data Rates for GSM Evolution
ETSI	European Telecommunications Standards Institute
FDPC	Fully Distributed Power Control algorithm
FCA	Fixed Channel Allocation
FDD	Frequency Division Duplex
GCOPC	Generic Constrained Optimum Power Control
GMSR	Generic Mobile-based Stepwise Removal algorithm
GSM	Global System for Mobile communication
GPRS	General Packet Radio Service
HCA	Hybrid Channel Allocation
HCR	High Chip Rate
HSCSD	High Speed Circuit Switched Data
HS-PDSCH	High Speed Physical Downlink Shared Channel
ILOPC	Iterative Lower-bounded Optimum Power Control
IMT-2000	International Mobile Telecommunications-2000
ITU	International Telecommunication Union
LCR	Low Chip Rate
MAC	Medium Access Control

MAPC	Modified Adaptive Power Control
MB	Movable Boundary
NSM	Normalized pathloss Sorting Method
P-CCPCH	Primary Common Control Physical Channel
PDCP	Packet Data Convergence Protocol
QPSK	Quadrature Phase Shift Keying
RCA	Random Channel Allocation
RLC	Radio Link Control
RNC	Radio Network Controller
RNS	Radio Network Sub-system
RRC	Radio Resource Control
SA	Static Allocation
SAA	Stepwise Allocation Algorithm
SAP	Slot Allocation method based on mobile-to-base stations Pathgains
SANP	Slot Allocation method based on mobile-to-base stations Normalized Pathgains
SMIRA	Stepwise Maximum-Interference Removal Algorithm
SOR	Successive OverRelaxation
SORA	Stepwise Optimal Removal Algorithm
SRA	Stepwise Removal Algorithm
SSP	Soft Switching Point
TDD	Time Division Duplex
TDMA	Time Division Multiple Access
TPC	Transmitted Power Command
TTI	Transmission Time Interval
UE	User Equipment
U-plane	User-plane
UMTS	Universal Mobile Telecommunications System
UTRA	UMTS Terrestrial Radio Access
UTRAN	UMTS Terrestrial Radio Access Network
VMM	Variance Minimization Method
WCDMA	Wideband Code Division Multiple Access

Index Notations

$\alpha_{i,n}$	The portion of $\mathcal{P}_{T,j,n}$ dedicated to mobile i during time slot n
β_d	The factor of remaining intracell interference in downlink
β_u	The factor of remaining intracell interference in uplink
γ_0	CIR target
$\gamma_{W,\ell}^*$	The maximum achievable CIR in link direction ℓ , using Wu matrix
$\lambda_{W,\ell}^*$	The real positive eigenvalue of Wu matrix $\mathbf{Z}_{W,\ell}$ for which the corresponding eigenvector has components of the same sign
γ_ℓ^*	The maximum achievable CIR in link direction ℓ , using the simplified matrix
λ_ℓ^*	The real positive eigenvalue of matrix \mathbf{Z}_ℓ for which the corresponding eigenvector has components of the same sign
$\rho(\mathbf{Z})$	The real positive eigenvalue of matrix \mathbf{Z} for which the corresponding eigenvector has components of the same sign (spectral radius)
$\overline{\gamma_{W,\ell}^*}$	The maximum achievable CIR in link direction ℓ , using Wu matrix in a constrained system
ℓ	The link transmission direction of mobile i during slot n ($\ell = d$ for downlink and $\ell = u$ for uplink)
τ	Type of the terminal ($\tau = b$ for a base station and $\tau = m$ for a mobile)
$\Gamma_{\ell,i,j,n}$	The CIR of mobile i served by base station j during slot n in link direction ℓ
Π	The set of base station indices
$\Psi_{i,j}$	The high interference-cells set associated to mobile i of cell j
a_r	Asymmetry rate between uplink and downlink cells during a crossed slot
i	Studied mobile index
j	The index of mobile server
k	Other mobile index
l	Other base station index
n	Time slot index
v_j	The variance of variables $z_{j,n}$ in cell j
z_i	The sum of mobile normalized pathgains
$z_{j,n}$	The sum of normalized pathgains of mobiles grouped in the subset $S_j^{(n)}$
A	The maximum allowed number of simultaneous active codes in a cell during a slot
$C_{\tau,i,n}$	The useful received power corresponding to mobile i during slot n
$C_{b,i,n}$	The useful power of a mobile i received by its server j during time slot n
$C_{m,i,n}$	The useful power received by mobile i during the time slot n
$G_{i,j}$	The pathgain between mobile i and its server j
$I_{\ell,i,n}$	The total interference power experienced by the useful signal of mobile i in the link direction ℓ during slot n

$I_{\text{intra},\ell,i,n}$	The intracell-interference power experienced by the useful signal of mobile i in the link direction ℓ during slot n
$I_{\text{inter},\ell,i,n}$	The total intercell-interference power experienced by the useful signal of mobile i in the link direction ℓ during slot n
$I_{\text{bm},i,n}$	The interference power induced by base stations of neighboring downlink-cells to mobile i during slot n
$I_{\text{mm},i,n}$	The interference power induced by mobiles of neighboring uplink-cells to mobile i during slot n
\mathbf{I}_N	The $N \times N$ identity matrix
M	The number of base stations
M_d	The number of active base stations in downlink-cells
M_u	The number of active base stations in uplink-cells
N	The total number of mobiles
N_0	The background noise power
N_j	The number of active mobiles in cell j
$\mathbf{N}_{\text{W},\ell}$	The vector of normalized thermal noise power to the pathgain between a mobile and its server
$P_{\tau,i,n}$	The transmitted power corresponding to mobile i during slot n
$P_{\text{b},i,n}$	The power transmitted by base station j to mobile i during time slot n
$P_{\text{m},i,n}$	The power transmitted by mobile i during slot n
\mathbf{P}_ℓ	The vector of transmitted powers in link direction ℓ
S_j	The set of mobiles connected to base station j
$S^{(n)}$	The set of active mobiles in the system during time slot n
$S_j^{(n)}$	The set of active mobiles connected to base station j during time slot n
T	The number of time slots in a frame
T_c	The number of crossed slots in a frame
T_d	The number of downlink time slots in a frame
T_e	Temperature parameter in simulated annealing
T_u	The number of uplink time slots in a frame
$Z_{i,l}$	The normalized pathgain between mobile i of cell j and base station l : $Z_{i,l} = \frac{G_{i,l}}{G_{i,j}}$
$\mathbf{Z}_{\text{W},\ell,u}$	Wu uplink normalized matrix in link ℓ
$\mathbf{Z}_{\ell,u}$	The simplified generic normalized matrix in link ℓ
\mathcal{B}	The set of acceptable power vectors
$\mathcal{C}_{\text{b},j,n}$	The useful power received by a base station j during slot n when optimal power control is applied
$\mathcal{I}_{\text{u},j,n}$	The total interference power experienced by the useful signal of each mobile in cell j transmitting during slot n
$\mathcal{I}_{\text{inter},\text{u},j,n}$	The total intercell-interference power experienced by the useful signal of each mobile in cell j transmitting during slot n
$\mathcal{I}_{\text{intra},\text{u},j,n}$	The intracell-interference power experienced by the useful signal of each mobile in cell j transmitting during slot n when optimal power control is applied
$\mathcal{I}_{\text{mb},j,n}$	The interference power induced by mobiles of neighboring uplink-cells to the useful signal of all mobiles in cell j transmitting during slot n
$\mathcal{I}_{\text{bb},j,n}$	The interference power induced by base stations of neighboring downlink-cells to the useful signal of all mobiles of cell j transmitting during slot n
\mathcal{N}	The number of all possible partitions in a TD-CDMA system
\mathcal{N}_j	The number of all possible partitions in a cell j of a TD-CDMA system
$\mathcal{P}_{\text{T},j,n}$	The total power transmitted by base station j during time slot n
$\mathcal{S}^{(p)}$	Mobile partition p

- $\mathcal{S}(N_j, T)$ Stirling number of the second kind for a set j with cardinality N_j divided into T subsets
- $\mathcal{Z}_{W,\ell,i,k}$ The element of the i th row and the k th column of Wu normalized matrix $\mathbf{Z}_{W,\ell,u}$

Time slot index n is omitted in some cases where only one time slot is investigated

Résumé

Les systèmes mobiles de la seconde génération ont été conçus pour offrir des services de transmission de la voix et des données à faibles débits. Par contre, les systèmes de communications mobiles de troisième génération doivent offrir une large gamme de services pour les utilisateurs: communication vocale de haute qualité, transmission de données à débits variables. De plus, ces systèmes doivent être capables de desservir avec un haut niveau de qualité de service tous les abonnés dont le nombre augmente rapidement et cause la saturation de la plupart des systèmes existant. L'objectif des systèmes mobiles de la troisième génération est donc d'offrir les mêmes services des systèmes fixes. Mais les caractéristiques de l'interface radio sont très différentes que celles des systèmes fixes et posent des problèmes additionnels à résoudre (interférences, effet de masque, mobilité, effet de multi-trajet, etc.). Ces problèmes sont les conséquences de l'instabilité de l'environnement radio et l'interaction entre les différents canaux (interférences). De ce fait, l'interface radio est considéré comme le goulet d'étranglement des réseaux mobiles.

La technique de multiplexage CDMA (*Code Division Multiple Access*) est utilisée dans les systèmes mobiles de troisième génération UMTS (*Universal Mobile telecommunication System*) sous deux variantes : l'une basée sur le CDMA pur, l'autre combinant le duplexage temporel TDD (*Time Division Duplex*) et le multiplexage temporel TDMA (*Time Division Multiple Access*) avec le CDMA. Dans les systèmes CDMA, tous les utilisateurs partagent la même bande passante. Malgré les caractéristiques des codes CDMA utilisés, l'orthogonalité ne peut pas être garantie dans tous les cas. Par conséquent, les signaux utiles d'un utilisateur sont interférés par les signaux des autres utilisateurs. De ce fait, la capacité de ces systèmes est limitée par l'interférence. Dans les systèmes utilisant le CDMA pur, la procédure au niveau du réseau la plus efficace pour réduire les interférences est le contrôle de puissance. Les algorithmes de contrôle de puissance tendent à optimiser la puissance de transmission afin de garantir le meilleur niveau de qualité de service à un ensemble défini des utilisateurs. En outre, la combinaison du TDMA et du TDD offre un nouveau degré de flexibilité dans la gestion de ressources. Ce degré de flexibilité permet aux systèmes de mieux exploiter les ressources radios, surtout lorsque le volume de trafic est beaucoup plus grand dans la voie descendante que dans la voie montante. Mais, l'exploitation de ce degré de flexibilité peut introduire des nouveaux types d'interférences (interférences mobile-mobile et station de base-station de base) qui peuvent dégrader le niveau de qualité de service. Dans cette optique, la conception des algorithmes d'allocation de slots efficaces devient vitale pour garantir un niveau adéquat de qualité de service pour le plus grand nombre d'utilisateurs.

Dans cette thèse, nous exploitons la flexibilité des systèmes TDMA-CDMA/TDD tout en conservant un faible niveau d'interférence. Tout d'abord, nous proposons un algorithme simple générique de contrôle de puissance optimal et nous l'appliquons à différents problèmes de gestion de puissance. Cet algorithme peut être utilisé dans la voie montante, la voie descendante et les slots croisés pour estimer la capacité maximale, la probabilité de blocage minimale, etc. De plus, nous proposons des améliorations simples au contrôle de puissance standardisé pour l'UMTS qui n'augmentent pas le volume de signalisation. Ces améliorations mènent à une augmentation significative de la capacité

en optimisant la puissance de transmission.

D'autre part, nous proposons des méthodes heuristiques et méta-heuristiques qui combinent le contrôle de puissance optimal et l'allocation de slots. Ces méthodes peuvent être utilisées pour estimer les bornes supérieures de capacité. De plus, elles peuvent être adaptées aux systèmes opérationnels en réorganisant les allocations de slots lorsque le niveau de qualité de service devient inacceptable. Finalement, nous proposons des méthodes d'évitement d'interférences mobile-mobile en utilisant les gains de parcours entre les mobiles et les stations de base. Ces méthodes mènent à une exploitation plus efficace de la flexibilité des systèmes TDMA-CDMA/TDD en conservant un bas niveau d'interférence.

1 Introduction

Le défi principal pour les systèmes de communications mobiles de la troisième génération est de faire face aux demandes des utilisateurs qui sont croissantes et complexes. En utilisant les avantages du mode d'accès multiple CDMA, le système universel de télécommunication mobile UMTS (Universal Mobile telecommunication System) garantira l'accès à des services allant de la simple téléphonie vocale jusqu'au multimedia à grande vitesse et de haute qualité, indépendamment de la localisation, du réseau ou du terminal utilisé.

1.1 Présentation du Système

Le nom UMTS a été choisi par l'organisme Européen de standardisation de télécommunications ETSI (*European Telecommunication Standard Institute*) pour les systèmes de la troisième génération. Ce système utilise, sur l'interface radio, la technique CDMA. Cette technique offre la possibilité de desservir simultanément plusieurs utilisateurs sur la même bande de fréquence.

Dans l'interface radio de l'UMTS, le mode UTRA FDD (*UMTS Terrestrial Radio Access Frequency Division Duplex*) utilisant le protocole WCDMA pur (*Wideband CDMA*) a été proposé pour la couverture globale et pour des services avec des trafics symétriques. Par contre, l'utilisation du mode de duplexage temporel TDD (*Time Division Multiple Access*) et du protocole de multiplexage temporel TDMA (*Time Division Multiple Access*) permet à l'UTRA TDD d'offrir des services asymétriques de hauts débits dans des micro et des pico cellules. Ce dernier mode utilise un protocole hybride TDMA-CDMA où les différents utilisateurs (ou même les différents services d'un même utilisateur) sont distribués sur des différents slots de temps avec la possibilité de desservir plusieurs utilisateurs pendant le même slot.

Dans le mode le plus courant, chaque porteuse de 5 MHz est divisée en 15 intervalles de temps et constitue une trame de 10 ms. Cette technique est compatible avec le mode TDD car elle possède un élément de multiplexage temporel. La bande de fréquence, le nombre d'intervalles de temps par trame radio, le type de modulation et d'autres paramètres du système sont les mêmes, ce qui permet de développer des terminaux simples qui peuvent supporter les deux modes.

La figure 1 montre la structure du canal physique dans une trame TDMA-CDMA. Ainsi, on peut remarquer dans cette figure la possibilité d'allouer à une communication plusieurs codes dans le même intervalle de temps (*code pooling*) ou plusieurs intervalles de temps (*time slot pooling*) afin d'augmenter le débit [FKWS01].

L'utilisation du mode de duplexage temporel et l'héritage de propriétés du multiplexage TDMA dans l'UTRA TDD lui offrent une spécificité par rapport à l'UTRA FDD.

- ◊ Le duplexage FDD a besoin d'une paire de bandes pour séparer les deux voies. Par contre, une seule bande non appariée est suffisante dans le mode TDD où les deux voies sont séparées dans le domaine temporel. Par ailleurs, la transmission est discontinue en multiplexage temporel, ce qui nécessite une synchronisation et un contrôle de temps.

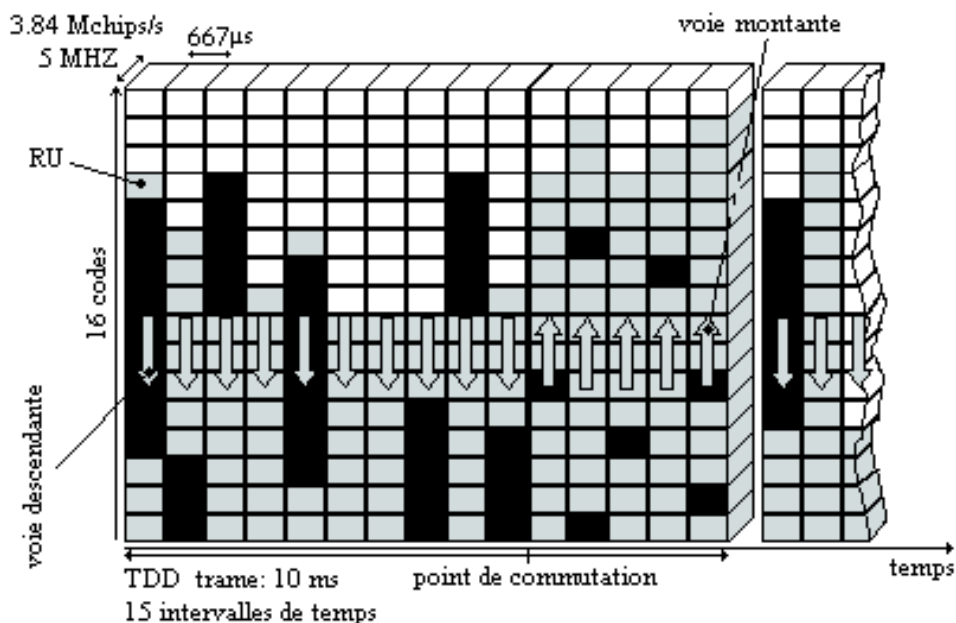


Figure 1: La structure du canal physique dans une trame TDMA-CDMA

- ◇ L'allocation de ressources est plus flexible dans le mode TDD. En effet, l'utilisation des points de commutation multiples ou dynamiques fait que le système s'adapte à la configuration de cellules qui peut être asymétrique et optimise l'utilisation des ressources radios.
- ◇ L'utilisation de la même fréquence dans les deux voies permet de contrôler l'évanouissement sélectif qui dépend de la fréquence. En se basant sur le signal reçu par un terminal TDD, on peut estimer le facteur d'évanouissement dans l'autre sens. L'utilisation de cette information dans le contrôle de puissance augmente la performance du système et permet l'utilisation de la boucle ouverte du contrôle de puissance. De plus, la nature réciproque du canal peut être utilisée dans la station de base si cette dernière utilise une diversité des antennes. En effet, l'antenne de la station de base qui reçoit le signal le plus fort peut être utilisée pour la transmission dans la voie descendante. Par conséquent, la séparation des mobiles dans l'espace pour la voie descendante peut être utilisée sans la nécessité d'avoir des antennes intelligentes dans le mobile [PN98].
- ◇ Contrairement à l'UTRA FDD où on utilise le *soft handover*, l'UTRA TDD utilise uniquement le *hard handover* où chaque mobile est relié à une seule station de base qui le dessert.
- ◇ Malgré ses avantages, le mode TDD présente un inconvénient important en introduisant de nouveaux types d'interférence : interférence mobile-mobile et interférence station de base-station de base. Ces interférences apparaissent lorsque deux cellules travaillent dans des voies différentes pendant le même intervalle de temps et utilisent la même fréquence (figure 3).

1.2 Contexte de la Thèse

Une partie de la thèse a été effectuée dans le cadre du projet PETRUS (Plate-forme d'Évaluation des Technologies Radio pour l'UMTS TDD et ses Services). PETRUS est un projet RNRT (Réseau

National de Recherche en Télécommunications) dont l'objectif est d'optimiser les techniques de détection conjointe et d'allocation de ressources radios dynamiques pour des systèmes offrant des services asymétriques.

PETRUS était une collaboration entre 5 partenaires : CEA-LETI, Mitsubishi Electric ITE, Supélec, Bouygues Telecom et GET/ENST Bretagne. Outre les études théoriques et les simulations, un banc de test a été développé pour émuler le canal radio et évaluer la performance des techniques de détection conjointes développées au sein du projet.

Les techniques de détection conjointe permettent à plusieurs utilisateurs de partager la même bande passante en utilisant des faibles facteurs d'étalement. Ces techniques utilisées dans le mode TDD sont très importantes pour la réduction des interférences intracellulaires. Néanmoins, les techniques de détection conjointe sont généralement très complexes et ne peuvent pas être implémentées dans des mobiles à prix économique. Pour cela, le premier objectif de PETRUS était d'étudier les techniques existantes et de proposer des nouvelles techniques qui offrent un compromis entre la complexité et le performance. En outre, ces techniques doivent être testées pour envisager les problèmes potentiels qui peuvent surgir dans les systèmes opérationnels.

Le second objectif de PETRUS est d'exploiter la flexibilité du mode TDD afin d'optimiser la gestion de ressources radios dans les systèmes offrant des services asymétriques. Pour cela, Les algorithmes d'allocation de slots dynamiques et les méthode d'évitement des interférence ont été étudiés et des nouveaux algorithmes ont été proposés. De plus, les algorithmes de contrôle de puissance ont été étudiés à cause de leur forte influence sur les algorithmes d'allocation de slots.

1.3 Objectives de la Thèse

Dans l'UTRA TDD, la combinaison d'un code et d'un intervalle de temps pour une seule bande de fréquence est appelée unité de ressource (RU : Ressource unit). Les interférences intracellulaires et intercellulaires, le nombre limité des séquences d'apprentissage, les contraintes sur les puissances émises et reçues et d'autres phénomènes réduisent le nombre d'unités de ressources qui peuvent satisfaire la qualité de service désirée. Par conséquent, la gestion de ressources radios joue un rôle important dans la conception des systèmes UTRA TDD. L'objectif de la gestion de ressources consiste alors à optimiser l'utilisation des unités de ressources offertes par le système pour maximiser la capacité de ce dernier.

Afin de garantir les niveaux de qualité de service imposés par les différents types d'application, des méthodes d'allocation de ressources raffinées sont nécessaires. Ces méthodes cherchent à diminuer le niveau d'interférence puisque la capacité d'un système utilisant le CDMA est limité par les interférences. L'objectif de ces méthodes est donc de garantir un niveau de qualité de service acceptable pour tous les utilisateurs avec une puissance de transmission minimale. Dans cette optique, les méthodes d'allocation de ressources sont destinées à optimiser l'utilisation de ressources limitées.

L'utilisation du multiplexage TDMA et du mode de duplexage TDD permet à l'UTRA TDD de gérer simultanément des flux hautement asymétriques et des flux symétriques. En revanche, les codes pseudo-aléatoires utilisés sont plus courts que ceux utilisés dans l'UTRA FDD. Par conséquent, les interférences sont plus élevées. Elles peuvent dégrader fortement la qualité de service si les ressources ne sont pas bien distribuées sur les différents canaux. Pour réduire l'effet des interférences pendant un slot, le contrôle de puissance doit être utilisé. En outre, le mode TDD de l'UMTS est spécifique en ce qu'il permet de combiner l'allocation de slots et le contrôle de puissance. Pour exploiter toutes les caractéristiques du mode TDD et pour améliorer les niveaux de qualité de service, il faut combiner ces deux techniques dans l'allocation de ressources. De plus, les interférences intracellulaire sont réduites en utilisant les techniques de détection conjointe [Ver98][KKB96][AW01].

L'objectif de cette thèse est d'exploiter la flexibilité du mode TDD en gardant un niveau adéquat de qualité de service. Dans toute la thèse, nous supposons que tous les utilisateurs demandent le même service. Nous supposons aussi que le système cherche à satisfaire tous les utilisateurs avec le même niveau de qualité de service. Dans la suite de la thèse, nous utilisons le rapport signal sur interférence et bruit (C/I) comme métrique de qualité de service. Par conséquent, notre objectif est d'utiliser la flexibilité du système TDMA-CDMA/TDD pour offrir quasiment le même niveau de C/I à tous les utilisateurs. Pour aboutir à cet objectif, cette thèse est divisée en quatre axes de recherche: contrôle de puissance optimal, contrôle de puissance adaptatif, combinaison d'allocation de slots et de contrôle de puissance optimales et l'évitement d'interférences.

2 Types d'Interférences dans l'UTRA TDD

La capacité d'un réseau utilisant la technique CDMA est limitée par l'interférence. Dans la voie montante la capacité est limitée par les interférences intercellulaires et intracellulaires qui augmentent la consommation de la puissance dans les mobiles tandis que dans la voie descendante, elle est généralement limitée par les interférences intercellulaires qui obligent les stations de base à transmettre avec des puissances totales non acceptables pour satisfaire la qualité de service. Pour cela, il faut bien étudier les différents types d'interférences et leurs influences sur le système.

La présence d'interférence intracellulaire est due au fait que les codes CDMA des différents utilisateurs de la même cellule peuvent avoir des corrélations à cause de l'effet du multitrajet dans les deux voies et de la perte de synchronisation dans la voie montante. Par conséquent, les interférences intracellulaires dans l'étude du mode TDD doivent être prises en compte. En effet, les codes CDMA ne sont pas assez longs dans le mode TDD pour que la corrélation entre les différents codes soit très petite. Par conséquent, les interférences intracellulaires ne sont pas négligeables. Par ailleurs, nous considérons qu'une technique de détection conjointe est utilisée et que la puissance des interférences intracellulaires est réduite; la puissance des interférences intracellulaires qui doit être ajoutée à la puissance des interférences intercellulaires pour un mobile i d'une cellule j est donnée par la formule suivante:

$$I_{\text{intra}} = \beta \cdot P,$$

où P est la puissance d'interférence de tous les mobiles de la cellule j reçue par le mobile i et β est une constante qui représente le taux de réduction d'interférence intracellulaire due aux orthogonalité des codes dans la voie descendante et à l'utilisation d'une technique de détection conjointe dans les deux voies.

La flexibilité de l'UTRA TDD et sa capacité à s'adapter à un trafic variable et asymétrique des systèmes futurs sont accompagnés par l'apparition de nouveaux types d'interférences qui limitent la capacité du système. En effet, deux types d'interférences intercellulaire apparaissent dans un système utilisant le mode de duplexage FDD : interférence d'une station de base sur un récepteur mobile dans la voie descendante (figure 2.a) et interférence d'un mobile sur une station de base écoutant l'interface radio dans la voie montante (figure 2.b). A ces deux types s'ajoutent deux nouveaux types d'interférences dans le mode de duplexage TDD : interférence entre les stations de base et interférence entre les mobiles (figure 3).

Le slot de temps pendant lequel toutes les stations de base d'un système transmettent, est appelé dans la suite slot descendant tandis que le slot de temps pendant lequel toutes les stations de base d'un système écoutent les canaux physiques est appelé slot montant. D'autre part un slot de temps est dit croisé si certaines stations de base y transmettent leurs signaux utiles et d'autres stations écoutent les canaux physiques.

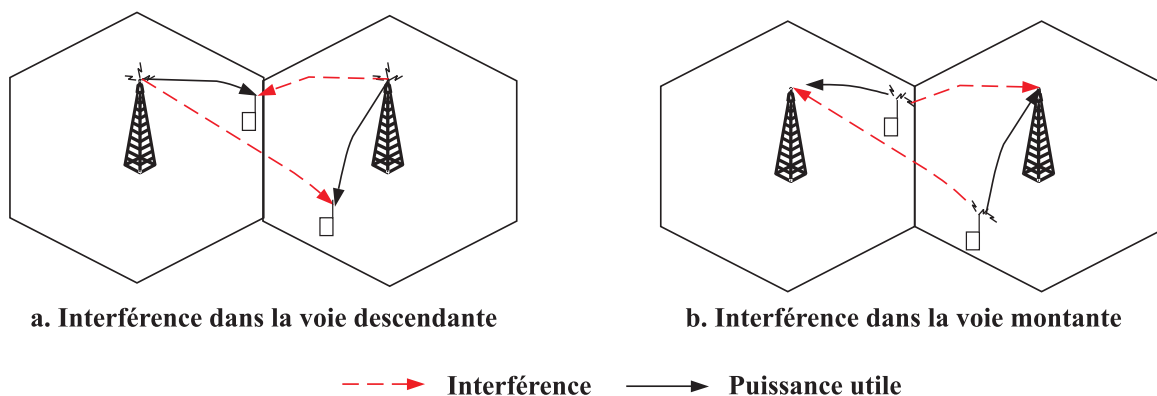


Figure 2: Interférence commune de deux modes de duplexage FDD et TDD

L'interférence d'une station de base sur un mobile apparaît dans le cas où un ensemble de stations de base voisines transmettent leurs signaux dans la voie descendante. Le mobile reçoit simultanément un signal utile de la station de base qui lui est associée et des puissances d'interférences des stations de base voisines qui transmettent pendant le même intervalle de temps. Ce cas apparaît pendant les slots descendants (figure 2.a).

D'autre part, un mobile i introduit une puissance d'interférence dans la réception d'une station de base voisine j si cette dernière écoute un signal émis par un mobile qui lui est attaché pendant le même intervalle où le mobile i émet son signal. Ce cas apparaît dans le cas de slots montants (figure 2.b).

Enfin, les interférences entre les stations de base et les interférences entre les mobiles ont lieu pendant les slots croisés. Pendant ces slots, un mobile écoutant son signal utile peut recevoir une puissance d'interférence d'un autre mobile d'une cellule voisine qui transmet pendant le même slot, alors une interférence inter mobiles apparaît. Pendant le même slot, la station de base qui dessert le dernier mobile reçoit une puissance d'interférence des stations de base qui travaillent dans la voie descendante. Ce phénomène est appelé interférence inter stations de base (figure 3).

3 Contrôle de Puissance

Afin d'obtenir le niveau de qualité de service imposé par les applications, les systèmes mobiles sont conçus, soit pour tolérer les faibles C/I, soit pour réduire les interférences. Le contrôle de

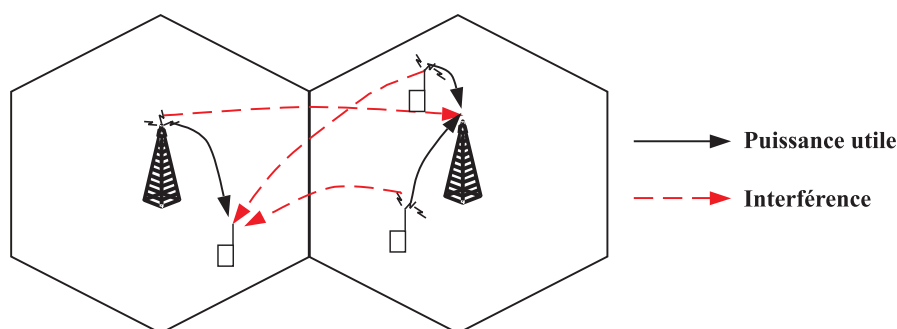


Figure 3: Interférence commune de deux modes de duplexage FDD et TDD

puissance est utilisé dans l'UTRA TDD pour limiter le niveau d'interférence intercellulaire et pour réduire la consommation de puissance dans les stations mobiles. Comme l'interférence est la limite principale de la capacité et comme la consommation de batterie va être très élevée, le contrôle de puissance efficace et rapide prend une grande importance dans la conception du système UMTS et surtout dans la voie montante. En effet, sans ce contrôle de puissance on peut avoir des interférences très élevées dues à la mauvaise distribution de puissances. Ces interférences réduisent la qualité de service et la capacité du système. Un contrôle de puissance est dit efficace s'il aboutit à la qualité de service désirée avec des puissances minimales.

3.1 Contrôle de Puissance Optimal et Centralisé

Dans la littérature, il existe plusieurs approches pour le but du contrôle de puissance: maximiser le débit maximal dans le système, minimiser la consommation d'énergie, offrir le C/I maximal à tous les utilisateurs, etc. Pour une distribution définie des mobiles et des gains de parcours, une approche importante pour le contrôle de puissance optimal est de maximiser le C/I minimum de tous les utilisateurs. Dans [GVGZ93], les auteurs ont démontré que cette approche revient à offrir le même C/I maximal à tous les utilisateurs (*CIR-balancing*). Dans la suite de la thèse, nous utilisons cette approche de contrôle de puissance optimal. Le contrôle de puissance optimal est utilisé, donc, pour trouver la distribution de puissances optimale qui assure le C/I maximum que peuvent atteindre tous les utilisateurs actifs.

Formulation du Problème

Le problème de contrôle de puissance optimal peut être formulé en un problème de programmation linéaire si certains métriques (gains de parcours, C/I, etc.) peuvent être communiquées à une unité centrale [BE64]. Dans [Aei73], l'auteur a introduit le concept de *CIR-balancing* pour la gestion des interférences dans les systèmes satellitaires. Dans ce modèle, tous les utilisateurs sont desservis avec le même C/I maximum. Ce concept a été étendu pour les systèmes CDMA [AN82][NA83] et FDMA (*Frequency-Division Multiple Access*) [Zan92b] sans bruit du fond. La solution du problème de *CIR-balancing* dans des systèmes sans bruit du fond est obtenue en utilisant les valeurs propres de la matrice des gains de parcours normalisés. Le C/I qui correspond à la valeur propre de plus grand module est le C/I maximum que peut atteindre les utilisateurs. Dans [Wu99], le contrôle de puissance optimal est généralisé pour prendre en compte les systèmes CDMA dans les voie montante et descendante avec ou sans bruit du fond. Contrairement au système FDMA, tous les utilisateurs d'une cellule doivent être considérés dans la matrice d'un système CDMA. Par conséquent, la taille de cette matrice devient rapidement très grande. Pour cela, un modèle simplifié du *CIR-balancing* est proposé dans [KP00][MH01][WSC01][WSW+03] pour la voie descendante. Dans ce modèle, la taille de la matrice dépend seulement du nombre des cellules dans le système. Néanmoins, ce contrôle de puissance simplifié n'a jamais été étudié pendant les slots croisés.

Contrôle de Puissance Optimal et Simplifié

Pour généraliser le contrôle de puissance optimal pour prendre en compte les slots croisés, nous avons conçu un modèle générique pour les deux voies de transmissions.

Dans la voie descendante, nous avons démontré que le contrôle de puissance optimal peut être appliqué sur les puissances totales transmises par les stations de base. On obtient les mêmes résultats que ceux obtenus lorsque le contrôle de puissance est appliqué aux puissances spécifiques des mobiles. Par conséquent, la taille de la matrice des gains de parcours normalisés obtenue est très réduite.

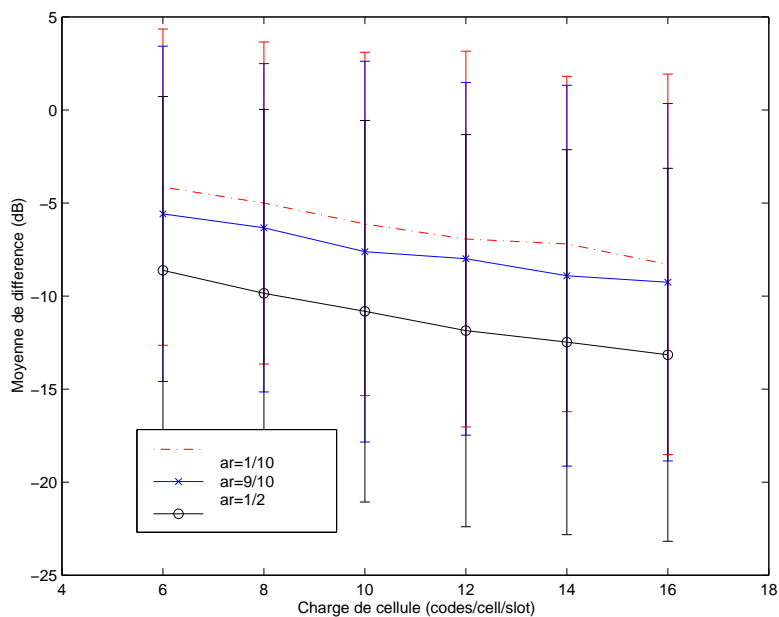


Figure 4: La différence entre le C/I maximum atteint dans les slots croisés et le C/I maximum atteint dans les slots montants

Dans la voie montante, nous avons démontré que le *CIR-balancing* correspond à la réception de tous les mobiles d'une cellule avec la même puissance. Par conséquent, le contrôle de puissance peut être appliqué sur les puissances reçues par les stations de base à la place des puissances de transmissions spécifiques des mobiles. Cette propriété permet de réduire la taille de la matrice des gains des parcours normalisé.

Dans un slot croisé, certains stations de base transmettent dans la voie descendante et certains mobiles transmettent dans la voie montante. Le contrôle de puissance dans ce cas est appliqué aux puissances de transmissions totales des stations de base actives dans la voie descendante et aux puissances reçues par les stations de base actives pendant la voie montante. Ce modèle converge au même niveau de C/I obtenu en utilisant le modèle traditionnel.

Dans la figure 4, nous présentons la moyenne de différence de C/I maximums obtenue en appliquant le contrôle de puissance optimal aux slots croisés et slots montants. Dans cette figure, plusieurs rapport d'asymétrie a_r ont été utilisés pour des différentes charges de cellules. Le rapport d'asymétrie est le rapport de nombre de cellules dans la voie montante et le nombre de cellules dans la voie descendante. Nous pouvons remarquer que les slots croisés ont généralement de C/I plus petits que ceux obtenus dans les slots montants et que cette différence augmente lorsque la charge augmente et lorsque a_r approche de 0.5. Néanmoins, le C/I maximum obtenu dans les slots croisés peut être, dans certains cas spécifiques, plus élevés que celui obtenu dans les slots montants.

Algorithmes d'Elimination des Mobiles

Dans certain cas, le contrôle de puissance ne peut pas garantir le C/I imposé par l'application. Ce phénomène est dû au fait que la distribution des gains de parcours des mobiles ne permet pas de fournir le C/I imposé. Pour remédier ce problème, des algorithmes d'élimination de mobiles sont proposés dans la littérature. L'algorithme exhaustif qui considère toutes les combinaisons possibles nécessitent un très grand nombre d'itérations pour se converger [Zan92b]. Pour cela,

des méthodes pas à pas "Stepwise Removal Algorithms" ont été proposées [Zan92b][LLS95][Wu99]. Dans ces algorithmes, un seul mobile est éliminé à chaque étape suivant des contraintes liées à l'algorithme. Ces contraintes dépendent des gains de parcours des mobiles et leurs puissances de transmission. Ces algorithmes sont utilisés pour les systèmes FDMA ou CDMA pur et aucun algorithme n'a été proposé pour les slots croisés. Les slots croisés diffèrent des autres types de slot par la présence des interférences mobiles-mobiles et stations de base-station de base. Pour prendre en compte ces interférences, nous avons proposé un algorithme qui utilise le modèle générique du contrôle de puissance optimal simplifié pour définir les contraintes d'élimination des mobiles. Cet algorithme a donné des C/I très proche des C/I donnés par un algorithme quasi-optimal. L'algorithme quasi-optimal étudie l'impact de l'élimination de chaque mobile sur le C/I.

Contrôle de Puissance Optimal avec Contraintes

Tous les algorithmes de contrôle de puissance étudiés dans la littérature prennent en compte la limite supérieure des puissances transmises dans les systèmes où le bruit du fond ne peut pas être négligé. Mais, aucun algorithme ne considère la limite inférieure qui peut dans certains cas être très contraignante pour un système mobile. Particulièrement, cette contrainte doit être considérée dans les systèmes peu chargés et dans les systèmes où la marge de contrôle de puissance est plus petite que la marge d'interférence (le cas d'un slot croisé où l'interférence entre deux mobiles proches peut être très élevée tandis que l'interférence reçues par les autres mobiles sont très faibles).

Nous avons proposé un algorithme itératif qui détermine si le système peut fournir le C/I imposé par tous les mobiles et qui détermine la valeur des puissances de transmissions dans le cas où les limites inférieures et supérieures sont prises en compte. En utilisant des lemmes que nous avons démontrées, l'algorithme construit itérativement l'ensemble des mobiles qui doivent transmettre avec la puissance minimale. A chaque étape, le contrôle de puissance est appliqué aux mobiles qui n'appartiennent pas à l'ensemble.

3.2 Contrôle de Puissance Iteratif

Le contrôle de puissance optimal maximise le C/I des utilisateurs en optimisant la transmission de puissances. Mais, ce type de contrôle de puissance nécessite la connaissance de tous les gains de parcours par une unité centrale. En revanche, ces données ne peuvent pas être communiquées à l'unité centrale puisqu'elles entraînent un trafic énorme de signalisation. Pour cela, des algorithmes itératifs et distribués de contrôle de puissance sont utilisés [Mey74][Zan92a][GVG94][LL96][HARW00][FM93][HY98]. Dans ces algorithmes, seulement des informations locales doivent être connues par les unités. Les algorithmes de contrôle de puissance pas-à-pas (ou contrôle de puissance en boucle fermée) sont les algorithmes itératifs les plus simples. De plus, les algorithmes pas-à-pas sont plus rapides que les autres algorithmes pour suivre les changements dans l'interface radio.

Formulation du Problème

Les algorithmes de contrôle de puissance pas-à-pas sont les algorithmes standardisés pour les deux voies du mode FDD et de la voie descendante du mode TDD. Dans ces algorithmes, un bit de contrôle est transmis par le récepteur selon la valeur du C/I mesuré. Si le C/I mesuré est plus grand que le C/I imposé, la valeur du bit de contrôle est mise 0. Sinon, cette valeur est mise à 1. En réponse à ce bit, l'émetteur diminue la puissance avec un pas généralement fixe si le bit de contrôle est mis 0 et augmente la puissance généralement avec le même pas si le bit est mis à 1. Deux problèmes apparaissent en utilisant ce type d'algorithme:

- ◊ S'il y a un changement brusque dans l'interface radio, l'algorithme ne peut pas le suivre puisqu'il utilise un pas fixe
- ◊ Le C/I oscille en permanence autour de la valeur imposée puisqu'il y a seulement deux commandes: augmenter ou diminuer la puissance

Contrôle de Puissance Adaptatif

Pour augmenter la vitesse de réaction des algorithmes de puissance aux variations brusques dans l'interface radio, des pas adaptatifs peuvent être utilisés à la place des pas fixes d'augmentation et de diminution de puissance [NLG02][NRB02]. Si une séquence de n bits de même nature est reçue par l'émetteur, le pas est augmenté. Si une séquence alternée de n bits est reçue par contre, le pas est diminué.

Pour résoudre le problème d'oscillation autour de C/I imposé, nous avons proposé des améliorations aux algorithmes adaptatifs. Dans la variante améliorée, nous avons défini une zone de stabilisation au dessus du C/I imposé. Cette zone de quelques dixième de dB est considérée comme une marge dynamique de C/I. Si le C/I est dans cette zone, le récepteur génère une alternance de bit (0 et 1) et l'émetteur stabilise la puissance en réponse à cette alternance.

Cet algorithme diminue d'une manière significative la probabilité d'échec. De plus, l'algorithme mène à une diminution de la puissance transmise dans le système. Ces améliorations sont réalisées en améliorant l'interprétation des bits de contrôle sans aucun changement sur le nombre de ces bits.

4 Allocation de Slots

L'allocation dynamique des slots DCA (*Dynamic Channel Allocation*) offre aux systèmes mobiles une plus grande flexibilité et une capacité à s'adapter aux variations des paramètres de l'interface radio. Les slots sont dynamiquement alloués aux liaisons radios suivant le trafic et la situation de l'interférence. Dans la norme 3GPP [TS202i], deux types d'allocations dynamiques sont définis:

- ◊ le DCA lent (*Slow DCA*) : allocation des slots pour les cellules
- ◊ le DCA rapide (*Fast DCA*) : allocation des slots pour les mobiles

Les techniques d'allocation de slots sont exécutées soit pour initialiser une liaison radio soit pour réorganiser les ressources dédiées à une ou plusieurs liaisons. Ces techniques cherchent à maximiser la capacité en variant la position et le nombre de points de commutation.

L'UTRA TDD est adapté à la couverture des zones de trafic élevé et asymétrique de données et de la voix. En général, le taux d'asymétrie entre la voie descendante et la voie montante n'est pas le même pour toutes les cellules. Pour pouvoir s'adapter à ce type de trafic, on doit concevoir des points de commutation dynamiques et adaptatifs dans les trames. Une technique proposée pour le trafic asymétrique est la technique d'allocation de ressources commune. Dans cette technique, toutes les cellules utilisent la même configuration de slots et le point de commutation peut changer dynamiquement. Par conséquent, les slots croisés ne sont jamais présents. Par contre, cette technique diminue la flexibilité de système TDD puisqu'elle oblige toutes les cellules à avoir la même distribution de slots sur les deux voies tandis que les cellules n'ont pas en général le même taux d'asymétrie entre les deux voies. Une autre technique est la technique d'allocation de ressources diversifiée. En utilisant cette technique, des slots peuvent être croisés. Pendant ces slots, des cellules travaillent dans la voie descendante et des autres dans la voie montante. Dans ce cas, des interférences de type mobiles-mobiles et stations de base-stations de base apparaissent et peuvent dégrader fortement la qualité de service.

4.1 Allocation de Slots Optimale

Le but de l'allocation de slot optimal est de trouver la répartition des mobiles sur les slots qui maximise le minimum de tous les C/I en utilisant le contrôle de puissance optimal. Ce type de problème est très complexe et la recherche de la solution optimale nécessite un très grand nombre d'itérations. Pour réduire le nombre d'itérations, nous avons proposé plusieurs méthodes heuristiques et meta-heuristiques basé sur la spécificité du mode TDD.

Algorithmes Heuristiques

Dans l'objectif de trouver des partitions qui donnent des valeurs de C/I proches de la valeur optimale et avec un nombre réduit d'itérations, deux méthodes ont été proposées : la méthode de minimisation de la variance et la méthode de tri suivant les affaiblissements. La première méthode cherche à égaliser les seuils de C/I des différentes cellules en mixant les mobiles de faibles gains de parcours avec les mobiles de forts gains de parcours dans chaque cellule sur un même slot. Par contre, la méthode de tri suivant les affaiblissements consiste à grouper dans un même slot un ensemble des mobiles ayant une bonne liaison (en général proches de leur station de base) avec des ensembles de mobiles ayant une mauvaise liaison (en général loin de leurs stations de base) des cellules voisines. La méthode de tri a donné les meilleurs résultats dans les systèmes sans bruit du fond tandis que la méthode de minimisation de la variance a donné les meilleurs résultats dans le cas inverse.

Un autre algorithme est conçu en se basant sur les résultats de deux méthodes. Cet algorithme, intitulé *Stepwise Allocation algorithm* (SAA), est un algorithme itératif. Il consiste à trier les mobiles suivant la somme de leur gains de parcours normalisés et d'allouer les slots aux mobiles de mauvaises liaisons au début. Les autres mobiles sont associés aux slots en commençant par les mobiles de plus mauvaises liaisons. Cet algorithme est basé sur l'idée que les mobiles de faibles liaisons sont les mobiles qui ont la plus grande influence sur la détermination du C/I dans un slot. Par conséquent, l'association de ces mobiles au début peut nous donner une idée sur le C/I qu'on peut avoir pendant le slot. Cet algorithme a donné des meilleurs C/I que les méthodes précédentes avec un nombre d'itérations beaucoup plus réduit.

Algorithmes Meta-Heuristiques

Un algorithme meta-heuristique contrôle l'exécution des méthodes heuristiques. Aux contraires des méthodes heuristiques, les algorithmes meta-heuristiques ne se terminent pas lorsqu'un optimum local est trouvé. L'une des méthodes heuristiques qui ne nécessite pas beaucoup de mémoire est le Recuit simulé (*Simulated annealing*). Cette méthode est une méthode itérative qui consiste de passer d'une configuration à une autre configuration voisine avec une certaine probabilité. Cette probabilité est égale à 1 si la nouvelle configuration donne des meilleurs résultats. La possibilité de passer à une configuration moins performante permet de s'échapper des optimums locaux.

L'algorithme proposé, intitulé *Re-Allocation Meta-heuristic Algorithm* (RAMA), peut prendre comme configuration initiale une configuration aléatoire ou une configuration obtenue par la méthode SAA. En partant de la configuration initiale, l'algorithme RAMA passe d'une configuration à une configuration voisine en utilisant le minimum de C/I comme métrique de comparaison entre les configurations. Deux configurations voisines sont deux configurations dans lesquelles un seul mobiles a changé de slot. Ce mobile est choisi du slot qui a le plus petit C/I et dans la cellule qui transmet avec la plus grande puissance. Le mobile peut être le mobile ayant la plus mauvaise liaison ou celui qui a la plus bonne liaison. Dans le premier cas, l'algorithme peut devenir instable. Pour cela, le mobile ayant la plus bonne liaison est choisi. Dorénavant, ce mobile sera associé au

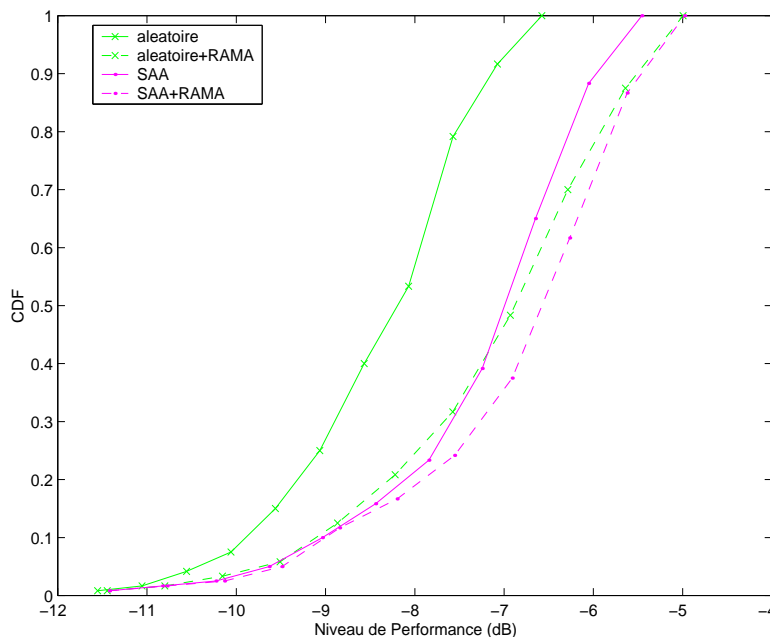


Figure 5: La distribution du CDF de niveau de performance pour un systèmes avec 7 cellules, 7 slots 5 mobiles/cellule/slot

slot ayant le C/I minimum le plus élevé et possédant de ressources libres. Cet algorithme a donné des meilleurs C/I que les méthodes heuristiques avec un nombre d'itérations réduit. De plus, il peut être utilisé dans les systèmes opérationnels.

Dans la figure 5, nous présentons les niveaux de performance obtenus en utilisant les méthodes suivantes: méthodes aléatoire, la méthode RAMA avec une configuration initiale aléatoire, la méthode SAA et la méthode RAMA avec une configuration initiale obtenue en utilisant la méthode SAA. Le niveau de performance est obtenu en maximisant le C/I minimum de tous les slots. Nous pouvons remarqué que les méthodes SAA et RAMA améliore d'une manière significatif le niveau de performance. De plus, les résultats de la méthodes RAMA ne dépendent pas beaucoup de la configuration initiale.

4.2 Méthodes d'Évitement d'Interférence

Dans un slot croisé, certaines cellules sont actives dans la voie montante tandis que des autres cellules sont actives dans la voie descendante. Une station de base écoutant les mobiles qu'elle dessert dans la voie montante reçoit des interférences de stations de base de la voie descendante. D'autre part, un mobile qui reçoit son signal pendant le slot croisé est interféré par des mobiles actifs dans la voie montante dans les cellules voisines.

Prenons le cas où un mobile de la voie descendante est très proche d'un mobile de la voie montante. Comme le second mobile est loin de sa station de base, sa puissance de transmission doit être élevée. De plus, la distance entre les deux mobiles est petite, ce qui implique une puissance d'interférence très élevée introduite par le second mobile au signal reçu par le premier. De même, le premier mobile est loin de sa station de base et la puissance transmise par la station de base à ce mobile est assez élevée. Par conséquent, l'interférence introduite par cette station de base au signal reçue par la seconde station de base est encore élevée. Par suite, la qualité de service est dégradée

dans les deux cellules et surtout dans la cellule de la voie descendante à cause de la faible distance entre les deux mobiles.

Maintenant, supposons qu'un mobile est accepté dans un slot croisé et qu'il est très loin de la station de base qui le dessert (mobile mauvais). Même si la qualité de service est conservée lors de l'allocation du slot à ce mobile, sa présence interdit les autres mobiles d'être desservis pendant ce slot. Par suite, l'effet de la présence d'un mobile mauvais pendant un slot croisé ne dégrade pas seulement la qualité de service pendant ce slot mais elle diminue également la capacité de ce slot. D'autre part, l'effet de ce mobile pendant un slot non croisé est beaucoup moins fort puisque la distance qui sépare les mobiles d'une cellule des stations de base voisines est assez élevée, d'où la nécessité de trouver des méthodes qui permettent d'identifier ce type de mobiles et de leur interdire d'être actifs pendant les slots croisés. L'estimation des gains de parcours entre les mobiles est très difficile ; pour cela, les méthodes proposées pour se prémunir contre les fortes interférences sont basées sur les gains de parcours entre le mobile et les stations de base.

Dans la littérature, on trouve plusieurs méthodes qui permettent de se prémunir contre une forte interférence dans les slots croisés [WC01][Lin01]. Mais, ces méthodes limitent trop la flexibilité du mode TDD parce que ce sont des méthodes d'évitements statiques; tous les mobiles et tous les cellules sont quasiment traités de la même façon pour tous les distributions des interférences. Pour résoudre ce problème, nous proposons deux méthodes. Dans la première méthode, on définit pour chaque mobile un ensemble de cellules interdites. Ces cellules correspondent aux stations de base avec lesquelles le mobile a un gain de parcours (respectivement un gain de parcours normalisé) plus grand qu'un certain seuil. Le mobile est interdit de transmettre dans la voie montante si au moins une de ses cellules interdites est active dans la voie descendante. En utilisant un seuil de gain de parcours, le nombre et l'identité des cellules varient suivant la position du mobile. Cette caractéristique augmente la flexibilité des méthodes et permet d'éviter les interférences très nuisible. De plus, la méthode basée sur le gain de parcours normalisé prend en compte la puissance de transmission de mobiles, ce qui permet de mieux détecter les interférences nuisibles.

5 Conclusions et Travaux Futurs

Le but de cette thèse est d'exploiter la flexibilité offerte par la combinaison de la technique TDMA et le mode de duplexage TDD dans les systèmes CDMA.

Tout d'abord, le contrôle de puissance a été étudié d'une façon approfondie car il a un impact important sur le comportement des systèmes CDMA. Pour cela, nous avons conçu un modèle générique du contrôle de puissance optimal simplifié qui peut être utilisé pendant les slots montants, descendants et croisés. La simplification du contrôle de puissance permet une convergence plus rapide vers la solution optimale à cause de la taille réduite des matrices. La convergence rapide permet l'utilisation du modèle dans les systèmes opérationnels et l'étude de performance des méthodes d'allocation de slots compliquées. En utilisant cet algorithmes, nous avons pu comparer la performance d'un système pendant un slot croisé et montant. Cette comparaison nous a permis de mieux comprendre le comportement des systèmes pendant les slots croisés. De plus, nous avons utilisé ce modèle pour proposer un algorithme d'élimination des mobiles qui diminue la probabilité d'échec sans une augmentation significatif de probabilité de blocage. D'autre part, un algorithme de contrôle de puissance qui prend en compte la limite inférieure de puissance de transmission a été proposé. Cet algorithme converge vers la solution optimale lorsqu'elle existe. Ces modèles centralisés peuvent être facilement généralisés pour prendre en compte les systèmes avec des différentes services. De plus, un algorithme décentralisé peut être conçu pour la voie montante en se basant sur ce modèle puisque dans cette voie on utilise une boucle ouverte de contrôle de puissance.

Puisque l'interface radio est en variation permanente, les algorithmes de contrôle de puissance

adaptatifs sont plus adéquats dans les systèmes opérationnels. Les algorithmes adaptatifs distribués souffrent du problème d'oscillation des C/I autour de la valeur imposée puisqu'ils utilisent seulement deux commandes: une pour augmenter la puissance et une autre pour la diminuer. Pour diminuer l'impact de ce problème nous avons proposé d'utiliser une zone de stabilisation au dessus de C/I imposé. Lorsque le C/I est dans cette zone, la puissance de transmission est stabilisé. Cet algorithme permet de diminuer la probabilité d'échec et la puissance de transmission.

Après l'étude du contrôle de puissance, nous avons formulé le problème d'allocation de slots en un problème d'optimisation. Dans ce problème, nous cherchons la configuration de mobiles qui maximise le C/I minimal. Comme ce problème est très complexe, nous avons utilisés des méthodes heuristique et meta-heuristiques basées sur la méthode de recuit simulé. Ces méthodes ont données des résultats satisfaisants comparés aux résultats des méthodes aléatoires. Le seul problème est qu'on ne peut pas les comparer à la méthode optimale. Pour avoir une idée sur la différence de performance entre les méthode proposées et la méthode optimale, on peut utilisé le modèle de contrôle de puissance optimal pour trouver des limites supérieures de la performance. Cette tâche est laissé pour un travail futur. Ces algorithmes ont été évalués dans la voie descendante seulement. Mais, elles peuvent être utilisés dans tous les types de slots.

Finalement, nous avons proposé des méthodes d'évitement d'interférence en utilisant les gains de parcours et les gains de parcours normalisés entre les mobiles et les stations de base voisines comme des indices pour l'interdiction de transmission. Ces méthodes diminuent la probabilité d'avoir des interférences très nuisibles en gardant la flexibilité des méthodes d'allocation avec points de commutations diversifiés.

Durant cette thèse, nous avons remarqué qu'il y a un manque d'étude pour l'optimisation d'allocation de slots. Les résultats de nos simulations ont montrés que l'allocation aléatoire peut offrir des bonnes performances dans certains cas. Nous avons proposés plusieurs méthodes qui offrent des meilleurs performances, mais nous ne pouvons pas savoir si ces méthodes donnent des performances assez proches de la solution optimale. Pour cela, il sera intéressant de trouver des méthodes qui donnent des bonnes approximations de la solution optimale. Ces méthodes peuvent être utilisées comme des références pour les méthodes d'allocation de slots.

Les nouvelles services des réseaux mobiles nécessitent une grande flexibilité de l'interface radio. Pour pouvoir assurer cette flexibilité, plusieurs systèmes mobiles peuvent être combinés. Pour cela, il faut développer des couche de contrôle capable d'assurer le meilleur niveau de C/I en se basant sur les interfaces existant et les contraintes introduites par les canaux radios. La méthode meta-heuristique de reallocation peut être adaptée pour prendre en compte plusieurs interfaces radios. De plus, le contrôle de puissance optimal et simplifié peut être généralisé pour tous les systèmes limités par l'interférence.

Abstract

The design of efficient radio resource management procedures has become a crucial need with the increased request for wireless data services. Moreover, heterogeneous quality of service requirements in new wireless networks create new challenges for radio resource management procedures.

In systems using the Code Division Multiple Access (CDMA) technique, all users share the same bandwidth. Therefore, the most important procedure to increase the capacity and ameliorate the quality of service level is the interference management. In the pure CDMA technique, power control is a widely used procedure for decreasing the interference and upholding required signal quality level. In addition to power control, the combination of Time Division Multiple Access (TDMA) and Time Division Duplex (TDD) techniques with CDMA provides a new degree of flexibility in managing the interference using slot allocation techniques. However, exploiting the flexibility of the TDD mode induces new challenges to mitigate such as pernicious mobile-to-mobile interference.

In this thesis, we exploit the flexibility of TDMA-CDMA/TDD systems and the characteristics of the CDMA technique. We propose power control algorithms combined with slot allocation techniques in order to provide required quality of service levels for users. First, we develop a simple generic optimum power control algorithm and we propose different schemes using this algorithm. The developed model can be applied to uplink, downlink and crossed slots to evaluate the system performance and can be used to design efficient distributed algorithms. Moreover, we propose simple modifications to the standardized closed loop power control of the UMTS (Universal Mobile Telecommunications system). The proposed modifications lead to a significant increase in system performance without increasing system complexity and signaling traffic.

We also propose heuristic and meta-heuristic methods combining the optimum power control and slot allocation techniques to find the upper bound of system performance in TDMA-CDMA/TDD systems. These methods can be adapted to real systems in order to reallocate radio resource units when the outage probability falls below a given threshold.

Finally, we investigate flexible channel allocation techniques to avoid high interference that can appear in systems supporting heterogeneous services and asymmetric traffic between uplink and downlink (i.e. mobile-to-mobile interference).

Chapter 1

Introduction

The exciting pace of wireless telecommunications system evolution has characterized the last few years. The fast evolution is the result of the huge success of digital mobile systems and the increasing demands of mobile users for Internet oriented applications. Thereby, operators tend to merge packet-switched oriented services prevalent on Internet and wireless telecommunications systems to fulfill the vision of: "*anyone, anytime and anywhere*" [Moh98]. These trends have been taken into account while planning third generation cellular systems.

The main objective of third generation cellular systems is to provide the same services now available in the fixed network (such as WWW-browsing, electronic mail, file transfer, audio and video broadcasts). These services impose different Quality of Service (QoS) requirements, such as high data rate, low delay and low error rate; for instance, interactive real-time services (e.g. telephony service) are more sensitive to the maximum delay than background services (e.g. E-mail). However, background services cannot tolerate errors, which can be tolerated by other services like video sessions and some interactive real time services. These differences in QoS requirements must be handled by third generation cellular systems.

Moreover, scarce resource units in the radio interface (e.g. bandwidth, time slot, codes) must be used efficiently to maximize the benefit of operators and to satisfy the majority of users. Therefore, efficient Radio Resource Management (RRM) techniques are crucial procedures in wireless telecommunications systems.

Every wireless system is characterized by a radio environment, geographical mobile distribution and the types of services offered to users; therefore, a specific RRM technique is designed for each type of wireless systems. Moreover, the asymmetry between uplink and downlink traffic of multimedia services and the fluctuations in their characteristics impose additional constraints. These constraints induce new challenges to RRM techniques. Nevertheless, the combination of the Time Division Duplex (TDD) mode and the Time Division Multiple Access (TDMA) technique provides high flexibility to RRM procedures. This flexibility can alleviate problems imposed by the nature of multimedia services and radio environment characteristics.

In this thesis, power control and slot allocation techniques are studied in micro- and small macro-cell environments. Our work can be divided into four RRM research fields: optimum power control algorithms, adaptive power control algorithms, optimum slot allocation techniques and interference avoidance methods. A simplified generic optimum power control algorithm is developed for uplink, downlink and crossed slots. The performance of this algorithm gives an upper bound for the performance of power control algorithms that can be implemented in real systems. Moreover, an iterative power control procedure is proposed as an evolution of existing techniques in standardization bodies. In order to optimize the use of radio resource units in the case of asymmetric

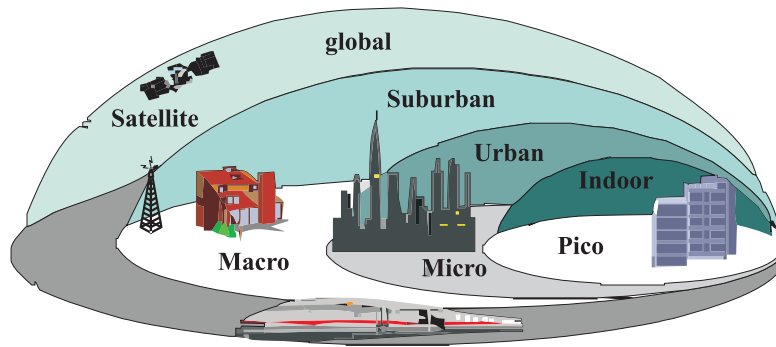


Figure 1.1: UMTS coverage: from indoor to global environment and from stationary users to high speed users

services, the flexibility of the TDMA component is exploited and some interference avoidance techniques are developed and studied. Furthermore, several heuristic and meta-heuristic slot allocation techniques combined with the optimum power control algorithm are proposed and compared to the optimal slot allocation when possible and to a random slot allocation.

1.1 Universal Mobile Telecommunications System

The main advantages of second-generation mobile systems (e.g. Global System for Mobile communication (GSM)) over their analog predecessors are higher capacity and lower battery consumption. However, the second-generation has retained the circuit-switched legacy of analog network, which is designed to carry voice traffic [Oli99]. Moreover, data rates in GSM were limited (e.g. 14.4 Kbps for voice traffic). Presently, the capabilities of second-generation systems is extended by adding some multimedia capabilities, such as the support for high bit rates and the introduction of packet data/IP access [DGNS98]. These improvements have been introduced by new technologies such as HSCSD (High Speed Circuit Switched Data), GPRS (General Packet Radio Service) or EDGE (Enhanced Data Rates for GSM Evolution) and allowed the increase of data rates up to 384 Kbps [LGT99].

In order to create a unified telecommunications system with multimedia capabilities, the International Telecommunication Union (ITU) has defined a framework for third generation telecommunications systems, called IMT-2000 (International Mobile Telecommunications-2000). Within the IMT-2000 framework, the Universal Mobile Telecommunications System (UMTS) has been developed and standardized by the Third Generation Partnership Project (3GPP).

1.1.1 Major Features of UMTS

One of UMTS objectives is to provide a global coverage for all types of users (figure 1.1); therefore, RRM procedures and radio access techniques are developed to cover users in indoor, outdoor, urban and rural environments with mobility ranging from pedestrian up to vehicular with very high speed.

Moreover, UMTS is intended to offer high quality multimedia services. These types of services require high data rates; therefore, the radio interface of UMTS is intended to allow up to 10.2 Mbps data rates [UMT04] in indoors and micro-cells. Furthermore, some multimedia services are not very sensitive to delay, and thus a packet-switched legacy can optimize the use of scarce radio resource units. This approach is considered by UMTS architecture (e.g. an all-IP architecture is proposed in Release 5 and 6 of 3GPP specifications). UMTS architecture allows also users to

Table 1.1: UMTS service classes

Traffic Class	Conversational	Streaming	Interactive	Background
Characteristics	Preserve time relation (variation) between information entities of the stream Conversational pattern (stringent and low delay)	Preserve time relation (variation) between information entities of the stream	Request/Response pattern Preserve payload content	Destination is not expecting the data within a certain time Preserve payload content
Mode	Circuit	Circuit, Packet	Packet	Packet
Type of asymmetry	Symmetric	Highly asymmetric	Asymmetric	Highly asymmetric
Sensitivity to errors	Slightly sensitive	Sensitive	Very sensitive	The most sensitive
Sensitivity to delay	The most sensitive	Very sensitive	sensitive	The least sensitive
Example	Voice	Streaming audio and video	Web-browsing	SMS, background download of emails

establish and manage several radio connections (or radio bearers) at the same time. For instance, a mobile user can, at the same time, download a file using ftp service and talk with another user via video teleconference.

The different types of UMTS services are grouped into four UMTS service classes according to their characteristics: conversational, streaming, interactive and background. This classification leads to an efficient management of radio resource units. The different classes take into account the restrictions and the limitations of the radio interface [TS204]. The main distinguishable factors among these classes is the sensitivity to delay, sensitivity to errors and asymmetry between uplink and downlink traffics (table 1.1).

The conversational class is the most sensitive class to delay, because it includes real-time services; the conversational nature of this class and the time relation between information entities of the stream must be preserved and thus, the delay must be low. Furthermore, the data processing at UMTS radio protocol stack should be as fast as possible. The most well known service of this class is the basic telephony service. Moreover, other multimedia and IP-based services such as voice over IP and video conferencing tools are also included in the conversational class. The maximum supported delay depends on the human perception of audio and video conversation. Besides, this service class is the least error sensitive class.

Another real-time service class is the streaming class. The QoS requirements of this class are also related to the human perception, since the destination of this class is always a human. In the streaming class, the time relation between information entities of the stream must be preserved to conserve the quality of the audio or the video. Therefore, a buffering process is used at the receiver side. Moreover, the streaming class requires sufficiently low bit-error-rate levels in order to offer satisfying QoS levels to users.

The interactive class includes application with a request-response pattern such as web-browsing. In this type of service, the user expects a response as fast as possible. Thus, this type of services is sensitive to overall round trip delay, which depends on the bit rate and the error rate.

Finally, users requesting an application of the background class, such as SMS or E-mail, do not expect data within a specified time. Thus, it is the least sensitive class to delay. However, this class is very sensitive to error rate.

In the radio interface, the delay for non-real time services can be measured by the number of retransmission for the same frame. The retransmission is due to error rates in frames. Moreover, the delay in real-time services is mainly due to the routing delay in the wired network. However, these services impose a bit error rate level. If this rate is not satisfied, the frame in question is dropped. As we will see in section 2.4.2, bit error and block error rates are increasing function of the CIR. Therefore, the QoS levels of all service classes in the radio interface can be evaluated using the CIR.

Another important characteristic of UMTS services is the asymmetry between uplink and downlink traffics. The services of the conversational class are typically symmetric due to the conversational nature of this class. Unlike the conversational class, other service classes require asymmetric traffic, with very high downlink to uplink load ratio; in some services, only signaling and request traffics are transmitted in uplink (e.g. Streaming services) (table 1.1). Obviously, spectrum efficiency is very sensitive to the asymmetry between the two link directions. Therefore, a fixed symmetric allocation for uplink and downlink bandwidths (e.g. UMTS FDD mode) may lead to a saturation of the loaded link whereas the second link is almost unused. Hence, systems that offer higher flexibility in resource distribution between uplink and downlink are more suited for asymmetric services (e.g. UMTS TDD mode). For this reason, TDD mode characteristics have been a hot subject in the last few years.

1.1.2 UMTS Network

UMTS network is divided into three interacting domains with standardized interfaces. The standardized interfaces facilitate network maintenance and allow operators to have different suppliers. The three interacting domains are: User Equipment (UE), UMTS Terrestrial Radio Access Network (UTRAN) and Core Network (CN) as depicted in figure 1.2 [HT00][LWN02]. UTRAN provides air interface access procedures for UE. CN insures information routing and switching between different UTRANs and between UTRAN and other telecommunications and service networks (GSM, fixed network, Internet network, Intelligent Network, etc.). CN also includes databases and network management functions. UEs and UTRAN are connected via the Uu interface, while UTRAN and CN are connected via the Iu interface. In this dissertation, only UTRAN and the Uu interface are investigated.

UTRAN is composed of several Radio Network Sub-systems (RNS) which can be interconnected via the Iur interface. This interconnection allows CN independent procedures between different RNS, such as handover. Therefore, CN is transparent for radio access technology-specific functions [HKK+00]. Each RNS comprises only one Radio Network Controller (RNC) and one or more base stations, which are referred as Node Bs.

A node B performs functions relevant to physical layer processing, such as spreading and modulation, coding and interleaving, rate adaptation, physical measurements and error handling. This network entity also performs some basic radio resource management operations such as micro-diversity/softer handover or closed-loop power control. Each Node B can serve one cell or more and may support either the TDD mode or the FDD mode, or both modes simultaneously.

The RNC controls slot allocation, call admission control, power control settings, hard handover,

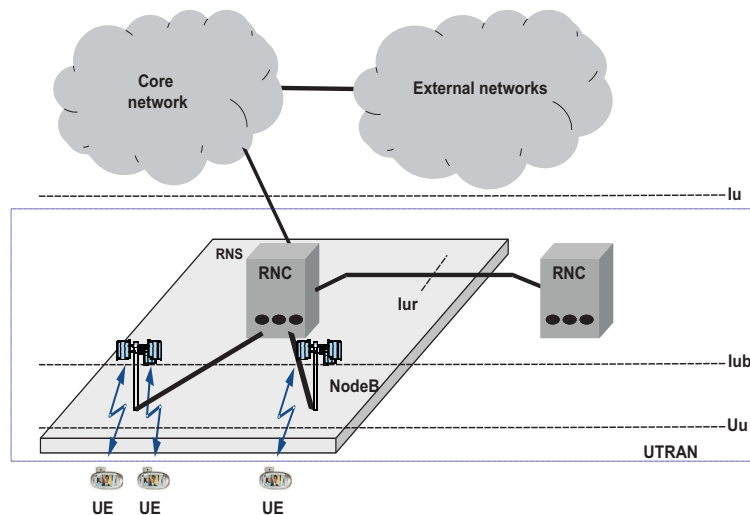


Figure 1.2: UMTS architecture

macro-diversity/soft-handover, ciphering, broadcast signaling, open-loop power control, etc. Node Bs of a given RNS are connected to the corresponding RNC via the Iub interface.

UTRAN is designed to support both FDD and TDD modes on the radio interface. Both modes use the same network architecture and the same protocols. Only the physical layer and the air interface Uu are specified separately.

1.1.3 Radio Interface Protocol Architecture

The radio interface protocol stack includes three layers as depicted in figure 1.3 [TS202h]: the physical layer (layer 1), the data link layer (layer 2) and the network layer (layer 3).

Physical Layer

All physical layer procedures are handled by Node Bs. The physical layer [TS202f][TS202g] offers services to the above MAC layer via radio transport channels, and controls the transfer of physical channels over the radio interface. The physical unit used in the air interface is a 10 ms frame. The period of a transport channel is a multiple of the basic radio frame period and is called Transmission Time Interval (TTI), where $TTI \in \{10, 20, 40, 80\}$ ms. Small values of TTI are suited for real time services such as voice in order to reduce the maximum delay.

Data Link Layer

The data link layer is split into four sub-layers: Radio Link Control (RLC), Medium Access Control (MAC), Packet Data Convergence Protocol (PDCP) and Broadcast/Multicast Control (BMC).

Mac Sub-layer: The MAC sub-layer [TS202a] is responsible for mapping logical channels onto appropriate transport channels. Logical channels are classified into control and traffic channels. The logical control channels transport Control-plane (C-plane) information, whereas the logical traffic channels transport User-plane (U-plane) information. One of MAC functionalities is priority handling between different data flows that share the same physical channel. The priority handling

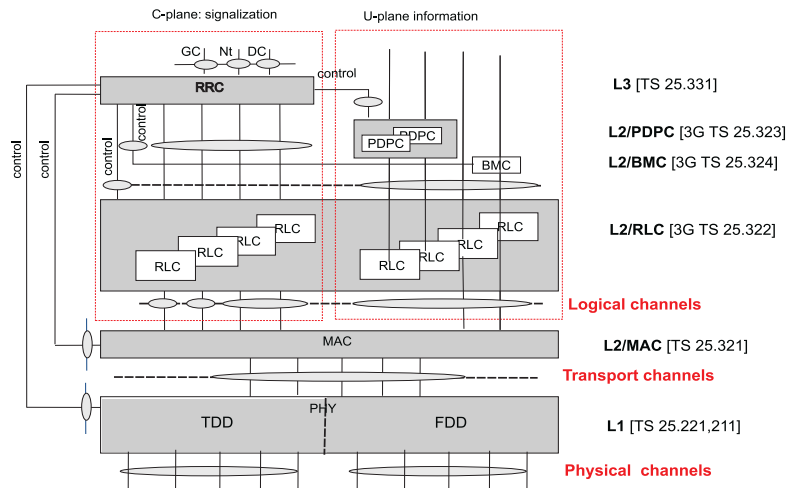


Figure 1.3: Radio interface protocol architecture

procedure is based on physical constraints, which are communicated via physical measurements and the QoS requirement fixed by higher layers. Another functionality of the MAC layer is the multiplexing and the demultiplexing of logical channels into and from the transport channels delivered to and from the physical layer.

RLC Sub-layer: The RLC sub-layer [TS202b] provides segmentation/reassembly and retransmission services for both user and control data. The radio resource control layer configures RLC instances in one of three modes: transparent mode, unacknowledged mode and acknowledged mode. In the transparent mode, no protocol overhead is added to higher layer data. In the unacknowledged mode, retransmission protocols are not used and error free data delivery is not guaranteed. Finally, the Automatic Repeat reQuest (ARQ) mechanism is used in the acknowledged mode in order to decrease the error rate. For all RLC modes, the physical layer estimates the Cyclic Redundancy Check (CRC) error detection and the result CRC is delivered to the RLC together with actual data [LWN02].

PDPC Sub-layer: The PDPC sub-layer exists only in the U-plane. The main function of this sub-layer [TS202c] is the compression of redundant protocol control information (e.g. TCP/IP and RTP/UDP/IP headers) in the transmission entity and the decompression in the receiving entity. Header compression decreases the header load and thus allows utilizing scarce radio resources more efficiently when transmitting IP packets over the radio interface. PDPC compression is possible because few TCP/IP header fields changing from one IP packet to another and the rest of header fields remain more or less the same.

BMC Sub-layer: The BMC sub-layer [TS202d] controls cell broadcast center messages over the radio interface and handles only U-plane information.

Network Layer

The network layer only contains the Radio Resource Control (RRC) layer. The RRC layer [TS202e] is the "head" layer in the UTRAN stack and controls all other layers. The main function of the

RRC layer is performing RRM procedures, which includes slot allocation and release, and the continuous control of QoS levels. Moreover, the RRC layer handles the control plan signaling of layer 3 between UTRAN and UEs. RRC signaling protocol is used to establish, reconfigure and release radio bearers. Furthermore, UE mobility is handled by an RRC protocol. The latter is used for setting up and controlling UE measurement reporting criteria (e.g. block or bit error rates, round trip time, etc.). These measurements allow the RRC layer to control the QoS levels of all links. Paging, ciphering control, initial cell selection and reselection, and open-loop power control are also part of the RRC connection management procedures. Moreover, the RRC layer controls layer 1 and layer 2 protocol entities. The RRC layer involves also some specific functionality for the TDD mode such as Dynamic Channel Allocation (DCA), handling of the outer-loop power control, and timing advance control.

1.2 UTRA TDD

In January 1998, European Telecommunications Standards Institute-Special Mobile Group (ETSI-SMG2), has agreed on the UMTS Terrestrial Radio Access (UTRA) system for third generation mobile radio systems with a dual mode scheme [SMG98]. Thereby, UMTS modes include UTRA FDD, which is characterized by a Frequency Division Duplex (FDD) mode [DBK⁺98], and UTRA TDD, which is characterized by a Time Division Duplex (TDD) mode [Pov97][PN98][Lem00][HKK⁺00][PHT97][ENS97][FJ02]. In order to move toward a compatible global third generation standard, the 3GPP body has tried to merge the European UTRA proposal with other proposals. Thus, two proposals were differentiated within the TDD mode: TDD High Chip Rate (HCR) mode with 3.84 Mcps (like the FDD mode) and TDD Low Chip Rate (LCR) mode with 1.28 Mcps. In 3GPP recommendations [TS202g], the physical layers of TDD LCR and TDD HCR modes are presented. Each proposal has a specific physical layer (i.e. chip rate, bandwidth, frame structure and the presence of an accurate synchronization scheme in the TDD LCR mode). Nevertheless, both proposals share the same higher layers (Layer 2 and 3). As it was agreed in the SMG2 group, operation should be possible within 2×5 MHz of allocated spectrum in UTRA FDD, 5 MHz in UTRA TDD HCR and 1.6 MHz in UTRA TDD LCR. The FDD mode uses a pure Wideband Code Division Multiple Access (WCDMA) technique in paired bands with equal spectrum allocated for uplink and downlink. The TDD HCR mode uses a hybrid Time Division Multiple Access-Code Division Multiple Access (TDMA-CDMA) technique and the TDD LCR uses a synchronous TDMA-CDMA technique in the unpaired band with a single bandwidth for the two link directions (figure 1.4). The UTRA FDD and the UTRA TDD HCR modes have been harmonized with respect to the basic physical parameters such as carrier spacing, chip rate, and frame length. Moreover, all modes use the same higher layer stack and the interworking with GSM is insured. Thereby, FDD/TDD dual mode operation is simplified. This simplification leads to the development of low cost mobiles [HKK⁺00].

UTRA FDD and UTRA TDD HCR are used in a complementary way to optimize the use of scarce radio resources; the FDD mode is deployed in macro- and micro-cell environments with data-rates up to 384 Kbps and high mobility; UTRA TDD HCR is used in micro- and pico-cell environments for licensed and unlicensed cordless applications and it supports data rates up to 2 Mbps. In addition, UTRA TDD HCR presents a flexibility in the distribution of radio resource units between uplink and downlink; this distribution is updated dynamically depending on traffic load. Therefore, UTRA TDD HCR is particularly well suited for environments with high traffic density and indoor coverage, where applications require high data rates and tend to create highly asymmetric traffic (e.g. Internet access). UTRA TDD LCR is designed to address all size of deploy-

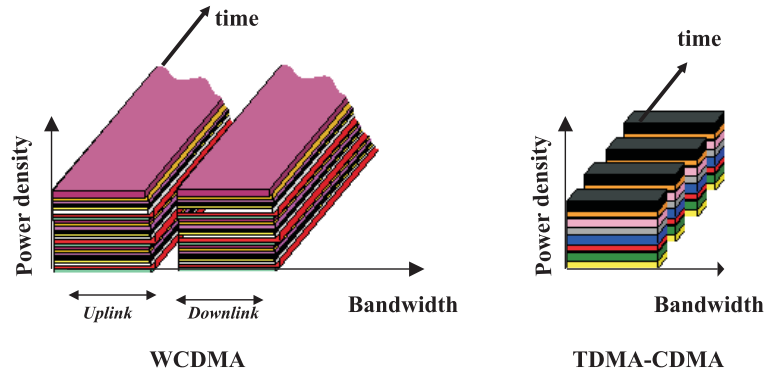


Figure 1.4: Resource distribution in FDD mode (left) and in TDD mode (right)

ment environments; from macro rural to densely populated urban areas and indoor applications, from stationary to high mobility users [AG02].

Unlike the FDD mode where soft- and softer-handover are implemented, only hard-handover is used in the TDD mode [HT00]. The soft-handover is used in WCDMA to mitigate cell-breathing¹. However, cell-breathing is not a major problem in the TDD mode due to joint detection techniques. The use of soft-handover requires high coordination between two base stations serving the same mobile in order to share the same slot or the mobile has to transmit (or receive) twice depending on the different allocation in cells. Moreover, the reception of the same signal from more than one transmitter increases the complexity of joint detection techniques and thus may increase intracell-interference. In other words, soft-handover will not be used in the TDD mode due to the high cost in terms of complexity without an important increase in QoS level.

The main parameters of UTRA are summarized in table 1.2. In this thesis, only UTRA TDD HCR is studied in details. In order to simplify the notation, we use UTRA TDD instead of UTRA TDD HCR in the following. The UTRA TDD interface is designed to cover "hot spots" such as airport, hotels and office buildings, which are characterized by high traffic load and asymmetric services. This interface is not intended to provide continuous coverage. Therefore, the UTRA network (UTRAN) is composed of a global UTRA FDD system with islands of UTRA TDD systems as depicted in figure 1.5. Hence, the continuity between different UTRA TDD systems is maintained by an UTRA FDD system. Thereby, a system with limited number of cells can be a good representation of TDD systems.

1.2.1 Physical Layer

UTRA TDD is based on a combination of time and code division multiple access techniques. The presence of TDMA frame structure is suited for TDD operations, while CDMA guarantees high system capacity.

Frame Structure

A TDD frame has a duration of 10 ms and is composed of 15 slots. At least one slot is reserved for broadcast in downlink and one slot is reserved to random access in uplink. Remaining slots can be allocated either for uplink or downlink in a cell. The boundaries between uplink and downlink slots

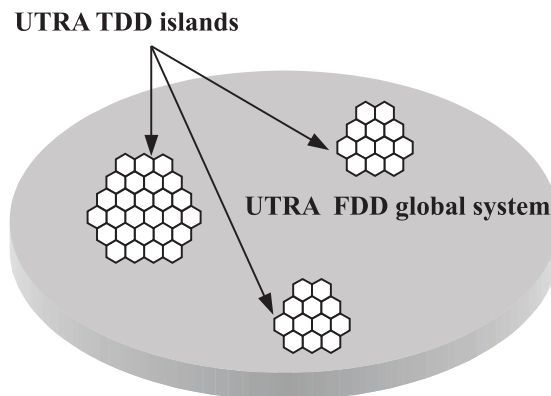
¹In WCDMA, cell coverage is reduced as the number of users increases due to the increase in intra-cell interference. This phenomena is called cell-breathing

Table 1.2: Main parameters of UTRA

	UTRA FDD	UTRA TDD HCR	UTRA TDD LCR
Multiple access	WCDMA	TD-CDMA	Synchronous TD-CDMA
Bandwidth	2×5 MHz	5 MHz	1.6 MHz
Frame length	10 ms		
Pulse shaping	Root raised cosine, roll-off = 0.22		
Spreading factor	DL: 2^n , $n = 2, 3, \dots, 9$	DL: 2^n , $n = 0$ or 4	
	UL: 2^n , $n = 2, 3, \dots, 8$	UL: 2^n , $n = 0, 1, \dots, 4$	
Multiple rate	Multicode and variable spreading	Multislot, multicode and variable spreading	
Duplex mode	FDD	TDD	
Joint detection	No	Yes	
Handover	Soft- and softer-handover	Hard-handover	
Modulation	QPSK		QPSK/8PSK
Chip rate	3.84 Mcps		1.28 Mcps
Frame structure	A 10 ms frame of 15 slots		Two 5 ms sub-frame of 7 slots each

in a cell are called switching points (figure 1.6). Moreover, the same slot may be used for uplink in some cells and for downlink in other cells. In this case, the slot is called *crossed slot*.

The maximum number of allocated codes during one slot is fixed to 16 in order to maintain the orthogonality between spreading codes. Each code is associated to one burst. A burst is subdivided into two data fields, one midamble field and a guard period field (figure 1.7). The guard period is used to cope with timing inaccuracies, power ramping and delay spread. Furthermore, the guard period mitigates propagation delay problem if no timing advance mechanism is used [HKK⁺00]. The midamble field is used to transmit training sequences, which are the key to estimate channel impulse responses. Data fields contain the data bits after modulation, multiplexing, interleaving, coding and spreading operations.

**Figure 1.5:** UTRA TDD islands in the global UTRA FDD system

cope with a limited number of codes. The number of codes that can be used simultaneously in one slot depends on channel characteristics and the length of the used midamble. Hence, the maximum number of allowed parallel codes must be strictly smaller than 16.

1.2.2 Benefits

Next generation mobile systems will be dominated by multimedia services. The majority of these services require low data rate in uplink and very high data rate in downlink. In this case, the paired spectrum of the FDD mode causes the saturation of the downlink while the uplink spectrum is almost unused. On the contrary, the variety of switching point configurations inherited from the TDMA technique allows flexible resource management in the TDD mode. This flexibility optimizes the use of the spectrum; in case of asymmetric services, more slots can be allocated for the saturated link direction.

Moreover, the same bandwidth is used for uplink and downlink in the TDD mode and thus, the two link directions of a mobile have the same radio characteristics (geometric pathloss, fading, multipath channel characteristics). This channel reciprocity can be exploited by some procedures to simplify the complexity of mobile equipments, such as: efficient open-loop power control, pre-RAKE diversity methods for reception at mobile, antenna diversity and pre-equalization methods for signal detection [JJ00][ENS97][Pov94][PYCW99][Haa00].

1.2.3 Drawbacks

Despite its benefits, the TDD mode presents some drawbacks. The most pernicious drawback is the presence of mobile-to-mobile and base station-to-base station interferences, which can lead to high outage and blocking probabilities. These interferences appear in crossed slots.

Moreover, the position of the mobile affects the delay between the transmission and the reception. This delay may in some cases be the source of interference between up- and downlink or between different slots. A guard period is reserved in each burst to decrease the probability of these interferences; this guard period must be proportional to the distance between the mobile and the base station. This constraint limits the use of the TDD mode to pico- and micro-cells. However, this problem may be alleviated by an efficient time advance implemented in mobiles as in UTRA TDD LCR systems.

Another drawback of the TDD mode is the need of synchronization between base stations. The synchronization is needed in order to decrease the intercell-interference, which appears due to the characteristics of the scrambling codes.

1.3 Context of the Thesis

A part of this thesis was realized in the framework of PETRUS (Plate-forme d'Evaluation des Technologies Radio pour l'UMTS TDD et ses Services). PETRUS is an RNRT (Réseau National de Recherche en Télécommunications) project that has started in 2001 and was completed in 2003. Five partners collaborated in this project: CEA-LETI, Mitsubishi Electric ITE, Supélec, Bouygues Telecom and GET/ENST Bretagne.

The objectives of the project was the optimization of joint detection and dynamic channel allocation techniques for TDMA-CDMA/TDD systems with asymmetric services. In addition to simulations and analytical demonstrations, a test-bed was designed to emulate the radio interface and to evaluate the performance of joint detection techniques proposed by the project for high data rate streaming services.

Joint detection is a set of specific techniques, which can be used in the TDD mode. Joint detection techniques allow several users to share the same bandwidth using short spreading codes. Therefore, joint detection techniques are very important to reduce intracell-interference. If we consider that mobile i in cell j experiences normally an intracell-interference I_{intra} , this intracell-interference is reduced by a factor β when the joint detection is used. The value of β depends on channel propagation characteristics and the number of mobiles in a slot [AWH02][AWBG02b][AWBG02a][WAH04]. The results of this work has been used to evaluate intracell-interference. Therefore, a platform was designed to emulate radio channels and test the performance of joint detection techniques when high bit rate, delay sensitive services are used.

Joint detection techniques are generally complicated. In order to be implemented in low-cost mobiles, joint detection techniques must be simplified. However, the simplification must not degrade the performance of joint detection techniques. Therefore, the first objective of PETRUS was to study existing techniques and design new techniques that make a compromise between performance and complexity. Moreover, these techniques should be tested to investigate the potential problems that may arise during implementation, such as quantification, synchronization, etc. This investigation aims to overcome the implementation problem, which are not yet studied in the literature.

The second objective of PETRUS was to exploit the flexibility of the TDD mode in managing asymmetric services. The flexibility of the TDD mode, inherited from the combination of the TDD mode and the TDMA technique, allows an efficient use of the spectrum. However, this flexibility induces new types of interference, such as mobile-to-mobile and base station-to-base station interferences. These interferences may drastically reduce the QoS level offered by the radio interface. In order to alleviate this problem, we have developed intelligent Dynamic Channel Allocation (DCA) techniques that take into account the specific characteristics of the TDD mode.

In PETRUS, ENST Bretagne has been responsible for DCA techniques development. First, existing DCA techniques have been introduced and studied. Second, we have designed an optimum power control algorithm. Thereafter, the optimum power control algorithm has been used to compare the performance of DCA techniques [NLBJK02]. Third, the impact of intracell-interference has been investigated using the optimum power control [NLAJ02]. Finally, a system level simulator has been developed and used to compare two new interference avoidance techniques [NL02a]. In all our models, we have used the results of joint detection techniques investigated by other members of the project.

In addition to our contribution in developing DCA techniques, we have designed and implemented a network architecture (i.e. physical architecture and higher layer protocols). This architecture was designed to alleviate control and synchronization problems in the interface between applications, and DSP and FPGA cards [NL03a]. This work is not presented in the following, because it is not in the scope of the thesis.

1.4 Thesis Scope and Outline

The diversified package of services in the fixed network will be present in next generation wireless networks. However, the radio access network is very different from the fixed access network and has more problems to alleviate. The additional problems appear due to the unstable nature of the radio environment and the interaction (i.e. interference) between users. Therefore, the radio resource management will be the bottleneck in network design.

In TDMA-CDMA/TDD systems, a radio resource unit is defined as a combination of a slot, a CDMA code and the specific power corresponding to the latter pair. To some extent, the capacity

of such a system is defined as the number of radio resource units served with an acceptable QoS level. In order to maximize the capacity in term of number of radio resource units, we can use three main RRM procedures: power control, slot allocation and code selection. For a given slot allocation, an intelligent code selection leads to an amelioration in the orthogonality between the codes of the same slot. Therefore, the intracell-interference can be reduced and the capacity is increased. Alternately, an efficient power control increases system capacity by essentially decreasing the intercell-interference. Moreover, the TDMA component of the TDD mode offers a new degree of flexibility in time domain. This flexibility allows the system of avoiding intercell-interference and intracell-interference using slot allocation. It must be noted that RRM procedures involve other procedures such as cell selection, handover and sectorization.

The main objective of this thesis is to exploit the flexibility of the TDD mode. This objective can be divided into two main issues: power control and slot allocation techniques. In the following chapters, we investigate these procedures in order to ameliorate the performance of next generation mobile networks. The document is organized as follows:

In chapter two, we introduce the concept of radio resource management procedures and their utilities. This introduction starts by the presentation of index notations. Thereafter, the interference profile in the TDD mode and the power budget are introduced. These presentations are very important to the comprehension of the developed RRM procedures, especially with the emerged mobile-to-mobile and base station-to-base station interference in the TDD mode. Being the main RRM tool that ameliorate CDMA system performance, power control is introduced. Moreover, the importance of slot allocation techniques is also emphasized in this chapter. In order to evaluate the performance of RRM procedures, we also introduce the performance measures used in this thesis.

In chapter three, we extend the existing optimum power control pattern to take into account intracell-interference reduction by using generic notations. Moreover, a simplified version of the optimum power control is developed. The simplified version can be applied to uplink, downlink and crossed slots. A generic mobile-based stepwise removal algorithm is also proposed to decrease the outage probability. Moreover, we develop a generic constrained power control algorithm that takes into account lower-bound power limitation. This limitation is generally omitted in power control algorithms though it can be very useful in systems where the interference power range is wider than the power control range.

In chapter four, we investigate step-by-step standardized power control algorithms. We study the performance of these algorithms within hostile environments where fast variation are frequent. We propose also an adaptive variant of the standardized algorithm. This variant ameliorates the performance of the step-by-step algorithm using simple modifications.

Chapter five deals with the problem of optimizing the use of radio resource units using a combination of optimum power control and slot allocation techniques. We define the optimization problem as a max-min-max problem with mixed-integer nonlinear constraints. As this problem is an NP-hard problem, we try to find quasi-optimal solutions using heuristic and meta-heuristic methods.

In chapter six, interference avoidance techniques are introduced and two new methods are proposed. These methods are based on the idea of approximating the pathgain between two mobiles by the pathgains between mobiles and base stations.

Through an analysis of the obtained results, we conclude on the interest of the proposed RRM procedures, and we discuss some perspectives opened by the work presented here.

Chapter 2

Radio Resource Management

The main problem in wireless telecommunications system is to satisfy both wireless operators and users. Wireless operators tend to use efficiently existing radio resource units, since they derive more benefits by being capable of providing services to the highest number of mobile or stationary users with a minimum infrastructure cost (number of base stations, number of reserved frequencies, etc.). On the other hand, users require a good QoS level. Some services need high bit rates and others have strict constraints on delay limits and bit error rates. Hence, a diversity of constraints are imposed by different users. In order to alleviate the problem of maximizing operator benefits while guaranteeing a reliable service diversity, efficient radio resource management (RRM) procedures should be used. RRM is a set of procedures that enable the system to offer reliable performance for a user while inducing the minimum interference to other users. Moreover, the interest for greedy multimedia services is expanding rapidly in new wireless systems (UMTS, 802.11x, WiMax). The highly varying user distribution, the extremely high data rate and the high number of different QoS requirements in multimedia services create new challenges for RRM procedures.

RRM procedures in TDMA-CDMA/TDD systems involve the distribution of existing codes, the distribution of free slots between users and the association of minimum powers that allow users to achieve desired QoS levels. In addition to the latter procedures, RRM [Zan97][ASPR+01][JFFP01] includes cell selection, call admission control, handover, etc. Due to interactions between the different procedures, it is suited to combine some of them to increase system performance. Depending on the type of offered services, propagation parameters and equipment limitations, different types of RRM procedures can be used. In this thesis, we only study power control and channel allocation techniques.

In this chapter, radio resource management techniques and their requirements are introduced. Index notations, power budget and interference profile in TDMA-CDMA/TDD systems are presented in section 2.1. In sections 2.2 and 2.3, power control and channel allocation techniques are set out and some of the existing techniques are presented. Performance evaluation metrics are presented in section 2.4. Finally, the chapter is summarized in section 2.5.

2.1 Interference in TDMA-CDMA/TDD Systems

The TDMA-CDMA/TDD system is one of future systems that have several interesting characteristics and techniques dedicated to alleviate the constraints imposed by service and environment diversity. During each slot, several users share the same bandwidth. The radio resource unit is therefore a combination of one slot, one CDMA code and the power associated to this pair. The limited number of CDMA codes and the effect of interference reduce the number of radio resource

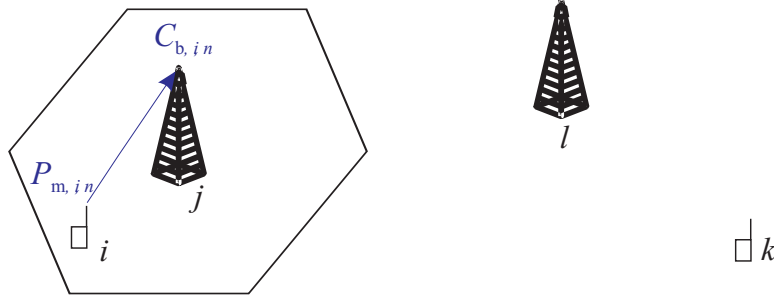


Figure 2.1: Mobile and base station notations

units. In order to use TDD techniques efficiently, it is necessary to analyze the interference profile, which has a significant impact on capacity and QoS levels. Moreover, the TDD mode allows the presence of new interference types that do not exist in other systems: mobile-to-mobile and base station-to-base station interferences. The new types of interference create complex and very influential interference situations.

In this dissertation, we suppose that a mobile is always served by the best-received base station. We assume that there is no special cell selection, such as cell selection based on load-balancing between cells. This assumption may lead to an increase in blocking and outage probability in few cases where some base stations are saturated and other base stations still have free radio resource units. Nevertheless, we take this assumption into account to decrease the impact of cell selection on the studied RRM strategies. We suppose also that joint detection techniques are used [Ver98][KKB96] in order to reduce intracell-interference, especially in the uplink transmission direction where code orthogonality is deteriorated.

In this section, we introduce some essential index notations and we present the power budget in uplink and downlink to facilitate the interference analysis.

2.1.1 Index Notations

In the following, we suppose that indices i and k always refer to mobiles. Index j refers to the base station that serves the considered mobile (i.e. mobile server) while index l refers to a neighboring cell (figure 2.1). We allocate lower index values to base stations and upper index values to mobiles. The set of base station indices is denoted by $\Pi = \{1, \dots, M\}$ whereas the set of mobiles connected to the base station j is denoted by S_j . N represents the total number of mobiles in the system. The number of active mobiles in cell j is denoted by N_j . Therefore, the range of mobile indices in cell j is $\left[M + \sum_{l=1}^{j-1} N_l + 1; M + \sum_{l=1}^j N_l \right]$. During slot n , $N^{(n)}$ mobiles are active in the system and $N_j^{(n)}$ mobiles are active in cell j . Moreover, the set of active mobiles in the system (respectively in cell j) during slot n is $S^{(n)}$ (respectively $S_j^{(n)}$). Therefore, we can write $S^{(n)} = \left\{ S_j^{(n)} \right\}_{j \in \Pi}$. In figure 2.2, mobile and base station indices are given for a simple system of three cells and one slot. It must be noted that $\Pi \cap (\cup_{j \in \Pi} S_j) = \emptyset$, where \emptyset is the empty set. Therefore, no ambiguity between mobile and base station indices can appear.

The useful received power corresponding to mobile i during slot n is denoted by $C_{\tau, i, n}$, where τ is the type of the receiver; the value of τ is either b or m whether the receiver is a base station or a mobile. The transmitted power corresponding to mobile i during slot n is denoted by $P_{\tau, i, n}$ where

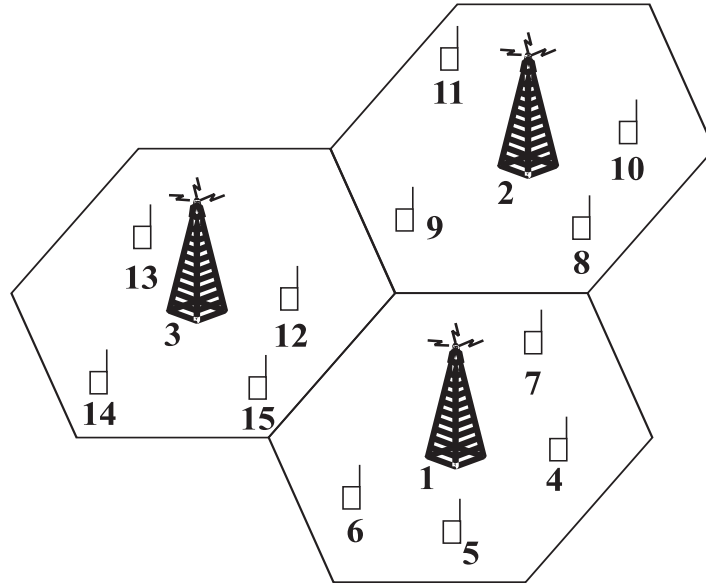


Figure 2.2: An example of mobile and base station indices: $\Pi = \{1, 2, 3\}$, $S_1 = \{4, 5, 6, 7\}$, $S_2 = \{8, 9, 10, 11\}$, $S_3 = \{12, 13, 14, 15\}$

the value of τ is either m or b whether the transmitter is mobile i or the transmitted power is the specific power transmitted by a base station to mobile i . Furthermore, $\mathcal{P}_{T,j,n}$ represents the total power transmitted by base station j during slot n (figure 2.3).

Moreover, if base station j is transmitting during slot n , the corresponding cell is called downlink-cell and if the mobiles of cell j are transmitting during slot n , cell j is called uplink-cell. During crossed slot n , we denote by $\Pi_{d,n}$ and $\Pi_{u,n}$ the sets of downlink-cells and uplink-cells respectively.

2.1.2 Normalized Pathgain

A widely used parameter for interference analysis and RRM procedure investigation is the normalized pathgain $Z_{i,l}$ between mobile i and neighboring base station l . The normalized pathgain $Z_{i,l}$ is the pathgain between mobile i and base station l normalized to the pathgain between mobile i

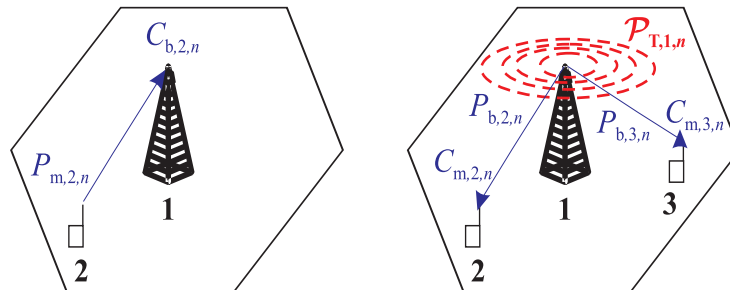


Figure 2.3: Power notations in uplink (left figure) and downlink (right figure) during slot n

and its server j :

$$Z_{i,l} = \frac{G_{i,l}}{G_{i,j}} \quad (2.1)$$

It is easy to see that $Z_{i,j} = 1$ when mobile i is served by base station j . $Z_{i,l}$ is a positive parameter smaller than unity: $Z_{i,l} \in [0, 1]$, because mobiles are served with the best-received base station. The Carrier-to-Interference ratio (CIR) of mobile i is very sensitive to the values of different $Z_{i,l}$; in a downlink-cell j , if $Z_{i,l}$ increases assuming constant transmitted powers, then the ratio of the received interference from base station l to the useful received power decreases (the same reasoning may be used for uplink). The advantage of the normalized pathgain over the simple pathgain is that the former take into account the pathgain between a mobile and its server. In other words, the normalized pathgain gives an idea about the ratio of the interference to the useful power and not only an idea about the interference power.

2.1.3 Power Budget

In downlink-cell j , the useful power $C_{m,i,n}$ received by mobile i during slot n is:

$$C_{m,i,n} = G_{i,j}P_{b,i,n}, \quad (2.2)$$

where $P_{b,i,n}$ is the power transmitted by base station j to mobile i during slot n and $G_{i,j}$ is the pathgain between mobile i and its server j .

Every base station j transmits a total power $\mathcal{P}_{T,j,n}$ during slot n :

$$\mathcal{P}_{T,j,n} = \sum_{i \in S_j^{(n)}} P_{b,i,n}. \quad (2.3)$$

This power is distributed between the mobiles of cell j in such a way that every mobile i receives:

$$C_{m,i,n} = G_{i,j}\alpha_{i,n}\mathcal{P}_{T,j,n}, \quad (2.4)$$

where $\alpha_{i,n}$ is the portion of $\mathcal{P}_{T,j,n}$ dedicated to mobile i during slot n . Thus:

$$\sum_{i \in S_j^{(n)}} \alpha_{i,n} = 1 \quad \forall j \in \Pi. \quad (2.5)$$

In uplink-cell j , the useful power of mobile i received by its server j during slot n is given by:

$$C_{b,i,n} = G_{i,j}P_{m,i,n}, \quad (2.6)$$

where $P_{m,i,n}$ is the power transmitted by mobile i during slot n .

In TDMA-CDMA/TDD systems, uplink and downlink have the same radio propagation characteristics; therefore, pathgains between mobile i and base station l in both transmission directions are the same:

$$G_{i,l} = G_{l,i} \quad (2.7)$$

2.1.4 Interference Profile

In CDMA systems, all transmitters use the same bandwidth; therefore, system capacity is limited by the interference profile and is called *soft capacity*. The soft capacity is the number of satisfied users, which changes depending on the interference profile.

In TDMA-CDMA/TDD systems, uplink and downlink share the same transmission bandwidth, so those two transmission directions can interfere with each other. Hence, five types of interference

Table 2.1: A summary of the interference characteristics in downlink and uplink

	The transmission direction of the interfered entity	Category	Type of slot
Mobile-to-mobile	Downlink	Same-entity	Crossed
Base station-to-mobile	Downlink	Different-entity	Uplink
Base station-to-base station	Uplink	Same-entity	Crossed
Mobile-to-base station	Uplink	Different-entity	Downlink
Intracell-interference	Downlink/uplink	Intracell	All

may appear: intracell, base station-to-mobile, mobile-to-base station, base station-to-base station and mobile-to-mobile interferences. Base station-to-base station and mobile-to-mobile interferences do not exist in WCDMA systems where uplink and downlink are separated in the frequency domain. The five types of interference can be grouped into three categories: intracell-interference, different-entity interference and same-entity interference. Different-entity interference includes base station-to-mobile and mobile-to-base station interferences. Same-entity interference includes base station-to-base station and mobile-to-mobile interferences. The characteristics of interference patterns in uplink and downlink are summarized in table 2.1.

The total interference power experienced by the signal of user i during slot n is given by:

$$I_{\ell,i,n} = I_{\text{intra},\ell,i,n} + I_{\text{inter},\ell,i,n}, \quad (2.8)$$

where $I_{\text{intra},\ell,i,n}$ and $I_{\text{inter},\ell,i,n}$ are respectively the intracell- and total intercell-interference powers experienced by the signal of user i , and ℓ is the link transmission direction of mobile i during slot n ($\ell = d$ for downlink and $\ell = u$ for uplink).

The only type of intercell-interference experienced by a mobile in pure uplink or downlink slots is a different-entity interference. However, the intercell-interference can include two types of interference in crossed slots depending on the type of the studied link direction; for a mobile i in a downlink-cell, the intercell-interference can be written as:

$$I_{\text{inter},d,i,n} = I_{\text{bm},i,n} + I_{\text{mm},i,n}, \quad (2.9)$$

where $I_{\text{bm},i,n}$ is the base station-to-mobile interference and $I_{\text{mm},i,n}$ is the mobile-to-mobile interference. Moreover, all mobiles in uplink-cells experience the same intercell-interference given by:

$$I_{\text{inter},u,i,n} = \mathcal{I}_{\text{mb},j,n} + \mathcal{I}_{\text{bb},j,n}, \quad (2.10)$$

where $\mathcal{I}_{\text{mb},j,n}$ is the mobile-to-base station interference and $\mathcal{I}_{\text{bb},j,n}$ is the base station-to-base station interference.

Intracell-Interference

In the same cell, orthogonal codes are used to separate different channels. Due to the quasi-synchronous transmission in uplink and the effect of multipath, the orthogonality may not be conserved between different channels. By using joint detection techniques, only a residual intracell-interference affects the CIR value. We denote by β_d and β_u the factors of remaining intracell-interference respectively in downlink and in uplink after the joint detection procedure. Generally,

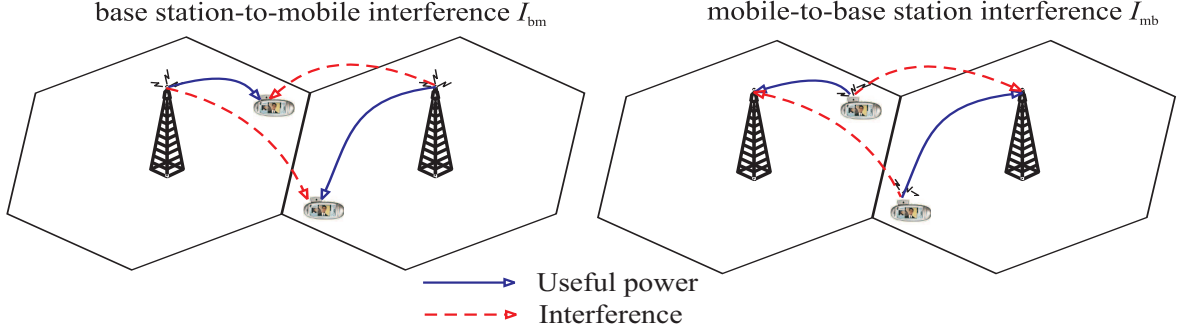


Figure 2.4: The interference received by mobiles from neighboring base stations and the interference received by base stations from neighboring mobiles.

these factors depend on both the interfered and the interfering codes. For simplicity, we suppose that the value of each factor is the same for all mobiles in a given link transmission direction. The values of these factors are taken from the results of the project PETRUS [AWH02].

In downlink-cell j , mobile i experiences intracell-interference $I_{\text{intra,d},i,n}$ during slot n :

$$I_{\text{intra,d},i,n} = \beta_d G_{i,j} \sum_{k \in S_j^{(n)} - \{i\}} P_{b,k,n} \quad (2.11)$$

Using equations (2.3) and (2.5), $I_{\text{intra,d},i,n}$ can be rewritten as:

$$I_{\text{intra,d},i,n} = \beta_d (1 - \alpha_{i,n}) G_{i,j} \mathcal{P}_{T,j,n} \quad (2.12)$$

In uplink-cell j , the useful signal of mobile i received by base station j experiences intracell-interference $I_{\text{intra,u},i,n}$ during slot n :

$$I_{\text{intra,u},i,n} = \beta_u \sum_{k \in S_j^{(n)} - \{i\}} G_{k,j} P_{m,k,n} \quad (2.13)$$

We have studied the impact of the intracell-interference in a technical report for PETRUS project [NLAJ02]. In [NLAJ02], we have noticed that the intracell-interference may dramatically decrease the system capacity. Therefore, it is preferred to consider its contribution in the total interference profile.

Different-Entity Interference

During slot n , some cells may be active in downlink. Mobile i served by one of these cells receives an intercell-interference power $I_{\text{bm},i,n}$ from neighboring base stations of downlink-cells as depicted in the left part of figure 2.4. $I_{\text{bm},i,n}$ is given by the following equation:

$$I_{\text{bm},i,n} = \sum_{l \in \Pi_{d,n} - \{j\}} G_{i,l} \left(\sum_{k \in S_l^{(n)}} P_{b,k,n} \right) \quad (2.14)$$

Using equation (2.3), $I_{\text{bm},i,n}$ can be rewritten as:

$$I_{\text{bm},i,n} = \sum_{l \in \Pi_{d,n} - \{j\}} G_{i,l} \mathcal{P}_{T,l,n}. \quad (2.15)$$

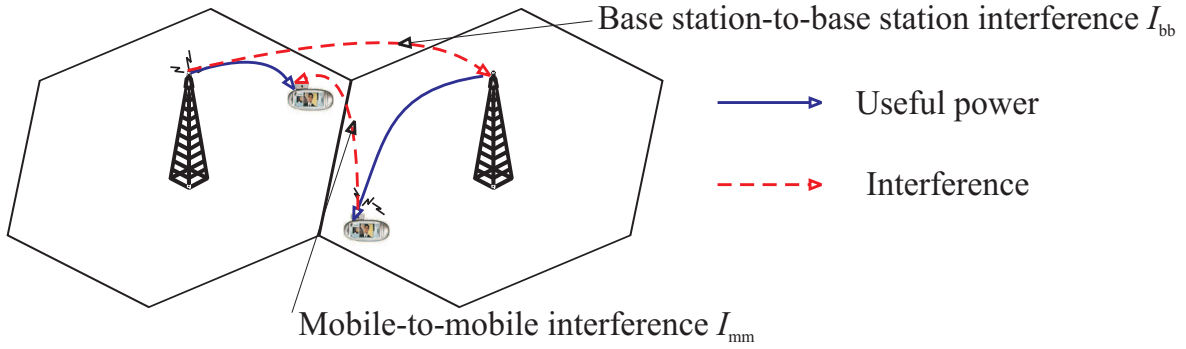


Figure 2.5: The interference received by a mobile from a neighboring mobile and the interference received by a base station from a neighboring base station during a crossed slot.

In uplink-cell j , all mobiles experience the same intercell-interference since they have the same receiver. Thus, the received signal of all active mobiles in uplink-cell j is interfered by the same power $\mathcal{I}_{\text{mb},j,n}$ induced by neighboring mobiles. $\mathcal{I}_{\text{mb},j,n}$ is given by the following equation:

$$\mathcal{I}_{\text{mb},j,n} = \sum_{l \in \Pi_{\text{u},n} - \{j\}} \left(\sum_{k \in S_l^{(n)}} G_{k,j} P_{\text{m},k,n} \right). \quad (2.16)$$

Same-Entity Interference

Due to the TDMA and TDD components, crossed slots may appear. In crossed slots, same-entity interference (i.e. mobile-to-mobile and base station-to-base station interference) occurs as depicted in figure 2.5. Same-entity interference may occur also if either base stations or mobiles are not synchronized or if neighboring operators use adjacent bandwidths. In our study, we consider that all slots are aligned and that neighboring operators do not interfere with each other. Hence, same-entity interference occurs only in crossed slots.

During crossed slot n , active mobile i in downlink-cell j receives interference power $I_{\text{mm},i,n}$ from neighboring mobiles, which are active in uplink. $I_{\text{mm},i,n}$ is given by the following equation:

$$I_{\text{mm},i,n} = \sum_{l \in \Pi_{\text{u},n}} \left(\sum_{k \in S_l^{(n)}} G_{k,i} P_{\text{m},k,n} \right), \quad (2.17)$$

where $G_{k,i}$ is the pathgain between mobiles k and i .

The received signal of active mobile i in uplink-cell j is interfered by neighboring base stations, which are active in downlink during the same crossed slot n . The base station-to-base station interference is the same for all mobiles of cell j and is denoted by $\mathcal{I}_{\text{bb},j,n}$. $\mathcal{I}_{\text{bb},j,n}$ is given by the following equation:

$$\mathcal{I}_{\text{bb},j,n} = \sum_{l \in \Pi_{\text{d},n}} G_{l,j} P_{\text{T},l,n}, \quad (2.18)$$

where $G_{l,j}$ is the pathgain between base stations l and j .

The best way to avoid base station-to-base station interference is by careful planning. Careful planning provides sufficient coupling loss between base stations. Unfortunately, mobile-to-mobile

interference cannot be avoided by network planning because mobile locations cannot be controlled. Furthermore, shadowing and multipath phenomena accentuate the problem of mobile-to-mobile interference. Hence, mobile-to-mobile interference is very difficult to estimate and need high signaling traffic to be communicated to base stations. However, high mobile-to-mobile interference appears when two close mobiles are active in opposite link directions. Generally, these mobiles are at cell borders. Using the latter property, dynamic channel allocation (DCA) and power control can be adapted to alleviate interference between mobiles. Many DCA techniques based on pathgains between mobiles and base stations are used to detect interfering mobiles with high pathgains toward interfered mobiles. Some of existing interference avoidance schemes are presented in chapter six.

2.2 Power Control

Power control is an essential tool used to insure continuous and reliable QoS levels for the maximum number of users in a cellular system. In order to satisfy this condition, power control process tries to allocate just the necessary power to each communication channel. With the necessary power, a communication channel should have an adequate QoS level without inducing extra interference to other channels. This result leads to an increase in system capacity without the degradation of QoS levels.

Moreover, the minimization of transmitted power leads to an increase in battery life. Battery life is very important to mobile telecommunication users, especially with the arrival of power greedy multimedia services; in addition to the transmission power, protocol stack processing and screen display of multimedia services require high amount of power. The high power consumption leads to a high decrease in battery life, which is very annoying for users. Therefore, it is very important to ameliorate the transmitted power management. Another important outcome of the power control is decreasing the electromagnetic radiation. Electromagnetic radiation affect especially mobile users which are very close to radiation sources.

The power control process of all channels must be harmonized (i.e. it is necessary to have some type of synchronization in the power control process) and the power step in iterative algorithms must be chosen very carefully to guarantee sufficient fast convergence. Otherwise, an incoherent channel-by-channel power control may lead to a power increase in all channels until the power reaches its maximum with an unacceptable QoS level. For example, the transmitted power of a user may be increased in order to improve its CIR, leading to lower BER. However, this power control leads to an increase in the interference experienced by other users, in turn increasing their powers. Therefore, the system suffers from a continuous interference increase, which leads to unacceptable CIRs for all users.

Power control algorithms may be classified into centralized or distributed, iterative or non-iterative, constrained or not constrained, synchronous or asynchronous algorithms.

In *synchronous* power control algorithms, all mobiles update their powers at the same time. Synchronous power control is difficult to be implemented, especially in uplink where the power update is controlled by different mobiles. In *asynchronous* power control algorithms, mobiles can update their powers at different moments [HC00].

In *Distributed* power control algorithms, the power level of each mobile is independently determined. Mobile power levels are determined using local information or measurements such as received power, CIR and pathloss toward base stations. Only some parameters are communicated by a central unit to conserve harmonization. In *centralized* power control algorithms however, all power levels are fixed by a central unit. The central unit must know all information concerning the radio interface. Centralized power control algorithms have better performance than distrib-

uted power control algorithms. This is due to the fact that centralized algorithms have better knowledge of the radio interface and allow better harmonization. However, centralized algorithms require high signaling traffic and exact information about all links (i.e. pathloss of all receivers with all transmitters, transmitted powers and the CIRs of all links), which might be very difficult to implement.

Non-iterative power control algorithms compute all link powers simultaneously. Therefore, this type of algorithms is centralized and synchronous. In *iterative* power control algorithms however, the power level is updated step-by-step to reach a specific CIR target. Hence, iterative power control algorithms may be asynchronous or distributed also.

A power control algorithm is called *unconstrained* if there is no upper nor lower limitations on the transmitted powers. In real systems however, transmitted powers are constrained by amplifier limitations. Therefore, *constrained* power control algorithms are generally investigated. Generally, only the maximum power limit is considered.

Interference situations in uplink and downlink are different due to the one-for-many transmission in downlink and the many-for-one transmission in uplink which can be treated as two problems with different approaches. Therefore, some algorithms have been developed especially for a given link direction; in [Kim99], a downlink power control was proposed to CDMA systems. In this algorithm, the signals of all users in a cell are received with the same CIR and a constraint is imposed on the total power transmitted by base stations during the convergence to CIR target. The dimension of the linear system used by the latter algorithm is reduced to the number of base stations rather than the number of mobile stations. The dimension reduction scheme was further generalized to take into consideration uplink, distributed algorithms [MH01][WSW+03], handover and different CIR targets [MH01]. A decentralized iterative version of these algorithms was introduced in [KP00] with convergence analysis.

2.3 Channel Allocation

Channel allocation is the process that distributes available slots over users while conserving an acceptable QoS level. The combination of the TDMA technique with the TDD mode in UTRA TDD provides a new degree of flexibility in time domain. This flexibility can be exploited in order to fairly distribute the interference across all slots and thus to satisfy all users. In this context, channel allocation is needed to mitigate the pernicious impact of interference. Channel allocation techniques are generally grouped into four basic categories [AZ98][Zan97]:

- ◇ Fixed Channel Allocation (FCA) techniques
- ◇ Dynamic Channel Allocation (DCA) techniques
- ◇ Hybrid Channel Allocation (HCA) techniques
- ◇ Random Channel Allocation (RCA) techniques

In a fixed channel allocation technique, cell planning is used to distribute available channels across cells in advance. However, the soft capacities of different slots in a CDMA system are not the same and cannot be estimated in advance. Therefore, the FCA technique may lead to high blocking probability in CDMA systems due to the fixed resource allocation (some slots have high interference profiles while other slots have very low interference profiles). In order to mitigate the poor spectral efficiency of FCA techniques, flexible DCA techniques may be used. In the DCA technique, slot configuration is updated in real time, depending on the interference situation of the

system [HM01]. However, DCA techniques must be used very carefully to avoid system instability and high outage probability. These phenomena can appear due to high interference powers in heavily loaded systems. A cell planning scheme can allocate a minimum fixed number of channels to each cell in order to guarantee the stability of loaded systems. The remaining channels are then allocated to cells using a DCA technique. This combination of FCA and DCA techniques is called hybrid allocation technique [KN96][Kun99]. Another allocation technique is the Random Channel Allocation (RCA) technique which is used mainly in narrowband FDMA systems. The basic idea of the RCA technique is to change channel distribution in a random and quasi-continuous manner to mitigate poor channel conditions (deep fade) in a static allocation.

DCA techniques take into account the interference situation and offer a flexible tool to manage available channels. Therefore, DCA techniques are crucial to an efficient use of the TDMA component in UTRA TDD which is an interference limited system. Moreover, DCA are needed to alleviate the additional interference patterns induced by the TDD mode [AJK99][HKK⁺00].

Dynamic channel allocation in UTRA TDD involves [TS202i]:

- ◊ Resource allocation for cells (slow DCA)
- ◊ Resource allocation for bearer services (fast DCA)

The slow DCA technique is responsible for distributing the available channels to cells depending on the traffic and interference fluctuations. The slow DCA must satisfy the following rules to minimize the interference and to improve system stability:

- ◊ Each slot is either used for uplink or downlink in a given cell. Moreover, a slot may be used for uplink in some cells, while it is used for downlink in other cell.
- ◊ The allocation of slots to cells can be dynamically rearranged in order to accommodate the traffic load in each cell.
- ◊ Slot reallocation uses interference measurements to avoid high interference situations (e.g. the same slot is not allocated to highly interfering cells).

Fast channel allocation refers to the allocation of one or multiple physical channels to one user according to a cell-related preference list derived from the slow DCA scheme. The fast DCA is thus particularly concerned by the multirate services which are achieved by pooling of resource units. This can be done in time domain (i.e. allocating multiple slots during one frame) or in code domain (i.e. allocating multiple codes during one slot). Any combination of the two methods is possible. Moreover, the fast DCA covers also the channel reallocation procedure. Channel reallocation is an important feature that enable the optimization of allocated channels management, because the interference situation is always in change.

The flexibility of the slow DCA technique optimizes the use of radio resource units in a system with different rate of asymmetry between uplink and downlink in different cells. According to the position of the switching point, slow DCA techniques may be divided into two categories: the common switching point technique and the diversified switching point technique. In the common switching point technique, all cells have the same slot configuration as depicted in figure 2.6. Slot configuration may be adjusted dynamically depending on different criteria such as the rate of uplink to downlink codes allocated in the system, the rate of blocking or outage probabilities between the two link directions, etc. This slot allocation is used to prevent the presence of same-entity interference. However, the common switching point technique does not efficiently exploit the bandwidth when the rate of asymmetry between uplink and downlink is not the same in all cells,

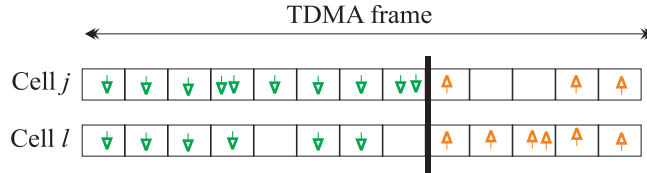


Figure 2.6: Example of slot configuration using the common switching point technique.

which is the most encountered case; therefore, a link direction may be saturated in a cell while the second link direction has free slots. This link saturation may induce high blocking probability.

In order to exploit efficiently the available channels, more flexibility must be given to each cell in adjusting its own switching point. This flexibility can be insured by using the diversified switching point technique. In the diversified switching point technique, each cell has an independent slot configuration as depicted in figure 2.7. This technique allows a full use of the spectrum and thus, maximum capacity may be reached. However, it authorizes the presence of crossed slots, where a set of cells is active in downlink and another set is active in uplink. In crossed slots, mobile-to-mobile and base station-to-base station interferences appear. Mobile-to-mobile interference is very difficult to measure and may induce very high outage probability when two close mobiles are active in opposite link directions during the same slot. Nevertheless, the diversified switching point technique outperforms the common switching point technique when an efficient call admission control is used. This result has been analytically proved by Jeon and Jeong in [JJ00] for simple configurations. Moreover, we have shown by simulation that the diversified switching point gives the best results for some mobile distributions [NL02b][NL04b][NL04a]. Therefore, the diversified switching point technique should be used carefully and must be combined with interference avoidance schemes. Interference avoidance schemes will be presented in chapter six.

When the diversified switching point is used, slot configuration is adjusted to reflect the link asymmetry in each cell. DCA does not statistically fix the configuration of the TDMA frame in order to support the variation of the asymmetry ratio between uplink and downlink. Instead, the distribution of slots to uplink or downlink changes dynamically. In [CYMH97], authors have proposed the Movable Boundary (MB) scheme to dynamically adjust the switching point in each cell of a TDMA/FDMA system. This scheme is also extended to CDMA/TDMA systems. When a new channel is required, the MB scheme sequentially searches the TDMA frame to find an adequate slot that may support the new channel. The uplink and downlink search are made in opposite direction as depicted in figure 2.8. The downlink search proceeds from left to right while the uplink search proceeds from right to left. The search continues until an available slot is allocated or until a slot allocated for the opposite link is encountered. Therefore, only one switching point may appear in each cell. Moreover, the probability that a crossed slot may appear at the beginning or at the end of the frame is less than the probability that a crossed slot may appear in central

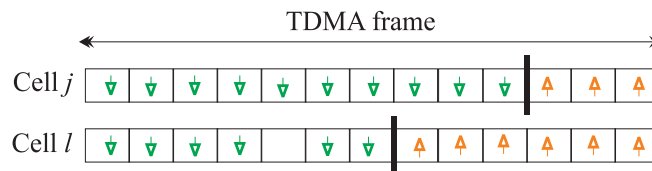


Figure 2.7: Example of slot configuration using the diversified switching point technique

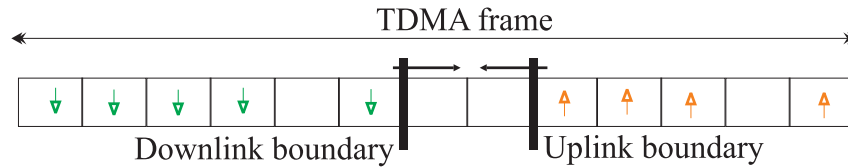


Figure 2.8: Uplink and downlink search for available channel using the movable boundary technique

slots. This property can be exploited to avoid high mobile-to-mobile interference by preventing mobiles that may generate high interference from being active in central slots. Therefore, mobiles that generate this kind of interference should be detected using an interference avoidance scheme [JJ00][WC01][Lin01][NL03b][NL04c]. The improved flexibility of the MB technique decreases drastically the blocking probability and increases the spectral efficiency of UTRA TDD. However, this improvement comes at the expense of allowing mobile-to-mobile and base station-to-base station interferences to appear.

Despite its flexibility, the MB technique does not exploit entirely the flexibility of TDMA/TDD structure. Lindström and Zander have proposed the Soft Switching Point (SSP) scheme in [LZ99] to mitigate the limitation of the MB scheme. In the SSP scheme, the search does not end when a slot used for opposed link direction is encountered. Instead, the search continues until there is no more free slots in the other side. Therefore, multiple switching points may appear and same-entity interferences are more frequent than in the MB scheme (figure 2.9). Despite its flexibility, this scheme needs to be used very carefully to guarantee the stability of the system. Otherwise, this method can lead to the saturation of a link direction while the other link uses partially its allocated slots. Therefore, a mechanism of slot release must be activated to reallocate slots for the uplink and downlink.

2.4 Performance Evaluation

2.4.1 Types of Simulations

In this thesis, we evaluate the proposed schemes using both snapshot simulations and discrete-time simulations.

In snapshot simulations, the system is frozen in time. Therefore, the pathgains of mobiles are considered as constant during each simulation. Snapshot simulation model can be seen as an observation of the system at a random instant. All system measures and parameters are considered as initialization values for radio resource management procedures. Radio resource management procedures are considered to be able to perform with infinitely fast updates such that pathgains

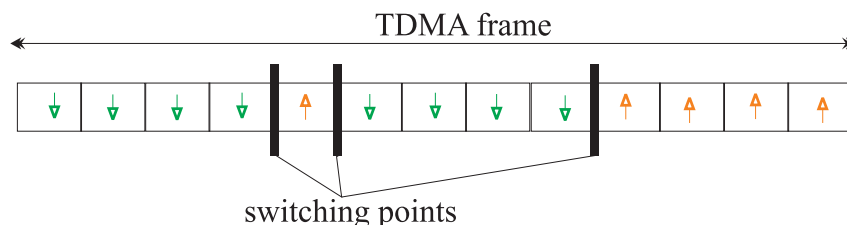


Figure 2.9: Frame configuration with multiple switching points using the SSP technique

are kept constant. Hence, the results of snapshot simulations can be considered as upper-bound of real performance. Snapshot simulations are very useful to study convergence and the impact of some parameters on procedure performances.

Discrete-time simulations are used to assess call admission control impact on procedure performances. In our discrete-time simulations, time separating two mobile arrivals and the duration of a call are generated using an exponential law.

2.4.2 Performance Measures

UMTS system is intended to offer a bunch of services that need different QoS requirements. These different requirements lead to a diversification of performance measures. Moreover, the primary performance measure may not be the same for users and operators. Certainly, users are interested in service quality (i.e. blocking probability, delays, data rates, BERs, etc.). Wireless operators however, tends to increase benefits. In this thesis, we only consider performance measures related to QoS requirements. The basic performance measures are: rate of convergence, carrier to interference ratio, E_b/N_0 , average transmitted power, blocking probability and outage probability.

Rate of Convergence

The rate of convergence is the average time needed to achieve a stable state in a system. This metric is averaged over all mobiles in a given mobile sample and all mobile samples.

E_b/N_0

In most cases, the QoS level can be specified in terms of error rate for all service classes [KH00]. The error rate is generally represented by the Bit Error Rate (BER). Furthermore, the BER is a function of E_b/N_0 . The E_b/N_0 of a mobile i in cell j during slot n , denoted by $\Upsilon_{i,j,n}$, is defined as the ratio of the useful received energy per bit to the sum of the spectral density of the interference power and the the spectral density power of thermal noise.

For static radio channels, E_b/N_0 is a time-constant metric. Therefore, the optimal BER with a QPSK modulation can be computed using E_b/N_0 by the following equation [Hay94]:

$$\text{BER} = \frac{1}{2} \text{erfc} \left(\sqrt{\Upsilon_{i,j,n}} \right), \quad (2.19)$$

where $\text{erfc}(\cdot)$ is the complementary error function.

However, this relation cannot be used when E_b/N_0 varies from a slot to another slot in the same TTI, because the relation between the BER and E_b/N_0 is not linear. Nevertheless, a mapping function between the BER and the geometric mean of E_b/N_0 has been retrieved by Holma in [Hol03]. The geometric mean $\Upsilon_{\text{TTI},i,j}$ is computed over one TTI (e.g. 30 slots for a voice service):

$$\Upsilon_{\text{TTI},i,j} = \sqrt[TTI]{\prod_{n=1}^{TTI} \Upsilon_{i,j,n}} = 10 \left(\frac{10 \log_{10} \prod_{n=1}^{TTI} \Upsilon_{i,j,n}}{10^{TTI}} \right) = 10 \left(\frac{\sum_{n=1}^{TTI} 10 \log_{10}(\Upsilon_{i,j,n})}{10^{TTI}} \right). \quad (2.20)$$

Therefore, the geometric mean is equivalent to an average of logarithmic E_b/N_0 values, i.e. average of E_b/N_0 values in dB:

$$\Upsilon_{\text{TTI},i,j} (\text{dB}) = \frac{\sum_{n=1}^{TTI} \Upsilon_{i,j,n}}{TTI} (\text{dB}). \quad (2.21)$$

Carrier-to-Interference Ratio

The Carrier-to-Interference Ratio (CIR) is a very important metric in the evaluation of QoS levels. The CIR of mobile i in cell j during slot n is given by:

$$\Gamma_{i,j,n} = \frac{C_{\ell,i,n}}{I_{\ell,i,n} + N_0}, \quad (2.22)$$

where $C_{\ell,i,n}$ is the useful received power, $I_{\ell,i,n}$ is the interference power and N_0 is background noise power. All these powers are measured in the radio frequency band, whereas the energy per bit and the spectral density of the interference power and of the thermal noise power are measured in the base band without spreading. Therefore, we have the following relation between E_b/N_0 and CIR:

$$\Upsilon_{i,j,n} = SF \times \Gamma_{i,j,n}, \quad (2.23)$$

where SF is the spreading factor.

The interference power is divided into intracell-interference $I_{\text{intra},\ell,i,n}$ and intercell-interference $I_{\text{inter},\ell,i,n}$ (see section 2.1). Therefore, the CIR can be rewritten as:

$$\Gamma_{i,j,n} = \frac{C_{\ell,i,n}}{I_{\text{intra},\ell,i,n} + I_{\text{inter},\ell,i,n} + N_0}. \quad (2.24)$$

In order to retrieve the relation between E_b/N_0 and the BER, the intracell-interference during slot n is approximated by equation (2.25) in cell j [AW01]:

$$I_{\text{intra},\ell,i,n} = \beta_{\ell} C_{\text{intra},\ell,i,n}, \quad (2.25)$$

where $C_{\text{intra},\ell,i,n}$ is the interference power measured before the despreading process (i.e. at the antenna level). The value of β_{ℓ} varies depending on receiver characteristics and the used techniques. When joint detection is used in a specific radio propagation pattern, the value of β_{ℓ} is 0.1 in downlink and 0.2 in uplink [AWH02].

As we have always a relation between the BER and the CIR, we will use in this thesis the CIR as a performance metric. Moreover, the geometric mean $\Gamma_{\text{TTL},i,j}$ (i.e. $\Upsilon_{\text{TTL},i,j}/SF$) is used to evaluate the system performance in discrete-time simulations (in this type of simulations, E_b/N_0 is not stable).

Averaged Transmitted Power

This metric can represent the average of the total transmitted power of base stations or the average of the specific power for each user.

Blocking Probability

The blocking probability is the ratio of refused codes to the total number of codes that request a connection. A mobile can request a connection that need several codes. The request of a mobile can be refused if the number of free codes in the system is less than the requested number of codes.

Outage Probability

The outage probability is the ratio of low quality codes to the total number of codes in a system. This ratio is averaged over the whole simulation. A mobile is considered with low quality connection if the geometric average of its CIR over a TTI period is less than a given threshold. The average value over a TTI period is used because error correction and retransmission mechanisms are executed using the TTI, which is generally two frames.

Confidence Interval

The confidence interval is a statistical tool that gives an idea about the precision of results. Since the number of users and simulation samples are large, we can use the student distribution to estimate the confidence interval [PW93]. This distribution allows us to find the interval of variation $[X_{\min}, X_{\max}]$ in which a random variable x can be found with a probability α :

$$\Pr(X_{\min} \leq x \leq X_{\max}) = \alpha.$$

Using Student distribution, we can write:

$$\begin{aligned} X_{\min} &= \bar{x} - \sigma t_{\alpha, n-1} \\ &\text{and} \\ X_{\max} &= \bar{x} + \sigma t_{\alpha, n-1}, \end{aligned}$$

where \bar{x} and σ are the mean and the standard deviation of x . $t_{\alpha, n-1}$ is a constant that can be obtained from the student table for n iterations and a probability α . For instance, $t_{95, 120} = 1.98$ is used in this dissertation.

If the confidence interval is wide, two interpretations can be made:

1. the number of simulation is not large enough. In this case, more simulation must be performed
2. the variance of the performance measure is very high due to variation in the system

2.5 Summary

In this chapter, we have presented the majority of notations that will be used in the thesis. Moreover, we have introduced the different types of interference that may appear in a TDMA-CDMA/TDD slot and we have represented their values as a function of powers and channel propagation parameters. Thereafter, we have presented briefly power control procedures and slot allocation techniques. Finally, we have introduced some metrics that will be used to evaluate the RRM procedure performances.

Chapter 3

Centralized Optimum Power Control

Power control is of great importance in reducing cochannel interference and increasing the capacity of mobile telecommunications systems. There are different approaches to the aim of power control (e.g. maximizing the total throughput of the system, minimizing the sum of all powers, CIR-balancing, etc.). For a given set of user geographic distribution and pathgains, an interesting and important approach is to find the power assignment that maximizes the minimum CIR of all users. It has been shown that the solution of this problem can be found if the CIR-balancing algorithm is performed [GVGZ93]. In the following, we call optimum power control the algorithm that maximizes the minimum CIR over all links. The aim of optimum power control procedure is therefore, to achieve CIR-balancing. In other words, the optimum algorithm computes the maximum achievable CIR that can be reached by all active communication links.

Optimum power control with CIR-balancing has been widely studied for Frequency-Division/Time-Division Multiple Access (FDMA/TDMA) cellular systems. In these systems, the CIR-balancing optimum power control was transformed to an eigenvalue problem using pathgain matrices. The same method was proposed to CDMA systems. In CDMA systems however, the size of the pathgain matrix is proportional to the square of the number of communication links. Thus, the computation of the eigenvalue may be infeasible in real time for CDMA systems with high loads. Therefore, simplified optimum power control algorithms have been proposed to reduce pathgain matrix size in the forward link [KP00][MH01][WSC01][WSW⁺03]. However, power control has not been sufficiently studied in crossed slots. In this chapter, we design a simplified generic optimum power control that can be used in uplink, downlink and crossed slots using a pretty small pathgain matrix.

This chapter is divided into five sections. In the first section, we define the optimum power control problem and we propose a generic equation of the CIR for only pure CDMA systems. In the second section, we formulate the latter problem as an optimization problem and we solve this problem using existing models and the new generic equation of the CIR. In the third section, the optimization problem is extended to TDMA-CDMA/TDD systems using a smaller pathgain matrix that reduces the complexity of the problem, though the same CIR is achieved by all users. In the fourth section, we present the existing removal algorithms for pure uplink and downlink slots and we propose a generic algorithm that can be used in crossed slots also. Before concluding, we propose an optimum power control algorithm in noisy systems that takes into account the lower-bound constraint on powers. This problem has not been studied as far as we know.

3.1 Problem Formulation

We remind that optimum power control is the power control algorithm that maximizes the minimum of the CIR of all simultaneous active mobiles. Based on existing models, we have formulated the optimum power control problem in CDMA systems as an optimization problem using a generic equation of the CIR. Therefore, we propose a new generic formulation of the CIR in the following.

We assume that the slot allocation procedure is already performed and that N mobiles are active during the studied slot. In all algorithms, we suppose that pathgains are stationary.

3.1.1 Generic Equation of the CIR in Pure CDMA Systems

The CIR equation is not the same in uplink and downlink. In the TDD mode however, the uplink and downlink use the same bandwidth. Thus, pathgains between two entities are the same in the two link directions. We develop a generic equation of the CIR to use the same notations in both link directions and to extend the model to crossed slots. We study the power control only in one slot; therefore, slot index n is omitted from all notations.

Uplink Slots

In uplink slot n , all cells are active in uplink. The CIR of mobile i in uplink-cell j can be written using equation (2.24):

$$\Gamma_{u,i,j} = \frac{C_{b,i}}{I_{\text{intra},u,i} + I_{\text{inter},u,i} + N_0},$$

where N_0 is the thermal noise power, $I_{\text{intra},u,i}$ and $I_{\text{inter},u,i}$ are respectively intracell-interference and intercell-interference powers experienced by the signal of mobile i . The intercell-interference $I_{\text{inter},u,i}$ in a system with only uplink-cells contains only mobile-to-base station interference and thus, $I_{\text{inter},u,i} = \mathcal{I}_{\text{mb},j}$. By substituting $C_{b,i}$, $I_{\text{intra},u,i}$ and $\mathcal{I}_{\text{mb},j}$ by their values from equations (2.6), (2.13) and (2.16), we can write:

$$\Gamma_{u,i,j} = \frac{G_{i,j}P_{m,i}}{\underbrace{\beta_u \sum_{k \in S_j - \{i\}} G_{k,j}P_{m,k}}_{I_{\text{intra},u,i}} + \underbrace{\sum_{l \in \Pi_u - \{j\}} \left(\sum_{k \in S_l} G_{k,j}P_{m,k} \right)}_{\mathcal{I}_{\text{mb},j}} + N_0}. \quad (3.1)$$

By dividing the numerator and the denominator of (3.1) by $G_{i,j}$, we obtain:

$$\Gamma_{u,i,j} = \frac{P_{m,i}}{\beta_u \sum_{k \in S_j - \{i\}} \frac{G_{k,j}}{G_{i,j}} P_{m,k} + \sum_{l \in \Pi_u - \{j\}} \left(\sum_{k \in S_l} \frac{G_{k,j}}{G_{i,j}} P_{m,k} \right) + \frac{N_0}{G_{i,j}}}.$$

Let $I_{N,u,i}$ be the total normalized interference experienced by the signal of mobile i . The total normalized interference is the ratio of the total interference to the pathgain of the mobile toward its server:

$$I_{N,u,i} = \frac{I_{\text{intra},u,i,n} + \mathcal{I}_{\text{mb},j}}{G_{i,j}}.$$

Thus, the CIR can be rewritten as:

$$\Gamma_{u,i,j} = \frac{P_{m,i}}{I_{N,u,i} + \frac{N_0}{G_{i,j}}}.$$

Using the values of the intracell-interference and intercell-interference of equation (3.1), we can write the total normalized interference as:

$$I_{N,u,i} = \beta_u \sum_{k \in S_j - \{i\}} \frac{G_{k,j}}{G_{i,j}} P_{m,k} + \sum_{l \in \Pi_u - \{j\}} \left(\sum_{k \in S_l} \frac{G_{k,j}}{G_{i,j}} P_{m,k} \right).$$

Moreover, the total normalized interference $I_{N,u,i}$ can be rewritten in matrix form:

$$I_{N,u,i} = (\mathbf{Z}_{W,u} \mathbf{P}_{W,u})_{i-M} - P_{m,i}, \quad (3.2)$$

where $\mathbf{P}_{W,u}$ is the power vector whose n th element is the power transmitted by mobile $(n + M)$, and $\mathbf{Z}_{W,u}$ is a normalized $(N \times N)$ matrix. The element of $\mathbf{Z}_{W,u}$ that corresponds to mobile i is defined by:

$$Z_{W,u,i-M,k-M} = \begin{cases} 1 & k = i \\ \beta_u \frac{G_{k,j}}{G_{i,j}} & k \neq i, k \in S_j \\ \frac{G_{k,j}}{G_{i,j}} & k \notin S_j \end{cases}$$

The translation in index is used because mobile indices begin at $M + 1$ and not at 1.

Thus, matrix $\mathbf{Z}_{W,u}$ can be written as:

$$\mathbf{Z}_{W,u} = \begin{bmatrix} 1 & \beta_u \frac{G_{M+2,1}}{G_{M+1,1}} & \dots & \frac{G_{M+N_1+1,1}}{G_{M+1,1}} & \dots & \dots & \frac{G_{M+N,1}}{G_{M+1,1}} \\ \beta_u \frac{G_{M+1,1}}{G_{M+2,1}} & 1 & \vdots & \frac{G_{M+N_1+1,1}}{G_{M+2,1}} & \dots & \dots & \frac{G_{M+N,1}}{G_{M+2,1}} \\ \vdots & \dots & 1 & \vdots & \vdots & \vdots & \vdots \\ \frac{G_{M+1,1}}{G_{M+N_1+1,2}} & \dots & \dots & 1 & \vdots & \vdots & \vdots \\ \vdots & \vdots & \vdots & \dots & 1 & \vdots & \frac{\beta_u G_{M,M}}{G_{M+N-N_N+1,M}} \\ \vdots & \vdots & \vdots & \vdots & \dots & 1 & \vdots \\ \frac{G_{M+1,1}}{G_{M+N,M}} & \vdots & \frac{G_{M+N_1,1}}{G_{M+N,M}} & \vdots & \beta_u \frac{G_{M+N-N_N+1,M}}{G_{M+N,M}} & \dots & 1 \end{bmatrix}$$

Matrix $\mathbf{Z}_{W,u}$ extends the matrix notation introduced by Wu in [Wu99] where the reduction of intracell-interference is not taken into account. Therefore, this matrix is called a Wu uplink matrix.

Using the elements of matrix $\mathbf{Z}_{W,u}$, we can write the CIR of mobile i as:

$$\Gamma_{u,i,j} = \frac{P_{m,i}}{\sum_{k=M+1}^{M+N} Z_{W,u,i-M,k-M} P_{m,k} - P_{m,i} + \frac{N_0}{G_{i,j}}}. \quad (3.3)$$

This notation can be used to write a unified equation for uplink and downlink.

Downlink Slots

In downlink slot n all cells are active in downlink. The CIR of mobile i in downlink-cell j can be written using equation (2.24):

$$\Gamma_{d,i,j} = \frac{C_{m,i}}{I_{\text{intra,d},i} + I_{\text{inter,d},i} + N_0},$$

where $I_{\text{intra,d},i}$ is the intracell-interference received by mobile i from its server and $I_{\text{inter,d},i}$ is the intercell-interference received by mobile i only from neighboring base stations of downlink-cells; therefore, $I_{\text{inter,d},i} = I_{\text{bm},i}$. By substituting $C_{m,i}$, $I_{\text{intra,d},i}$ and $I_{\text{bm},i}$ by their values from equations (2.2), (2.11) and (2.14), we can write:

$$\Gamma_{d,i,j} = \frac{G_{i,j}P_{b,i}}{\underbrace{\beta_d G_{i,j} \sum_{k \in S_j - \{i\}} P_{b,k}}_{I_{\text{intra,d},i}} + \underbrace{\sum_{l \in \Pi_d - \{j\}} G_{i,l} \left(\sum_{k \in S_l} P_{b,k} \right)}_{I_{\text{bm},i}} + N_0}. \quad (3.4)$$

By dividing the numerator and the denominator of (3.4) by $G_{i,j}$ and using the definition of the normalized pathgain, we obtain:

$$\Gamma_{d,i,j} = \frac{P_{b,i}}{\beta_d \sum_{k \in S_j - \{i\}} P_{b,k} + \sum_{l \in \Pi_d - \{j\}} Z_{i,l} \left(\sum_{k \in S_l} P_{b,k} \right) + \frac{N_0}{G_{i,j}}}.$$

Using the same definition as in uplink, we denote by $I_{N,d,i}$ the total normalized interference experienced by the signal of mobile i in downlink. Using the same approach as in uplink we can write:

$$\Gamma_{d,i,j} = \frac{P_{b,i}}{I_{N,d,i} + \frac{N_0}{G_{i,j}}}.$$

Moreover, the total normalized interference $I_{N,d,i}$ can be rewritten in matrix form:

$$I_{N,d,i} = (\mathbf{Z}_{W,d} \mathbf{P}_{W,d})_{i-M} - P_{b,i}, \quad (3.5)$$

where $\mathbf{P}_{W,d}$ is the power vector whose n th element is the power transmitted to mobile $(n + M)$, and $\mathbf{Z}_{W,d}$ is a downlink normalized $(N \times N)$ matrix. The element of $\mathbf{Z}_{W,d}$ that corresponds to mobile i is defined by:

$$Z_{W,d,i-M,k-M} = \begin{cases} 1 & k = i \\ \beta_d & k \neq i, k \in S_j \\ Z_{i,l} & k \in S_l \end{cases}$$

Thereafter, the downlink normalized $(N \times N)$ matrix $\mathbf{Z}_{W,d}$ can be written as:

$$\begin{bmatrix} 1 & \beta_d & \cdots & \beta_d & Z_{M+1,2} & \cdots & Z_{M+1,2} & \cdots & Z_{M+1,M} \\ \beta_d & 1 & \vdots & \beta_d & Z_{M+2,2} & \cdots & Z_{M+2,2} & \cdots & Z_{M+2,M} \\ \vdots & \cdots & \cdots \\ \beta_d & \vdots & \vdots & 1 & \vdots & \vdots & \vdots & \cdots & \cdots \\ Z_{M+N_1+1,1} & \cdots & \cdots & Z_{M+N_1+1,1} & 1 & \vdots & \beta_d & Z_{M+N_1+1,3} & \cdots \\ \vdots & \vdots & \vdots & \vdots & \cdots & 1 & \beta_d & \vdots & \cdots \\ Z_{M+N_1+N_2,1} & \vdots & \vdots & Z_{M+N_1+N_2,1} & \beta_d & \cdots & 1 & Z_{M+N_1+N_2,1} & \cdots \\ \vdots & 1 & \beta_d \\ Z_{M+N,1} & \vdots & Z_{M+N,1} & \vdots & \vdots & \vdots & \vdots & \cdots & 1 \end{bmatrix}$$

The matrix $\mathbf{Z}_{W,d}$ is also called a Wu downlink matrix.

Using the elements of matrix $\mathbf{Z}_{W,d}$, the CIR of mobile i can be written as:

$$\Gamma_{d,i,j} = \frac{P_{b,i}}{\sum_{k=1+M}^{N+M} \mathcal{Z}_{W,d,i-M,k-M} P_{b,k} - P_{b,i} + \frac{N_0}{G_{i,j}}}. \quad (3.6)$$

Generic Equation

Finally, uplink and downlink CIR can be represented by one equation that includes both equations (3.3) and (3.6):

$$\Gamma_{\ell,i,j} = \frac{P_{\tau,i}}{\sum_{k=1+M}^{N+M} \mathcal{Z}_{W,\ell,i-M,k-M} P_{\tau,k} - P_{\tau,i} + \frac{N_0}{G_{i,j}}}, \quad (3.7)$$

where τ is the type of the transmitter in link direction ℓ :

$$\begin{cases} \tau = m & \text{for } \ell = u \\ \tau = b & \text{for } \ell = d \end{cases} \quad (3.8)$$

3.1.2 Optimization Problem Formulation

The optimum power control problem has been widely studied. In 1964, Bock and Ebstein have found that power control problem can be formulated as a linear programming problem if certain metrics (such as pathloss, CIR, noise etc.) can be communicated to a central unit [BE64]. Aein has introduced the concept of CIR-balancing to investigate cochannel interference management in satellite systems [Aei73]. In this concept, all active communication links must be served with the same achievable CIR. A CIR target is considered achievable, if there is a positive power vector \mathbf{P}_ℓ for which all links are received with a same CIR equal to or greater than the CIR target. This concept has been extended to noiseless CDMA systems by Nettleton and Alavi [AN82][NA83] and for noiseless FDMA/TDMA systems by Zander [Zan92b]. It was found that the CIR-balancing problem can be formulated as an eigenvalue problem of the normalized pathgain matrix if the thermal noise is neglected. The common CIR that corresponds to the eigenvalue is the largest achievable CIR level and thus, this power control is called optimum power control. Moreover, the existence and uniqueness of the CIR-balancing problem solution is a consequence of the Perron-Frobenius theorem [GVGZ93][Gan71]. In [Wu99], optimum power control performance was extended to CDMA systems in uplink and downlink for noisy and noiseless systems.

In the following, we generalize the latter optimum power control for CDMA systems to take into consideration the intracell-interference, which is reduced by joint detection techniques (see § 2.1.4). In some cases, we use the notation of CIR-balancing instead of optimum power control to emphasize the fact that all users are received with the same CIR.

Using the existing models, we can write the following definitions that are used to define our objective.

Definition 3.1 Let $A = [a_{i,j}]$ and $B = [b_{i,j}]$ be $M \times N$ matrices. $A \geq B \Leftrightarrow a_{i,j} \geq b_{i,j} \quad \forall i, j$.

Definition 3.2 A CIR level γ is considered *achievable* in link direction ℓ if there exists a power vector $\mathbf{P}_\ell \geq 0$ such that $\Gamma_{\ell,i,j} > \gamma, \forall i \in S_j, j \in \Pi$.

The power vector \mathbf{P}_ℓ is an N -dimensional vector whose r th element is $P_{\tau,r+M}$.

Definition 3.3 The *maximum achievable* CIR is given by [GZY95]:

$$\gamma_{\mathbf{W},\ell}^* = \max_{\mathbf{P}_\ell \in \mathcal{B}} \left(\min_{1+M \leq i \leq N+M} \Gamma_{\ell,i,j} \right),$$

where \mathcal{B} is the set of feasible power vectors. The set of feasible power vectors is fixed by operators due to the limitation of amplifiers. Moreover, operators limit transmitted power in order to decrease the interference pattern. In general, the power of a transmitter must be within a given interval $[P_{\ell,\min}, P_{\ell,\max}]$.

Remark 3.1 If we consider all power distributions of a given system and we select the minimum CIR achieved in each distribution. The maximum of the latter CIR is the maximum achievable CIR.

From its definition, we can deduce that the optimum power control problem is to find $\gamma_{\mathbf{W},\ell}^*$ and the corresponding power vector.

Let γ be the minimum CIR in a system when the power vector \mathbf{P}_ℓ is used:

$$\gamma = \min_{1 \leq r \leq N} \Gamma_{\ell,r+M,j}. \quad (3.9)$$

Therefore, all other users have a CIR higher than γ and we can write the following inequality using equation (3.7):

$$\frac{P_{\tau,i}}{\sum_{k=1+M}^{N+M} \mathcal{Z}_{\mathbf{W},\ell,i-M,k-M} P_{\tau,k} - P_{\tau,i} + \frac{N_0}{G_{i,j}}} \geq \gamma \quad \forall i \in S_j, j \in \Pi,$$

and thus:

$$\frac{1+\gamma}{\gamma} P_{\tau,i} \geq \sum_{k=1+M}^{N+M} \mathcal{Z}_{\mathbf{W},\ell,i-M,k-M} P_{\tau,k} + \frac{N_0}{G_{i,j}}.$$

This equation can be rewritten in matrix form using Wu matrices:

$$\boxed{\frac{1+\gamma}{\gamma} \mathbf{P}_\ell \geq \mathbf{Z}_{\mathbf{W},\ell} \mathbf{P}_\ell + \mathbf{N}_{\mathbf{W},\ell}}, \quad (3.10)$$

where $\mathbf{N}_{\mathbf{W},\ell}$ is a $N \times 1$ vector representing the normalized thermal noise power to the pathgain between a mobile and its server. The element of $\mathbf{N}_{\mathbf{W},\ell}$ that corresponds to mobile i is defined by:

$$\mathcal{N}_{\mathbf{W},\ell,i-M} = \frac{N_0}{G_{i,j}}.$$

We denote by (O_{C_1,C_2}) the name of the optimization problem where O represents the objective function (e.g. Γ for maximizing the CIR and P for minimizing the sum of powers), and C_1 and C_2 correspond to the two constraints; in C_1 , we emphasize the existence of background noise (i.e. > 0 in noisy system and 0 in noiseless system). Moreover, C_1 may show the value of the desired CIR when a CIR target is required. In C_2 , we show the power solution space represented by the second set of constraints.

Using definition (3.3), and equations (3.9) and (3.10), the optimum power control problem is transformed to an optimization problem that solves the inequality (3.10):

$$\boxed{\begin{array}{ll} (\Gamma_{\mathbf{N}_{\mathbf{W},\ell},\mathcal{B}}) & \text{maximize } \gamma \\ & \text{subject to } \frac{1+\gamma}{\gamma} \mathbf{P}_\ell \geq \mathbf{Z}_{\mathbf{W},\ell} \mathbf{P}_\ell + \mathbf{N}_{\mathbf{W},\ell} \\ & \text{and } \mathbf{P}_\ell \in \mathcal{B} \end{array}}$$

In noisy systems, another optimization problem is also widely investigated. In this problem, a CIR target γ_0 is fixed by the network. The objective of the optimum power control in this case is to find the power vector \mathbf{P}_ℓ of least total (i.e. sum) power achieving γ_0 for all mobiles:

$$\begin{array}{ll} \left(\mathbf{P}_{\{\gamma_0, \mathbf{N}_{W,\ell}, \mathcal{B}\}} \right) & \text{minimize} \quad \sum_{k=1}^{N+M} P_{\tau,k} \\ & \text{subject to} \quad \frac{1+\gamma_0}{\gamma_0} \mathbf{P}_\ell \geq \mathbf{Z}_{W,\ell} \mathbf{P}_\ell + \mathbf{N}_{W,\ell} \\ & \text{and} \quad \mathbf{P}_\ell \in \mathcal{B} \end{array}$$

3.2 Optimum Power Control in Pure CDMA Systems

In this section, we extend the existing optimum power control algorithms using the generic equations in the presence of residual intracell-interference.

3.2.1 Centralized Unconstrained Optimum Power Control

The solution of centralized unconstrained optimum power control problem is the solution of the optimization problem $(\Gamma_{\mathbf{N}_{W,\ell}, \mathcal{B}})$, where \mathcal{B} is the Euclidean space $\mathbb{R}^{+N} = \{\mathbf{P}_\ell : \mathbf{P}_\ell \geq 0\}$.

Noiseless Systems

In the following, we consider that thermal noise is neglected. Therefore, the optimization problem can be written in the following matrix form:

$$\begin{array}{ll} (\Gamma_{0, \geq 0}) & \text{maximize} \quad \gamma \\ & \text{subject to} \quad \frac{1+\gamma}{\gamma} \mathbf{P}_\ell \geq \mathbf{Z}_{W,\ell} \mathbf{P}_\ell \\ & \text{and} \quad \mathbf{P}_\ell \geq 0 \end{array} \quad (3.11)$$

In order to solve this problem, we make use of the properties of matrix $\mathbf{Z}_{W,\ell}$ and the following proposition.

Proposition 3.1 (Perron-Frobenius Theorem [Gan71])

If \mathbf{Z} is a square nonnegative irreducible¹ matrix. Then:

- \mathbf{Z} has exactly one real positive eigenvalue $\rho(\mathbf{Z}) = \lambda^*$ for which the corresponding eigenvector has components of the same sign
- λ^* is the eigenvalue of \mathbf{Z} with the maximum modulus and is referred to be the spectral radius of \mathbf{Z}
- the minimum real λ that verifies the inequality: $\lambda \mathbf{P} \geq \mathbf{Z} \mathbf{P}$ which has solution for $\mathbf{P} \geq 0$ is $\lambda = \lambda^*$
- λ^* increases when any entry of \mathbf{Z} increases

¹A square matrix is called reducible if the indices $1, 2, \dots, n$ can be divided into two disjoint nonempty sets i_1, i_2, \dots, i_μ and j_1, j_2, \dots, j_ν (with $\mu + \nu = n$) such that $a_{i_\alpha j_\beta} = 0$, for $\alpha = 1, 2, \dots, \mu$ and $\beta = 1, 2, \dots, \nu$. A square matrix which is not reducible is said to be irreducible [Gan71].

- e. λ^* has an upper-bound the maximum sum of elements in lines or columns, and a lower-bound the minimum of these sums

The spectral radius λ^* has a major impact on the convergence of inherited iterative methods [Zan92a] and has been used as a measure of congestion in [Han99].

In the two link directions, $\mathbf{Z}_{W,\ell}$ is a nonnegative, irreducible matrix. This can be proved using the same procedure presented in [GVGZ93]. From property (a) and (c) of the Perron-Frobenius theorem, the minimum real that verifies the inequality: $\lambda \mathbf{P}_\ell \geq \mathbf{Z}_{W,\ell} \mathbf{P}_\ell$ which has solution for $\mathbf{P}_\ell \geq 0$ is $\lambda_{W,\ell}^* = \rho(\mathbf{Z}_{W,\ell})$. However, we have:

$$\lambda = \frac{1 + \gamma}{\gamma}.$$

Therefore, the maximum achievable CIR is given by [Zan92b]:

$$\gamma_{W,\ell}^* = \frac{1}{\lambda_{W,\ell}^* - 1}. \quad (3.12)$$

It is also shown in [GVGZ93], that:

$$\max_{\mathbf{P}_\ell \geq 0} \left(\min_{1+M \leq i \leq N+M} \Gamma^{\ell,i,j} \right) = \gamma_{W,\ell}^* = \min_{\mathbf{P}_\ell \geq 0} \left(\max_{1+M \leq i \leq N+M} \Gamma^{\ell,i,j} \right),$$

and therefore $\gamma_{W,\ell}^*$ is unique. Furthermore, the last result shows that maximizing the minimum CIR is equivalent to CIR-balancing. Therefore, when the power vector solution is used in the system, the inequality in the optimization problem ($\Gamma_{0,\geq 0}$) become an equality:

$$\frac{1 + \gamma_{W,\ell}^*}{\gamma_{W,\ell}^*} \mathbf{P}_{W,\ell}^* = \mathbf{Z}_{W,\ell} \mathbf{P}_{W,\ell}^*.$$

Furthermore, the eigenvector solution $\mathbf{P}_{W,\ell}^*$ of matrix $\mathbf{Z}_{W,\ell}$ corresponding to $\lambda_{W,\ell}^*$ is the power vector that allows all users to be received with the maximum achievable CIR $\gamma_{W,\ell}^*$. The power vector solution can be multiplied by a positive constant κ and the CIR is always the optimum solution:

$$\frac{1 + \gamma_{W,\ell}^*}{\gamma_{W,\ell}^*} (\kappa \mathbf{P}_{W,\ell}^*) = \mathbf{Z}_{W,\ell} (\kappa \mathbf{P}_{W,\ell}^*),$$

and therefore, the power solution is an infinite set of parallel positive vectors to vector $\mathbf{P}_{W,\ell}^*$.

Moreover, the property (e) of the Perron-Frobenius theorem gives the limits of $\lambda_{W,\ell}^*$:

$$\min_{1+M \leq r \leq N+M} \sum_{c=1+M}^{N+M} \mathcal{Z}_{W,\ell,r-M,c-M} \leq \lambda_{W,\ell}^* \leq \max_{1+M \leq r \leq N+M} \sum_{c=1+M}^{N+M} \mathcal{Z}_{W,\ell,r-M,c-M} \quad (3.13)$$

and

$$\min_{1+M \leq c \leq N+M} \sum_{r=1+M}^{N+M} \mathcal{Z}_{W,\ell,r-M,c-M} \leq \lambda_{W,\ell}^* \leq \max_{1+M \leq c \leq N+M} \sum_{r=1+M}^{N+M} \mathcal{Z}_{W,\ell,r-M,c-M}. \quad (3.14)$$

From these two properties, we can deduce that $\lambda_{W,\ell}^* \geq 1$ because $\text{diag}(\mathbf{Z}_{W,\ell})$ is the unity matrix, where $\text{diag}(\mathbf{Z}_{W,\ell})$ is the $N \times N$ diagonal matrix with diagonal elements equal to the diagonal elements of matrix $\mathbf{Z}_{W,\ell}$. Thus, $\gamma_{W,\ell}^*$ is always positive and we can always find a solution for the optimum power control problem.

An important conclusion in [Wu99] is that, as in the FDMA/TDMA case, the maximum achievable CIR are the same in uplink and downlink if the same matrices are used in both link directions. This property, called system-wide CIR-balancing, is retrieved when the extended model is used with matrices $\mathbf{Z}_{W,u}$ and $\mathbf{Z}_{W,d}$.

Noisy Systems

Thermal noise may be neglected in case of large number of simultaneous active mobiles where the interference is much more important than thermal noise. However, the maximum number of simultaneous active codes in a cell is limited to 16 in the TDD mode. Thus, it is more convenient to consider thermal noise in the TDD mode. In noisy systems, we solve the optimization problems $(\Gamma_{\geq 0, \geq 0})$ and $(\mathbf{P}_{\{\gamma_0, \geq 0\}, \geq 0})$ using the following propositions.

Proposition 3.2 let ε be a strictly positive constant with $\varepsilon < \gamma_{W,\ell}^*$, where $\gamma_{W,\ell}^*$ is the solution of the optimization problem for noiseless systems $(\Gamma_{0, \geq 0})$, then there exists a positive power vector \mathbf{P}_ℓ for which $\frac{1+\gamma_{W,\ell}^*-\varepsilon}{\gamma_{W,\ell}^*-\varepsilon}\mathbf{P}_\ell \geq \mathbf{Z}_{W,\ell}\mathbf{P}_\ell + \mathbf{N}_{W,\ell}$.

Proof. We have $\varepsilon > 0$ and $\rho(\mathbf{Z}_{W,\ell}) = \frac{1+\gamma_{W,\ell}^*}{\gamma_{W,\ell}^*}$, then $\frac{1+\gamma_{W,\ell}^*-\varepsilon}{\gamma_{W,\ell}^*-\varepsilon} > \rho(\mathbf{Z}_{W,\ell})$. From theorem 3.9 in [Var62] for irreducible square matrix $\mathbf{Z}_{W,\ell}$, we have the following equivalent: For all $c > \rho(\mathbf{Z}_{W,\ell})$, $c\mathbf{I}_N - \mathbf{Z}_{W,\ell}$ is nonsingular and $(c\mathbf{I}_N - \mathbf{Z}_{W,\ell})^{-1} > 0$. Thus, matrix $\left(\frac{1+\gamma_{W,\ell}^*-\varepsilon}{\gamma_{W,\ell}^*-\varepsilon}\mathbf{I}_N - \mathbf{Z}_{W,\ell}\right)$ is nonsingular and $\left(\frac{1+\gamma_{W,\ell}^*-\varepsilon}{\gamma_{W,\ell}^*-\varepsilon}\mathbf{I}_N - \mathbf{Z}_{W,\ell}\right)^{-1} > 0$. Let $\mathbf{P}_\ell = \left(\frac{1+\gamma_{W,\ell}^*-\varepsilon}{\gamma_{W,\ell}^*-\varepsilon}\mathbf{I}_N - \mathbf{Z}_{W,\ell}\right)^{-1}\mathbf{N}_{W,\ell}$. Therefore, $\mathbf{P}_\ell > 0$. Therefore, there exist at least a positive power vector \mathbf{P}_ℓ satisfying $\frac{1+\gamma_{W,\ell}^*-\varepsilon}{\gamma_{W,\ell}^*-\varepsilon}\mathbf{P}_\ell = \mathbf{Z}_{W,\ell}\mathbf{P}_\ell + \mathbf{N}_{W,\ell}$. ■

Proposition 3.3 let ε be a strictly positive constant and $\gamma_{W,\ell}^*$ be the solution of the optimization problem for noiseless systems $(\Gamma_{0, \geq 0})$, then for all positive power vectors \mathbf{P}_ℓ we have:

$$\frac{1 + \gamma_{W,\ell}^* + \varepsilon}{\gamma_{W,\ell}^* + \varepsilon} \mathbf{P}_\ell < \mathbf{Z}_{W,\ell} \mathbf{P}_\ell + \mathbf{N}_{W,\ell}.$$

Proof. Assume that there exists a power vector for which we can write:

$$\frac{1 + \gamma_{W,\ell}^* + \varepsilon}{\gamma_{W,\ell}^* + \varepsilon} \mathbf{P}_\ell \geq \mathbf{Z}_{W,\ell} \mathbf{P}_\ell + \mathbf{N}_{W,\ell}.$$

Hence, $\left(\frac{1+\gamma_{W,\ell}^*+\varepsilon}{\gamma_{W,\ell}^*+\varepsilon}\mathbf{I}_N - \mathbf{Z}_{W,\ell}\right)\mathbf{P}_\ell \geq 0$ and $\gamma_{W,\ell}^* + \varepsilon$ is a feasible solution of the noiseless optimum power control problem $(\Gamma_{0, \geq 0})$. This result contradicts the fact that $\gamma_{W,\ell}^*$ is the maximum achievable CIR. Thus, $\frac{1+\gamma_{W,\ell}^*+\varepsilon}{\gamma_{W,\ell}^*+\varepsilon}\mathbf{P}_\ell < \mathbf{Z}_{W,\ell}\mathbf{P}_\ell + \mathbf{N}_{W,\ell}$. ■

Conclusion 3.1 From propositions 3.2 and 3.3, we can deduce that the maximum achievable CIR $\gamma_{W,\ell}$ for an unconstrained optimum power control problem in a noisy system is always smaller than the maximum achievable CIR $\gamma_{W,\ell}^*$ in a noiseless system. The value of $\gamma_{W,\ell}$ is the nearest value to $\gamma_{W,\ell}^*$ for which the matrix $\frac{1+\gamma_{W,\ell}}{\gamma_{W,\ell}}\mathbf{I}_N - \mathbf{Z}_{W,\ell}$ can be inverted. $\gamma_{W,\ell}^*$ is a simple root of $\frac{1+\gamma_{W,\ell}}{\gamma_{W,\ell}}\mathbf{I}_N - \mathbf{Z}_{W,\ell}$ determinant. Therefore, $\gamma_{W,\ell}^*$ cannot be achieved with finite power vector.

In order to solve the optimization $(\mathbf{P}_{\{\gamma_0, \geq 0\}, \geq 0})$, γ_0 must be therefore smaller than $\gamma_{W,\ell}^*$. Otherwise, γ_0 is not achievable. The power vector with the least total power is computed using the following corollary:

Corollary 3.1 For all $\gamma_0 < \gamma_{\mathbf{W},\ell}^*$, $(\mathbf{P}_{\{\gamma_0, \geq 0\}, \geq 0})$ is a linear optimization problem whose solution is the solution of the following system of linear equations:

$$\left(\frac{1 + \gamma_0}{\gamma_0} \mathbf{I}_N - \mathbf{Z}_{\mathbf{W},\ell} \right) \mathbf{P}_{\mathbf{W},\ell} = \mathbf{N}_{\mathbf{W},\ell}. \quad (3.15)$$

Proof. We have shown in proposition 3.2, that $(\mathbf{P}_{\{\gamma_0, \geq 0\}, \geq 0})$ has feasible solutions for every $\gamma_0 < \gamma_{\mathbf{W},\ell}^*$ that satisfies equation (3.15). Therefore, we must only prove that the solution of equation (3.15) minimizes the sum $\sum_{i=1+M}^{N+M} P_{\tau,i}$. Let \mathbf{P}_ℓ be a solution of $\frac{1+\gamma_0}{\gamma_0} \mathbf{P}_\ell \geq \mathbf{Z}_{\mathbf{W},\ell} \mathbf{P}_\ell + \mathbf{N}_{\mathbf{W},\ell}$, then $\left(\frac{1+\gamma_0}{\gamma_0} \mathbf{I}_N - \mathbf{Z}_{\mathbf{W},\ell} \right) \mathbf{P}_\ell \geq \mathbf{N}_{\mathbf{W},\ell}$. Therefore, we can use equation (3.15) to write:

$$\left(\frac{1 + \gamma_0}{\gamma_0} \mathbf{I}_N - \mathbf{Z}_{\mathbf{W},\ell} \right) \mathbf{P}_\ell \geq \left(\frac{1 + \gamma_0}{\gamma_0} \mathbf{I}_N - \mathbf{Z}_{\mathbf{W},\ell} \right) \mathbf{P}_{\mathbf{W},\ell}.$$

Hence, $\left(\frac{1+\gamma_0}{\gamma_0} \mathbf{I}_N - \mathbf{Z}_{\mathbf{W},\ell} \right) (\mathbf{P}_\ell - \mathbf{P}_{\mathbf{W},\ell}) \geq 0$. However, $\left(\frac{1+\gamma_0}{\gamma_0} \mathbf{I}_N - \mathbf{Z}_{\mathbf{W},\ell} \right)^{-1} \geq 0$ because $\mathbf{Z}_{\mathbf{W},\ell}$ is an irreducible square matrix; therefore $(\mathbf{P}_\ell - \mathbf{P}_{\mathbf{W},\ell}) \geq 0$ and $\mathbf{P}_\ell \geq \mathbf{P}_{\mathbf{W},\ell}$. Consequently:

$$P_{\tau,k} \geq P_{\mathbf{W},\tau,i} \quad \forall i \in S_j, j \in \Pi.$$

Hence, the sum of powers in vector \mathbf{P}_ℓ is higher than the sum of powers in $\mathbf{P}_{\mathbf{W},\ell}$ and the corollary is proved. ■

Remark 3.2 From the demonstration of corollary 3.1, we can note that all solutions of inequality $\frac{1+\gamma_0}{\gamma_0} \mathbf{P}_\ell \geq \mathbf{Z}_{\mathbf{W},\ell} \mathbf{P}_\ell + \mathbf{N}_{\mathbf{W},\ell}$ have elements higher or equal to the optimal solution of $(\mathbf{P}_{\{\gamma_0, \geq 0\}, \geq 0})$.

3.2.2 Centralized Constrained Optimum Power Control

Constrained power control was studied in [GZY95] where the maximum allowed power vector is denoted by $\mathbf{P}_{\ell,\max} = \{P_{\ell,\max}\}$. In this case, the CIR-balancing power control problem is to find the maximum achievable CIR $\overline{\gamma_{\mathbf{W},\ell}^*}$ that can be reached by a power vector less than $\mathbf{P}_{\ell,\max}$:

$\left(\Gamma_{\geq 0, \{0 \leq \mathbf{P}_\ell \leq \mathbf{P}_{\ell,\max}\}} \right)$	maximize γ subject to $\frac{1+\gamma}{\gamma} \mathbf{P}_\ell \geq \mathbf{Z}_{\mathbf{W},\ell} \mathbf{P}_\ell + \mathbf{N}_{\mathbf{W},\ell}$ and $0 \leq \mathbf{P}_\ell \leq \mathbf{P}_{\ell,\max}$
--	--

Remark 3.3 The study of constrained power control algorithms are interesting only in noisy systems; in noiseless systems, we can find a power vector \mathbf{P}_ℓ parallel to $\mathbf{P}_{\mathbf{W},\ell}$ and satisfying the constraints of the optimization problem $\left(\Gamma_{0, \{0 \leq \mathbf{P}_\ell \leq \mathbf{P}_{\ell,\max}\}} \right)$.

Let $\overline{\gamma_{\mathbf{W},\ell}^*}$ be the maximum achievable CIR by a constrained optimum power control in a noisy system:

$$\overline{\gamma_{\mathbf{W},\ell}^*} = \max_{0 \leq \mathbf{P}_\ell \leq \mathbf{P}_{\ell,\max}} \left(\min_{1+M \leq i \leq N+M} \Gamma_{\ell,i,j} \right).$$

It can be shown, as in [GZY95], that the upper bound of $\overline{\gamma_{W,\ell}^*}$ is $\gamma_{W,\ell}^*$ and the maximum achievable CIR can be reached with at least one user transmitting with the maximum power. Therefore $\overline{\gamma_{W,\ell}^*}$, can be written as:

$$\overline{\gamma_{W,\ell}^*} = \left\{ \gamma; \max_{1+M \leq i \leq N+M} \left[\left(\frac{1+\gamma}{\gamma} I_N - \mathbf{Z}_{W,\ell} \right)^{-1} \mathbf{N}_{W,\ell} \right]_i = P_{\max} \right\}. \quad (3.16)$$

A centralized constrained power control can be formulated using (3.16) in order to find the maximum achievable CIR $\overline{\gamma_{W,\ell}^*}$. This can be done iteratively by choosing a first value of γ near to zero and computing the maximum transmitted power:

$$P_{\max} = \max_{1 \leq r \leq N} \left[\left(\frac{1+\gamma}{\gamma} I_N - \mathbf{Z}_{W,\ell} \right)^{-1} \mathbf{N}_{W,\ell} \right]_r. \quad (3.17)$$

The CIR value γ is increased with small steps until $\left| P_{\max} - \max_{1+M \leq i \leq N+M} P_\ell \right|$ is sufficiently small.

3.3 Simplified Generic Optimum Power Control

The computation complexity of the solution for optimum power control problems in noisy and noiseless systems depends on pathgain matrix dimensions; the size of a pathgain matrix is proportional to the square of the number of mobiles in the system (i.e. for N active mobiles, we have an $N \times N$ matrix). Moreover, each line of the pathgain matrix corresponds to an equation to solve. For instance, consider a system of 25 cells where 8 mobiles are active simultaneously in each cell. In this case, we must solve 200 equations for each mobile distribution. In other words, we must perform the inverse of a 200×200 matrix in noisy systems or find the eigenvalue of the latter matrix in noiseless systems. Therefore, a simplified pathgain matrix leading to the same results is very advantageous in high loaded systems, which will be the case in future wireless networks. Moreover, the optimum power control has not been studied during crossed slots as far as we know.

In this section, we introduce a simplified generic optimum power control algorithm that can be used for uplink, downlink and crossed slots. Similarly to existing simplified optimum power control algorithms, the proposed algorithm is based on a pathgain matrix whose size is proportional to the square of the number of cells. Despite its pretty small size, the proposed algorithm achieves the same maximum achievable CIR as the complex algorithm.

We assume that slot allocation is done and we analyze the optimal power control in a crossed slot. Uplink and downlink slots are special cases of crossed slots and thus, only crossed slots are investigated.

We first rewrite CIR equations in downlink- and uplink-cells independently as a function of the total interference profile. The CIR-balanced power control problem in TDMA-CDMA/TDD systems is then formulated as an eigenvalue problem by combining the linear equations of downlink- and uplink-cells.

In downlink-cells, the power control algorithm is applied to total powers transmitted by base stations instead of specific powers of mobiles. Alternately, the power control algorithm in uplink-cells is applied to the received power in base stations (intracell CIR-balancing).

We show in the following that these considerations do not affect the optimum power control performance. Thus, the maximum achievable CIR is retrieved without approximation.

In crossed slot n , each type of cells (i.e. uplink- and downlink-cells) is studied independently. Equations obtained in both links are combined to form one matrix equation.

Let γ_n be the CIR that can be reached by all active mobiles during slot n , then:

$$\boxed{\Gamma_{i,j,n} \geq \gamma_n \quad \forall i \in S_j^{(n)}, j \in \Pi}, \quad (3.18)$$

where $\Gamma_{i,j,n}$ is the estimated CIR of mobile i during slot n .

3.3.1 Unconstrained Power Control in Noiseless Systems

We first consider a noiseless system and we suppose that all users request the same type of service (i.e. the same processing gain, BER and data rate). Our objective is to find the maximum achievable CIR that can be reached by all mobiles in a crossed slot with the presence of residual intracell-interference. In other words, we try to solve $(\Gamma_{0,\geq 0})$ with a simpler method.

The interference pattern in crossed slots is different than in pure uplink and downlink slots, due to the presence of mobile-to-mobile and base station-to-base station interferences (see section 2.1.4). Therefore, the CIR equations for downlink- and uplink-cells must be rewritten.

Uplink-Cells

The CIR of mobile i in uplink-cell j during slot n is given by:

$$\Gamma_{i,j,n} = \frac{C_{b,i,n}}{I_{u,i,n}}, \quad (3.19)$$

where $I_{u,i,n}$ is the total interference experienced by the signal of mobile i , and it is given by equation (2.8):

$$I_{u,i,n} = I_{\text{intra},u,i,n} + I_{\text{inter},u,i,n},$$

where $I_{\text{intra},u,i,n}$ and $I_{\text{inter},u,i,n}$ are respectively intracell- and total intercell-interference powers experienced by the signal of user i .

Proposition 3.4 If the CIR-balanced power control is applied in a system where only one service is offered, all mobiles of an uplink-cell are received with the same power.

Proof. If the CIR-balanced power control is applied, intracell CIR-balancing is certainly applied in each cell j . Therefore, all communication links of cell j must be received with the same CIR [Zan92b][Aei73]:

$$\Gamma_{i,j,n} = \Gamma_{j,n} \text{ for all } i \in [1 + M, N + M]. \quad (3.20)$$

Moreover, all communication links in cell j are interfered by the same intercell-interference $\mathcal{I}_{\text{inter},u,j,n}$ because they have the same receiver:

$$I_{\text{inter},u,i,n} = \mathcal{I}_{\text{inter},u,j,n} \quad \forall i \in S_j^{(n)}. \quad (3.21)$$

Furthermore, the intracell-interference experienced by the signal of mobile i can be written as:

$$I_{\text{intra},u,i,n} = \beta_u (C_{\text{intra},u,j,n} - C_{b,i,n}),$$

where $C_{\text{intra},u,j,n}$ is the total power received from all mobiles of cell j . Therefore, we can write the CIR of two mobiles i and k of cell j as:

$$\Gamma_{j,n} = \frac{C_{b,i,n}}{\mathcal{I}_{\text{inter},u,j,n} + \beta_u (C_{\text{intra},u,j,n} - C_{b,i,n})} = \frac{C_{b,k,n}}{\mathcal{I}_{\text{inter},u,j,n} + \beta_u (C_{\text{intra},u,j,n} - C_{b,k,n})}.$$

Therefore:

$$C_{b,i,n} = C_{b,k,n},$$

and all mobiles of uplink-cell j are received with the same power. ■

Using proposition 3.4, we can represent the received power of all mobiles in cell j by a unique notation $C_{b,j,n}$ specific to base station j :

$$\boxed{C_{b,i,n} = C_{b,j,n} \quad \forall i \in S_j^{(n)}}. \quad (3.22)$$

Thereby, the intracell-interference given in equation (2.13) can be formulated as:

$$I_{\text{intra,u},i,n} = \beta_u \sum_{k \in S_j^{(n)} - \{i\}} C_{b,j,n}.$$

Hence, all mobile signals in cell j experience the same intracell-interference $\mathcal{I}_{\text{intra,u},j,n}$ given by:

$$\boxed{\mathcal{I}_{\text{intra,u},j,n} = \beta_u (N_{j,n} - 1) C_{b,j,n} \quad \forall i \in S_j^{(n)}, j \in \Pi_{u,n}}. \quad (3.23)$$

In crossed slots, the useful signal of mobile i in uplink-cell j experiences a total intercell-interference induced by neighboring base stations of downlink-cells and neighboring mobiles of uplink-cells. This total interference is given by equation (2.9):

$$I_{\text{inter,u},i,n} = \mathcal{I}_{\text{mb},j,n} + \mathcal{I}_{\text{bb},j,n}.$$

Certainly, the same interference $\mathcal{I}_{\text{mb},j,n}$ from neighboring mobiles of uplink cells is experienced by the signals of all mobiles in cell j . From equations (2.6), (2.16) and (3.22), we can write:

$$\mathcal{I}_{\text{mb},j,n} = \sum_{l \in \Pi_{u,n} - \{j\}} \left(\sum_{k \in S_l^{(n)}} \frac{G_{k,j}}{G_{k,l}} C_{b,l,n} \right).$$

If some cells are active in downlink, an extra intercell-interference $\mathcal{I}_{\text{bb},j,n}$ is added by base stations of these cells. From equation (2.18), we can write:

$$\mathcal{I}_{\text{bb},j,n} = \sum_{l \in \Pi_{d,n}} G_{l,j} \mathcal{P}_{T,l,n}.$$

As all mobiles of cell j have the same receiver, therefore $I_{\text{inter,u},i,n}$ is also the same and can be replaced by $\mathcal{I}_{\text{inter,u},j,n}$:

$$\mathcal{I}_{\text{inter,u},j,n} = \sum_{l \in \Pi_{u,n} - \{j\}} \left(\sum_{k \in S_l^{(n)}} \frac{G_{k,j}}{G_{k,l}} C_{b,l,n} \right) + \sum_{l \in \Pi_{d,n}} G_{l,j} \mathcal{P}_{T,l,n}.$$

Moreover, all mobiles of cell j experience the same intracell-interference $\mathcal{I}_{\text{intra,u},j,n}$ (equation 3.23). Therefore, all mobiles of cell j experience the same total interference $\mathcal{I}_{u,j,n}$. $\mathcal{I}_{u,j,n}$ can be rewritten using equation (2.1) as:

$$\underbrace{\mathcal{I}_{u,j,n} = \beta_u (N_{j,n} - 1) C_{b,j,n} + \sum_{l \in \Pi_{u,n} - \{j\}} \left(\sum_{k \in S_l^{(n)}} Z_{k,j} C_{b,l,n} \right) + \sum_{l \in \Pi_{d,n}} G_{l,j} \mathcal{P}_{T,l,n}}_{\text{The same for all mobiles of cell } j}, \quad (3.24)$$

As a consequence of the latter conclusions, we can rewrite the CIR of all mobiles of cell j as:

$$\Gamma_{j,n} = \frac{\mathcal{C}_{b,j,n}}{\mathcal{I}_{u,j,n}} \quad (3.25)$$

Conclusion 3.2 We can stress that equation (3.25) is quite similar to equation (3.19). Nevertheless, in (3.25) we have proved that for all mobiles of cell j the CIR depends only on cell j . Therefore, the CIR of all mobiles i of cell j can be represented by only one value $\Gamma_{j,n}$ given by equation (3.25).

By substituting the value of $\Gamma_{j,n}$ from (3.25) in (3.18) and adding $\mathcal{C}_{b,j,n}$ to both sides of the last inequality, we obtain:

$$\frac{1 + \gamma_n}{\gamma_n} \mathcal{C}_{b,j,n} \geq \mathcal{C}_{b,j,n} + \mathcal{I}_{u,j,n}. \quad (3.26)$$

Conclusion 3.3 The linear system using only equations (3.26) is equivalent to the linear system used by Wu in [Wu99] due to proposition (3.4).

Downlink-Cells

The CIR of mobile i in downlink-cell j during slot n is given by:

$$\Gamma_{i,j,n} = \frac{C_{m,i,n}}{I_{d,i,n}}, \quad (3.27)$$

where $I_{d,i,n}$ is the total interference experienced by the signal of mobile i , and it is given by equation (2.8):

$$I_{d,i,n} = I_{\text{intra,d},i,n} + I_{\text{inter,d},i,n},$$

where $I_{\text{intra,d},i,n}$ and $I_{\text{inter,d},i,n}$ are respectively intracell- and total intercell-interference powers experienced by the signal of user i .

In crossed slot n , the useful received power by mobile i of downlink-cell j is given by equation (2.4):

$$C_{m,i,n} = G_{i,j} \alpha_{i,n} \mathcal{P}_{T,j,n}.$$

In addition to the useful power, mobile i receives intracell-interference $I_{\text{intra,d},i,n}$ due to the presence of other active mobiles in cell j . This interference is given by equation (2.12):

$$I_{\text{intra,d},i,n} = \beta_d G_{i,j} (1 - \alpha_{i,n}) \mathcal{P}_{T,j,n}.$$

Moreover, the useful signal of mobile i experiences a total intercell-interference $I_{\text{inter,d},i,n}$ induced by base stations of neighboring downlink-cells and mobiles of neighboring uplink-cells. $I_{\text{inter,d},i,n}$ is given by equation (2.9):

$$I_{\text{inter,d},i,n} = I_{\text{bm},i,n} + I_{\text{mm},i,n}.$$

Neighboring base stations of downlink-cells induce interference $I_{\text{bm},i,n}$ given by equation (2.15):

$$I_{\text{bm},i,n} = \sum_{l \in \Pi_{d,n} - \{j\}} G_{i,l} \mathcal{P}_{T,l,n}.$$

If some cells are active in uplink, an extra intercell-interference $I_{\text{mm},i,n}$ is added by mobiles of these cells. Furthermore, if all mobiles of uplink-cells are received with the same power, we can rewrite equation (2.17) by using equations (2.6) and (3.22):

$$I_{\text{mm},i,n} = \sum_{l \in \Pi_{\text{u},n}} \left(\sum_{k \in S_l^{(n)}} \frac{G_{k,i}}{G_{k,l}} \right) \mathcal{C}_{b,l,n}.$$

Therefore, we can write the total interference $I_{d,i,n}$ experienced by mobile i as:

$$I_{d,i,n} = \beta_d G_{i,j} (1 - \alpha_{i,n}) \mathcal{P}_{\text{T},j,n} + \sum_{l \in \Pi_{\text{d},n} - \{j\}} G_{i,l} \mathcal{P}_{\text{T},l,n} + \sum_{l \in \Pi_{\text{u},n}} \left(\sum_{k \in S_l^{(n)}} \frac{G_{k,i}}{G_{k,l}} \right) \mathcal{C}_{b,l,n}, \quad (3.28)$$

and the CIR of mobile i is thus:

$$\Gamma_{i,j,n} = \frac{\alpha_{i,n} G_{i,j} \mathcal{P}_{\text{T},j,n}}{I_{d,i,n}}. \quad (3.29)$$

By substituting the value of $\Gamma_{i,j,n}$ from (3.29) in (3.18) and using (2.1), we obtain:

$$\frac{\alpha_{i,n}}{\gamma_n} \mathcal{P}_{\text{T},j,n} \geq \beta_d (1 - \alpha_{i,n}) \mathcal{P}_{\text{T},j,n} + \sum_{l \in \Pi_{\text{d},n} - \{j\}} Z_{i,l} \mathcal{P}_{\text{T},l,n} + \sum_{l \in \Pi_{\text{u},n}} \left(\sum_{k \in S_l^{(n)}} \frac{G_{k,i}}{G_{i,j} G_{k,l}} \right) \mathcal{C}_{b,l,n}. \quad (3.30)$$

By making the sum over all mobiles of cell j , using equation (2.5) and adding $\mathcal{P}_{\text{T},j,n}$ to both sides of the last inequality, we obtain:

$$\frac{1 + \gamma_n}{\gamma_n} \mathcal{P}_{\text{T},j,n} \geq \mathcal{P}_{\text{T},j,n} + \mathfrak{S}_{d,j,n}, \quad (3.31)$$

where $\mathfrak{S}_{d,j,n}$ is the sum of all normalized interferences experienced by all mobiles of cell j and it is given by:

$$\mathfrak{S}_{d,j,n} = \beta_d (N_{j,n} - 1) \mathcal{P}_{\text{T},j,n} + \sum_{l \in \Pi_{\text{d},n} - \{j\}} \left(\sum_{i \in S_j^{(n)}} Z_{i,l} \mathcal{P}_{\text{T},l,n} \right) + \sum_{l \in \Pi_{\text{u},n}} \left(\sum_{i \in S_j^{(n)}} \sum_{k \in S_l^{(n)}} \frac{G_{k,i}}{G_{i,l} G_{k,l}} \right) \mathcal{C}_{b,l,n}. \quad (3.32)$$

Generic Model

By combining equations (3.31) for all downlink-cells and (3.26) for all uplink-cells, we obtain a system of M inequalities which can be represented by the following matrix inequality:

$$\boxed{\frac{1 + \gamma_n}{\gamma_n} \mathbf{R}_n \geq \mathbf{Z}^{(n)} \mathbf{R}_n}, \quad (3.33)$$

where $\mathbf{R}_n = [R_{j,n}]$ is the $M \times 1$ vector with elements:

$$R_{j,n} = \begin{cases} \mathcal{P}_{\text{T},j,n} & \forall j \in \Pi_{\text{d},n} \\ \mathcal{C}_{b,j,n} & \forall j \in \Pi_{\text{u},n} \end{cases} \quad (3.34)$$

$\mathbf{Z}^{(n)}$ is an $M \times M$ non negative matrix with elements:

$$\mathbf{Z}_{j,l,n} = \begin{cases} 1 + \beta_d (N_{j,n} - 1) & \forall j, l \in \Pi_{d,n}, j = l \\ \sum_{i \in S_j^{(n)}} Z_{i,l} & \forall j, l \in \Pi_{d,n}, j \neq l \\ \sum_{i \in S_j^{(n)}} \sum_{k \in S_l^{(n)}} \frac{G_{k,i}}{G_{i,j} G_{k,l}} & \forall j \in \Pi_{d,n}, l \in \Pi_{u,n} \\ 1 + \beta_u (N_{j,n} - 1) & \forall j, l \in \Pi_{u,n}, j = l \\ \sum_{k \in S_l^{(n)}} Z_{k,j} & \forall j, l \in \Pi_{u,n}, j \neq l \\ G_{l,j} & \forall j \in \Pi_{u,n}, l \in \Pi_{d,n} \end{cases} \quad (3.35)$$

Example 3.1 The following matrix represents the simplified normalized pathgain matrix of a system with two downlink-cells (cell 1 and 2), two uplink-cells (cell 3 and 4) and with 4 mobiles in each cell:

$$\mathbf{Z}^{(1)} = \begin{pmatrix} 1 + 3\beta_d & \sum_{i=5}^8 Z_{i,2} & \sum_{i=5}^8 \sum_{k=13}^{16} \frac{G_{k,i}}{G_{i,1} G_{k,3}} & \sum_{i=1}^8 \sum_{k=17}^{20} \frac{G_{k,i}}{G_{i,1} G_{k,4}} \\ \sum_{i=9}^{12} Z_{i,1} & 1 + 3\beta_d & \sum_{i=9}^{12} \sum_{k=13}^{16} \frac{G_{k,i}}{G_{i,2} G_{k,4}} & \sum_{i=9}^{12} \sum_{k=17}^{20} \frac{G_{k,i}}{G_{i,2} G_{k,4}} \\ G_{3,1} & G_{3,2} & 1 + 3\beta_u & \sum_{k=17}^{20} Z_{k,3} \\ G_{4,1} & G_{4,2} & \sum_{k=13}^{16} Z_{k,4} & 1 + 3\beta_u \end{pmatrix}$$

It must be noted that vector \mathbf{R}_n includes total base station transmitted powers in downlink-cells and received powers in uplink-cells. From the Perron Frobenius theorem (proposition 3.1), the maximum value γ_n^* of γ_n that can be reached during slot n with positive powers is obtained when the matrix inequality (3.33) became an equality:

$$\mathbf{Z}^{(n)} \mathbf{R}_n^* = \frac{1 + \gamma_n^*}{\gamma_n^*} \mathbf{R}_n^*, \quad (3.36)$$

and the value of γ_n^* is given by the following equation:

$$\gamma_n^* = \frac{1}{\lambda_n^* - 1}, \quad (3.37)$$

where λ_n^* is the largest real eigenvalue of matrix $\mathbf{Z}^{(n)}$ and \mathbf{R}_n^* is the corresponding eigenvector.

Equation (3.36) allows us to write the CIR in a crossed slot using the generic equation of section 3.1.1:

$$\Gamma_{i,j,n} = \frac{R_{j,n}}{\sum_{l \in \Pi} \mathbf{Z}_{j,l,n} R_{l,n} - R_{j,i}} \quad \forall i \in S_j^{(n)}. \quad (3.38)$$

Proposition 3.5 If the intracell and intercell CIR-balanced power control are used, the set of relations (3.31) and (3.26) in all cells gives the same achievable CIR as in [Wu99] which is the maximum achievable CIR.

Proof. Equation (3.18) has a only one optimal solution [Zan92b] and the two linear system satisfy the latter equation. Therefore, the set of relations (3.31) and (3.26) in all cells gives the same achievable CIR as in [Wu99]. Moreover, this proposition has been proved using simulations in [NL04b]. ■

From proposition 3.5, we can deduce that the maximum achievable CIR γ_n^* during slot n is computed using the eigenvalue λ_n^* of matrix $\mathbf{Z}^{(n)}$. Moreover, the set of eigenvectors of $\mathbf{Z}^{(n)}$ corresponding to λ_n^* represents the set of power vectors. The elements of the normalized vector of this set represent the total transmitted powers in downlink-cells and the received powers in uplink-cells needed to guarantee a CIR equal to γ_n^* in all channels. Hereafter, we must only find how these powers are distributed to mobiles. This distribution is performed in the following.

Specific Power Distribution

If the power vector \mathbf{R}_n^* is used, all mobiles will have a CIR equal to γ_n^* . Moreover, the transmitted power of a mobile i in an uplink-cell j is deduced from $\mathcal{C}_{b,j,n}$ using equations (2.6) and (3.22):

$$P_{m,i,n} = \frac{\mathcal{C}_{b,j,n}}{G_{i,j}} \quad \forall i \in S_j^{(n)}$$

In order to compute the power transmitted to each mobile in downlink-cell j , we derive the following system of equations from relations (3.29) and (3.36):

$$\gamma_n^* = \begin{cases} \frac{\alpha_{i,n} \mathcal{P}_{T,j,n}}{I_{d,i,n}/G_{i,j}} & \forall i \in S_j^{(n)}, j \in \Pi \\ \frac{\mathcal{P}_{T,j,n}}{\mathfrak{S}_{d,j,n}} & \forall j \in \Pi \end{cases}$$

From this system, we can write the following equation:

$$\alpha_{i,n} = \frac{\mathcal{P}_{T,j,n}}{\mathfrak{S}_{d,j,n}} \times \frac{I_{d,i,n}/G_{i,j}}{\mathcal{P}_{T,j,n}}.$$

Therefore:

$$\alpha_{i,n} = \frac{\beta_d (1 - \alpha_{i,n}) \mathcal{P}_{T,j,n} + \sum_{l \in \Pi_{d,n} - \{j\}} Z_{i,l} \mathcal{P}_{T,l,n} + \sum_{l \in \Pi_{u,n}} \left(\sum_{k \in S_l^{(n)}} \frac{G_{k,i}}{G_{i,j} G_{k,l}} \right) \mathcal{C}_{b,l,n}}{\beta_d (N_{j,n} - 1) \mathcal{P}_{T,j,n} + \sum_{l \in \Pi_{d,n} - \{j\}} \left(\sum_{i \in S_j^{(n)}} Z_{i,l} \mathcal{P}_{T,l,n} \right) + \sum_{l \in \Pi_{u,n}} \left(\sum_{i \in S_j^{(n)}} \sum_{k \in S_l^{(n)}} \frac{G_{k,i}}{G_{i,j} G_{k,l}} \right) \mathcal{C}_{b,l,n}}.$$

By solving this equation, we obtain the value of $\alpha_{i,n}$ given by:

$$\alpha_{i,n} = \frac{\beta_d \mathcal{P}_{T,j,n} + \underbrace{\sum_{l \in \Pi_{d,n} - \{j\}} Z_{i,l} \mathcal{P}_{T,l,n} + \sum_{l \in \Pi_{u,n}} \left(\sum_{k \in S_l^{(n)}} \frac{G_{k,i}}{G_{k,l} G_{i,j}} \mathcal{C}_{b,l,n} \right)}_{\text{Specific to mobile } i}}{\beta_d N_{j,n} \mathcal{P}_{T,j,n} + \underbrace{\sum_{i \in S_j^{(n)}} \sum_{l \in \Pi - \{j\}} Z_{i,l} \mathcal{P}_{T,l,n} + \sum_{i \in S_j^{(n)}} \sum_{l \in \Pi_{u,n}} \sum_{k \in S_l^{(n)}} \frac{G_{k,i}}{G_{i,j}} \mathcal{C}_{b,l,n}}_{\text{The same for all mobiles of cell } j}}.$$

By multiplying the nominator and the denominator of the latter equation by $G_{i,j}$, we can write:

$$\alpha_{i,n} = \frac{\beta_d G_{i,j} \mathcal{P}_{T,j,n} + \sum_{l \in \Pi_{d,n} - \{j\}} G_{i,l} \mathcal{P}_{T,l,n} + \sum_{l \in \Pi_{u,n}} \left(\sum_{k \in S_l^{(n)}} \frac{G_{k,i}}{G_{k,l}} \mathcal{C}_{b,l,n} \right)}{\beta_d N_{j,n} G_{i,j} \mathcal{P}_{T,j,n} + \sum_{i \in S_j^{(n)}} \sum_{l \in \Pi - \{j\}} G_{i,l} \mathcal{P}_{T,l,n} + \sum_{i \in S_j^{(n)}} \sum_{l \in \Pi_{u,n}} \sum_{k \in S_l^{(n)}} \frac{G_{k,i}}{G_{k,l}} \mathcal{C}_{b,l,n}} \quad (3.39)$$

Conclusion 3.4 We can deduce that $\alpha_{i,n}$ is the ratio of the total power received by mobile i to the sum of total powers received by all mobiles of cell j . From equation (3.39), we can see that

the value of $\alpha_{i,n}$ depends on two separated parts: the intercell-interference and the the total power received by mobile i . Therefore, power distribution in a downlink-cell does not only depend on the pathgains of mobiles toward their servers, but also on pathgains of these mobiles toward interfering entities.

System-Wide CIR Balancing

If we suppose that we have the same mobile distribution and radio characteristics for pure uplink and downlink slots, the pathgain matrix elements during uplink and downlink slots are respectively given by:

$$\mathcal{Z}_{u,j,l,n} = \begin{cases} \sum_{k \in S_l^{(n)}} Z_{k,j} & \forall j, l \in \Pi_{u,n}, j \neq l \\ 1 + \beta(N_{j,n} - 1) & \forall j, l \in \Pi_{u,n}, j = l \end{cases} \quad (3.40)$$

$$\mathcal{Z}_{d,j,l,n} = \begin{cases} \sum_{i \in S_j^{(n)}} Z_{i,l} & \forall j, l \in \Pi_{d,n}, j \neq l \\ 1 + \beta(N_{j,n} - 1) & \forall j, l \in \Pi_{d,n}, j = l \end{cases} \quad (3.41)$$

Therefore $Z_{u,j,l,n} = \sum_{k \in S_l^{(n)}} Z_{k,j} = Z_{d,l,j,n}$ when $j \neq l$ and $Z_{u,j,j,n} = Z_{d,j,j,n}$. Thus, the uplink pathgain matrix is the transpose of the downlink pathgain matrix. In this case, the maximum achievable CIR in uplink and in downlink are identical and are deduced from the eigenvalue of (3.40) and (3.41). This result extends the result presented by Zander for FDMA/TDMA systems [ZF94].

3.3.2 Performance Analysis using Simplified Generic Optimum Power Control

In the following, we use the simplified generic optimum power control algorithm to investigate the performance of TDMA-CDMA/TDD system during crossed slots. System performance during these slots is compared to system performance during uplink slots where the intracell-interference is higher than in downlink slots. The simplified generic optimum power control is used to compute the maximum achievable CIR.

System performance is evaluated in a simulation platform with 25 hexagonal cells. The cell radius is 100 meters. A wraparound technique is applied to guarantee that each cell is completely surrounded by a symmetric pattern. All pathgains are assumed to be known through intelligent measuring. We assume that a mobile is always served by the best-received base station. The values of residual intracell-interference factors in downlink and uplink β_d and β_u are 0.1 and 0.2. We also assume that all mobiles request the same type of services. An Okumura-hata-cost231 model with shadowing is used [AG03][NL03b]. Minimum distances of 0.2 m between mobiles and 1 m between mobiles and base stations are considered.

In the following, we introduce the concept of slot capacity as a performance measure during a slot. Slot capacity K_n of slot n is the total maximum number of active mobiles that can be served during slot n with a CIR target γ_0 :

$$K_n = \max \left(\sum_{j \in \Pi} \text{card} \left(S_j^{(n)} \right) \right) \text{ with } \Gamma_{i,j,n} \geq \gamma_0 \text{ for } i \in \bigcup_{j \in \Pi} S_j^{(n)}, \quad (3.42)$$

where $\text{card}(S)$ is the cardinality of the set S . The maximum cardinality is computed by removing the least number of mobiles that guarantee a CIR higher than γ_0 for the remaining users (the mobile removing algorithm is introduced in section 3.4.2).

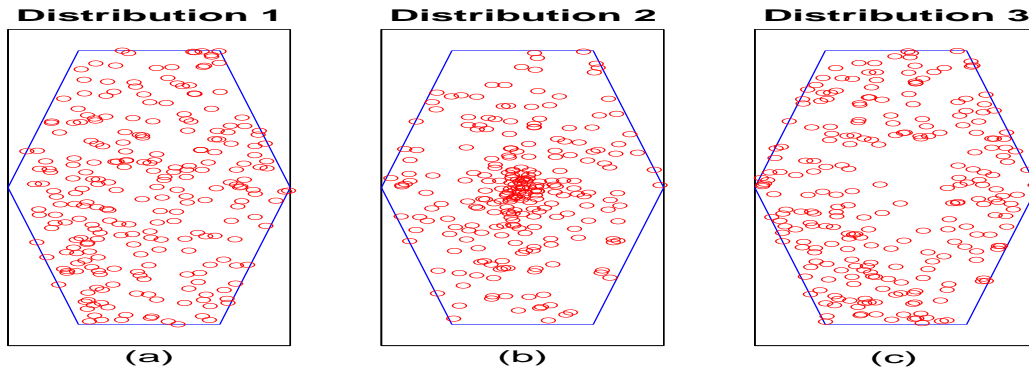


Figure 3.1: The three types of mobile distribution: uniform mobile distribution (a), mobiles close to base stations (b) and mobiles close to cell borders (c)

Three types of geographic mobile distributions are used. In the first distribution, mobiles are uniformly distributed inside cells. In the second distribution, mobiles are concentrated close to base stations while in the third distribution, mobiles are concentrated in cell borders (figure 3.1). The aim of using different types of mobile distribution is to show that crossed slots are suited in some situations where mobile-to-mobile interferences are not very high.

In order to compare the performance of crossed slots to the performance of uplink slots, we simulate 1000 different geographical mobile samples for each type of mobile distribution. In each sample, we assume that slot allocation is already performed and we study only one slot. Furthermore, we assume that the same mobiles are allocated to the crossed slot and to the uplink slot. In crossed slots, uplink- and downlink-cells are randomly distributed with asymmetry rate $a_r = M_u / (M_d + M_u)$, where M_u and M_d are the number of uplink- and downlink-cells respectively. In figure 3.2, the probability density function (pdf) of the CIR is plotted for the three distributions in uplink and crossed slots. The plotted figures correspond to a cell load of 6 codes/cell/slot and an asymmetry rate of 1/10. The average maximum achievable CIR is the highest when the uplink is used and when mobiles are distributed using the second distribution. Furthermore, the range of pdf is very large in crossed slots while it is very narrow in uplink slots. We have evaluate also the confidence interval and we have found the same results; the range of confidence interval is higher in crossed slots than in uplink slots. These results are not presented here. The high variation in the maximum achievable CIR in crossed slots is due to the high number of parameters affecting the pathgain matrix. In uplink slots, only pathgains between mobiles and base stations have an impact on the pathgain matrix. In crossed slots however, new types of pathgains (i.e. pathgains between mobiles and pathgains between base stations) appear. Pathgains between mobiles are highly related to mobile positions and shadowing factors with high variance. Hence, the pathgain matrix in crossed slots may change drastically depending on mobile positions.

In figure 3.3, the crossed slot capacity is plotted as a function of the asymmetry rate for the three types of mobile distributions. The horizontal lines represent the uplink slot capacity, which are independent from the asymmetry rate.

As it is expected, the slot capacity is at its highest level when the second distribution is used while it is at its lowest level when the third distribution is used; in the third distribution, the presence of a high number of active mobiles in uplink in some cells and in downlink in other cells at cell borders increases the probability of high mobile-to-mobile interference. Moreover, mobiles at cell borders need more powers than other mobiles to achieve γ_0 . Therefore, the third distribution has the lowest maximum achievable CIR while the second distribution has the highest one. Moreover,

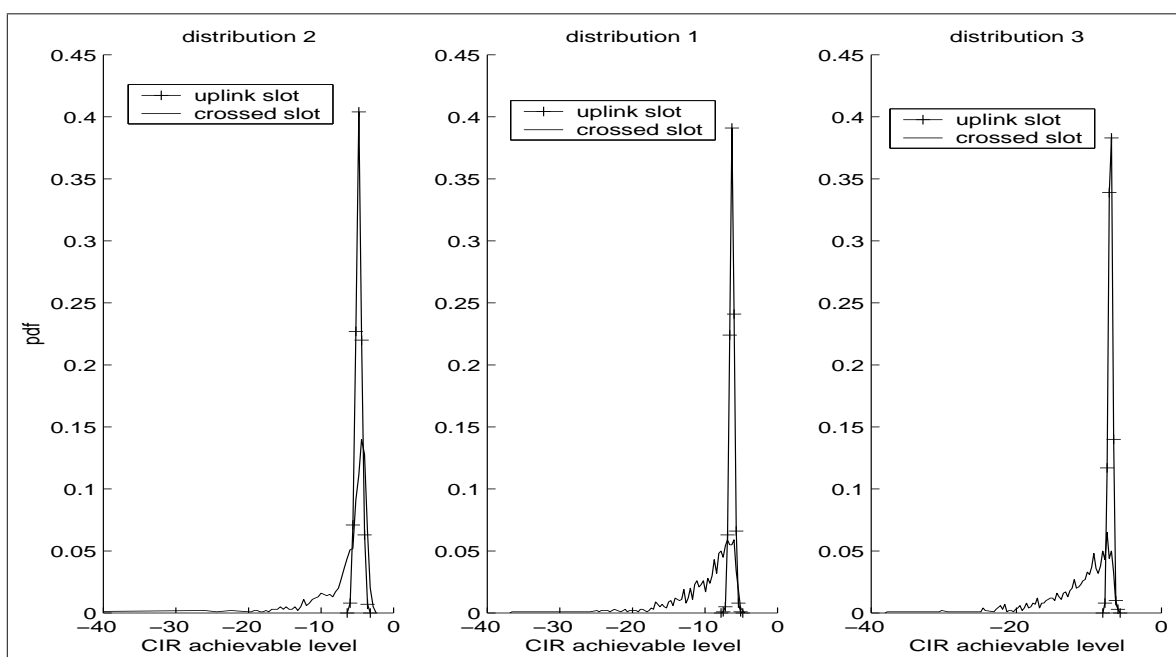


Figure 3.2: The pdf of the maximum achievable CIR for uplink and crossed slots

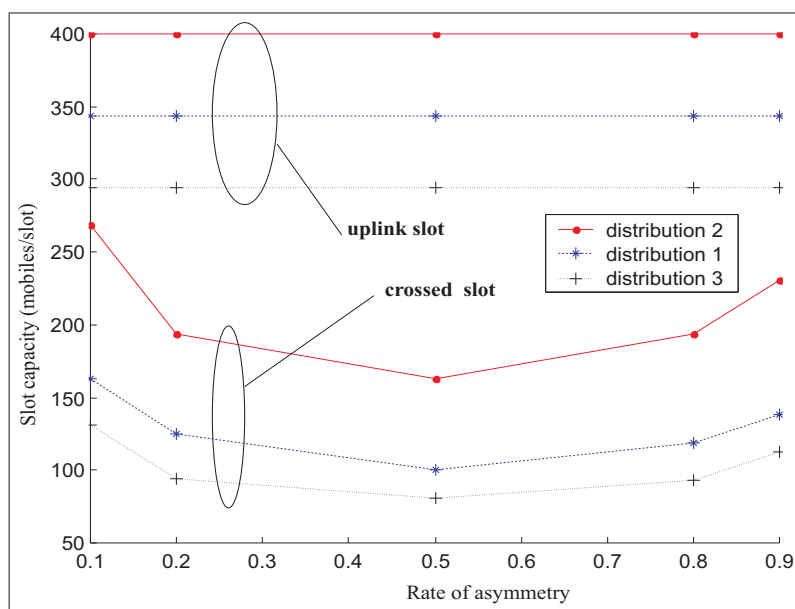


Figure 3.3: Slot capacity for $\gamma_0 = -10$ dB

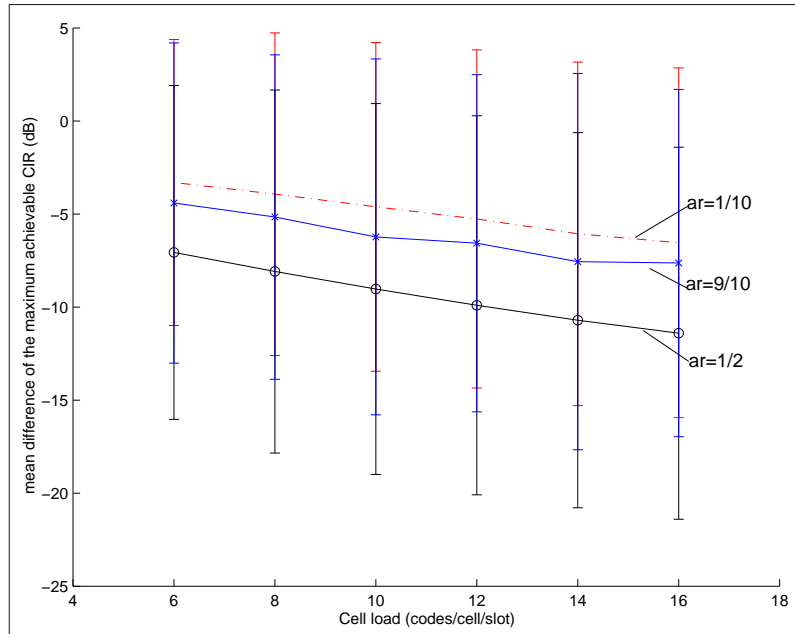


Figure 3.4: The mean difference between the maximum achievable CIR in crossed and uplink slots

the crossed slot capacity is at its lowest level when the asymmetry rate is 0.5. At this rate, the number of active mobiles in uplink and in downlink is at its maximum. Thus, the probability that high mobile-to-mobile and base station-to-base station interferences affect the system is at its maximum. The crossed slot capacity is higher when $a_r = 1/10$ than when $a_r = 9/10$, because $\beta_u > \beta_d$, and thus the intracell-interference impact is higher in uplink than in downlink. Thus, when the number of uplink-cells is higher than the number of downlink-cells, the intracell-interference impact is increased.

The average difference between the maximum achievable CIR in crossed and the maximum achievable CIR in uplink slots is plotted in figure 3.4 with the confidence interval for three values of the asymmetry rate using the first distribution. Results show that the performance in crossed slots become closer to the performance in uplink slots for very high or very low values of a_r in particular when a_r is at its maximum where the slot become almost a pure downlink slot; for very high value of a_r (resp. very low value of a_r), the number of uplink (resp. downlink) cells is very low and the probability of having high mobile-to-mobile or base station-to-base station interference is very low.

Due to the high range of confidence interval, we can note that the maximum achievable CIR in crossed slots can be higher than its value in uplink slots in some cases (e.g. the difference can reach 5 dB). However, the performance in uplink is better in most cases and the enhancement in the uplink case can reaches 20 dB for high loads. In figure 3.2, we can see also that the maximum achievable CIR in crossed slots is higher than its value in uplink slots for some mobile distribution samples, especially when the second distribution is used.

Summary

In this section, we have proposed a unconstrained simplified generic optimum power control algorithm for noiseless systems. This algorithm was used to study the performance of TDMA-CDMA/TDD systems during crossed slots by considering the uplink slot as a reference. The impact of different mobile distributions inside cells, the cell load and the rate of asymmetry on the

system performance during crossed slots were investigated. Simulation results have shown that in some distributions where mobiles are concentrated close to base stations, the system performance may be better during crossed slots than during uplink slots. However, the system performance in crossed slots varies in a large range depending on pathgain distributions. Therefore, a dramatic degradation may appear when high mobile-to-mobile interference appears. Nevertheless, some improvements may appear in other cases. Therefore, crossed slots have to be allocated very carefully to a low number of mobiles and intelligent slot allocation techniques must be used to exploit the flexibility of TDMA-CDMA/TDD systems without increasing the outage probability. This trade-off may be achieved by using crossed slots for cells where mobiles are concentrated near to base stations and by using some techniques to avoid high interference.

3.4 User Removal Algorithms

If we consider that all mobiles of an unconstrained system require the same CIR level γ_0 , this level must be less than the maximum achievable CIR $\gamma_{W,\ell}^*$ in order to be achieved by all mobiles. Otherwise, all CIRs will drop below the required level and all users will be unsatisfied. This is due to the fact that the system cannot support all active mobiles at the same time with the fixed CIR target [ZKAQ01]. An optimal removal algorithm was introduced in [Zan92b] to minimize the outage probability, which is the percentage of unsatisfied users:

$$P_{out} = \Pr(\text{received CIR} < \gamma_0) \quad (3.43)$$

In this algorithm, a minimum number of users must be disconnected in order to make the CIR level achievable. In other word, the largest submatrix $\mathbf{Z}_{W_s,\ell}$ of $\mathbf{Z}_{W,\ell}$ must be formed by removing the minimum number of rows-columns in order to obtain $\gamma_{W_s,\ell}^* \geq \gamma_0$ (s stands for subsystem). Moreover, Wu [Wu99] has demonstrated that the removal algorithm has the same performance in uplink and downlink of CDMA systems. In figure 3.5, we present the impact of CIR-balancing when $\gamma_0 < \gamma_{W,\ell}^*$, when $\gamma_0 > \gamma_{W,\ell}^*$, and when a user removal algorithm is used [ZKAQ01].

3.4.1 Stepwise Removal Algorithms for Pure Downlink and Uplink Slots

An optimal removal algorithm involves an exhaustive investigation of all mobile removal combinations, in order to minimize the outage probability. This algorithm, called *brute force* search, was proposed in [Zan92b] as an optimal solution. However, the computation complexity of this algorithm increases exponentially with the number of users in the system. Therefore, stepwise methods have been proposed as suboptimal solutions with lower complexity to FDMA/TDMA systems [Zan92b][LLS95].

All removal algorithms involve two steps. The first step is common between all algorithms and it consists of computing $\gamma_{W,\ell}^*$ that corresponds to matrix $\mathbf{Z}_{W,\ell}$. If $\gamma_{W,\ell}^* \geq \gamma_0$ the eigenvector $\mathbf{P}_{W,\ell}^*$ is used, otherwise we set $\mathbf{Z}_{W_s,\ell} = \mathbf{Z}_{W,\ell}$ and we execute step 2.

The second step of the Brute Force Algorithm (BFA) consists of removing all combinations of at most $N - 2$ users and computing the eigenvalue of each submatrix. The algorithm starts by removing only one user and computes the eigenvalue of each submatrix until the CIR constraint is fulfilled. If not, all combinations of disconnecting two mobiles are investigated and so on. If the CIR requirement is not fulfilled, then $N - 1$ arbitrary users are disconnected and the requirement is fulfilled with only one active user without interference. This algorithm converges to the optimal solution in term of outage probability. However, the computation of the eigenvalue must be repeated

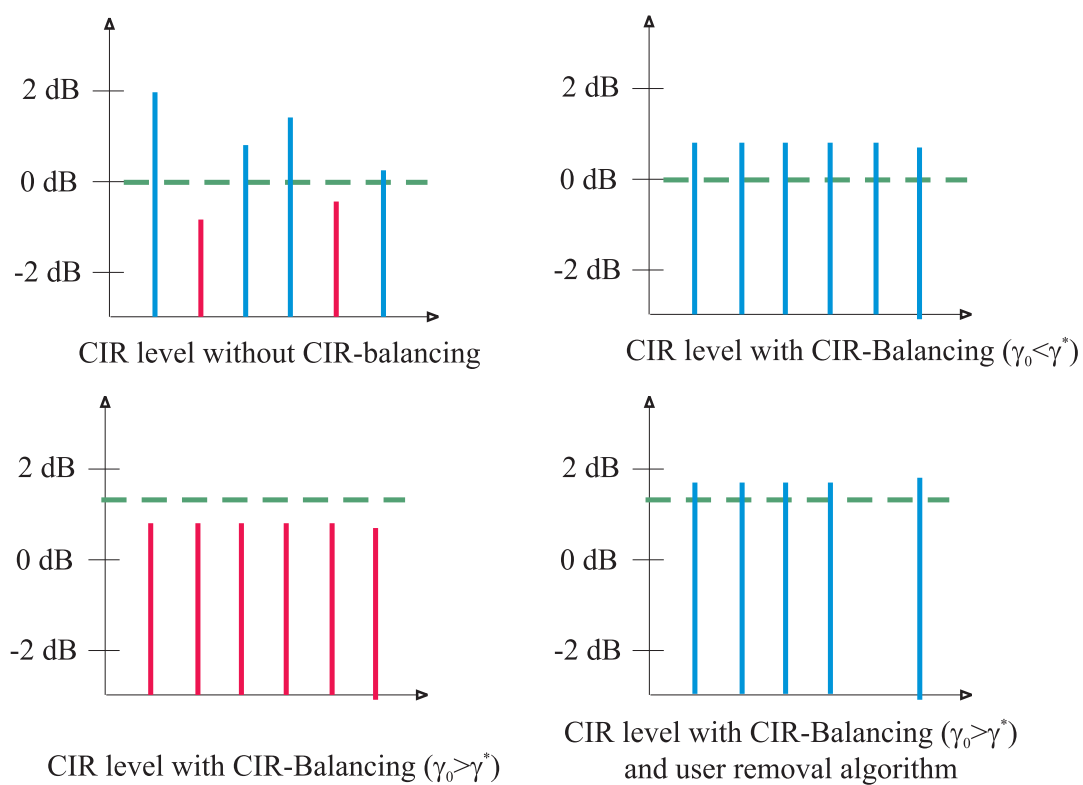


Figure 3.5: Example of the CIR level with and without CIR-Balancing and with user removal algorithm

$\binom{N}{\eta} = \frac{N!}{(N-\eta)!\eta!}$ to analyze the impact of disconnecting a set of η users. Therefore, we must compute the eigenvalues of $\sum_{\eta=1}^{N-2} \binom{N}{\eta} = (1+1)^N - N - 2 = 2^N - N - 2$ matrices in the worst case. The high complexity of the exhaustive algorithm leads to high computation time; therefore, the pathgain matrix in an operational system may change faster than the convergence rate of the algorithm.

Stepwise removal algorithms were proposed as suboptimal solutions to alleviate computation complexity. In the second step of these algorithms, a user k is removed from the system; user k must satisfy some constraints fixed by the algorithm. After mobile removal, an $(N-1) \times (N-1)$ submatrix $\mathbf{Z}_{W_s, \ell}$ is formed and the eigenvalue is computed. This step is repeated until the optimum computed CIR is higher than the required CIR.

In the Stepwise Removal Algorithm (SRA) proposed in [Zan92b], the removed mobile i is the mobile that maximizes the maximum of row and column sums:

$$s = \max_{1+M \leq i \leq N+M} \left(\sum_{k=1+M}^{N+M} \mathcal{Z}_{W, \ell, i-M, k-M}, \sum_{k=1+M}^{N+M} \mathcal{Z}_{W, \ell, k-M, i-M} \right)$$

The removal constraint is based on the properties of the eigenvalue $\lambda_{W, \ell}^*$; from equations (3.13) and (3.14), we can deduce that the upper bound of $\lambda_{W, \ell}^*$, and thus the lower bound of $\gamma_{W, \ell}^*$, is limited by the maximum row and column sums; therefore, the minimization of this maximum might maximize $\gamma_{W, \ell}^*$ for a fixed number of users.

In the worst case, the SRA algorithm can converge after $N-2$ computations of eigenvalues; therefore the SRA algorithm requires less computation time than BFA. However, the SRA algorithm maximizes only the lower bound of $\gamma_{W_s, \ell}^*$ at each step and therefore, the computed $\gamma_{W_s, \ell}^*$ may not be the optimum CIR at the studied step.

An algorithm was proposed in [LLS95] to ameliorate SRA by maximizing $\gamma_{W_s, \ell}^*$ at each step. In the proposed algorithm, called Stepwise Maximum-Interference Removal Algorithm (SMIRA), mobile i is removed in a given step if it generates the highest interference in the system and thus the following sum is maximized:

$$s = \max_{1+M \leq i \leq N+M} \left(\sum_{k=1+M}^{N+M} P_{\tau, k} \mathcal{Z}_{W, \ell, i-M, k-M}, P_{\tau, i} \sum_{k=1+M}^{N+M} \mathcal{Z}_{W, \ell, k-M, i-M} \right)$$

The first sum corresponds to the total interference received by user i while the second corresponds to the sum of the interferences induced by user i to other users. At each step ν in the algorithm, $(N-\nu)$ submatrices are formed by disconnecting a different user in each submatrix. Thereby, $\gamma_{W_s, \ell}^*$ is computed for each submatrix. This algorithm converges to a lower outage probability than SRA but it is more complex: at worst case, the algorithm may compute the eigenvalue of $(N-1) + (N-2) + \dots + 2 = \frac{N(N-1)}{2} - 1$ matrices.

These algorithms have been proposed for FDMA systems, but can be used for CDMA systems also. In [Wu99], the Stepwise Optimal Removal Algorithm (SORA) was proposed to CDMA systems. In SORA, if the removal of mobile k maximizes $\gamma_{W_s, \ell}^*$ at a given iteration, the corresponding user is disconnected. The proposed algorithm is an optimum stepwise algorithm in the term of maximizing $\gamma_{W_s, \ell}^*$ at each step. Moreover, SORA converges after the computation of the eigenvalue of $\frac{N(N-1)}{2} - 1$ like SMIRA.

Stepwise removal algorithms cannot converge to the optimal solution because the optimal solution involves the removal of a set of η users. These users may not satisfy the constraint of stepwise removal algorithms in all steps, because the optimum solution takes into account the mutual impact of the η users, which is not the case in stepwise removal algorithms. In table 3.1, the characteristics of different user removal algorithms are presented: the performance of these methods are sorted

Table 3.1: The characteristics of different user removal algorithms

User removal algorithm	performance	complexity	Same-entity interference
Brute Force Algorithm (BFA)	1	4	No
Stepwise Optimal Removal Algorithm (SORA)	2	2	No
Stepwise Maximum-Interference Removal Algorithm (SMIRA)	2	2	No
Stepwise Removal Algorithm (SRA)	4	1	No

from the highest performance (1) to the lowest performance (4); the complexity also is sorted from the least complex (1) to the most complex (4) algorithm; same-entity interference consideration is also presented.

3.4.2 Generic Mobile-based Stepwise Removal Algorithm

Existing stepwise removal algorithms treat only pure uplink and downlink slots, where same-entity interferences do not appear. Therefore, we propose the Generic Mobile-based Stepwise Removal (GMSR) algorithm that can be applied to all types of slots. The aim of the GMSR algorithm is to minimize the outage probability by eliminating mobiles with high normalized pathgains.

In existing works mobile-based stepwise removal algorithms are only studied in systems with different-entity interferences. In the following, we extend the existing algorithms to take into account same-entity interferences.

Algorithm Description

The GMSR algorithm is based on the algorithm in [WSC01] where an interference index $\iota_{i,j}$ is associated to mobile i of cell j . However, the interference index in [WSC01] cannot be used in crossed slots because it does not consider same entity-interference; therefore we define a new interference index by:

$$\iota_{i,j} = \begin{cases} \beta_d + \sum_{l \in \Pi_{d,n} - \{j\}} Z_{i,l} + \sum_{l \in \Pi_{u,n}} \sum_{k \in S_l^{(n)}} \frac{G_{k,i}}{G_{i,j} G_{k,l}} & \text{if } j \in \Pi_{d,n} \\ \beta_u + \sum_{l \in \Pi_{u,n} - \{j\}} Z_{i,l} + \sum_{l \in \Pi_{d,n}} G_{j,l} & \text{if } j \in \Pi_{u,n} \end{cases} \quad (3.44)$$

The elements of $\iota_{i,j}$ represent the intracell, the mobile-to-mobile, the base station-to-base station and the mobile-to-base station effect on the interference level experienced by the mobile. A mobile with high value of $\iota_{i,j}$ is considered as a mobile that suffers from high interference and thus can induce high interference to other mobiles.

Let us look at equation (3.44). We can find the elements of the simplified normalized pathgain matrix $\mathbf{Z}^{(n)}$ defined in equation (3.35). The elements of an active mobile in uplink appear in the column corresponding to its server. On the contrary, the elements of an active mobile in downlink appear in the row corresponding to its server. The asymmetry between uplink and downlink is due to the fact that the pathgain matrix in uplink is the transpose of the pathgain matrix in downlink.

Moreover, the eigenvalue of the pathgain matrix is bounded by row and line sums [Gan71]. The removal algorithm must remove the mobile with the highest contribution either in line or in row

sums to minimize the outage probability. Hence, the mobile with the highest interference index must be removed.

In the GMSR algorithm, mobiles are removed until all remaining mobiles have a CIR larger than γ_0 . Hence, the outage probability is given by:

$$P_{out} = 1 - \frac{N_r}{N^{(n)}},$$

where N_r and $N^{(n)}$ are respectively the number of remaining mobiles and the initial number of mobiles during slot n .

The GMSR algorithm is described as follows:

Step 1: Set $N_r = N^{(n)}$

Step 2: Determine γ^* corresponding to $\mathbf{Z}^{(n)}$

Step 3: If $\gamma^* \geq \gamma_0$, then all mobiles are satisfied and halt

Step 4: Remove mobile i with the highest $\nu_{i,j}$, decrease N_r and build the matrix $\mathbf{Z}_s^{(n)}$ by eliminating the elements of mobile i

Step 5: Determine γ^* corresponding to $\mathbf{Z}_s^{(n)}$

Step 6: If $\gamma^* \geq \gamma_0$, then all mobiles are satisfied and halt

else repeat from step 4

As the SRA algorithm, the GMSR algorithm can converge after $N - 2$ computations of eigenvalues.

Simulations and Results

A CDMA cellular system of 5×5 blocks is considered to investigate the performance of the proposed algorithm. The block size is 200×200 meters. Only one slot of the TDMA frame is studied. It is supposed that all cells have the same number of simultaneous active mobiles and this number is limited to 16 as in the UMTS TDD mode. The values of β_d and β_u are respectively 0.1 and 0.2.

We compare the performance of the GMSR algorithm to the performance of the so-called quasi-optimal algorithm in term of outage probability. At each step in the quasi-optimal algorithm, $\mathbf{Z}_s^{(n)}$ is built by removing remaining mobiles one-by-one and testing γ^* for each mobile removal. The removed mobile of the step is the mobile for which $\mathbf{Z}_s^{(n)}$ gives the highest γ^* . The latter algorithm is not optimal because it does not consider all combination of mobile removal in different steps.

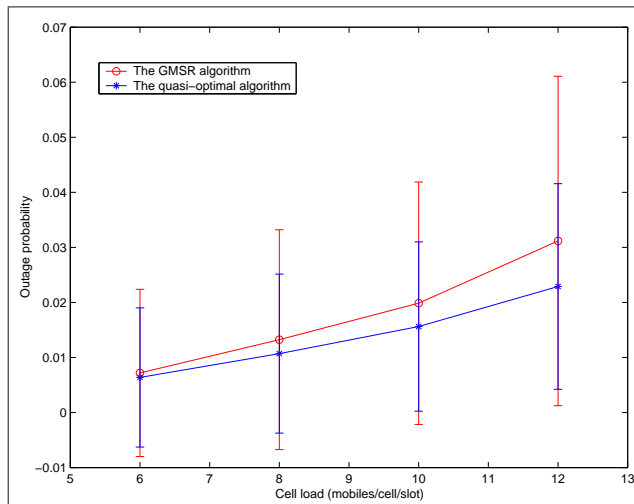
The assumed propagation model is an Okumura-hata-cost231 model with shadowing:

$$P_r = P_e \frac{k}{d_{x,y}^\gamma} a_{x,y}, \quad (3.45)$$

where P_r and P_e are respectively the received and the transmitted powers, k and γ are constants [AG03], which depend on the type of environment, and d is the distance between the transmitter and the receiver. Factor $a_{x,y}$ models the shadowing effect. It is a time constant, log-normal variable with zero mean [NL03b] (table 3.2). The shadowing factor variance and the pathloss constant between two mobiles are very high compared to those between two base stations due to the low altitude of mobile antennas. The presented results are the results of 500 different mobile samples

Table 3.2: Propagation model constants (from [AG03])

	$BS - BS$	$BS - MS$	$MS - MS$
k [dB]	-112.7	-127.7	-147.4
γ [dB]	35.5	35.5	40
$\text{var}[a_{x,y}]$ [dB]	4.24	6	7.34

**Figure 3.6:** The average outage probability of the GMSR and the quasi-optimal algorithms as a function of the cell load

with $\gamma_0 = -12$ dB. Moreover, we assume that the number of uplink-cells and downlink-cells are equal.

In figure 3.6, the average outage probability is plotted as a function of the cell load for the GMSR algorithm and the quasi-optimal algorithm. We can see that the outage probability given by the GMSR algorithm is slightly higher than the outage probability given by the quasi-optimal algorithm. Moreover, the difference between these probabilities increases when cell load increases.

As we can see in figure 3.7, the average difference between the two algorithms is not high. It must be noted also, that the proposed algorithm decreases the outage probability for some mobile samples. The difference increases with the increase of the cell load, because the number of cases to investigate increases in this case. However, the computation time in the quasi-optimal algorithm is very high because all mobile removal are investigated in each step. On the other hand, only one mobile elimination is investigated in the proposed algorithm.

3.5 Lower-Bounded Constrained Power Control

Generally, transmitter amplifiers have lower-bound limitations on transmitted power. In systems with low loads or having highly asymmetric distribution of loads between cells, the convergence vector of power control procedure may involve some powers smaller than the minimum acceptable level. In other words, the range of interference in different cells is wider than the range of power control. Therefore, the study of lower-bounded constrained power control may be an interesting subject for some systems. However, this type of power control has not been studied as far as we

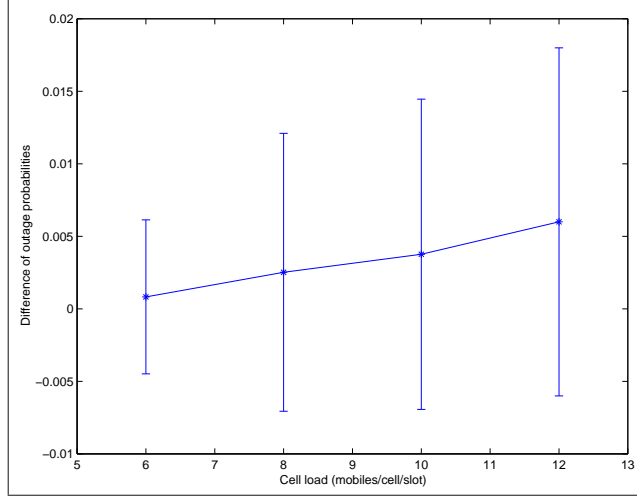


Figure 3.7: The average difference between the outage probability of the quasi-optimal algorithm and the outage probability of the proposed algorithm with confidence interval

know. In this section, we propose a method to assess the feasibility of constrained power control with a CIR target γ_0 and a method to compute the power vector. We study the power control only in one slot; therefore, slot index n is omitted from all notations.

3.5.1 Problem Formulation

The constrained power control problem is defined with the following linear optimization problem:

$$\begin{array}{ll}
 (\mathbf{P}_{\{\gamma_0, \geq 0\}, \{P_{\min} \leq P \leq P_{\max}\}}) & \text{minimize} \quad \sum_{k=1+M}^{N+M} P_k \\
 & \text{subject to} \quad \frac{1+\gamma_0}{\gamma_0} \mathbf{P} \geq \mathbf{Z}_W \mathbf{P} + \mathbf{N}_W \\
 & \text{and} \quad P_{\min} \leq P \leq P_{\max}
 \end{array}$$

In this section, we assume that γ_0 is feasible, i.e. γ_0 is smaller than the Perron-Frobenius CIR. In section 3.2.1, we have shown that the unconstrained minimization problem can be solved only by finding the solution \mathbf{P}_W of equation (3.15). However, this solution does not take into account the upper-bound and lower-bound constraints of powers. In the following, we solve the optimization problem $(\mathbf{P}_{\{\gamma_0, \geq 0\}, \{P_{\min} \leq P \leq P_{\max}\}})$ using an iterative algorithm.

Upper-Bound Constraint

The upper-bound constraint is very deterministic: if at least one element of \mathbf{P}_W is higher than P_{\max} , then the problem is not feasible in the sense of finding a power vector satisfying the upper-bound constraint and offering a CIR higher than γ_0 for all mobiles. This conclusion is deduced from the remark noted in the corollary 3.1; it was shown that the elements of all solutions satisfying the inequality $\frac{1+\gamma_0}{\gamma_0} \mathbf{P} \geq \mathbf{Z}_W \mathbf{P} + \mathbf{N}_W$ are at least equal to the elements of \mathbf{P}_W solution of equation (3.15). Therefore, if one element of \mathbf{P}_W is higher than P_{\max} , all power vector solutions with elements smaller than P_{\max} cannot satisfy the inequality.

Lower-Bound Constraint

Unlike the upper-bound constraint, the lower-bound constraint is more flexible; if some elements of \mathbf{P}_W are smaller than P_{\min} , we can always find a new power vector satisfying the CIR and lower-bound power constraints. Nevertheless, finding a power solution satisfying the upper-bound power constraint in addition is not always guaranteed. If we only increase low powers until the minimum level is reached, the CIR of others links may fall below the required level. Therefore, it is interesting to study the problem of the lower-bound constraint to limit the outage probability.

In the following, we propose an iterative algorithm that find the minimum power vector (i.e. with the minimum sum of elements) satisfying all the constraints of the optimization problem ($\mathbf{P}_{\{\gamma_0, \geq 0\}, \{P_{\min} \leq P \leq P_{\max}\}}$) if a feasible solution exists. Certainly, this method determines if the system has a feasible solution. The proposed method is developed using the Wu matrix introduced in section 3.1.1. It can be extended to use the simplified normalized matrix also.

A simple method to find a feasible method in a lower-bounded constrained problem is to take the vector \mathbf{P}_W , solution of $\frac{1+\gamma_0}{\gamma_0}\mathbf{P} = \mathbf{Z}_W\mathbf{P} + \mathbf{N}_W$ and multiplied it by a constant c . The constant c is the ratio of P_{\min} to the minimum power in \mathbf{P}_W . $c\mathbf{P}_W$ is a solution of $\frac{1+\gamma_0}{\gamma_0}\mathbf{P} \geq \mathbf{Z}_W\mathbf{P} + \mathbf{N}_W$ (see the proof of proposition A.1) that satisfies the lower-bound constraint. However, we cannot guarantee that this solution satisfies the upper-bound constraint. Moreover, it is not the optimum solution in term of minimizing the sum of powers because we have always one user with γ_0 and other users have CIRs higher than γ_0 , which is not always the case in the optimum solution as we will demonstrate in the following. Therefore, our objective is to find the set of mobiles that must transmit with P_{\min} such that the sum of powers in the power vector solution is minimized.

3.5.2 Optimization Problem Solution

In order to to solve the constrained power control problem, we introduce useful propositions in Appendix A and the following definition:

Definition 3.4 We call P a feasible power for equation i if the following constraint is satisfied:

$$\frac{1 + \gamma_0}{\gamma_0} P \geq \sum_{k=1}^N \mathcal{Z}_{W,i,k} P + N_{W,i}.$$

In other words, P_W is a feasible power for equation i if the CIR constraint of user i is fulfilled when this power is used by all transmitters.

In the following, we propose an iterative lower-bounded power control algorithm and a generic constrained optimum power control algorithm that takes into account lower-bound and upper-bound constraints.

Iterative Lower-bounded Optimum Power Control Algorithm

Using propositions of appendix A, we define an Iterative Lower-bounded Optimum Power Control (ILOPC) algorithm that converges to the solution of ($\mathbf{P}_{\{\gamma_0, \geq 0\}, \{P_{\min} \leq P \leq P_{\max}\}}$):

Step 1: Compute \mathbf{P}_W

Step 2: If $\mathbf{P}_W \geq \mathbf{P}_{\min}$, \mathbf{P}_W is the solution and halt

Step 3: Build the set of indices E_S corresponding to equations for which P_{\min} is feasible (see definition 3.4) and the corresponding powers in \mathbf{P}_W are smaller than P_{\min}

- Step 4:** Set $P_{W,i}$ to P_{\min} for $i \in E_S$ and computes the remaining powers of the power vector \mathbf{P}_W by solving the corresponding equations
- Step 5:** Find the set U of unsatisfied mobiles for which the CIR is smaller than the CIR target (from proposition A.3, U is always a subset of E_S).
If U is empty, \mathbf{P}_W is the solution and halt
- Step 6:** Set $E_S = E_S - U$ and repeat from step 4 (from proposition A.4, powers corresponding to indices in set U cannot be set to P_{\min} in a feasible solution)

Generic Constrained Optimum Power Control Algorithm

If the upper-bound constraint is imposed, a new algorithm based on the ILOPC algorithm is used. This algorithm, called Generic Constrained Optimum Power Control (GCOPC) algorithm, is described below:

- Step 1:** Compute \mathbf{P}_W
- Step 2:** if at least one element of \mathbf{P}_W is higher than P_{\max} , the system is unfeasible and halt
- Step 3:** If $\mathbf{P}_W \geq \mathbf{P}_{\min}$, \mathbf{P}_W is the solution and halt
- Step 4:** Build the set of indices E_S corresponding to equations for which P_{\min} is feasible and the corresponding powers in \mathbf{P}_W are smaller than P_{\min}
- Step 5:** Set $P_{W,i}$ to P_{\min} for $i \in E_S$ and computes the remaining powers of the power vector \mathbf{P}_W by solving the corresponding equations
- Step 6:** If at least one element of \mathbf{P}_W is higher than P_{\max} , the system is unfeasible and halt
- Step 7:** Find the set U of unsatisfied mobiles for which the CIR is smaller than the CIR target.
If U is empty, \mathbf{P}_W is the solution and halt
- Step 8:** Set $E_S = E_S - U$ and repeat from step 4

In the worst case, the algorithm needs at maximum $\text{card}(E_S)$ iterations to converge.

The GCOPC method can be used for all centralized power control algorithm and for all types of pathgain matrices (Wu matrix, generic simplified matrix, FDMA matrix, etc.). Moreover, the GCOPC method can be slightly modified to take into account different levels of lower-bounds and upper-bounds in the system.

3.6 Concluding Remarks

In this chapter, we have extended the optimum power control algorithm in CDMA noisy and noiseless systems using a generic equation of the CIR. The extended algorithm takes into account residual intracell-interference and specific TDD interferences during crossed slots. Moreover, we have developed a generic optimum power control algorithm using a simplified pathgain matrix that converges to the same maximum achievable CIR as existing algorithms. In this algorithm, we control the total transmitted powers by base stations in downlink and the received powers in uplink, instead of the specific transmitted powers of mobiles. The simplified generic algorithm can be used for uplink, downlink and crossed slots to investigate the performance of the system during these

slots and may be used to estimate system capacity. Due to its simplicity, the proposed algorithm allows us to study complex slot allocation algorithms and the behavior of the system using different propagation models. Moreover, the proposed centralized approach can be used to design simple efficient distributive power control algorithms.

Based on the simplified algorithm, we have proposed a generic mobile-based stepwise removal algorithm that decreases the outage probability by removing some mobiles. As far as we know, the generic mobile-based stepwise removal algorithm is the first mobile stepwise removal algorithm that can be applied to crossed slots.

Moreover, we have proposed an iterative optimum power control that allows all mobiles of achieving a CIR target in a noisy lower-bounded and upper-bounded system. We have shown that the proposed algorithm converges to the power vector with the least sum of powers.

Chapter 4

Iterative Power Control

In next generation mobile networks, the demand on high data rate services is expected to increase. The high data rate services need more power than the current voice-dominated service, and thus the interference in next generation mobile networks is expected to increase. Moreover, UMTS uses the CDMA technique, which is an interference-limited technique. Therefore, interference reduction and power control are essential features to increase system capacity.

Power control is a very active field of research in mobile telecommunications systems and much work has been intended to optimize the transmitted power. Centralized optimum power control algorithms require measuring all pathgains and communicating this measurement to a central unit. This task is highly complex and is very difficult to be implemented, especially in highly loaded radio systems. Instead, algorithms that needs less information, such as iterative power control algorithms, are more attractive for real systems. The design of these algorithms is based on centralized optimum power control algorithms and they generally converge to the same maximum achievable CIR as centralized algorithms.

The radio interface is a very hostile environment due to interference and unstable radio propagation characteristics. Therefore, pathgains are not stationary and experience high fluctuations. Pathgains fluctuations may lead to QoS level degradation if the power control scheme is not fast enough. Therefore, adaptive power control are used to assess this problem.

In this chapter, we present the existing iterative power control algorithms for noiseless and noisy systems. In section 4.2, we present the standardized power control for UMTS systems and we propose an adaptive variant of this algorithm that mitigates the problem of pathgain fluctuations.

4.1 Iterative Power Control Algorithms

In this section, we present the existing iterative power control algorithms in noisy and noiseless systems, where all power update steps are allowed. We assume that these algorithms are performed to N simultaneous active mobiles.

4.1.1 Iterative Optimum Power Control Algorithms

Iterative power control algorithms that converge to the Perron-Frobenius value are grouped into the iterative optimum power control class. In this type of algorithms, users start their transmission with an initial power vector \mathbf{P}_0 and update their powers in a distributed manner until the convergence of the algorithm. A generic formulation of the distributed form of these algorithms can be represented by an algorithm Ψ :

$$P_{\tau,i}^{(\nu+1)} = \Psi \left(\mathcal{E}_{P_{\tau,i}}^{(\nu)}, \Gamma_{\ell,i,j}^{(\nu)} \right),$$

where the subscript ν denotes the iteration number and $\mathcal{E}_{P_{\tau,i}}^{(\nu)}$ is the set of previous transmitted powers of mobile i until iteration ν . The cardinality of $\mathcal{E}_{P_{\tau,i}}^{(\nu)}$ depends on the order of power control algorithm (e.g. for second order algorithms, $\mathcal{E}_{P_{\tau,i}}^{(\nu)} = \{P_{\tau,i}^{(\nu-1)}, P_{\tau,i}^{(\nu)}\}$). In these algorithms, the receiver measures the CIR and reports its value to the transmitter.

In this type of power control algorithms, fast convergence rate is needed to cope with possible changes in pathgain matrix. A centralized version of iterative algorithms can be used also. In this type of algorithms, all information are reported to a central unit that distributes power decision throughout the network.

Distributed Balanced Algorithm

The first distributed optimum power control algorithm was proposed by Meyerhoff [Mey74] to estimate the maximum achievable CIR in satellite systems. This algorithm is derived from the well-known numerical linear algebra method, *Power method*, that is used to compute the dominant eigenvalue of nonnegative matrices [GVL96]. In [Zan92a], Zander has extended the latter algorithm to FDMA systems and the new algorithm has been called Distributed Balanced (DB) algorithm. This algorithm can be represented by:

$$P_{\tau,i}^{(\nu+1)} = c^{(\nu)} P_{\tau,i}^{(\nu)} \left(1 + \frac{1}{\Gamma_{\ell,i,j}^{(\nu)}} \right),$$

where $c^{(\nu)}$ is a normalization factor communicated by a central unit and that can be changed at each iteration. The normalization factor is used to guarantee that the transmitted power is neither too high nor too low. An ideal value of $c^{(\nu)}$ is given in [Zan92a]:

$$c^{(\nu)} = \frac{1}{\max_{1+M \leq i \leq N+M} \left(P_{\tau,i}^{(\nu)} \right)}.$$

Distributed Power Control Algorithm

The distributed balanced algorithm has been enhanced by a the Distributed Power Control (DPC) algorithm in [GVG94]:

$$P_{\tau,i}^{(\nu+1)} = \frac{c^{(\nu)} P_{\tau,i}^{(\nu)}}{\Gamma_{\ell,i,j}^{(\nu)}}.$$

Fully Distributed Power Control Algorithm

It has been shown that DB and DPC algorithms converge to the maximum achievable CIR for noiseless systems with only local measurements and the normalization factor $c^{(\nu)}$. However, these algorithms require a normalization procedure in each iteration. In this procedure, all entities must communicate with a central unit to compute factor $c^{(\nu)}$, which is required by the power control algorithm; therefore, these algorithms are not fully distributed and induce an extra signaling traffic. In order to alleviate this problem, the Fully Distributed Power Control (FDPC) algorithm has been

proposed in [LL96]. The FDPC algorithm uses the same equation of DPC algorithm with some modifications:

$$P_{\tau,i}^{(\nu+1)} = \frac{\min\left(\Gamma_{i,j}^{(\nu)}, c\right)}{\Gamma_{i,j}^{(\nu)}} P_{\tau,i}^{(\nu)},$$

where c is a constant fixed by the network without global information exchanging, and $P_{\tau,i}^{(0)} = 1$ for all i . This algorithm converges to the maximum achievable CIR $\gamma_{\mathbf{W},\ell}^*$ (see § 3.2.1) with probability one if $c \leq \gamma_{\mathbf{W},\ell}^*$:

$$\lim_{\nu \rightarrow \infty} \Gamma_{i,j}^{(\nu)} = \gamma_{\mathbf{W},\ell}^*.$$

However, the transmitted powers of all users decrease with time and $\lim_{\nu \rightarrow \infty} P_{\tau,i}^{(\nu)} = 0$; therefore the algorithm cannot be implemented in real systems where a lower-bound limits transmitted powers. Authors of [LL96] have proposed a variant where a protection power value δ is used to prevent transmitting power from dropping too low:

$$P_{\tau,i}^{(\nu+1)} = \max\left(\frac{\min\left(\Gamma_{i,j}^{(\nu)}, c\right)}{\Gamma_{i,j}^{(\nu)}} P_{\tau,i}^{(\nu)}, \delta\right).$$

As a result of this modification, the convergence of the FDPC algorithm is no more guaranteed.

Balanced Distributed Power Control Algorithm

The FDPC algorithm has been enhanced by the Balanced Distributed Power Control (BDPC) algorithm [HARW00] by limiting the transmitted power in a fixed range:

$$P_{\tau,i}^{(\nu+1)} = \eta_{\tau,i}^{(\nu)} P_{\tau,i}^{(\nu)}$$

where:

$$\eta_{\tau,i}^{(\nu)} = \begin{cases} \frac{\min\left(\Gamma_{i,j}^{(\nu)}, c\right)}{\Gamma_{i,j}^{(\nu)}} & \text{if } P_{\tau,i}^{(\nu)} \geq P^{\text{UpBound}} \\ \eta_{\tau,i}^{(\nu-1)} & \text{if } P^{\text{LowBound}} \leq P_{\tau,i}^{(\nu)} \leq P^{\text{UpBound}} \\ \frac{\max\left(\Gamma_{i,j}^{(\nu)}, c\right)}{\Gamma_{i,j}^{(\nu)}} & \text{if } P_{\tau,i}^{(\nu)} \leq P^{\text{LowBound}} \end{cases}$$

and P^{UpBound} , P^{LowBound} are the upper and lower bounds of transmitted powers, which are fixed in advance. The convergence of the BDPC algorithm is slightly slower than the convergence of the DPC algorithm but the former insures that powers are in given range.

The speed of convergence of these algorithms is an decreasing function of the ratio between the second-largest and the largest eigenvalue of matrix $\mathbf{Z}_{\mathbf{W},\ell}$ [Zan92a].

4.1.2 Iterative Algorithms in Noisy Systems

In noisy systems where a CIR target γ_0 is required by users, the power control problem is equivalent to the optimization problem $(P_{\{\gamma_0, \geq 0\}, \geq 0})$. We can prove as in corollary 3.1, that the latter optimization problem is equivalent to solve equation $\mathbf{A}_{\mathbf{W},\ell} \mathbf{P}_{\mathbf{W},\ell} = \hat{\mathbf{N}}_{\mathbf{W},\ell}$, where $\mathbf{A}_{\mathbf{W},\ell} = ((1 + \gamma_0) I_N - \gamma_0 \mathbf{Z}_{\mathbf{W},\ell})$

and $\hat{\mathbf{N}}_{W,\ell} = \gamma_0 \mathbf{N}_{W,\ell}$. Unlike previous algorithms, the optimization problem ($\mathbf{P}_{\{\gamma_0, \geq 0\}, \geq 0}$) is based on the simultaneous Jacobi Over-Relaxation (JOR) method [GVL96], where the matrix $\mathbf{A}_{W,\ell}$ is split into two matrix $\mathbf{A}_{W,\ell} = \tilde{\mathbf{M}}_{W,\ell} - \tilde{\mathbf{L}}_{W,\ell}$. A general power update is given by:

$$\mathbf{P}_{W,\ell}^{(\nu)} = \tilde{\mathbf{M}}_{W,\ell}^{-1} \tilde{\mathbf{L}}_{W,\ell} \mathbf{P}_{W,\ell}^{(\nu)} + \tilde{\mathbf{M}}_{W,\ell}^{-1} \hat{\mathbf{N}}_{W,\ell}$$

The iterative algorithm converges to the solution of $\mathbf{A}_{W,\ell} \mathbf{P}_{W,\ell} = \hat{\mathbf{N}}_{W,\ell}$ for any $\mathbf{P}_{W,\ell}^{(0)}$, if and only if the Perron-Frobinus eigenvalue of $\tilde{\mathbf{M}}_{W,\ell}^{-1} \tilde{\mathbf{L}}_{W,\ell}$ is smaller than unity [Ber03]: $\rho(\tilde{\mathbf{M}}_{W,\ell}^{-1} \tilde{\mathbf{L}}_{W,\ell}) < 1$. Matrices $\tilde{\mathbf{M}}_{W,\ell}$ and $\tilde{\mathbf{L}}_{W,\ell}$ should be chosen carefully to conserve consistency and convergence. Depending on the choice of these matrices, several algorithms can be derived.

Foschini and Miljanic Algorithm

Iterative power control algorithms in noisy systems were first introduced by Foschini and Miljanic [FM93]. Each user proceeds to iteratively update its transmitted power to the necessarily level needed to achieve the desired QoS level by supposing that other users will conserve their power levels. However, other users are proceeding in a similar way. Nevertheless, if $\gamma_0 \leq \gamma^*$ all users achieve the desired CIR level γ_0 no matter what initial power is used. In this algorithm, $\tilde{\mathbf{M}}_{W,\ell} = \frac{1}{\beta} \mathbf{I}_N$ and $\tilde{\mathbf{L}}_{W,\ell} = \frac{1}{\beta} \mathbf{I}_N - \mathbf{A}_{W,\ell}$:

$$P_{\tau,i}^{(\nu+1)} = (1 - \beta) P_{\tau,i}^{(\nu)} + \beta \frac{\gamma_0}{\Gamma_{\ell,i,j}^{(\nu)}} P_{\tau,i}^{(\nu)},$$

where β is a constant fixed by the network. This algorithm converges to γ_0 if all eigenvalue modulus of matrix $(\mathbf{I}_N - \beta \mathbf{A}_{W,\ell})$ are strictly less than unity. Moreover, the convergence speed of the algorithm is an increasing function of β . Therefore, high values of β are suited but must satisfy the convergence constraint and it is found to be in the interval $[0, 1]$ [Ber03]. The fastest convergence of the algorithm for which convergence is assured was found for $\beta = 1$ [FM93]. For this value of β , the Foshini-Miljanic (FM) algorithm becomes the DPC algorithm:

$$P_{\tau,i}^{(\nu+1)} = \frac{\gamma_0}{\Gamma_{\ell,i,j}^{(\nu)}} P_{\tau,i}^{(\nu)},$$

and the convergence condition becomes $\rho(\mathbf{I}_N - \mathbf{A}_{W,\ell}) < 1$ and thus γ_0 must be less than $\rho(\mathbf{Z}_{W,\ell})$.

Mitra has extended the latter algorithm with $\beta = 1$ to an asynchronous version [Mit93]. Author has proved that the algorithm converges to the CIR level despite that user power updates are not harmonized.

Distributed Constrained Power Control Algorithm

The power limitation constraint was considered in the Distributed Constrained Power Control (DCPC) algorithm [GZ94][GZY95]. The DCPC algorithm is a constrained version of the Foschini and Miljanic algorithm and converges in both synchronous and asynchronous modes:

$$P_{\tau,i}^{(\nu+1)} = \min \left(\frac{\gamma_0}{\Gamma_{\ell,i,j}^{(\nu)}} P_{\tau,i}^{(\nu)}, P_{\ell,\max} \right),$$

where $P_{\tau,i}^{(0)}$ is chosen arbitrary in the interval $[0, P_{\ell,\max}]$. A variant of this algorithm is used in uplink of the TDD mode.

It is reported that DCPC converges with a geometric rate to a fixed CIR. However, this rate becomes slow when approaching the fixed CIR level [HY98].

Second Order Constrained Power Control Algorithms

All previous iterative algorithms use only $P_{\tau,i}^{(\nu)}$ to compute $P_{\tau,i}^{(\nu+1)}$. A second order constrained algorithm based on the Successive OverRelaxation (SOR) [GVL96] method was proposed in [JK00] to increase the rate of convergence. The second order algorithm is defined by the following equation:

$$P_{\tau,i}^{(\nu+1)} = \min \left[P_{\ell,\max}, \max \left(0, c^{(\nu)} \frac{\gamma_0}{\Gamma_{\ell,i,j}^{(\nu)}} P_{\tau,i}^{(\nu)} + (1 - c^{(\nu)}) P_{\tau,i}^{(\nu-1)} \right) \right],$$

where $P_{\tau,i}^{(0)}$ and $P_{\tau,i}^{(1)}$ are chosen arbitrary in the interval $[0, P_{\ell,\max}]$, and $c^{(\nu)}$ is the relaxation parameter and it is a nonincreasing sequence of control parameters. Therefore, the algorithm is not fully distributed. It was shown in [JK00], that the convergence of second-order algorithm is much faster than first order algorithms when a good relaxation parameter is used, in particularly near to the convergence point.

4.1.3 Other Power Control Algorithms

Power control is a very studied field of research in mobile telecommunications systems. Therefore, a high number of power control algorithms were proposed to enhance the convergence speed of the previous algorithms. In the following we cite only the principles of some existing algorithms.

A cooperative power control based on FDPC algorithm is proposed in [SW99a] for CIR-balancing. In this semi-distributed algorithm, communication between base stations are incorporated to estimate the minimum CIR, which is in turn used by the power update process. This algorithm has shown better performance than DB and DPC algorithms.

A general power control algorithm was suggested by Jantti and Kim [JK03]. In the block-distributed algorithm of the latter paper, different degree of distributiveness are allowed depending on the size of blocks. This leads to a different degree of availability and reliability of used pathgains. The main idea of this algorithm is to exploit the information about some measured blocks of pathgains to increase the convergence rate. The convergence rate is increased when more pathgain information are communicated to central units (i.e. when the block size is increased). When the block size is reduced to one user, the DCPC algorithm is retrieved.

In the last few years, a powerful technique, known as krylov subspace technique [GVL96], was developed to solve linear algebra systems. This method outperforms the successive overrelaxation technique used in the second-order power control algorithm. A centralized algorithm, called Generalized Minimum RESidual (GMRES) algorithm, based on the krylov subspace technique was introduced in [LG02]. The GMRES algorithm is particularly suited in system with high loads as UMTS, due to its fast convergence.

4.2 Standardized Power Control

Despite the benefits of the optimum power control, its centralized implementation is very complex and induces heavy signalization traffic. Therefore, iterative power control algorithms are the best candidates to be used in mobile telecommunications systems. The simplest iterative power control algorithm is the step-by-step power control. In this type of algorithms, the power is either increased or decreased as a reaction to some specific receiver commands.

4.2.1 3GPP Power Control Algorithms

Power control algorithms in UMTS were specified in the 3GPP standardization forum [TS203a] [TS203b] for FDD and TDD modes respectively. Proposals for UMTS involve a combination of inner-loop and outer-loop power control.

The main objective of the outer-loop is to dynamically adjust the target CIR, called CIR_{target} , according to a fixed Block-Error Rate (BLER) or Bit-Error Rate (BER) depending on propagation channel characteristics. The outer-loop power control procedure is performed by mobiles and RNC equipment. The CIR_{target} of a given radio channel is achieved by the inner-loop power control. Inner-loop power control algorithm is performed by both mobiles and Node Bs [TS203c].

Inner-loop power control algorithms in the downlink of the TDD mode and in both link directions of the FDD mode are based on a closed-loop control, whereas an open-loop control is used in uplink of the TDD mode. The closed-loop power control algorithm is used after an initial phase that uses an open-loop power control algorithm [TS203a].

The drawback of the power control variant in the TDD mode is that the rate of the feedback command in slow rate applications is reduced to 100 Hz compared to 1500 Hz in the FDD mode [KLR03].

Uplink Inner-loop Power Control Algorithm

Unlike the FDD mode, the TDD mode uses the same bandwidth for uplink and downlink. Therefore, channel propagation characteristics are the same in both link directions. Thus, measurements taken in a given link direction can be used for the second link direction procedures and open-loop power control can be used. This type of power control is therefore used in uplink inner-loop power control of the TDD mode; in each cell, a broadcast channel can be transmitted over one or several downlink slots (e.g. the Primary Common Control Physical Channel P-CCPCH carrying the Broadcast channel BCH). The broadcast channel is transmitted with a fixed power, which allows mobiles to measure their pathgains toward base stations. Furthermore, each base station broadcasts the interference profile I_{BTS} of uplink slots and the CIR_{target} of each mobile (figure 4.1). These information are used to adjust mobile powers by using the following equation in the logarithmic scale:

$$P_{m,i} = \alpha L_{P-CCPCH} + (1 - \alpha)L_0 + I_{BTS} + CIR_{target} + C \quad (4.1)$$

where $L_{P-CCPCH}$ represents the measured pathloss and L_0 the long term average pathloss. The Constant C is communicated by the network. This constant allows the network operator to adjust the power of mobiles. The weighting parameter α is calculated by mobiles and reflects the reliability of the downlink pathloss estimation as a measure of uplink pathloss. The method to compute α is

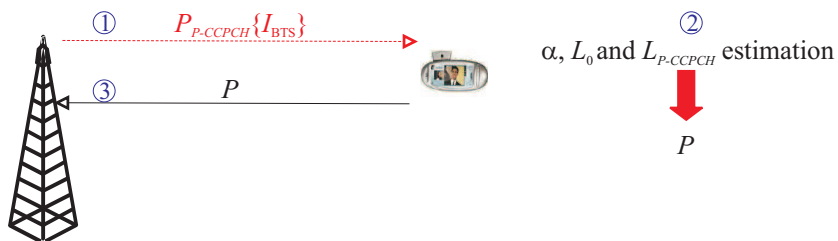


Figure 4.1: Uplink inner-loop power control algorithm steps (UTRA TDD)

not defined in the standard, but a useful function might include the length of the delay between the downlink and uplink slots.

We can easily justify equation (4.1) using the following equations. The open-loop power control is based on DPC algorithm presented in section 4.1.1:

$$P_{m,i}^{(\nu+1)} (\text{dBm}) = \text{CIR}_{target} (\text{dB}) - \Gamma_{i,j}^{(\nu)} (\text{dB}) + P_{m,i}^{(\nu)} (\text{dBm})$$

The difference $P_{m,i}^{(\nu)} - \Gamma_{i,j}^{(\nu)}$ in the DPC algorithm is approximated by the sum of the interference profile and the weighted pathloss by combining equations (3.19) and (2.6) in logarithmic scale:

$$\Gamma_{i,j}^{(\nu)} (\text{dB}) \simeq P_{m,i}^{(\nu)} (\text{dBm}) - I_{BTS} (\text{dBm}) - L (\text{dB})$$

This approximation is used to allow the algorithm to follow the fluctuation of pathgains. Therefore:

$$P_{m,i}^{(\nu+1)} (\text{dBm}) \simeq \text{CIR}_{target} (\text{dB}) + I_{BTS} (\text{dBm}) + L (\text{dB})$$

Downlink Inner-loop Power Control Algorithm

The downlink inner-loop power control procedure of the TDD mode is the same as the inner-loop of the FDD mode. Two algorithms were proposed in 3GPP specifications for the FDD mode [TS203a]. In the first algorithm, the transmitted power is updated each slot while it may be updated once each 5 slots in the second algorithm. Only the first algorithm is evaluated in the following; each slot, the mobile estimates the received CIR and compares it to CIR_{target} . When the estimated CIR, called CIR_{est} , is higher than CIR_{target} , the Transmitted Power Command (TPC) is set to "0" and the transmitted power is decreased by Δ_{step} dB. Otherwise, the TPC is set to "1" and the transmitted power is increased by Δ_{step} dB (figure 4.2). The same procedure is used for downlink inner-loop power control of the TDD mode. However, the frequency of the feedback is 1 TPC each frame (i.e. 15 times slower than the first algorithm of the FDD mode) [TS203b]. In most UMTS formats, the TPC command is repeated on two bits as an error-protection redundancy. The power control step is fixed by higher layers and it depends on radio and service parameters. Several values of the order of 1 dB are proposed in the specification [TS203a].

4.2.2 Problem Formulation

Iterative power control algorithms under discrete power level, such as closed-loop power control algorithms, were studied in [ARZ98] and it was shown that oscillations around the convergence point may appear. Alternately, an asynchronous discrete power control was proposed in [HC00]. The power update in the asynchronous discrete algorithm is done using a single bit up/down command. Authors have shown by simulation that the average number of users in the convergence

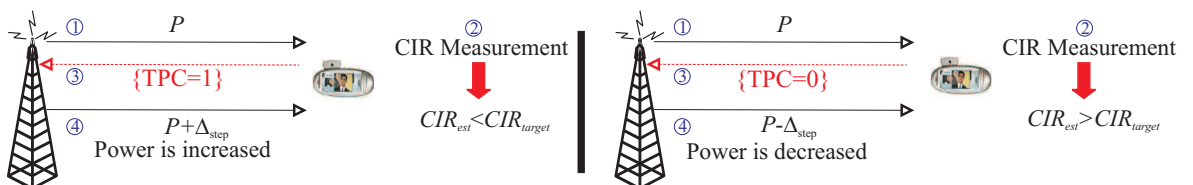


Figure 4.2: Downlink inner-loop power control algorithm steps

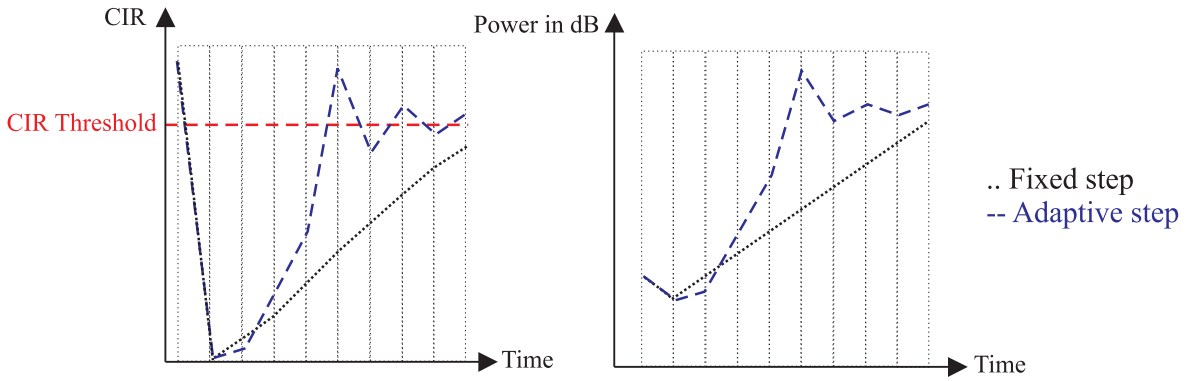


Figure 4.3: A comparison between fixed-step and adaptive-step power control convergence

zone is a decreasing function of the bit error rate that can change bit command information. A two bit up/down power control algorithm was proposed in [SW99b] to reduce the impact of the bit error rate.

Adaptive Steps

In wireless telecommunications systems, frequent fluctuations occur in the radio interface. Hence, the received CIR may change significantly and very fast. In many cases, the presently-proposed 3GPP power control cannot track these variations because the power update step in the 3GPP power control algorithm is fixed. In other words, the power is updated with a fixed step whatever the magnitude of variations in pathloss and interference profile. This leads to the degradation of QoS levels and some channels may be dropped. In figure 4.3, the CIR of a mobile is dropped to a low level suddenly (e.g. a big obstacle appears between the mobile and its server). For small Δ_{step} , the convergence of the fixed-step power control is very slow. However, if high value of Δ_{step} is used always, the oscillation around the CIR_{target} will have high variance. In order to avoid this type of situation, adaptive-step power control may be used. In this type of power control, the power-update step accommodates CIR fluctuations. Some methods were proposed to increase the adaptation of the power control algorithm by using asymmetric power control steps: different step values for increasing and decreasing power [KLR03]. Other methods suggest an adaptive power variation step in order to decrease oscillations around CIR_{target} and to increase the speed of the power control when the difference between CIR_{est} and CIR_{target} is very high [NLG02][NRB02]. In the Adaptive-Step Power Control (ASPC) algorithm proposed in [NLG02], if the base station detects the same TPC from a mobile in a set of consecutive slots, the step dedicated to this mobile is increased. On the contrary, if an alternative sequence of up and down TPCs of a mobile are received by a base station, the step dedicated to this mobile is reduced. The authors of [VRK00][VKK01][RVK01] propose a self-tuning predictor algorithm where the TPC is coded on 2, 3 or 4 bits instead of one. In these latter papers, the parameters of the power control change according to the quality measurements of the system level, which can be deduced from the command and the CIR error history. The self-tuning predictor algorithm ameliorates significantly system performance, but imposes some modifications on the Uu interface which is standardized by 3GPP bodies.

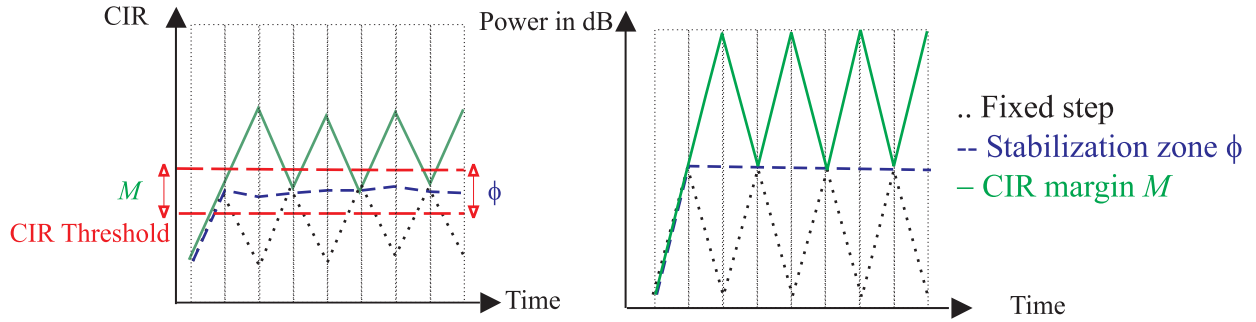


Figure 4.4: Solving the oscillation problem by using either a CIR margin or a stabilization zone

CIR Margin

Adaptive power control algorithms reduce oscillations around the CIR_{target} . However, the limited amplifier precision prevents transmitters from using very low power control steps; therefore, oscillations are not totally eliminated. The CIR oscillation is due to the fact that the power is either increased or decreased even if the CIR is very close to CIR_{target} . Therefore, the received CIR may oscillate around CIR_{target} with high variance. One solution to the oscillation problem is to use a CIR margin M and to define $CIR_{target} + M$ as the new CIR target. The new CIR target is called CIR_{target}^M . When the estimated CIR of a mobile is close to CIR_{target}^M , a power decrease may degrade the CIR of the mobile in the next slot if the margin is not high enough. Therefore, a high CIR margin is suited to minimize the outage probability. However, increasing M decreases the system maximum capacity due to the high value of CIR_{target}^M . Moreover, the power consumption is an increasing function of CIR_{target}^M . Hence, a trade-off must be taken between the maximum capacity, power consumption and the outage probability.

Stabilization Zone

In order to alleviate the latter problem, we propose an adaptive-step power control with stabilization zone Φ in [NNL04a] (figure 4.4). In the stabilization zone, the transmitted power is kept stable by a specific algorithm. Therefore, the CIR may be kept at a quasi-fixed level above the CIR_{target} . The stabilization zone can be considered as an adaptive CIR margin.

4.2.3 Modified Adaptive Power Control

In existing power control algorithms, a mobile can request only a power decrease or increase from its server. However, the mobile cannot inform its server that CIR_{est} is very close to CIR_{target} and that the power must be stabilized. Thus, CIR_{est} can always oscillate even if the radio interface parameters are stable. Our proposed algorithm adds intelligence to mobiles in order to command the base station to stabilize its power. Unlike the algorithm of [NRB02], the proposed algorithm does not need more TPC bits than the conventional WCDMA power control algorithm. Nevertheless, we show by simulation that the use of a stabilization zone decreases, at the same time, outage probability and power consumption.

The Modified Adaptive Power Control Algorithm

We propose the Modified Adaptive Power Control (MAPC) algorithm as an evolution of the existent adaptive power control algorithms. The aim of the MAPC algorithm is to reduce the oscillation variance around the CIR_{target} by creating a stabilization zone Φ above the CIR_{target} and to reduce power consumption. The MAPC algorithm combines adaptive-step power control algorithm with the new concept of stabilization zone to completely eliminate oscillations. When CIR_{est} of a mobile is in the stabilization zone, the mobile generates an alternative TPC sequence (up and down). Consequently, the base station reduces the power step dedicated to this mobile and stabilizes its transmitted power. The MAPC algorithm uses also an adaptive power control step to mitigate the impact of the radio interface variation. Moreover, the MAPC algorithm leads to the stabilization of the received CIR above the desired value with the same signalization load as the 3GPP power control algorithm. Furthermore, the use of a stabilization zone decreases the needed margin value, which can be omitted also; therefore, the system maximum capacity is increased and the power consumption is reduced. This algorithm may be used for both link directions in the FDD mode and for the downlink of the TDD mode (i.e. for closed-loop power control).

We have proposed another adaptive power control algorithm in [NNL04b] that decreases power consumption though the same outage probability is maintained. However, this algorithm is not presented in the dissertation because its performance is quite similar to the performance of the MAPC algorithm in term of outage probability.

Mobile Station Algorithm

In the MAPC algorithm, each mobile station compares CIR_{est} with CIR_{target} and generates TPC commands according to the following algorithm (figure 4.5):

- ◇ If $CIR_{est} > CIR_{target} + \Phi$, then the transmitted TPC is set to "0" requesting a transmit power decrease.
- ◇ If $CIR_{target} \leq CIR_{est} \leq CIR_{target} + \Phi$, then the transmitted TPC is the complementary of the previous TPC (saved in the command register) requesting an unchanged transmitted power. In this interval, mobiles generate alternative up and down TPC commands.
- ◇ If $CIR_{est} < CIR_{target}$, then the transmitted TPC is set to "1" requesting a transmit power increase.
- ◇ The TPC is saved in a command register of one bit.

Parameter Φ (in dB) is the range of the stabilization zone. For each mobile, RRC layer in the core network sets CIR_{target} and Φ based on the system load, the service type and radio interface characteristics. These parameters are sent to mobile stations via signalization channels.

Base Station Algorithm

We remind that the CIR_{target} is fixed by the outer-loop power control. The inner-loop of the MAPC algorithm has to be executed by the base station in the network side to increase the algorithm speed. The base station receives the TPC commands from mobile stations and analyzes the command of each mobile station independently. After each power control iteration, these commands are saved in a command register, where only one bit is dedicated to each mobile.

Each base station executes the following algorithm to set the power of a mobile (figure 4.6):

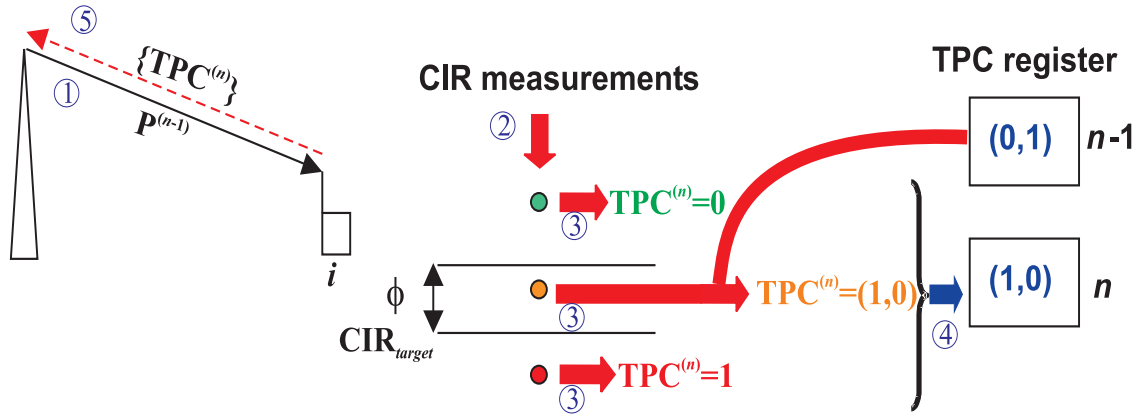


Figure 4.5: MAPC algorithm steps in mobiles

- ◇ If the instantaneous and the saved TPC commands are the same, the transmitted power is updated using the previous Δ_{step} , which is then multiplied by μ .
- ◇ If the instantaneous TPC command is different from the saved command, Δ_{step} is divided by λ and the transmitted power is maintained stable.
- ◇ The TPC command is saved in the command register and the power control step is saved in a 3 bit register (i.e. only 8 values of power control steps are allowed).

Parameters λ , μ , κ and the initial value of Δ_{step} , are fixed by the RRC layer in the core network. Furthermore, the power control step margin is limited by the precision of the used amplifier and is always in the interval $[\Delta_{min}; \Delta_{max}]$ where only Δ_n values are allowed. The value of Δ_n must be lower than 8 to fit with the register size.

4.2.4 Simulation Model

The MAPC algorithm is evaluated by simulation using Matlab. It is compared to the 3GPP closed-loop power control variant and to the ASPC algorithms [NLG02]. An outdoor Manhattan scenario

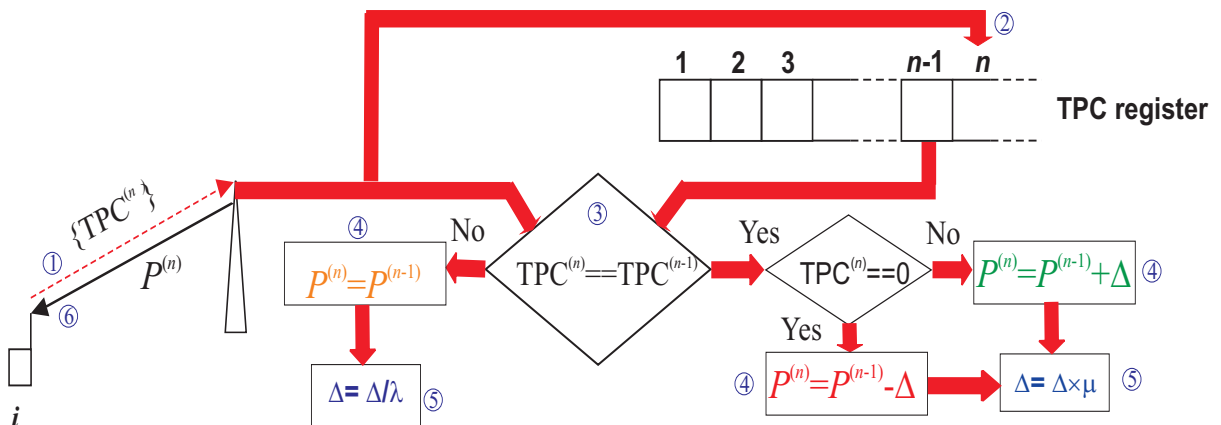


Figure 4.6: MAPC steps in base stations (all equations are in dB)

Table 4.1: Power limits and receiver thermal noise power

	BS	MS channel
Max Tx Power [dBm]	33	20
Power control range [dB]	30	25
Receiver thermal noise power [dBm]	-	-98

with 5×5 blocks is used to evaluate power control algorithms. The block size is 200×200 meters. Mobiles are uniformly distributed and each mobile is served by the best-received base station. A wrap-around technique is used in order to overcome cell boundary effects. Only FDD mode system is simulated. The performance of the TDD mode in term of outage probability and power consumption will be the same for the same channel propagation characteristics. Only, the convergence time is higher in the TDD mode than in the FDD mode (i.e. it is multiplied by 15).

Common channel powers, call dropping, call admission control, and error detection and correction are not considered in simulations. These procedures are not considered to reduce their impact and amplify the power control impact on QoS levels.

The assumed propagation model is an Okumura-Hata-Cost231 model with shadowing; the path-gain between mobile i and base station j is modeled as $G_{i,j} = a_{i,j}/d_{i,j}^{3.5}$, where $d_{i,j}$ is the mobile-to-base distance expressed in meters and the coefficient $a_{i,j}$ models the shadowing effect. The coefficient $a_{i,j}$ is a log-normal random variable with zero mean and 10 dB standard deviation [UMT98]. A correlation coefficient of 0.5 is considered between the shadow fading coefficients of a mobile and neighboring base stations.

The simulated service is 8 kbps circuit-switched service with 100% activity factor. The CIR_{target} is $\gamma_0 = -17$ dB and a perfect CIR estimation is considered. The transmitted power limits and the receiver thermal noise power are presented in table 4.1. The characteristics of mobiles correspond to class 3 mobiles defined in [TS202]. The initial transmitted powers have random values between the minimum value and 10% of the maximum transmitted power.

We have investigated several combinations of ASPC and MAPC algorithm parameters (i.e. λ , μ , Φ and M) and we have deduced that the values in table 4.2 are the optimal values in term of minimizing the outage probability for the studied system. In these simulations, the values of Φ and M ranged from 0 to 1 dB with a 0.1 dB step. The results of these simulations are not shown in this thesis. In real systems, these values can be determined in the dimensioning phase of the network.

Algorithm performance is evaluated using frame-outage probability, which is the probability that the geometric average of CIR $\Gamma_{TTI,i,j}$ over one Transmission Time Interval (TTI, i.e. 20 ms) falls below CIR_{target} (see section 2.4).

4.2.5 Simulation Results

First, we evaluate the system performance by Monte Carlo simulations for 100 independent mobile configurations. In each configuration, 600 slots are simulated (i.e. 400 ms) with the 3GPP variant

Table 4.2: Power control parameters

initial Δ_{step}	λ	μ	Δ_{max}	Δ_{min}	Δ_n	Φ	M_{MAPC}	M_{ASPC}
1 dB	2	4	4 dB	0.25 dB	5	0.3 dB	0 dB	0.2 dB

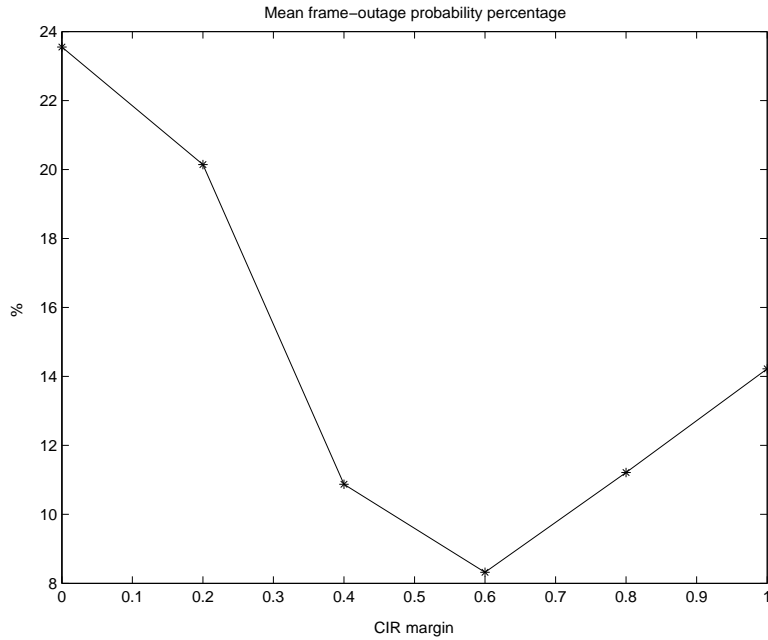


Figure 4.7: The mean frame-outage probability percentage for different values of the margin M when the 3GPP power control algorithm is used in a system with 26 mobiles/cell.

algorithm, the ASPC algorithm and the MAPC algorithm. The limited simulation time does not affect the mean frame-outage probability nor the mean total transmitted power due to the fast convergence of the three algorithms (i.e. less than 100 slots). After the convergence, the system hold on in a periodic state, where the same performance is repeated at a fixed period. We assume that mobiles are active in the downlink during all simulation time. The mean transmitted power and the mean frame-outage probability are averaged over the simulation period.

CIR Margin Impact

In figure 4.7, we present the impact of CIR margin (without stabilization zone) on the mean frame-outage probability when the 3GPP power control algorithm is used in a system with 26 mobiles/cell. The minimum mean frame-outage probability (8.3 %) is reached with a 0.6 dB CIR margin, and therefore, system maximum capacity is reached with a 0.6 dB CIR margin. For a cell load of 26 mobiles/cell, the mean frame-outage percentage is drastically reduced when the optimal CIR margin is used (from 23.6% without CIR margin to 8.3% with the optimal CIR margin). Moreover, we studied the impact of CIR margin for different cell loads and we have always found the same optimal CIR. As we can see, the optimal CIR margin is equal to the half of the power control step. This can be justified by the fact that within the stable phase, the majority of mobile CIRs oscillate around CIR_{target}^M with a standard deviation around 0.5 dB. Therefore, the CIR of these mobiles do not fall below CIR_{target} which is equivalent to $\text{CIR}_{target}^M - 0.5$ in this case.

Stabilization Zone Impact

The impact of the stabilization zone size combined with a CIR margin on the MAPC algorithm is shown in figure 4.8 for a cell load of 26 mobiles/cell. This figure shows that the optimal value of Φ is 0.3 dB with no CIR margin. For these parameters, the mean frame-outage probability is 0.4%.

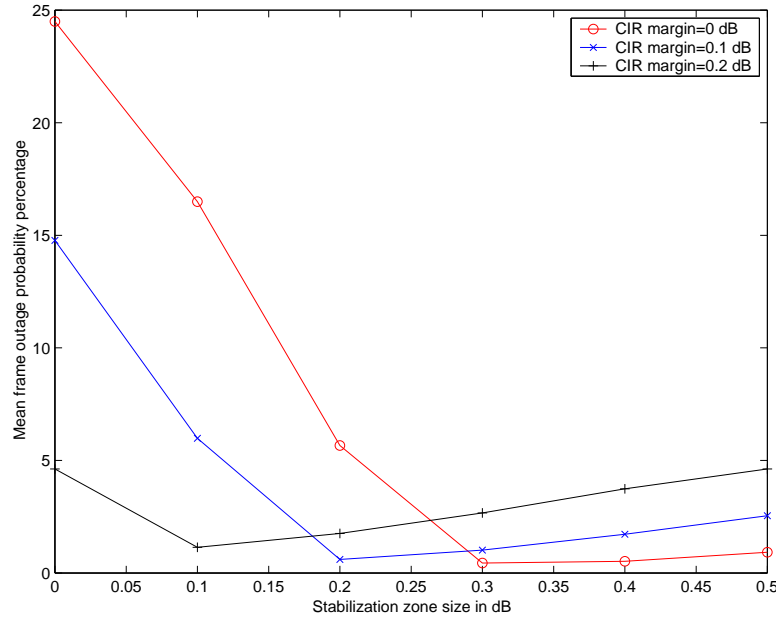


Figure 4.8: The mean frame-outage probability percentage as a function of Φ for different values of M and with a cell load of 26 mobiles/cell.

Furthermore, the optimal value of Φ as a function of the CIR margin is a decreased function as expected. Besides, we notice that the stabilization zone size changes slightly the mean frame-outage probability when no CIR margin is used and Φ is greater than 0.3 dB. This behavior makes the algorithm more feasible in systems where CIR measure sensitivity is not very high.

Power Control Algorithms Performance

In figure 4.9, the mean frame-outage probability percentage is plotted as a function of the cell load. The 95% confidence interval is also plotted in this figure. The plotted results are the best results obtained by the studied algorithms: the 3GPP algorithm with a 0.6 dB CIR margin, the ASPC with 0.2 dB margin and the MAPC algorithm with a stabilization zone of 0.3 dB.

The MAPC algorithm gives the lowest frame-outage probability. The difference in the mean frame-outage probability percentages between the MAPC algorithm and existing algorithms is an increasing function of cell load. This property makes the MAPC algorithm suited in systems with high traffic load.

It should be noted that the mean frame-outage probability is considered without error detection and correction; therefore, the capacity of a real system will be higher when these procedures are used.

In figure 4.10, the mean total transmitted power is plotted as a function of cell load. This figure shows that the MAPC algorithm reduces the transmitted power of at least 1 dB from the ASPC algorithm for high loads and more than 3 dB from the 3GPP algorithm with the least outage probability. Furthermore, the power increase in adaptive algorithm is a convex function of cell load, while it is a concave function in the 3GPP algorithm; therefore, the convergence of total transmitted powers to the maximum allowed power is slower in adaptive algorithms. In a dynamic system where pathgains are not fixed and where the instantaneous cell load is variable, the mean

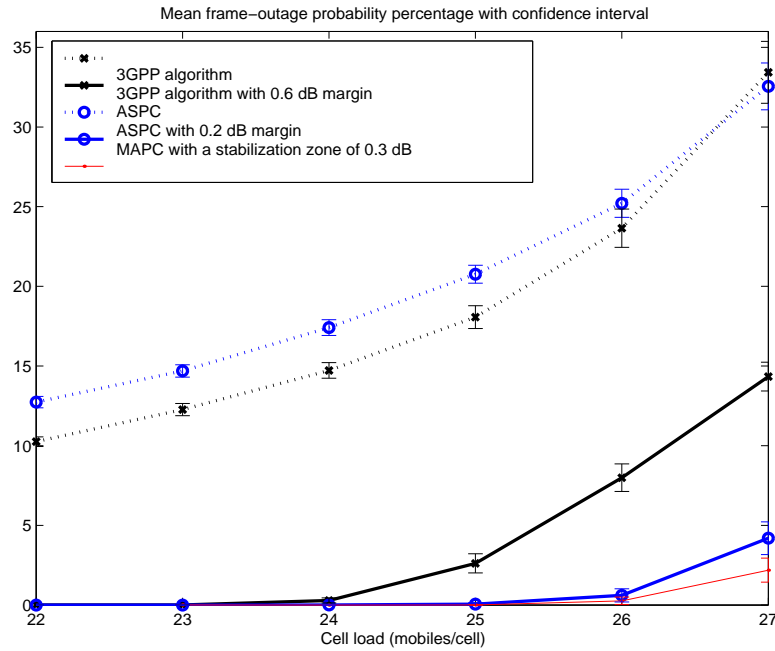


Figure 4.9: The mean frame-outage probability percentage for different cell loads and a fixed mobile configuration.

power consumption is thus, reduced by adaptive algorithms.

Finally, figure 4.11 represents the convergence rate of the three algorithms. The presented convergence rate is averaged over all mobile configurations. In this figure, we can see that the adaptive algorithms have approximately the same convergence rate. Moreover, the convergence of these algorithms is faster than the convergence of the 3GPP algorithm. An interesting behavior of the 3GPP algorithm can be noted in this figure: the outage probability decreases to a low level than it increases. This behavior can be explained by the fact that at a given instant, the CIRs of some mobiles are above CIR_{target}^M with a margin. However, the power control tends to decrease the power of these mobiles until all CIRs are near to CIR_{target}^M . Thereby, the CIR of all mobiles oscillate around CIR_{target}^M .

TPC Error Impact

We investigate the impact of errors in TPC commands to the performance of power control algorithms. Fixed BER rate value of 5%, 10% and 15% are used [KLR02]. In figure 4.12, we present the mean-frame outage probability for the MAPC algorithm when TPC BER is 10%. From this figure, it can be seen that even when TPC errors occur, the MAPC is still providing the lowest outage probability compared to other algorithms, even if TPC errors are not considered for the latter algorithms.

In figure 4.13, the impact of the TPC BER on the mean-frame outage probability given by the MAPC is presented. It can be seen that this probability is increasing almost linearly with the TPC BER. Moreover, an increase of 100% can be noticed when the TPC BER is 15%.

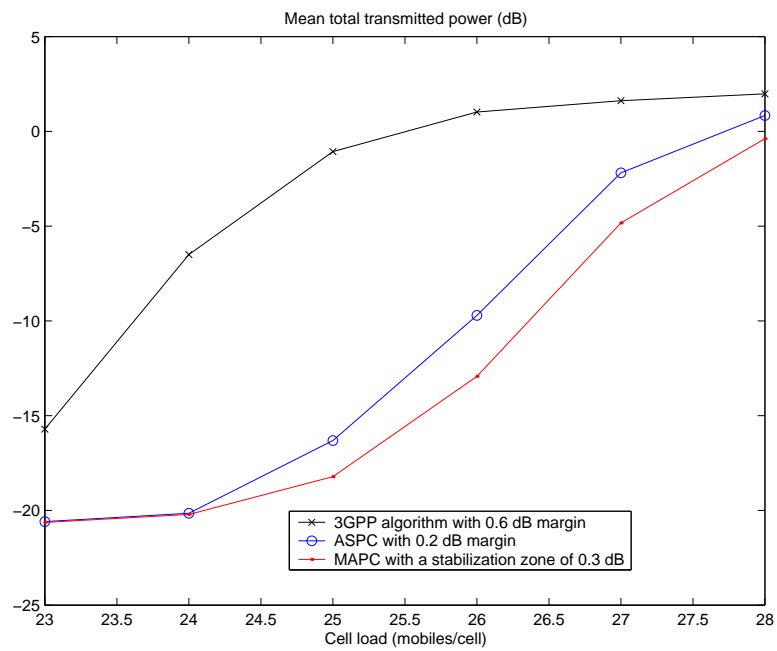


Figure 4.10: The mean total transmitted power as a function of the cell load

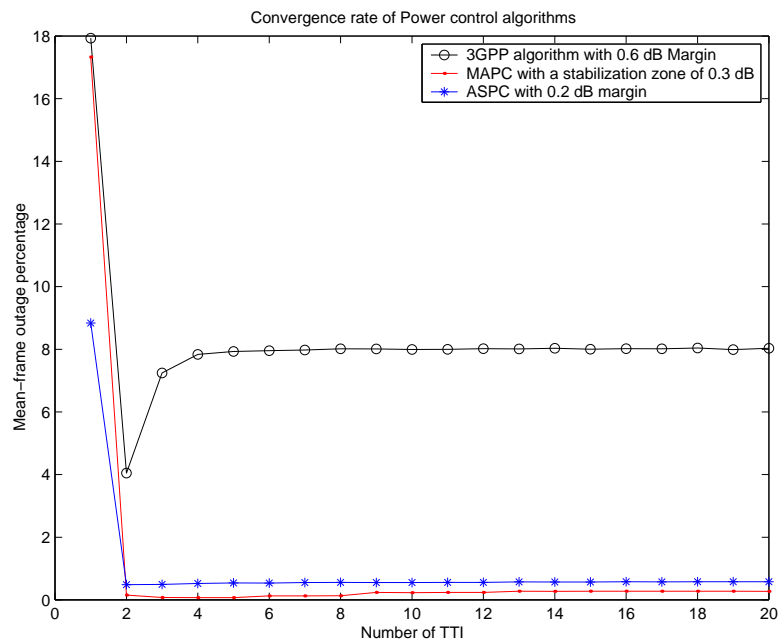


Figure 4.11: Convergence rate of power control algorithms when 26 mobiles/cell/slot are active simultaneously

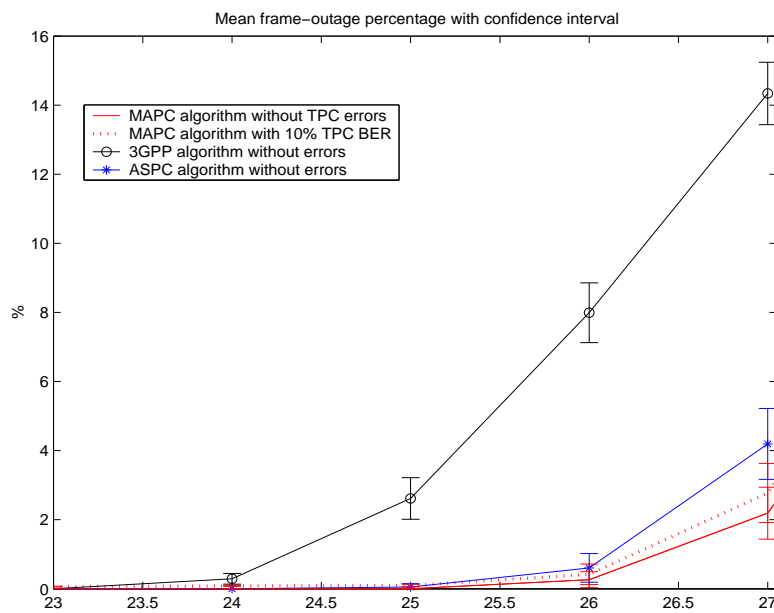


Figure 4.12: The mean frame-outage probability percentage as function of cell load with TPC errors

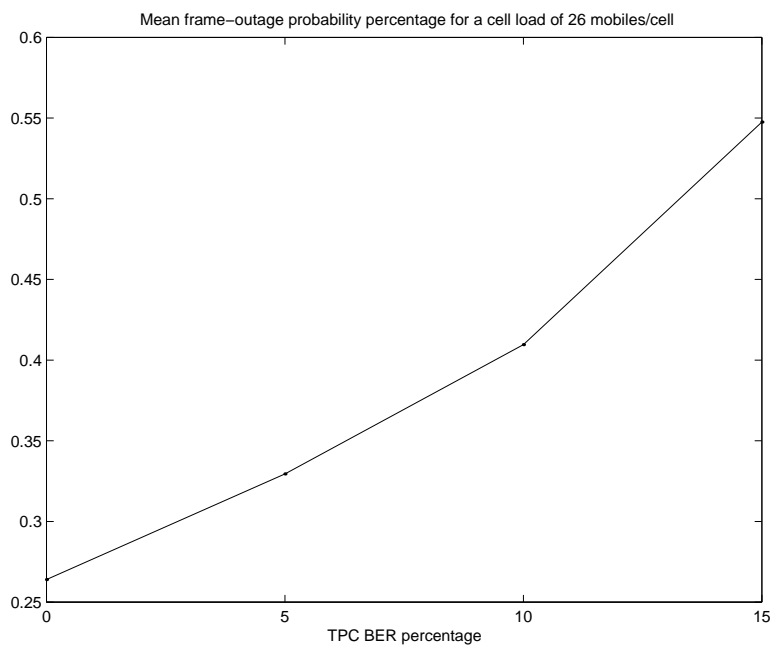


Figure 4.13: The TPC BER impact on the mean-frame outage probability for a cell load of 26 mobiles/cell

4.3 Concluding Remarks

In this chapter, we have presented the existing iterative power control algorithms and the standardized power control for CDMA systems. Thereafter, we have emphasized the fact that the standardized power control algorithm cannot always track fluctuations in pathgains. Therefore, we have proposed a variant of the standardized algorithm that improves system performance in term of outage probability and power consumption. In order to limit oscillations, the modified adaptive power control algorithm forces the receiver to transmit an alternate sequence of up and down commands in a stabilization zone above the CIR target. The transmitter responds to this sequence by a power stabilization. Hence, only the interpretation of the TPC commands is ameliorated. Nevertheless, the proposed algorithm has shown better performance than the 3GPP and an existing adaptive algorithm; system maximum capacity is increased and the power consumption is reduced. This advantage is due to the elimination of the CIR margin. Moreover, the MAPC algorithm has shown good immunity to TPC errors.

A dynamic stabilization zone that depends on radio and services characteristics may be used for each mobile to increase the algorithm performance. This is left for future research.

Chapter 5

Slot Allocation Techniques

The combination of the TDD mode and the TDMA technique offers a new degree of flexibility to UMTS systems. The new degree of flexibility may increase the system capacity and the QoS levels of active channels if it is wisely used. Slot allocation techniques allow the RNC to control the assignment of slots to users in order to exploit the TDMA/TDD flexibility. In this chapter, we investigate the optimal slot allocation that maximizes the minimum achievable CIR by all mobiles when optimum power control is used during each slot. This field of research has not been well studied in literature for TDMA-CDMA/TDD systems.

In the optimal slot allocation, an exhaustive search investigates all slot allocation possibilities. Due to the complexity of the exhaustive method, we propose optimal slot allocation techniques that approximate the optimal solution of allocation in term of maximizing the lowest CIR in the system. In these techniques, we have combined heuristic and meta-heuristic slot allocation techniques with the simplified optimal power control procedure. Meta-heuristic techniques can be adapted to operational systems using measurements. In this chapter, we investigate the performance of algorithms in downlink slots only. These methods can be easily adapted to uplink and crossed slots using the generic normalized matrix introduced in chapter three.

5.1 Problem Formulation

In UTRA FDD, radio interface capacity is an decreasing function of interference profiles. Interference profile is very sensitive to pathloss matrices. The pathloss matrix of a system depends on mobile positions and fading. Therefore, the capacity of UTRA FDD is not deterministic and thus, it is called soft capacity. Similarly to UTRA FDD, the soft capacity of UTRA TDD is limited by interference profile. However, UTRA TDD can exploit the flexibility of its TDMA and TDD components to change the pathloss matrix of each slot. In UTRA TDD, each frame is divided into 15 slots. Furthermore, each slot can be allocated to 16 CDMA codes in each cell if a processing gain of 16 is used. These codes can be allocated for either downlink or uplink channels in each cell. This flexibility can drastically increase overall system capacity. Capacity increase is possible only if the flexibility is carefully used.

5.1.1 System Model

The studied system is a synchronized bunched system [BPZ97][MLG99]. A bunch is a centralized cellular system where a central unit controls a set of remote antenna units. In this system, all pathgains are assumed to be known through intelligent measuring [LZ99].

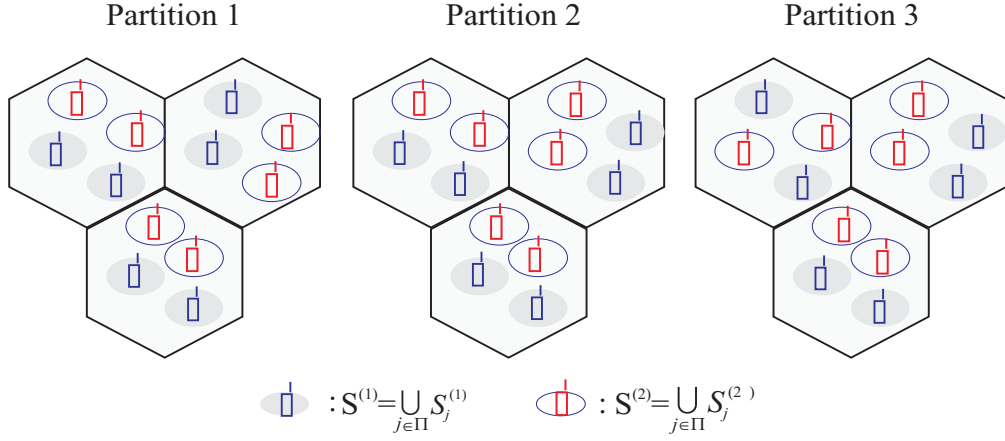


Figure 5.1: Three partition examples from the 108 possible set partitions with the same number of mobiles in slots ($T = 2$, $M = 3$, $N = 12$)

In the studied system, N mobiles are uniformly distributed to M cells. By convention, indices i and k always refer to mobiles while indices j and l refer to base stations. Furthermore, index j refers to the base station that serves mobile i (see section 2.1.1). Moreover, mobiles are supposed to be served by the best received base station.

Let T_d be the number of slots used for downlink. We assume that each mobile is assigned to one slot in the TDMA frame. The set S_j of mobiles communicating with base station j might be divided into T_d subsets $\{S_j^{(n)}\}_{n \in \{1, \dots, T_d\}}$, where $S_j^{(n)}$ is the set of mobiles connected to base station j during slot n . Moreover, we denote by $S^{(n)}$ the set of all active mobiles during slot n .

Due to synchronization, slots between cells are aligned in time (i.e. slot n is the same in all cells). Hence, there is no interference between different slots.

5.1.2 Optimization Problem Definition

In order to define the problem and try to find adequate solutions, we introduce some propositions and definitions in the following.

Definition 5.1 A mobile partition of mobile set $\Omega = \bigcup_{j \in \Pi} S_j$ into T_d subsets (figure 5.1) is defined by the unique set partition $\mathcal{S}^{(p)} = \{S^{(1)}, S^{(2)}, \dots, S^{(T_d)}\}$, where:

$$\begin{aligned} \bigcup_{n \in \{1, \dots, T_d\}} S^{(n)} &= \Omega \\ \bigcap_{n \in \{1, \dots, T_d\}} S^{(n)} &= \emptyset. \end{aligned}$$

Definition 5.2 A slot allocation in a system with T_d slots corresponds to mobile partition $\mathcal{S}^{(p)}$ of a set of mobiles into T_d subsets.

For each partition $\mathcal{S}^{(p)}$, a specific transmitted power vector $\Psi = \{\mathbf{P}_{\ell,1}, \mathbf{P}_{\ell,2}, \dots, \mathbf{P}_{\ell,T_d}\}$ can be allocated to mobiles. Depending on Ψ , a vector of CIR $\Gamma = \{\Gamma_{i,j,n}\}_{i \in S_j^{(n)}, j \in \Pi}$ is reached by mobiles.

We remind that $S^{(n)} = \{S_j^{(n)}\}_{j \in \Pi}$.

Our objective is to find the slot allocation that maximizes the minimum CIR of all mobiles in a system where all pathgains are known. Therefore, for a given mobile geographical distribution, our problem is to find the partition $\mathcal{S}^{(p)}$ and the set of power vectors Ψ that maximizes the CIR of all mobiles. This can be formulated as follows:

$$\begin{array}{ll}
\text{maximize} & \min_{i \in \Omega} (\Gamma_{i,j,n}) \\
\text{subject to} & \frac{1+\Gamma_{i,j,n}}{\Gamma_{i,j,n}} P_{b,i,n} \geq \beta_d \sum_{k \in S_j^{(n)}} P_{b,k,n} + \sum_{l \neq j} \frac{G_{i,l}}{G_{i,l}} \left(\sum_{k \in S_l^{(n)}} P_{b,k,n} \right) \\
& \quad + \frac{N_0}{G_{i,j}}, \quad \text{for all } i \in S_j^{(n)}, j \in \Pi, n \in \{1, \dots, T_d\} \\
\text{and} & \mathbf{P}_\ell \in \mathcal{B} \\
& \mathcal{S}^{(p)} = \{S^{(1)}, S^{(2)}, \dots, S^{(T_d)}\} \subset \mathcal{X}
\end{array}$$

where \mathcal{X} is the set of all acceptable partitions of mobiles into T_d nonempty slots. These partitions must satisfy also the limitations in the number of codes that can be handled by a slot.

Proposition 5.1 If we consider a given allocation of two slots with the same maximum achievable CIR. The additional allocation of the two slots to the same new mobile does not give always the same maximum achievable CIR.

Proof. We take an example of a system with two cells and two slots in order to prove the proposition. Let $\mathbf{Z}^{(1)}$ and $\mathbf{Z}^{(2)}$ be the simplified normalized matrices associated to the two slots (see chapter 3). We assume that $\mathbf{Z}^{(2)} = (\mathbf{Z}^{(1)})^t$, where $(\mathbf{Z}^{(1)})^t$ is the transpose of $\mathbf{Z}^{(1)}$. Therefore, the maximum achievable CIR is the same in both slots (see the system-wide CIR balancing property in 3.3.1). The matrix $\mathbf{Z}^{(1)}$ is given by:

$$\mathbf{Z}^{(1)} = \begin{pmatrix} K_1 & \mathcal{Z}_1 \\ \mathcal{Z}_2 & K_2 \end{pmatrix},$$

where K_1 and K_2 correspond to intracell-interferences experienced by mobiles of the first and second cells respectively. If new mobile i in the first cell is allocated to the two slots, the normalized pathgains can be written as:

$$\mathbf{Z}^{(1)} = \begin{pmatrix} K_1 + \beta & \mathcal{Z}_1 + z \\ \mathcal{Z}_2 & K_2 \end{pmatrix} \quad \mathbf{Z}^{(2)} = \begin{pmatrix} K_2 + \beta & \mathcal{Z}_2 + z \\ \mathcal{Z}_1 & K_1 \end{pmatrix},$$

where z is the normalized pathgain of mobile i toward base station 2 and β is the residual intracell-interference factor. Thus, the maximum achievable CIR in both slots are given by:

$$\begin{aligned}
\gamma_1^* &= \frac{2}{K_1 + K_2 + 1 + \sqrt{(K_1 + \beta - K_2)^2 + 4(\mathcal{Z}_1 + z)\mathcal{Z}_2}}, \\
\gamma_2^* &= \frac{2}{K_1 + K_2 + 1 + \sqrt{(K_2 + \beta - K_1)^2 + 4(\mathcal{Z}_2 + z)\mathcal{Z}_1}}.
\end{aligned}$$

If $\gamma_1^* = \gamma_2^*$, then $(N_2 + \beta - K_1)^2 + 4(\mathcal{Z}_2 + z)\mathcal{Z}_1 = (N_1 + \beta - K_2)^2 + 4(\mathcal{Z}_1 + z)\mathcal{Z}_2$ and therefore:

$$z = \frac{\beta(N_2 - K_1)}{2(\mathcal{Z}_2 - \mathcal{Z}_1)}.$$

Therefore, only one value of z can give the same maximum achievable CIR in the two slots. ■

Conclusion 5.1 From proposition 5.1, we can deduce that slot allocation techniques cannot be based only on the previous CIR in the chosen slot and mobile pathgains, but the interaction between all mobiles must also be considered. This conclusion must be taken into account when slot allocation strategies are designed.

Slot Allocation Optimization Problem

In order to evaluate slot allocation techniques, we define the performance-index.

Definition 5.3 In a given partition $\mathcal{S}^{(p)}$, let $\{\gamma_n^{*(p)}\}_{n \in \{1, \dots, T_d\}}$ be the set of the maximum achievable CIRs in T_d slots using the optimum power control in each slot. The performance-index of partition $\mathcal{S}^{(p)}$ is therefore, the minimum power-balanced CIR in all slots:

$$\gamma_{min}^{*(p)} = \min_{n \in \{1, \dots, T_d\}} \gamma_n^{*(p)}, \quad (5.1)$$

where $\gamma_n^{*(p)}$ is the maximum achievable CIR during slot n of partition $\mathcal{S}^{(p)}$.

Proposition 5.2 In either noisy or noiseless systems, the mobile partition that maximizes the minimum power-balanced CIR in all slots (i.e. the performance-index) is the partition that maximizes the minimum CIR of all mobiles.

Proof. We demonstrate the proposition for noiseless systems and the same demonstration can be made for noisy systems. Let $\hat{\mathcal{S}}$ be the partition that maximizes the minimum power-balanced CIR in all slots $\hat{\gamma}_{min}^* = \min_{n \in \{1, \dots, T_d\}} \hat{\gamma}_n^*$. This partition is found by comparing all CIRs obtained after the application of the CIR-balancing power control to slots in all partitions. We remind that when the CIR-balancing power control is applied within a slot, all mobiles achieve the same CIR.

We assume that there exists another partition $\mathcal{S}^{(p)}$ that maximizes the minimum CIR of all mobiles $\Gamma_{min}^{(p)} = \min_{n \in \{1, \dots, T_d\}} \Gamma_{min, n}^{(p)}$, where $\Gamma_{min, n}^{(p)}$ is the minimum CIR during slot n . This partition is obtained by comparing the minimum CIR computed without CIR-balancing procedure during slots. Without loss of generality, we suppose that the minimum CIR is found during slot n . We have seen in chapter 3 that maximizing the minimum CIR for a set of active mobiles during a slot corresponds to CIR-balancing. Therefore, the minimum CIR in each slot of partition $\mathcal{S}^{(p)}$ can be maximized by using the CIR-balancing procedure:

$$\Gamma_{min, n}^{(p)} \leq \gamma_n^{*(p)} \quad \forall n \in \{1, \dots, T_d\},$$

where $\gamma_n^{*(p)}$ is the maximum achievable CIR during slot n and $\Gamma_{min, n}^{(p)}$ is the minimum CIR during slot n without CIR-balancing procedure. Hence:

$$\Gamma_{min}^{(p)} = \min_{n \in \{1, \dots, T_d\}} \Gamma_{min, n}^{(p)} \leq \min_{n \in \{1, \dots, T_d\}} \gamma_n^{*(p)} = \gamma_{min}^{*(p)}.$$

However, $\gamma_{min}^{*(p)} \leq \hat{\gamma}_{min}^*$ (by definition of $\hat{\gamma}_{min}^*$) and therefore, $\hat{\gamma}_{min}^*$ is the highest minimum CIR that can be reached in the considered noiseless system. ■

By using proposition 5.2, we can rewrite our objective as:

Find the mobile partition $\hat{\mathcal{S}}$ that maximizes the performance-index.

In other words, our objective is to find the solution of the following Slot Allocation Optimization (SAO) problem:

$$\begin{aligned}
(SAO) \quad & \text{maximize} \quad \gamma_{min}^{*(p)} \\
& \text{subject to} \quad \frac{1+\Gamma_{i,j,n}}{\Gamma_{i,j,n}} P_{b,i,n} \geq \beta_d \sum_{k \in S_j^{(n)}} P_{b,k,n} + \sum_{l \neq j} \frac{G_{i,l}}{G_{i,l}} \left(\sum_{k \in S_l^{(n)}} P_{b,k,n} \right) \\
& \quad \quad \quad + \frac{N_0}{G_{i,j}} \quad \text{for all } i \in S_j^{(n)}, j \in \Pi, n \in \{1, \dots, T_d\} \\
& \text{and} \quad \quad \gamma_{min}^{*(p)} = \min_{n \in \{1, \dots, T_d\}} \gamma_n^{*(p)} \\
& \quad \quad \mathbf{P}_\ell \in \mathcal{B} \\
& \quad \quad \mathcal{S}^{(p)} = \{S^{(1)}, S^{(2)}, \dots, S^{(T_d)}\} \subset \mathcal{X}
\end{aligned}$$

Complexity of the Problem

Using proposition 5.2, the global optimization problem can be divided into two maximization problems to reduce its complexity: the first maximization computes the maximum achievable CIR during a slot, while the second maximization find the partition that maximizes the performance-index. Moreover, we have N nonlinear constraints where the variables are either natural numbers (e.g. N_j) or real numbers (e.g. $P_{b,i,n}$). Therefore, this problem is a max-min-max problem with mixed-integer nonlinear constraints, which is known to be an NP-hard problem.

The direct solution to find the optimal partition is to study all possible partitions. However, the number of possible partitions to investigate increases exponentially with the number of mobiles. We denote by \mathcal{N} the total number of partitions. If partition $\mathcal{S}^{(p)}$ can be deduced from partition $\mathcal{S}^{(a)}$ only by a simple permutation of slots, only one of these partitions is investigated. The number of all possible partitions is therefore given by (see appendix B):

$$\mathcal{N} = \frac{\prod_{j \in \Pi} \mathcal{N}_j}{T_d!}, \quad (5.2)$$

where \mathcal{N}_j is the number of all possible partitions in cell j :

$$\mathcal{N}_j = T! \times \mathcal{S}_A(N_j, T), \quad (5.3)$$

where A is the maximum allowed number of simultaneous active codes in a cell during a slot (e.g. 8 codes/cell/slot), $\mathcal{S}_A(N_j, T_d)$ the number of all possible partitions with nonempty slots, where each slot can be associated to A codes at maximum. $\mathcal{S}_A(N_j, T)$ is given by the following recurrence equation:

$$\mathcal{S}_A(N_j, T) = \begin{cases} 1 & \text{if } T = 1 \\ 0 & \text{if } N_j > A \times T \\ \mathcal{S}(N_j, T) & \text{if } N_j - A \leq T - 1 \\ \sum_{k=0}^v \binom{k-1}{N_j-1} \mathcal{S}_A(N_j - k, T - 1) & \text{Otherwise} \end{cases} \quad (5.4)$$

where $\binom{c}{N_j}$ is the binomial coefficient, $\mathcal{S}(N_j, T)$ is the Stirling number of the second kind (i.e. the number of ways of partitioning a set of N_j elements into T_d nonempty sets):

$$\mathcal{S}(N_j, T_d) = \frac{1}{T_d!} \sum_{n=0}^{T_d-1} (-1)^n \binom{n}{T_d} (T_d - n)^{N_j},$$

and ϱ and v are the minimum and the maximum numbers of elements that can be allocated to the first subset.

The factor ϱ is used to guarantee that at least one element is associated to the first subset and to limit the number of the remaining elements to $A(T-1)$ at maximum, i.e. the number of remaining elements can be supported by the $T-1$ slots. Therefore, ϱ is given by:

$$\varrho = \max(1, N_j - A(T-1)). \quad (5.5)$$

The factor v is used to limit the number of elements in the first subset to A and to guarantee that at least one element is associated to each remaining subset. Therefore, v is given by:

$$v = \min(A, N_j - (T-1)) \quad (5.6)$$

It must be noted that all possible permutations of slots are considered in \mathcal{N}_j . We do not consider partitions with empty slots because we can always find a partition that gives at least the same performance when this slot is allocated to one mobile.

If we consider that all slots are allocated for approximately the same number of mobiles in each cell, the number \mathcal{N}_j is reduced to:

$$\mathcal{N}_j = \frac{N_j!}{\left[\left[\frac{N_j}{T_d}\right]!\right]^\varepsilon \left[\left(\left[\frac{N_j}{T_d}\right] - 1\right)!\right]^{T_d - \varepsilon}} \quad (5.7)$$

where ε is the remainder of the ratio N_j/T_d (see appendix B).

We consider a system with 196 mobiles uniformly distributed to 7 cells and 7 slots to give an idea on the magnitude of the number \mathcal{N} . The number of possible partitions when all slots have the same number of mobiles in each cell is around 1.5×10^{135} (this number increases to 2×10^{161} if we consider all possible partitions with 8 codes/slot at maximum). This number represents only the number of partitions to investigate. We must also add the complexity of the CIR-balancing power control (i.e. the first maximization). The complexity of this algorithm may be very high, especially in noisy constrained systems. The computation time needed to investigate all partitions, even in this special case, range from several days to several months depending on the complexity of tested algorithms and computing power. Therefore, we propose heuristic and meta-heuristic¹ algorithms that converge to partitions with high performance-indices. It must be noted here, that the simplified generic optimum power control reduces drastically the computation time.

5.2 Optimal Slot Allocation Algorithms

In this section, we propose two heuristic slot allocation algorithms that investigate a small number of partitions and gives high performance-indices. Moreover, an heuristic slot allocation algorithm that distributes mobiles over slots based on fixed constraints is also proposed. Results of this section are used to better understand the impact of mobile partitions over slots on performance-index levels. The main idea of the proposed methods is to find partitions where the achievable CIRs over all slots are as similar as possible. In other words, we search for the partition that minimizes the variance of maximum achievable CIRs over slots :

$$\text{Minimize } \text{var}(\gamma_n),$$

¹A meta-heuristic algorithm controls the execution of a simpler heuristic method, and unlike a one-pass heuristic, does not automatically terminate once a locally optimal solution is found.

where γ_n is the maximum achievable CIR during slot n for either noisy or noiseless systems.

Before the presentation of the proposed methods, we emphasize a remark that we have noticed during the analysis of these methods.

Remark 5.1 If the maximum achievable CIR during a slot is higher than the maximum achievable CIR during another slot for a noiseless system, this result do not always hold on when the background noise is added. This phenomena is due to power limitations that decrease the maximum achievable CIR. The CIR decrease of a mobile is related to the pathgain between the mobile and its server and not only to normalized pathgains. Therefore, the CIR decrease in different slots is not the same when the background noise is added. Thus, optimal partitions in noisy and noiseless systems may not be the same.

5.2.1 Heuristic Methods for Partition Search

We propose two methods that allow the system to achieve high enough performance-indices by investigating a reduced number of partitions. Each method is divided into two basic steps to reduce the complexity of the search process:

Step 1: We investigate partitions in each cell j to build M_d partitions (i.e. one partition in each cell) $\{\mathcal{S}_j^{(p)} = \{S_j^{(1)}, S_j^{(2)}, \dots, S_j^{(T_d)}\}\}_{j=1 \dots M_d}$ using heuristic methods

Step 2: We investigate all possible combinations of the obtained partitions to build the global partition $\mathcal{S}^{(p)} = \{S^{(1)}, S^{(2)}, \dots, S^{(T_d)}\}$, where p is partition index. We select the partition that maximizes the performance-index. Each global partition is formed by combining the elements of sets $\mathcal{S}_j^{(p)}$. Each block $S^{(n)}$ of partition $\mathcal{S}^{(p)}$ includes one block from each cell:

$$S^{(n)} = \bigcup_{j \in \Pi, p_{j,n} \in \{1, \dots, T_d\}} S_j^{(p_{j,n})},$$

where subsets $S_j^{(p_{j,n})}$ must verify the following constraint:

$$\bigcap_{n \in \{1, \dots, T_d\}} S_j^{(p_{j,n})} = \emptyset \quad \forall j \in \Pi.$$

Once the partition $\mathcal{S}^{(p)}$ is built, simplified normalized pathgain matrices $\{\mathbf{Z}^{(n)}\}_{n \in \{1, \dots, T_d\}}$ are formed.

A mobile is called high-gain (resp. low-gain) mobile if the sum of its normalized pathgains toward neighboring base stations is higher (resp. smaller) than a threshold. In general, low-gain mobiles are close to their base servers.

Variance Minimization Method

The main idea of the Variance Minimization Method (VMM) is to allocate a slot to a combination of low-gain and high-gain mobiles in each cell. This strategy leads to approximately similar pathgain profiles in all cells during a given slot. In the first step, we study each cell j independently: for set S_j , we investigate all possible partitions $\mathcal{S}_j^{(p)}$. We denote by $z_{j,n}$ the sum of normalized pathgains of mobiles grouped in subset $S_j^{(n)}$. The variable $z_{j,n}$ is the element sum of the j th line of matrix

$\mathbf{Z}^{(n)}$ without the diagonal element:

$$z_{j,n} = \sum_{l \in \Pi - \{j\}} \mathcal{Z}_{j,l,n} = \sum_{l \in \Pi - \{j\}} \left(\sum_{i \in S_j^{(n)}} Z_{i,l} \right).$$

The simplest way to obtain similar power-balanced CIR over all slots is to build similar matrices $\mathbf{Z}^{(n)}$. In noiseless systems, the power-balanced CIR during slot n is limited by the minimum and the maximum sums of elements in each line of matrix $\mathbf{Z}^{(n)}$ (see equation 3.13). Moreover, the power-balanced CIR in noisy systems is upper-bounded by the power-balanced CIR without background noise. Therefore, we search for the partition that minimizes the difference between the variables $z_{j,n}$ in each cell. One method to do so, is to minimize the variance v_j of variables $z_{j,n}$ in each cell j :

$$v_j = \text{var}_{n \in \{1, \dots, T_d\}} (z_{j,n}) = \frac{1}{T_d + 1} \sum_{n=1}^{T_d} (z_{j,n} - \bar{z}_j)^2,$$

where \bar{z}_j is the mean value of variables $z_{j,n}$.

Hence, we choose in each cell j the partition that minimizes v_j (step 1 of the VMM). Once found, all combinations of the partitions of the first step are investigated to find the global partition. The global partition $\hat{\mathcal{S}}$ must maximizes the performance-index.

In each cell, the VMM investigates only partitions that have approximately the same number of users. In other word, $S_j^{(n)}$ contains $\lceil N_j / (M_d T_d) \rceil - 1$ or $\lceil N_j / (M_d T_d) \rceil$ mobiles of cell j , where $\lceil x \rceil$ is the upper-bound integer of x . We consider only partitions with a fair distribution of mobiles in the same cell to slots. We investigate only these partitions to take into account the intracell-interference which is not considered in normalized pathgains. In figure 5.2, we compare the performance-index when only fair partitions are taken and when all partitions are considered in a cell. We can see that the results are very close. Moreover, the average difference between the performance-indices of the first and the second cases is 0.18 dB. Therefore, considering only fair partitions increases slightly the performance-index in addition to the drastic decrease in the number of partitions to investigate.

In figure 5.3, a partition obtained by the mean of the VMM is presented for a system of two cells and two slots. In each cell, two high-gain mobiles and two low-gain mobiles are active.

The number of partitions to investigate in this method is given by the following equation:

$$\mathcal{N} = M_d \mathcal{N}_j + (T_d!)^{M_d - 1}, \quad (5.8)$$

where \mathcal{N}_j is the number of partitions investigated in cell j . For the general case \mathcal{N}_j can be computed using equation (5.3). When fair mobile distribution to slots is used, \mathcal{N}_j can be computed using equation (5.7).

Hence, the number of investigated partitions is decreased, particularly when the number of cells increases. For a bunched system where $M_d = 7$, $T_d = 7$ and $N = 196$, the number of investigated partitions is around 16×10^{21} . Hence, we obtain a reduction of 10^{113} from the number of total possible partitions.

Normalized Pathloss Sorting Method

The main idea of the Normalized pathloss Sorting Method (NSM) is to allocate the same slot to mobiles that have similar normalized pathgains in each cell and associate a set of high-gain mobiles

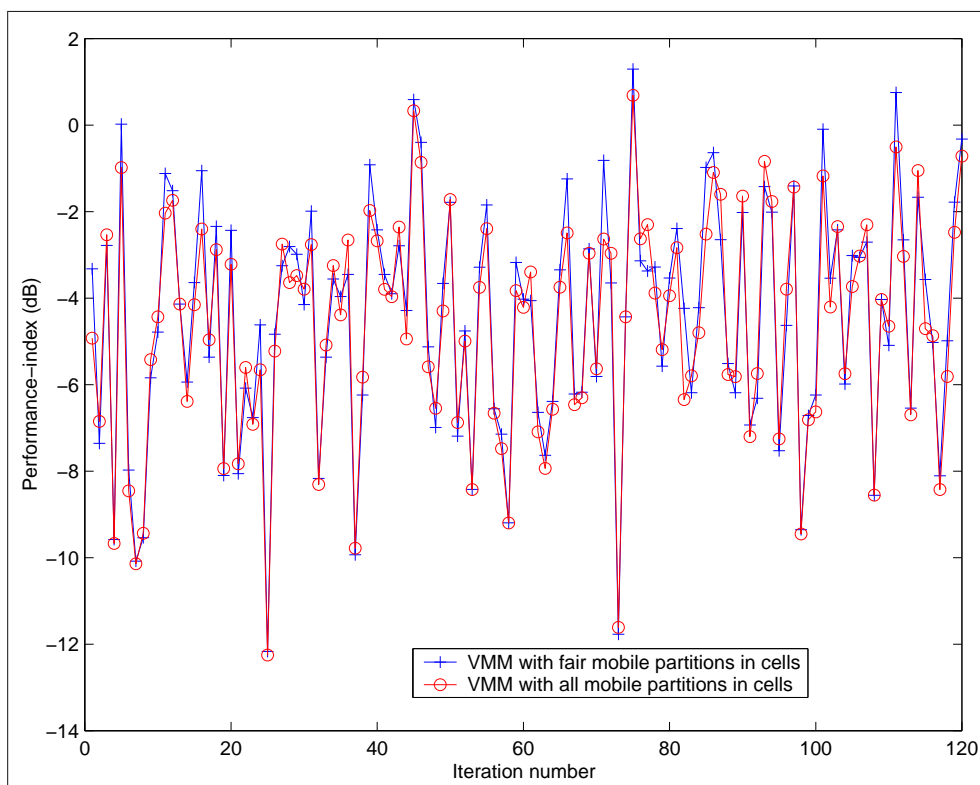


Figure 5.2: Comparison between the VMMs with fair mobile partitions and all mobile partitions in the same cell (a system with 2 cells, 2 slots and 16 mobiles is considered)

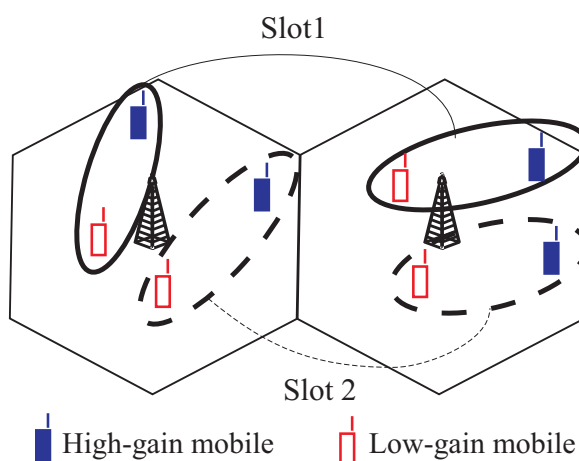


Figure 5.3: Example of a partition using the variance minimization method

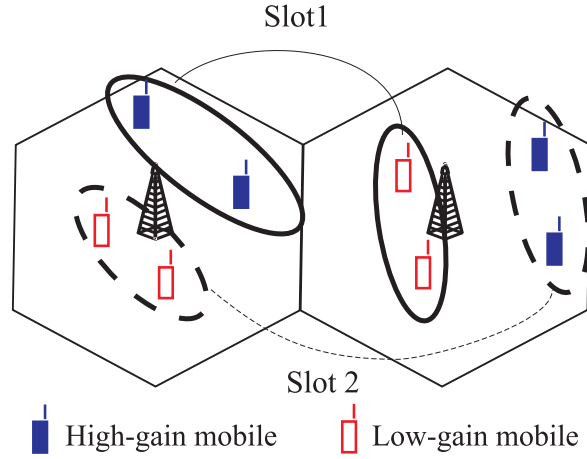


Figure 5.4: Example of a partition using the normalized pathloss sorting method

of a cell to sets of low-gain mobiles of neighboring cells. Therefore, similar maximum achievable CIRs are obtained by compensating the presence of high-gain mobiles in some cells by the presence of low-gain mobiles in other cells. This objective is achieved in the second step of the method, which is the same as the second step of the VMM.

In the NSM, we associate to each mobile i a parameter $z_i = \sum_{l \in \Pi - \{j\}} Z_{i,l}$, which is the sum of mobile normalized pathgains. The NSM sorts mobiles of each cell using parameters z_i . Thereafter, each $N_{j,n}$ consecutive mobiles of each cell j are grouped in a subset $S_j^{(n)}$. The number of mobiles in cells is fixed in such a way that we obtain a fair mobile partition to limit intracell-interference. Hence, we obtain T_d subsets in each cell. These subsets will be used in the second step to find the global partition that maximizes the performance-index.

Figure 5.4 presents the same system as in the previous section but with mobiles distributed using the normalized pathloss sorting method.

The number of partitions to investigate in this method is given by the following equation:

$$\mathcal{N} = M_d + (T_d!)^{M_d - 1}.$$

The number of investigated partitions is decreased compared to the exhaustive search, particularly when the number of cells increases. Moreover, the NSM becomes more interesting than the VMM in term of simplicity when the number of mobiles in cells increases. For a bunched system where $M_d = 7$, $T_d = 7$ and $N = 196$, the number of investigated partitions is around 16×10^{21} . Hence, we obtain a reduction of 10^{113} to the number of total possible partitions. In this example, we have approximately the same number of partitions in both methods. This is due to the high number of slots and cells. In this case, the second step investigates more partitions than the first step. The latter is the only difference between the two methods.

5.2.2 Stepwise Allocation Algorithm

The Stepwise Allocation Algorithm (SAA) is an iterative slot allocation algorithm that distributes a set of mobiles to free slots. In the SAA, all mobiles of the system are sorted using parameters z_i . It must be noted that the sorting process is done for all mobiles and not for mobiles in each cell independently as in the NSM. We remind that mobile i with high z_i generates high interference. Therefore, the T_d mobiles with the highest z_i are the first mobiles distributed to the T_d slots (i.e.

each slot is allocated to one mobile). Thereafter, the best slot is allocated to a mobile starting by the mobile with the highest z_i . The best slot is the slot where the maximum CIR is achieved. We describe the SAA by the following iterations:

Step 1: Sort all mobiles in the system using parameters z_i and build the set of sorted mobile indices \mathcal{M}

Step 2: Initialization phase: allocate the T_d slots to the worst T_d mobiles (i.e. with highest z_i)

Step 3: Remove the allocated mobiles from \mathcal{M}

Step 4: Computes the power-balanced CIR in all slots

Step 5: Take the worst mobile in \mathcal{M} and determine its server; allocate the best slot (relative to this server) to the worst mobile

Step 6: Remove the allocated mobile from \mathcal{M}

Step 7: If $\mathcal{M} = \emptyset$, halt.

Else, Repeat from Step 4.

In this algorithm, we distribute worst mobiles over slots at the beginning. Worst mobiles are mobiles that generate the highest interference due to their high normalized pathgains. Therefore, pathgains of these mobiles give an idea about the lower-bound of the maximum achievable CIR during a slot. Hence, the allocation of these mobiles at the beginning allows us to have a perspective on the power-balanced CIR that can be achieved during each slot. Using this method, we can achieve a fair distribution of maximum achievable CIR to slots.

The number of power-balanced CIR to investigate in this method is equal to the number of mobiles in the system. Therefore, the SAA is the simplest heuristic method.

5.3 Channel Re-allocation Algorithms

In this section, we propose a channel re-allocation technique, called the Re-Allocation Meta-heuristic Algorithm (RAMA). The proposed algorithm uses the principle of simulated annealing [Ing93][KCK00][KGV83][Can96]. The RAMA is designed using results of methods presented in section 5.2. Moreover, the RAMA can be used in operational systems when the QoS level falls below the desired threshold in a given slot.

5.3.1 Simulated Annealing

Simulated annealing is a general technique to find a good solution to difficult optimization problems. This technique is commonly known as the oldest among the meta-heuristic methods and one of the first algorithms that has an explicit strategy to avoid local minima. A meta-heuristic algorithm (like simulated annealing, tabu search, Ant colony method, etc.) controls the execution of a simpler heuristic method, and unlike a one-pass heuristic, does not automatically terminate once a locally optimal solution is found. The fundamental idea of simulated annealing is to allow moves that leads to worse quality than the current solution in order to escape from local minima. The probability of doing such a move is a time decreasing function. Simulated annealing has been used to solve several types of problems such as computer-aided design of integrated circuits, image processing, and channel allocation in TDMA/FDMA systems [KCK00].

Generally, a set \mathcal{X} of solutions is defined for an optimization problem. An optimization problem consists of finding a solution $x \in \mathcal{X}$ that minimizes a cost function $C(x)$. Simulated annealing tends to approximate the optimal solution by using the local search scheme. For performing a local search, the neighbors of each element x must be known. Therefore, we must define a neighborhood structure \mathcal{N}_e , where $\mathcal{N}_e(x)$ is the neighborhood of element x . $\mathcal{N}_e(x)$ is the set of possible new solutions to which we can transit from solution x .

The novel scheme in simulated annealing is that a neighbor \bar{x} can replace a solution x , even if the cost function increases, i.e. $C(\bar{x}) > C(x)$. This move is allowed with given probability. More precisely, the solution \bar{x} replaces the solution x with an acceptance probability $\Pr(x, \bar{x})$:

$$\Pr(x, \bar{x}) = \min \{1, \exp(-(C(\bar{x}) - C(x))/T_e)\}, \quad (5.9)$$

where T_e is a positive control parameter called *Temperature*. Temperature T_e decreases gradually to zero during the algorithm execution. By definition of the acceptance probability, all transitions to solutions that decrease the cost function are accepted. Moreover, the acceptance probability decreases when $C(\bar{x}) - C(x)$ increases, to avoid solution with very high cost function. In other hand, $\Pr(x, \bar{x})$ is an increasing function of T_e . Therefore, the probability of accepting a high cost solution decreases gradually. The initial value of T_e is set to a relative high value, allowing a frequent transition from x to \bar{x} at the beginning. This scheme allows the system to avoid local optima.

When the temperature becomes sufficiently small (i.e. frozen state), the solution is stabilized for many iterations and thereafter the algorithm will halt. The best available solution is retained as the approximate optimal solution.

5.3.2 Re-Allocation Meta-heuristic Algorithm

The aim of the Re-Allocation Meta-heuristic Algorithm (RAMA) is to maximize the performance-index by reallocating new slots to active mobiles. The RAMA is applied to the downlink of the TDD mode, and can be adapted to other type of slots.

The initial solution may be a random partition or a partition resulting from one of heuristic slot allocation techniques. The initial solution represents the state of a system at a given instance. The RAMA can be described as follows:

1. Determine an initial temperature T_e
2. Find the *Transit solution* \bar{x} of x from $\mathcal{N}_e(x)$ and computes $\Pr(x, \bar{x})$
3. Transit to solution \bar{x} with probability $\Pr(x, \bar{x})$
4. If the system reaches a stable state (i.e. a transition is done), then go to step 5.
Otherwise, repeat from step 2 using x .
5. If T_e is small enough, then go to step 6.
Otherwise, reduce T_e using the cooling function and return to step 2 using \bar{x}
6. Halt after saving the best computed solution as an approximation of the optimal solution

In order to apply the RAMA, we have to define solution space \mathcal{X} , cost function C , neighborhood structure \mathcal{N}_e , transit solution and cooling function.

Solution space Solution space involves all global mobile partitions $\mathcal{S}^{(p)}$ that satisfy the following constraints:

1. All mobiles are served
2. The number of simultaneous active mobiles (i.e. active during the same slot) in each cell is less than a given threshold A

Cost function Cost function $C(x)$ is the inverse of the performance-index and it is defined as follows:

$$C(x) = \frac{1}{\left(\min_{n \in \{1, 2, \dots, T_d\}} \gamma_n^*\right)},$$

where γ_n^* is the maximum achievable CIR during slot n computed using the CIR-balancing power control algorithm.

Neighborhood structure The neighborhood structure of a solution x is built by changing the allocated slot of only one mobile.

Transit solution The transit solution involves two process:

1. Find the mobile that must be reallocated
2. Find the new slot that will be allocated to the chosen mobile

Two strategies are used to choose the transit solution. In both strategies, the chosen mobile must be active during the worst slot ws . The worst slot ws stands for the slot where $\gamma_{ws}^* = \min_{n \in T_d} \gamma_n^*$. Moreover, the mobile is chosen from mobiles served by base station wb transmitting with the highest power during slot ws . We choose this base station, because it is the base station that imposes the CIR constraint in a noisy system. Thereafter, the mobile to reallocate is chosen using one of two strategies:

1. Worst Mobile Move (WMM) strategy: select mobile i with the highest sum of normalized pathgains z_i . The chosen mobile is therefore, the mobile that experiences the highest intercell-interference power if all base stations are transmitting with the same power.
2. Best Mobile Move (BMM) strategy: select mobile i with the lowest sum of normalized pathgains z_i . The chosen mobile is therefore, the mobile that experiences the lowest intercell-interference power if all base stations are transmitting with the same power.

The WMM strategy allows fast convergence, while the BMM strategy guarantees stability in the system (i.e. the minimum CIR does not fall to low values) as depicted in figure 5.5. In this figure, we take a sample of geographical mobile distribution in a system with seven cells, seven slots and five mobiles/cell/slots. We can see that the WMM strategy leads to a degradation in the QoS level, even if it allows a faster convergence. On the contrary, the BMM strategy converges more slowly but with an increasing QoS level. We tested several mobile geographical distributions and noticed the same behavior in almost all cases.

The new slot is selected from the solution space and must have the highest maximum achievable CIR. If the transition is not accepted, another slot is selected with the same constraint until no

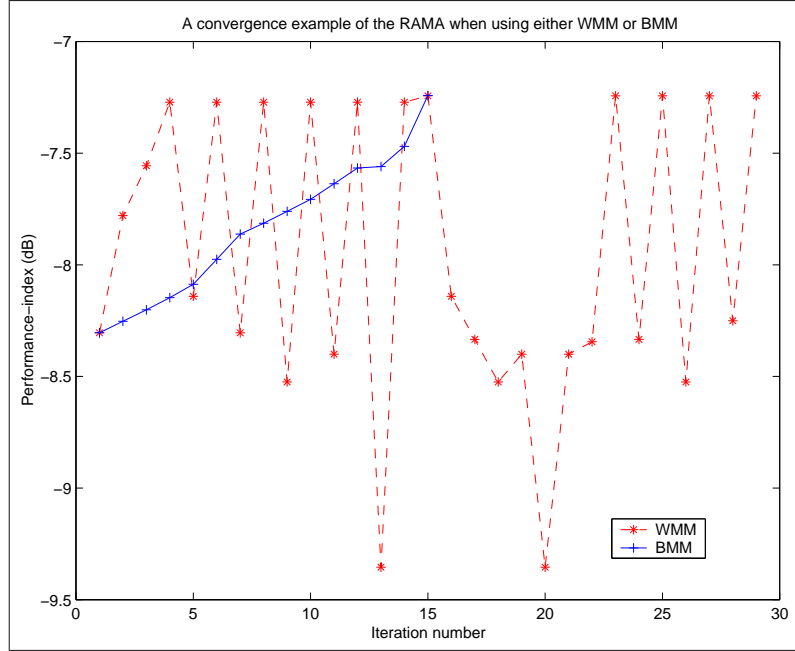


Figure 5.5: A convergence example of the RAMA when using either WMM or BMM strategies in a system of 7 cells, 7 slots and 5 mobiles/cell/slot

slots are left or the transition is accepted. If all slots are investigated without success, the chosen mobile is dropped and a new mobile is chosen from the same cell until all mobiles of this cell are tested without success. All other cells are then tested, starting by the base station with the second highest transmitted power.

Cooling function The cooling function decreases gradually the temperature parameter T_e using the following equation:

$$T_e^{(\text{new})} = r * T_e^{(\text{old})},$$

where r is a predefined constant satisfying: $0 < r < 1$.

The power-balanced CIR is sensitive to the interaction between mobiles (see conclusion 5.1). Therefore, a normal search can converge toward a local optimum; assume that we have a partition, where the performance-index is higher than all other performance-indices in neighborhood partitions. This partition can be considered as the optimum partition if the transition probability is always equal to zero when the cost function increases. However, there is a possibility to reach partitions by reallocating more than one mobile and obtain higher performance-indices due to the interaction between mobiles. In order to avoid these local optima we have used simulated annealing. Another method is to investigate all combinations of mobile re-allocation. This scheme increases exponentially the number of investigated partitions.

Operational Channel Re-allocation Algorithm

The RAMA can be modified to be integrated in real systems. In this case, the algorithm reacts when the CIR falls below the CIR target. The end-condition can be the state where all mobile signals are received with the CIR target.

Table 5.1: Simulation parameters [TS202j]

Thermal noise power	Max BTS power
-98 dBm	33 dBm

The sum of the normalized pathgains $z_{i,n}$ of mobile i can be measured using the broadcast channel. If we assume that mobile i receives intercell-interference $I_{\text{inter,d},i,n}$ during slot n , where P-CCPCH is transmitted. As the P-CCPCH is transmitted with a fixed power $P_{P\text{-CCPCH}}$, the sum of the normalized pathgains can be computed by the following equation:

$$z_{i,n} = \frac{I_{\text{inter,d},i,n}}{P_{P\text{-CCPCH}} G_{i,j}}, \quad (5.10)$$

where $G_{i,j}$ can be measured by estimating the received signal from the server j . The BMM strategy is more suited in operational systems due to its stability. Therefore the combination of the modified RAMA and the BMM strategy can be implemented in operational systems to decrease the outage and blocking probabilities.

Another method that can be used is to reallocate the mobile with lowest specific transmitted power in the worst cell and during the worst slot.

5.4 Simulations and Results

All slot allocation techniques are evaluated using snapshot simulations. We made simpler comparison in [NL02b] with a different propagation model. We here present more detailed simulations.

5.4.1 System Model

The simulated system is an UTRA TDD system of M_d cells and T_d slots. The simulation area is finite, i.e. no wraparound is used. This implies that border effects will affect the results but that will be the case in a real UMTS TDD systems as well. We consider hexagonal macrocells with 1 km radius. Mobiles are assumed connected to the best server and they are uniformly distributed to cells.

The constraint on transmitted powers and the value of thermal noise power are presented in table 5.1 [TS202j].

The assumed propagation model is a Xia-Bertoni model [MBX93][FC02] with shadowing:

$$P_r = P_e \frac{k}{d_{x,y}^\gamma} a_{x,y}, \quad (5.11)$$

where P_r and P_e are respectively the received and the transmitted powers, k and γ are constants [AG03], which depend on the type of environment (table 5.2), and d is the distance between the

Table 5.2: Propagation model and simulated annealing parameters

k [dB]	γ [dB]	std[$a_{x,y}$] [dB]	MCL [dB]	initial T_e	r
-128.1	37.6	7	70	1	0.9

transmitter and the receiver. Factor $a_{x,y}$ models the shadowing effect. It is a time constant, log-normal variable with zero mean [NL03b] (table 5.2). Simulation minimum coupling loss (MCL) between mobiles and base stations [TS202j] and simulated annealing parameters are also given in table 5.2.

CIR-balancing power control is used to find the maximum achievable CIR during slots. A joint detection technique is used to decrease intracell-interference ($\beta_d = 0.1$) [Ver98]. The maximum number of codes per slot is reduced to eight in each cell to reduce the complexity of the joint detection technique.

We denote by γ_o^* and γ_r^* the performance-indices given by the exhaustive and the random methods respectively. Moreover, we denote by γ_m^* the performance-index given by method m, where m can be replaced by a method abbreviation. In all simulations, we consider 120 samples of geographical mobile distributions.

We want to evaluate the performance of the different methods and to compare these methods to the exhaustive method, which necessarily gives the optimal solution. However, the high number of iterations needed to simulate a big system prevent us from simulating such a system. Therefore, we simulate a system with only two cells and two slots. It can be considered a very limited system. However, with 16 mobiles there are 2 450 different possible allocations. It is then possible to investigate this case. For more complex systems, we only compare the different methods to the random allocation.

5.4.2 Noiseless System

First, we assume that background noise is neglected. In this system, we evaluate the performance of the NSM and the VMM.

System without Shadowing

The performance-indices are evaluated in a system with two cells, two slots and 16 mobiles without shadowing factor. The performance-indices comparison is represented in table 5.3, where $E(x)$ and $Std(x)$ are the mean value and the standard deviation of variable x respectively. In figure 5.6, we represent the Cumulative Distribution Function (CDF) of the performance-indices given by the exhaustive method, the NSM, the VMM and the random method. From these results, we can see that the VMM and the NSM give higher performance-indices than the random method (a mean difference of 1.7 and 0.7 dB respectively). Moreover, the NSM gives higher performance-indices than the VMM (i.e. a mean difference of 1 dB). The variation range of the VMM (5 dB) is wider than variation range of the NSM (3 dB).

Table 5.3: Comparison between the performance-indices given by the exhaustive method, the NSM, the VMM and the random method in a noiseless system with 2 cells, 2 slots and 16 mobiles without shadowing

Tested method	Versus exhaustive		Versus random	
	$E(\gamma_m^* - \gamma_o^*)$	$Std(\gamma_m^* - \gamma_o^*)$	$E(\gamma_m^* - \gamma_r^*)$	$Std(\gamma_m^* - \gamma_r^*)$
Normalized pathloss sorting method (NSM)	-0.2 dB	0.3 dB	1.7 dB	1 dB
Variance minimization method (VMM)	-1.3 dB	0.8 dB	0.7 dB	0.8 dB

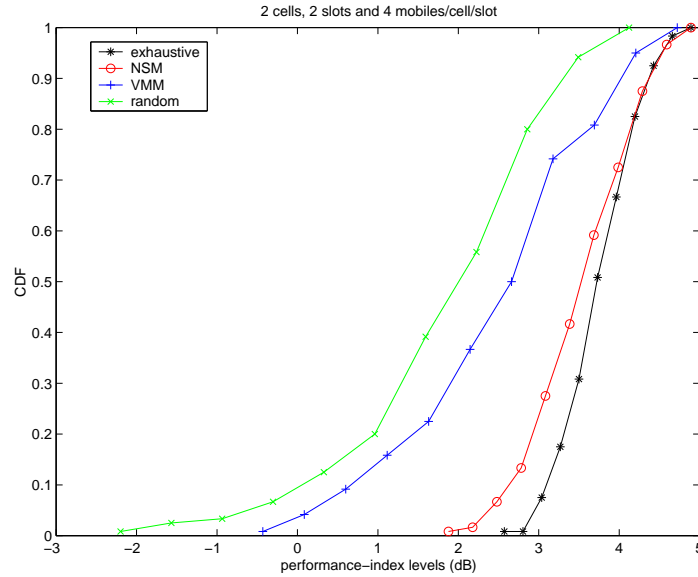


Figure 5.6: The CDF of the performance-indices given by the exhaustive method, the NSM, the VMM and the random method in a noiseless system with 2 cells, 2 slots and 16 mobiles without shadowing

In this simple system, the NSM gives partitions with performance-indices very close to optimal values and allows a drastic reduction of the number of studied partitions.

System with Shadowing

First, we consider a system with two cells, two slots and 16 mobiles with shadowing. A comparison between the performance-indices given by the exhaustive method, the NSM, the VMM and the random allocation is presented in table 5.4 and figure 5.7. We can see that the NSM gives always the best results (only 0.5 dB less than the optimum in average). We notice also that performance-indices are decreased when shadowing effect is considered. Moreover, differences between the performance-indices of the proposed methods and the performance indices of the exhaustive and the random methods increase also. Moreover, the mean difference between the NSM and VMM performance-indices increases to 1.5 dB. Finally, the range of variations of all methods has significantly increased.

Second, we compare the NSM and the VMM in a system with 36 mobiles distributed uniformly over three cells and three slots. In this simulation, we have noticed that the performance-index given by the NSM is always higher than the one given by the VMM.

From these results, we can see that the NSM gives higher performance-indices than the VMM in all cases where the background noise is neglected. Moreover, the difference between the optimal

Table 5.4: Comparison between the performance-indices given by the exhaustive method, the NSM, the VMM and the random method in a noiseless system with 2 cells, 2 slots and 16 mobiles with shadowing

Tested Method	Versus exhaustive		Versus random	
	$E(\gamma_m^* - \gamma_o^*)$	$Std(\gamma_m^* - \gamma_o^*)$	$E(\gamma_m^* - \gamma_r^*)$	$Std(\gamma_m^* - \gamma_r^*)$
NSM	-0.5 dB	0.6 dB	2.1 dB	1.1 dB
VMM	-1.9 dB	1 dB	0.6 dB	0.9 dB

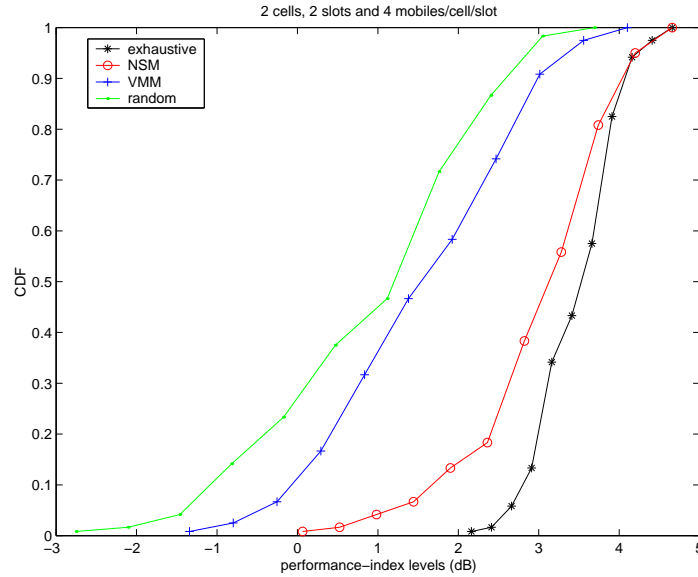


Figure 5.7: The CDF of the performance-indices given by the exhaustive method, the NSM, the VMM and the random method in a noiseless system with 2 cells, 2 slots and 16 mobiles with shadowing

performance-index and the performance-indices given by the NSM and the VMM increases when the shadowing factor is taken into account.

5.4.3 Noisy Systems

In the following, we evaluate the performance of the NSM, the VMM and the SAA. Moreover, we investigate the performance of the RAMA after an initial allocation based on a random distribution or SAA.

System Without Shadowing

We compare the NSM and the VMM with the exhaustive method in a system with two cells, two slots and 16 mobiles without shadowing factor. Results are shown in table 5.5. We can see that the VMM performance is ameliorated compared to the NSM performance due to the consideration of background noise (a mean difference of 0.5 dB between the performance-index given by the VMM and the performance-index given by the NSM); when the NSM is used, a base station transmits with very high power while other base stations are transmitting with low powers during each slot. Base stations with high powers correspond to cells where high-gain mobiles are allocated. The high variance in transmitted powers leads to high decrease between the maximum achievable CIR in noiseless and noisy systems.

In figure 5.8, we represent the CDF of the performance-indices. We can see that the curves are relatively close to each others. This is mainly due the small number of slots and thus the small number of possible partitions.

In the same system, we investigate the performance of the SAA. In figure 5.9-A, we can see that the SAA gives approximately the same results as the VMM with a drastic decrease of computation time (from 72 iterations in the VMM to 15 iterations in the SAA).

Moreover, we evaluate the performance-indices given by the RAMA after an initialization phase with random distribution or the SAA. The results are given in table 5.6. When a random distribution

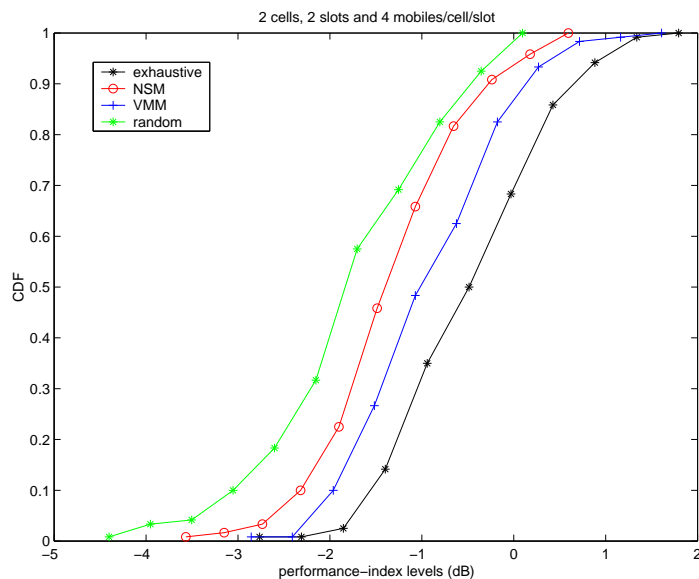


Figure 5.8: The CDF of the performance-indices given by the exhaustive method, the NSM, the VMM and the random method in a noisy system with 2 cells, 2 slots and 16 mobiles without shadowing

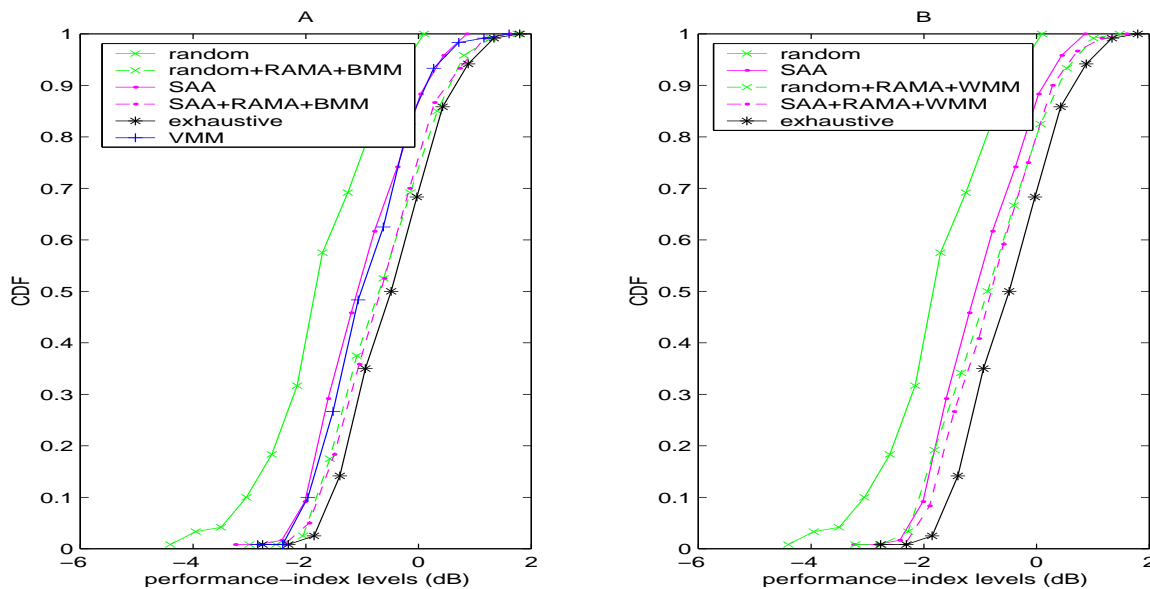


Figure 5.9: The CDF of the performance-indices given by the random method, the RAMA, the SAA, the exhaustive method and the VMM in a noisy system of 16 mobiles without shadowing

Table 5.5: Comparison between the performance-indices given by the exhaustive method, the NSM, the VMM and the random method in a noisy system with 2 cells, 2 slots and 16 mobiles without shadowing

Tested method	Versus exhaustive		Versus random	
	$E(\gamma_m^* - \gamma_o^*)$	$Std(\gamma_m^* - \gamma_o^*)$	$E(\gamma_m^* - \gamma_r^*)$	$Std(\gamma_m^* - \gamma_r^*)$
Normalized pathloss sorting method (NSM)	-0.9 dB	0.4 dB	0.4 dB	0.7 dB
Variance minimization method (VMM)	-0.5 dB	0.3 dB	0.9 dB	0.7 dB

is considered, the mean difference between the performance-indices given by the RAMA based on BMM and WMM is around 0.2 dB. Moreover, the mean difference between the performance-indices given by the RAMA and the random method is approximately 1.1 and 0.8 dB for BMM and WMM strategies respectively. When the SAA is used instead of the random method as an initialization algorithm, the performance-index is slightly increased. Therefore, we achieve the same performance-index as if we use the random initialization. This means that the performance of the RAMA is independent of the initial partition in this simple case. Moreover, figure 5.9 shows that the RAMA gives higher performance-indices than the VMM. It must be noted that the mean number of iterations when the RAMA is used, is around 10. Therefore, the RAMA is the fastest method and it gives the highest performance-indices.

System with Shadowing

First, we consider a noisy system with two cells, two slots and 16 mobiles. The performance-indices given by the exhaustive method, the NSM, the VMM and the random method are presented in figure 5.10 and table 5.7. We can see that the VMM and the NSM gives better results than the random method (a mean difference of 0.5 and 0.2 respectively). Moreover, the VMM gives always higher performance-indices than the NSM in the presence of the shadowing effect (a mean difference of 0.3 dB). Furthermore, the range of variations is higher than the range of variations in systems without shadowing; performance-indices range between -12 dB and 2 dB, while they range only between 5 dB and 2 dB in systems without shadowing.

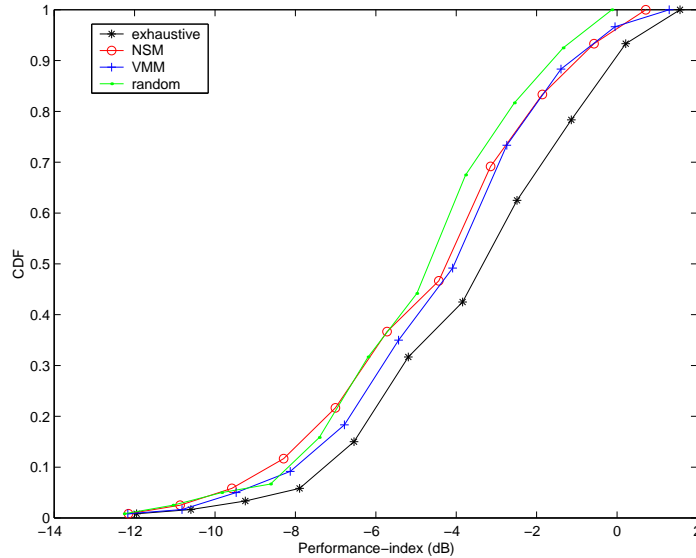
In table 5.8, we represent the performance-indices given by the RAMA after an initialization phase with random distribution or the SAA. When a random distribution is considered, the mean difference between the performance-indices given by the RAMA and the optimal performance-index

Table 5.6: Comparison between the performance-indices given by the random method, the RAMA and the BMM, the RAMA and the WMM, the SAA, the exhaustive method and in a noisy system of 16 mobiles without shadowing

Tested method	Versus exhaustive		Versus random	
	$E(\gamma_m^* - \gamma_o^*)$	$Std(\gamma_m^* - \gamma_o^*)$	$E(\gamma_m^* - \gamma_r^*)$	$Std(\gamma_m^* - \gamma_r^*)$
Random+RAMA+BMM	-0.2 dB	0.1 dB	1.1 dB	0.7 dB
Random+RAMA+WMM	-0.4 dB	0.2 dB	0.8 dB	0.7 dB
SAA	-0.5 dB	0.4 dB	0.7 dB	0.7 dB
SAA+RAMA+BMM	-0.2 dB	0.2 dB	1.1 dB	0.7 dB
SAA+RAMA+WMM	-0.3 dB	0.2 dB	1 dB	0.7 dB

Table 5.7: Comparison between the performance-indices given by the exhaustive method, the random method, the NSM and the VMM in a noisy system with 2 cells, 2 slots and 16 mobiles with shadowing

Tested method	Versus exhaustive		Versus random	
	$E(\gamma_m^* - \gamma_o^*)$	$Std(\gamma_m^* - \gamma_o^*)$	$E(\gamma_m^* - \gamma_r^*)$	$Std(\gamma_m^* - \gamma_r^*)$
Normalized pathloss sorting method (NSM)	-1.2 dB	0.6 dB	0.2 dB	0.8 dB
Variance minimization method (VMM)	-0.8 dB	0.5 dB	0.5 dB	0.7 dB

**Figure 5.10:** the CDF of the performance-indices given by the exhaustive method, the NSM, the VMM and the random method in a noisy system with 2 cells, 2 slots and 16 mobiles with shadowing

is around 0.3 dB. Moreover, the mean difference between the performance-indices given by the RAMA and the random method is approximately 1.1 dB for both strategies (BMM and WMM). The performance of the RAMA is less dependent on the initial partition in this simple case with shadowing. Moreover, figure 5.11 shows that the SAA and the RAMA gives higher performance-indices than the VMM. We emphasize that the number of investigated partitions by the RAMA in this case is around 9 partitions. Moreover, the RAMA converges faster if the SAA gives the initialization partition or if the WMM strategy is used.

Second, we compare the NSM and the VMM in a system with 36 mobiles distributed uniformly over three cells and three slots. In this simulation, we notice that the performance-index given by the VMM is ameliorated compared to the one given by the NSM (0.7 dB of difference).

In figure 5.12, we represent the CDF of the performance-indices of the SAA and the RAMA. We can see that the SAA and the RAMA give approximately the same performance-indices. Moreover, we notice that the mean difference between the RAMA performance-indices and the performance-index given by the random method increases when the number of mobiles increases (from 1.1 to 1.3 dB). It must be noted here that the VMM investigate 17 334 partitions, while the SAA investigates only 34 partitions and the RAMA investigates 30 partitions in average.

Finally, we evaluate the RAMA and the SAA performance in a system with seven cells, seven

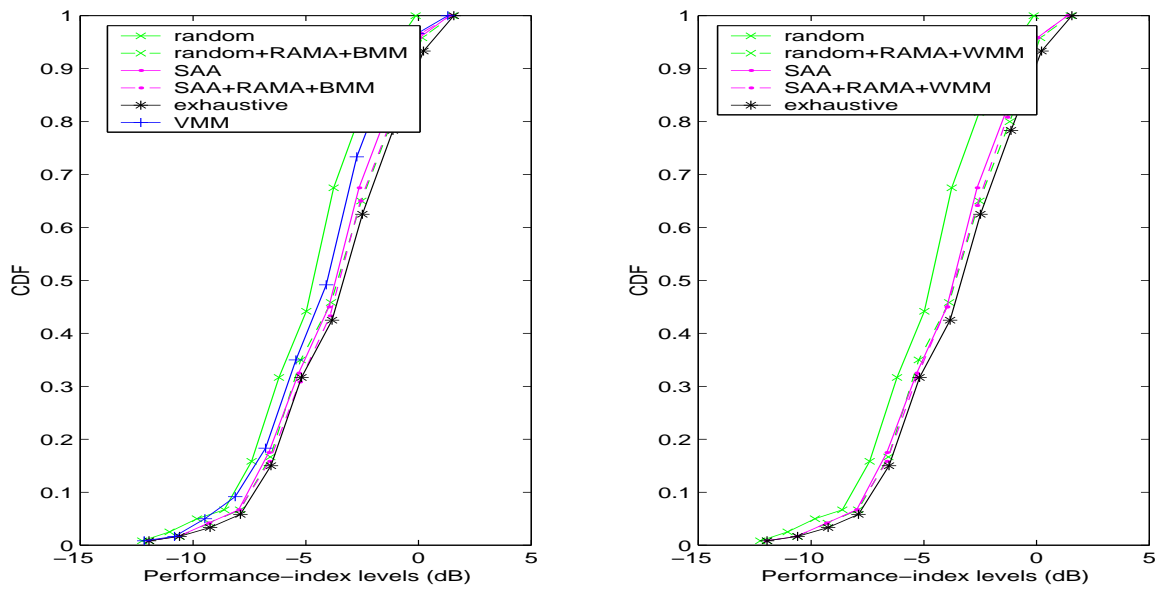


Figure 5.11: The CDF of the performance-indices given by the random method, the RAMA, the SAA, the exhaustive method and the VMM in a noisy system of 16 mobiles with shadowing

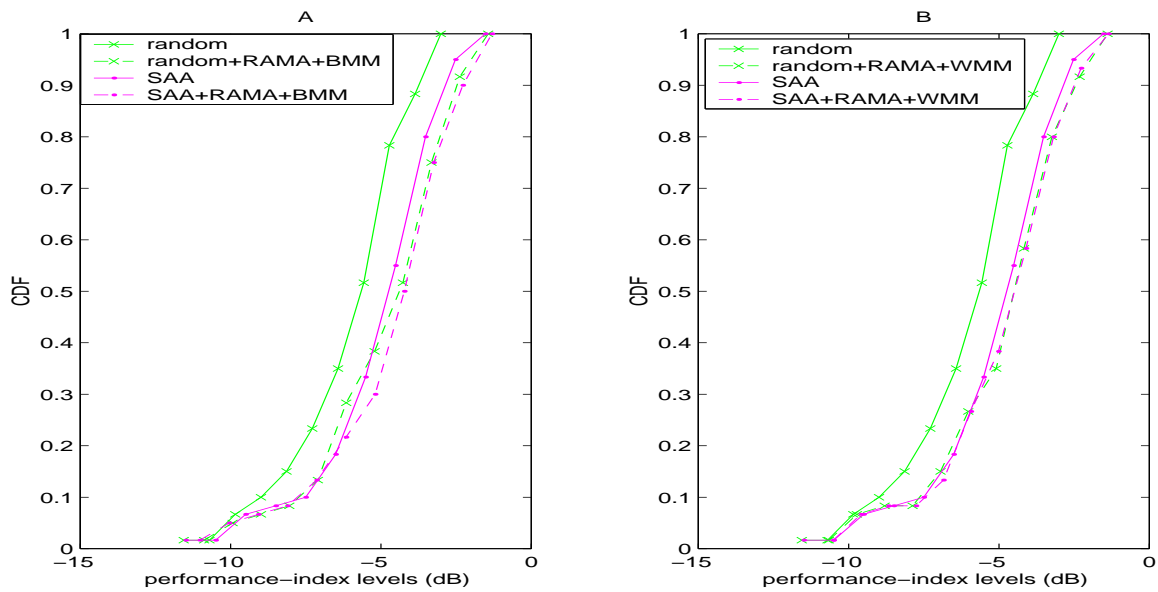


Figure 5.12: The CDF of the performance-indices given by the random method, the RAMA, the SAA and the exhaustive method in a noisy system of 36 mobiles with shadowing

Table 5.8: Comparison between the performance-indices given by the random method, the RAMA and the BMM, the RAMA and the WMM, the SAA and the exhaustive method in a noisy system of 16 mobiles with shadowing

Tested method	Versus exhaustive		Versus random	
	$E(\gamma_m^* - \gamma_o^*)$	$Std(\gamma_m^* - \gamma_o^*)$	$E(\gamma_m^* - \gamma_r^*)$	$Std(\gamma_m^* - \gamma_r^*)$
Random+RAMA+BMM	-0.3 dB	0.4 dB	1.1 dB	0.7 dB
Random+RAMA+WMM	-0.3 dB	0.4 dB	1.1 dB	0.7 dB
SAA	-0.4 dB	0.4 dB	1.1 dB	0.8 dB
SAA+RAMA+BMM	-0.3 dB	0.3 dB	1.1 dB	0.8 dB
SAA+RAMA+WMM	-0.3 dB	0.3 dB	1.1 dB	0.8 dB

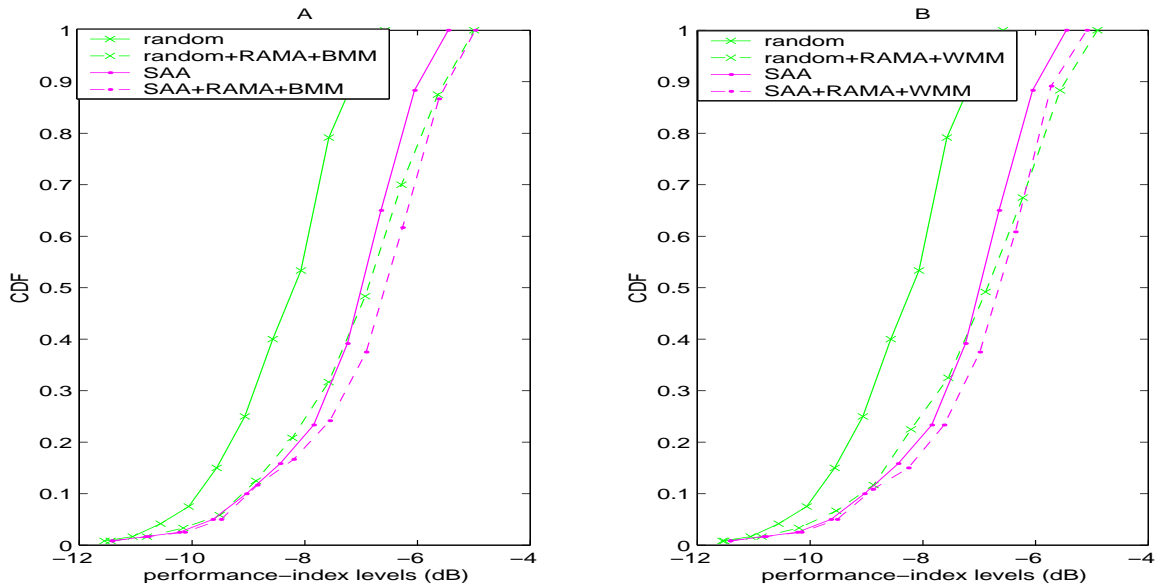


Figure 5.13: The CDF of the performance-indices given by the random method, the RAMA, the SAA and the exhaustive method in a noisy system of 245 mobiles with shadowing

slots and five mobiles/cell/slot (245 mobiles in the system). Results shown in figure 5.13 confirm that the difference between the performance-indices given by the heuristic and meta-heuristic methods, and the random method increases as the number of slots and cells increases.

In table 5.9, we show the difference between the performance-index given by the random allocation and the performance-indices given by the RAMA when it is combined with different strategies. It can be seen that this difference has increased to 1.4 dB when the SAA is used. Moreover, we notice that the performance-index given by the WMM strategy is higher than the one given by the BMM strategy.

In table 5.10, we show the number of partitions investigated by the different methods. It can be noticed that the number of partitions increases when using the WMM strategy. This is due to the instability of this method. Finally, we emphasize that the number of all possible partitions in this system is around 10^{174} .

Table 5.9: Comparison between the performance-indices given by the random method, the RAMA and the BMM, the RAMA and the WMM and the SAA in a noisy system of 245 mobiles with shadowing

Tested method	$E(\gamma_m^* - \gamma_r^*)$	$Std(\gamma_m^* - \gamma_r^*)$
Random+RAMA+BMM	1.2 dB	0.6 dB
Random+RAMA+WMM	1.3 dB	0.7 dB
SAA	1.1 dB	0.6 dB
SAA+RAMA+BMM	1.4 dB	0.6 dB
SAA+RAMA+WMM	1.4 dB	0.6 dB

Table 5.10: Iteration number in a noisy system of 245 mobiles with shadowing

Tested method	Number of iterations
Random+RAMA+BMM	32
Random+RAMA+WMM	77
SAA	239
SAA+RAMA+BMM	239+28
SAA+RAMA+WMM	239+42

5.5 Summary

In this chapter, we have studied the optimization of slot allocation using heuristic and meta-heuristic algorithms. Simulation results have shown that in noiseless system grouping high-gain mobiles in the same cell and compensating the presence of high-gain mobiles in some cells by the presence of low-gain mobiles in other cells is better than grouping high-gain and low-gain mobiles in each cell. However, these results are inverted when the background noise is added. Moreover, we have found that distributing high-gain mobiles at the beginning leads to very satisfactory results with low complexity. Due to its fast convergence, this algorithm may be used in operational systems.

Using these results, we have proposed meta-heuristic methods based on simulated annealing. Simulation results have shown that these methods give higher performance-indices than heuristic methods with fewer investigated partitions. All proposed methods have ameliorate the performance-index given by a random slot allocation. The difference between the performance-indices given by these methods and the performance-index given by the random allocation increases as the number of mobiles, slots or cells increases. Moreover, this difference increases also when the shadowing factor is considered. However, we still unable to know how much the performance-indices of these methods are close to the optimum solution in complex systems.

Moreover, we have proposed an operational scheme based on the meta-heuristic algorithms. This scheme can exploit the measurements information in the system to perform an iterative reallocation based on simulated annealing.

Chapter 6

Interference Avoidance Techniques

System capacity and achievable QoS levels are very sensitive to interference in CDMA systems. Moreover, the impact of interference is higher in the TDD mode than in the FDD mode due to the length of CDMA codes. Nevertheless, the TDD mode provides a flexibility in time domain due to the combination of the TDD mode and the TDMA technique. This flexibility is insured by slot allocation techniques that are used to avoid congestion and high interference profiles. However, the TDD flexibility must be used wisely to avoid high outage probability that may be induced due to high mobile-to-mobile interference in crossed slots.

In this chapter, we propose two new interference-avoidance methods that decrease the probability of high mobile-to-mobile interference, though blocking probability is kept at an acceptable level. In the first section, the problem of high mobile-to-mobile interference is introduced and some existing methods are presented and criticized. In sections 2 and 3, we propose two new interference-avoidance methods for which a guideline for implementation is presented in section 4. In section five, we analyze the performance of the proposed methods using simulations. Finally, we conclude with a brief summary.

6.1 Problem Formulation

In crossed slots, mobile-to-mobile and base station-to-base station interferences may appear (fig. 6.1). Mobile-to-mobile interference may induce very high outage probability when two close mobiles are active in opposite link directions during the same slot. Nevertheless, it was noticed in sections 2.3 and 3.3.1 that slot allocation techniques with crossed slots outperforms slot allocation techniques without this type of slot, if an efficient call admission control is used or if the fast DCA takes into account a condition that may reduce mobile-to-mobile interference.

Mobile-to-mobile interference is very difficult to estimate and need high signaling traffic to be communicated to central units. However, pernicious mobile-to-mobile interference appears when two close mobiles are active in opposite link directions. Generally, these mobiles are at cell borders. Hence, many algorithms based on pathgains between mobiles and base stations are used to detect this type of mobiles in order to reduce the probability of high mobile-to-mobile interference [WC01][Lin01]. The aim of these methods is to reduce the outage probability without a significant increase in the blocking probability.

6.1.1 Different Time Slot Allocation Based on Region Division

In the so-called "Different time slot Allocation based on Region Division" (DARD) method [WC01], each cell is divided into two zones: the inner zone near to the base station and the outer zone that

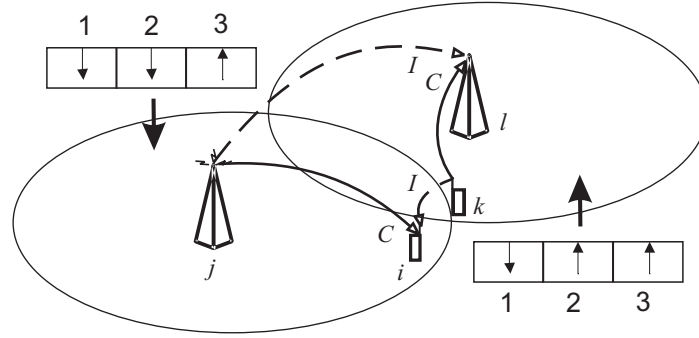


Figure 6.1: Crossed time slot (slot 2) in a system with two cells

encloses the first one (figure 6.2). The inner zone is a circle of radius R_0 . The main idea of this method is that mobiles at cell borders are the main source of high mobile-to-mobile interference. Therefore, crossed slots can be allocated only to mobiles of the inner zone for both links. This method decreases the outage probability by decreasing the number of mobiles allowed to be active in crossed slots. However, the DARD method does not take into account mobile pathgains with interfering cells, which is very important in real systems where shadowing can appear; in such systems, a mobile of the inner cell may have a high pathgain with mobiles of a neighboring cells if there is no obstacles that separate them. Moreover, this method can significantly increase the blocking probability in some cases as we will see in section 6.5.

6.1.2 Disjoint Base Station Sets Method

The Disjoint Base station Sets (DBS) method has been proposed in [Lin01] to mitigate the problem of shadowing factor. In the DBS method, each mobile builds a set of its n strongest base stations using pathgains. Two mobiles, from different cells, transmitting in opposite link directions can share a slot if their sets of strongest base stations are disjoint (figure 6.3). This method takes into account the interfering cells. However, the number of forbidden cells to a given mobile is fixed to 2 and this number is independent of mobile positions. Therefore, a mobile close to its server is forbidden from being active in crossed slots with mobiles of the most interfering cell even if that mobile does not generate high mobile-to-mobile interference. Moreover, only one cell is considered forbidden to a mobile: if a mobile is at the border of two cells, it can generate high interference toward mobiles of the non forbidden neighboring cell.

6.2 Slot Allocation Method Based on Mobile-to-Base Station Pathgains

In this section, we propose a Slot Allocation method based on mobile-to-base station Pathgains (SAP). The SAP is inspired from the disjoint base station sets and the different time slot allocation based on region division methods.

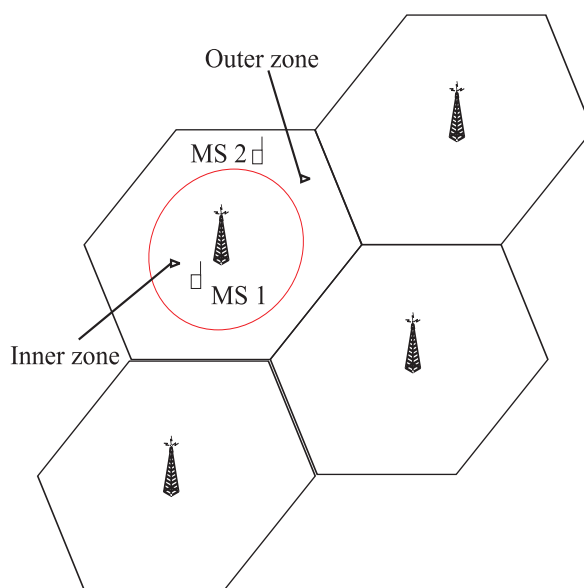


Figure 6.2: The inner zone and the outer zone of the DARD method. Mobile MS2 is forbidden to share a crossed slot with mobiles of neighboring cells in contrary to MS1

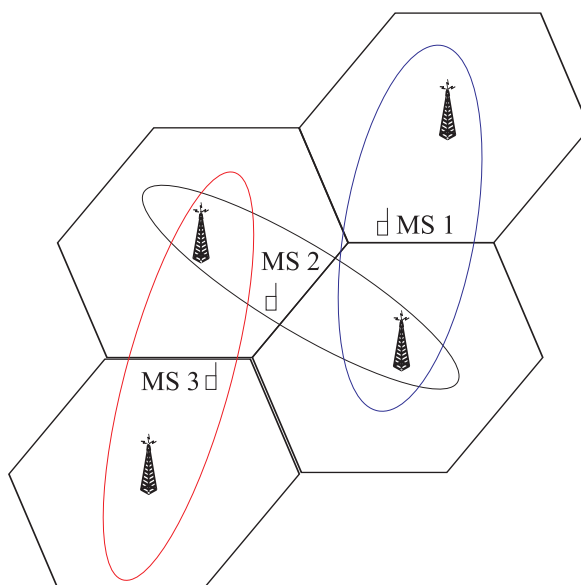


Figure 6.3: The set of the 2 strongest base stations for 3 mobiles (DBS method). The sets of MS1 and MS2 are not disjoint. Therefore, they can not share the same slot in different link direction in contrary to MS1 and MS3

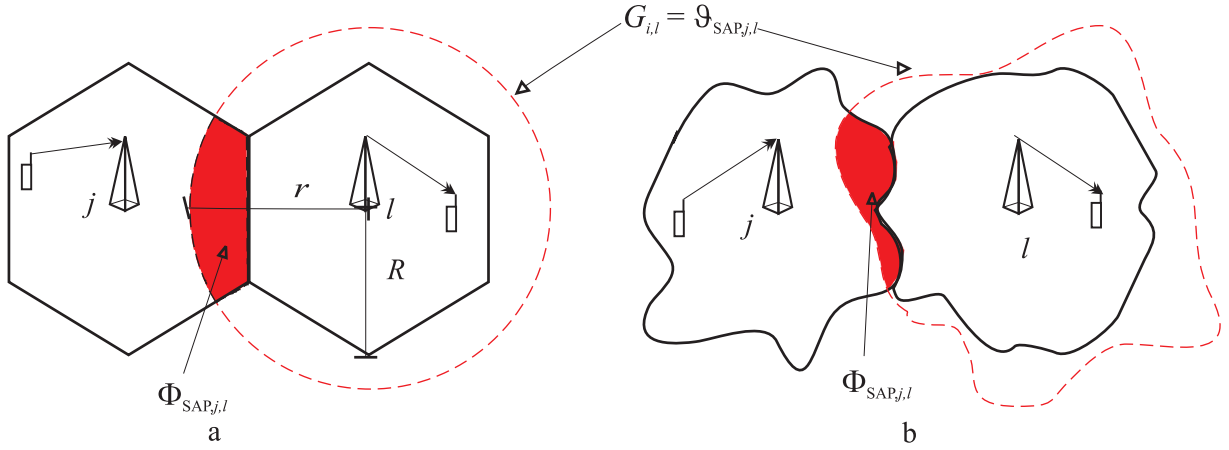


Figure 6.4: Forbidden zone in cell j when the slot allocation method based on mobile-to-base station pathgains (SAP) is used: (a) without shadowing (b) and with shadowing

6.2.1 Main Idea

The main idea of the proposed method is to reduce the outage probability without limiting the flexibility of the slot allocation technique. This objective can be reached if we can predict the existence of close mobiles transmitting in opposite link directions. A mobile that has a high pathgain toward a neighboring base station is expected to be close to the border of the cell served by the latter base station; thus, there is a high probability that this mobile can introduce high mobile-to-mobile interference. Therefore, it is more suitable to prevent this type of mobiles from being active in crossed slots with mobiles of close cells.

In SAP, mobile i of cell j can be active with mobiles of cell l which are active in the opposite link direction, if the following constraint is satisfied:

$$G_{i,l} \leq \vartheta_{SAP,j,l}, \quad (6.1)$$

where $G_{i,l}$ is the pathgain of mobile i toward neighboring base station l and $\vartheta_{SAP,j,l}$ is a specific threshold between cells j and l . This threshold depends on radio characteristics and the services offered to mobiles.

6.2.2 SAP Behavior in Hexagonal Networks

In a regular hexagonal cellular network, cell area where crossed slots are not allowed may be calculated. Assuming an Okumura-Hata propagation model without shadowing, the pathgain between mobile i and base station l may be written as:

$$G_{i,l} = k/d_{i,l}^\gamma, \quad (6.2)$$

where $d_{i,l}$ is the distance between mobile i and base station l . Constants k and γ are radio propagation constants. From equations (6.1) and (6.2), we can deduce that the zone $\Phi_{SAP,j,l}$ of cell j where mobiles are forbidden from being active in uplink though mobiles of cell l are active in downlink is limited by the boundary of cell j and a circle. The center of this circle is the base station l and its radius equal to $(k/\vartheta_{SAP,j,l})^{1/\gamma}$.

If the shadowing effect is considered, pathgains become random variables and $\Phi_{SAP,j,l}$ becomes an irregular curve as depicted in figure 6.4.

6.3 Slot Allocation Method Based on Mobile-to-Base Station Normalized Pathgains

Two mobiles with the same pathgain toward a neighboring base station may transmit with different powers depending on their pathgains toward their server; therefore, these mobiles may introduce different interference powers to the neighboring base stations. Hence, uplink power effect must be considered in the slot allocation constraint to decrease the outage probability.

6.3.1 Main Idea

The Slot Allocation method based on mobile-to-base station Normalized Pathgains (SANP) uses the normalized pathgain $Z_{i,l}$ instead of the pathgain $G_{i,l}$. We remind that $Z_{i,l} = G_{i,l}/G_{i,j}$, where j is the index of the cell on which mobile i is camping.

In SANP, mobile i of cell j can be active with mobiles of cell l which are active in the opposite link direction, if the following constraint is satisfied:

$$Z_{i,l} \leq \vartheta_{\text{SANP},j,l}, \quad (6.3)$$

where $\vartheta_{\text{SANP},j,l}$ is a specific threshold between cell j and l , which depends on radio characteristics and the services offered to mobiles.

SANP has the same advantages of SAP over other interference avoidance methods and gives better results due to the consideration of power impact.

6.3.2 SANP Behavior in Hexagonal Networks

In a regular hexagonal cellular network, cell area where crossed slots are not allowed may be specified. From equations (2.1), (6.2) and (6.3), we can deduce that the zone $\Phi_{\text{SANP},j,l}$ of cell j where mobiles are prevented from being active in uplink thought mobiles of cell l are active in downlink is limited by the boundary of cell j and a circle. If we consider a Cartesian coordinate system associated with cell j , the center o of the latter circle has the coordinates $\left(-\frac{DS^2}{1-S^2}, 0\right)$, and the radius r of this circle is given by:

$$r = D \left(\frac{S}{1-S^2} \right), \quad (6.4)$$

where $D = \sqrt{3}R$ is the inter-base station distance, R is the radius of the cell j circumscribed circle and S is a constant given by the following equation:

$$S = \vartheta_{\text{SANP},j,l}^{1/\gamma} \quad (6.5)$$

If the shadowing effect is considered, the pathgain becomes a random variable and $\Phi_{\text{SANP},j,l}$ becomes an irregular curve as depicted in figure 6.5.

6.4 Guideline for Implementation

In order to implement one of interference avoidance methods, we define a set of cells $\Psi_{i,j}$ for each mobile i of cell j . The set $\Psi_{i,j}$, called high interference-cells set, is defined by the following formula:

$$\begin{cases} \Psi_{i,j} = \{l/G_{i,l} \geq \vartheta_{\text{SAP},j,l}\} & \text{for SAP} \\ \Psi_{i,j} = \{l/Z_{i,l} \geq \vartheta_{\text{SANP},j,l}\} & \text{for SANP} \end{cases}$$

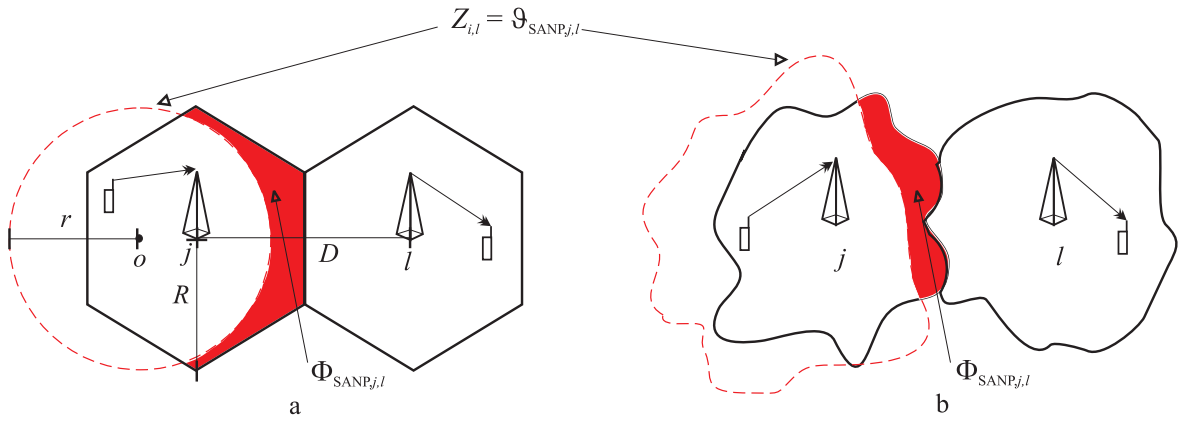


Figure 6.5: Forbidden zone in cell j when the slot allocation method based on normalized mobile-to-base station pathgains (SANP) is used: (a) without shadowing (b) and with shadowing

A slot n can be allocated to mobile i if each cell of set $\Psi_{i,j}$ is either active in uplink or not active during this slot. Moreover, slot n cannot be allocated to mobile i if at least one cell of the set $\Psi_{i,j}$ is active in downlink.

In UTRA TDD, base stations transmit with a constant power on the Primary Common Control Physical Channel (P-CCPCH). The value of this power and the CIR target are broadcast to all mobiles. Similarly, values of $\vartheta_{SAP,j,l}$ or $\vartheta_{SANP,j,l}$ for each cell can be also broadcasted on the same channel. Moreover, mobiles can measure the received powers from the most favorable base stations (typically 6) in P-CCPCH and estimate their pathgains toward these cells. Thereafter, each mobile i builds its high interference-cells set $\Psi_{i,j}$. This set $\Psi_{i,j}$ is communicated to the RNC unit of the system only at the call initialization and when the set changes. Consequently, the RNC can allocate slot n for the uplink traffic of mobile i , if each cell of the set $\Psi_{i,j}$ is either active in uplink or not active during slot n . Moreover, the RNC can take a reallocation decision based on the instantaneous high interference-cells sets of mobiles.

The slot allocation technique is different for downlink channels; let us assume that cell j is allocating a downlink resource to mobile i during a slot n . If cell l is active in uplink during slot n , than base station l receives a base station-to-base station interference $\mathcal{I}_{bb,l,j}$ from cell j . Otherwise, if cell l is active in downlink, mobiles of this cell receive base station-to-mobile interference from cell j . The mean value of the latter interference is very comparable to $\mathcal{I}_{bb,l,j}$ (figure 6.6). Thus, it is not suitable to prevent mobiles of cell j with high pathgain or normalized pathgain toward base station l from being active in downlink during slot n . Moreover, Base station-to-base station interference may be avoided by cell planning (e.g. limiting maximum transmitted powers by base stations, taking sufficient base station-to-base station distances, decreasing antenna tilt and sectorization).

6.5 Interference Avoidance Techniques Analysis

In the DBS method, the number of forbidden cells is fixed. This property decreases the flexibility (i.e. increases blocking probability) of the system by preventing mobiles, close to their servers, from being active in crossed slots with the forbidden cell. In addition, some mobiles can be close to borders of two cells. These mobiles are forbidden from being active in crossed slots with only one of these cells. However, they can generate very high mobile-to-mobile interference to other cells and increase the outage probability.

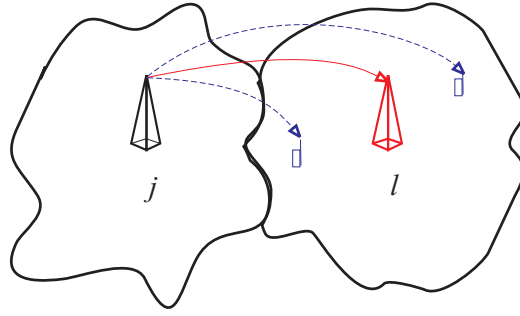


Figure 6.6: Base station-to-base station interference in crossed slot (solid line) and base station-to-mobile interference (dashed lines)

The DARD method prevents mobiles of the forbidden zones from being active in uplink if one of neighboring cells is active in downlink. This slot allocation is forbidden even if the only active cell in downlink is very far from the considered mobile. This procedure increases significantly the blocking probability. This problem can be solved by using the proposed methods where the number of forbidden cells varies depending on mobile positions and their environment.

Due to the dynamic nature of the proposed interference avoidance methods, the blocking probability in the system is smaller than the one found in a system using DARD and DBS methods. In figure (6.7), we can see that the forbidden zone in cell j is reduced when using SAP or SANP with the same cell slot-configuration; hence, the mean number of mobiles that can be active in the studied slot is higher when using the proposed method, and thus the blocking probability of the overall system is reduced. It must be noted that the forbidden zone is reduced without significantly increasing the probability of having high mobile-to-mobile interference.

We remind that a mobile with high normalized pathgains is called high-gain mobile. High-gain mobiles are generally at the border of cells. These mobiles generate high interference and may have low CIR. If the surface of $\Phi_{\text{SANP},j,l}$ (or $\Phi_{\text{SAP},j,l}$) increases, the number of high-gain mobiles during an uplink slots (without crossed slots) increases and thus, the interference received by cell j in these slots increases. On the other hand, if the surface of $\Phi_{\text{SANP},j,l}$ (or $\Phi_{\text{SAP},j,l}$) decreases, the probability of finding two close mobiles transmitting in opposite link directions during a crossed slot increases; thus, the probability of high mobile-to-mobile interference increases. Therefore, a compromise must be taken between these two constraints by using a suitable threshold $\vartheta_{\text{SANP},j,l}$ (or $\vartheta_{\text{SAP},j,l}$). Suitable values of $\vartheta_{\text{SANP},j,l}$ (or $\vartheta_{\text{SAP},j,l}$) can be estimated using radio planning tests and may be changed in time depending on the history of measures.

6.5.1 System Model

The proposed interference avoidance methods are evaluated in an UTRA TDD system of 12 cells and 12 time slots. In this system, we assume that three slots among 15 are reserved for broadcast, random access and signaling channels. The simulation area is finite, i.e. no wraparound is used. This implies that border effects will affect the results but that will be the case in a real UMTS TDD system as well.

In this system, the SANP is compared to the diversified switching point technique and to the common switching point technique. The SAP method has been evaluated in [NL03b] and it has been shown by simulation that it outperforms the existing interference avoidance methods presented in section 6.1.

In the common switching point technique, the switching point is the same for all cells and it

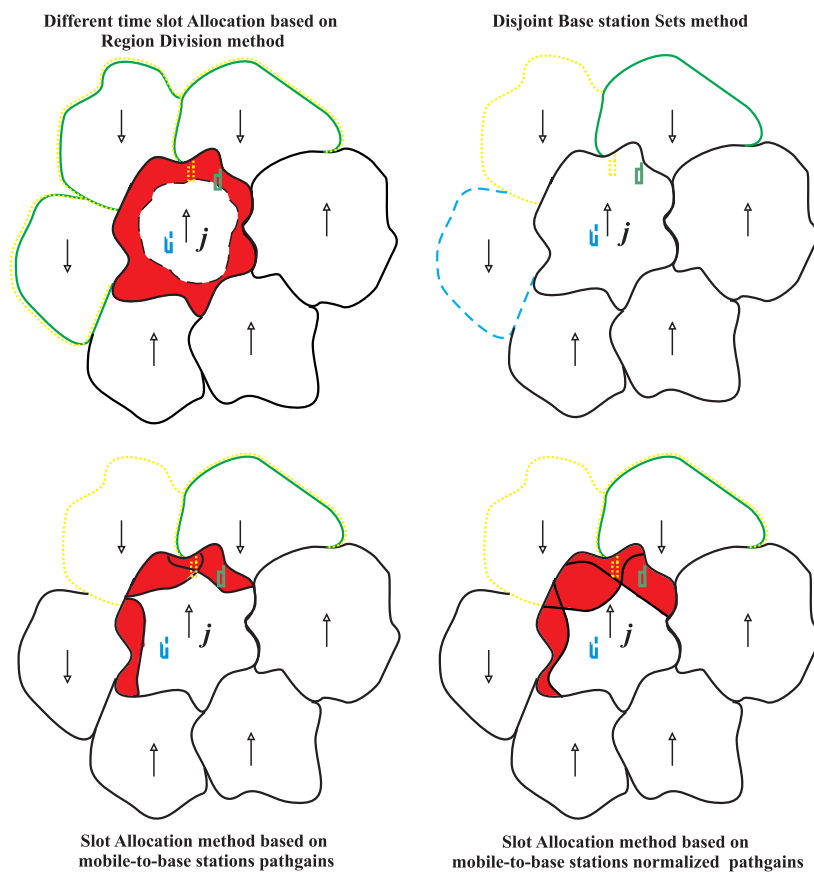


Figure 6.7: Forbidden cells for three mobiles when an interference avoidance method is used (Forbidden cells of a mobile have the same line pattern as the mobile)

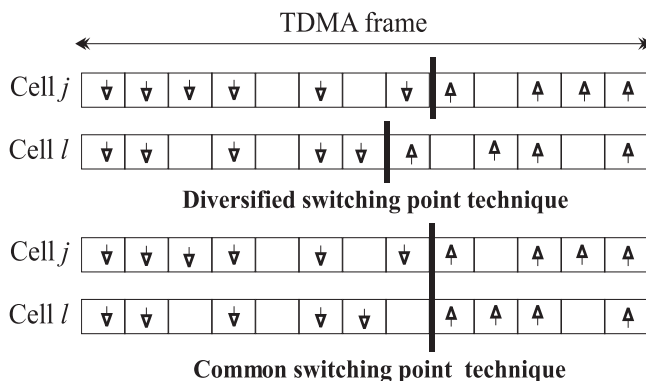


Figure 6.8: The diversified and common switching point techniques

varies according to the ratio of total traffic in the two links. In the diversified switching point technique, each cell has only one specific switching point that varies according to the ratio of traffic between uplink and downlink in the cell (figure 6.8). Interference avoidance methods are combined with the diversified switching point technique.

The studied slot allocation methods determine the set of slots that can be used by a new mobile in uplink and downlink. Thereafter, a slot with free codes is chosen randomly from the set of allowed slots. This random procedure is used to increase the probability of high mobile-to-mobile interference. Therefore, the proposed methods are evaluated in worst situations.

In real systems, there is a mixture of different services in each cell. In our simulation model, we assign one type of services to a cell in order to have a simple configuration where crossed slots are suitable. We consider two types of circuit switched services: asymmetric data service in the 3 central cells and symmetric speech service in the nine other cells (figure 6.9). For both services, calls are generated according to a Poisson process assuming mean call duration of 120 seconds [UMT98]. Data service needs one code in uplink and five codes in downlink with a spreading gain of 13.9 dB, while voice service needs one code in each link with the same spreading gain as data service.

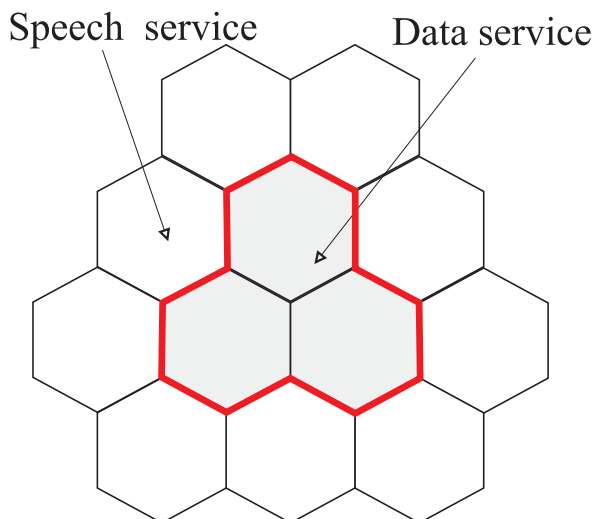


Figure 6.9: Traffic distribution over cells

Table 6.1: Simulation parameters [TS202j]

	uplink	downlink
CIR_{target} [dB]	-7.8	-10.2
Thermal noise power [dBm]	-103	-98
Max Tx power [dBm]	21	20
Max BTS power [dBm]	-	33
Mobile Power cntrl range [dB]	65	25
BTS power cntrl range [dB]	-	30

We consider small hexagonal macrocells with 0.3 km radius. Mobiles are assumed connected to the best server and they are uniformly distributed to cells. Furthermore, we assume that all cells have the same mean load (simultaneous active code number). The arrival rates for data and voice users are λ_d and λ_v respectively. These rates have to satisfy the following equation in order to have the same mean load in all cells:

$$9c_d\lambda_d = 3c_v\lambda_v, \quad (6.6)$$

where c_d and c_v are the number of codes in both uplink and downlink used by data and voice users respectively. The constraint on transmitted powers, the CIR target and the value of thermal noise are presented in table 6.1 [TS202j].

The assumed propagation model is an Okumura-hata-cost231 model with shadowing:

$$P_r = P_e \frac{k}{d^{\gamma}} a_{x,y}, \quad (6.7)$$

where P_r and P_e are respectively the received and the transmitted powers, k and γ are constants [AG03], which depend on the type of environment (table 6.2), and d is the distance between the transmitter and the receiver. Factor $a_{x,y}$ models the shadowing effect. It is a time constant, log-normal variable with zero mean [NL03b] (table 6.2). Simulation minimum coupling loss (MCL) between different transmitters and receivers [TS202j] are also given in table 6.2. It can be noted that the shadowing factor variance and path losses between two mobiles are very high compared to those between two base stations due to the low altitude of mobile antennas.

In UTRA TDD, open-loop and closed-loop power control procedures are used respectively in uplink and downlink. The use of closed-loop power control induces an oscillation in the received CIR. Thus, perfect open-loop power control is used in both links to decrease the effect of power control on the instantaneous CIR of mobiles when the performance of slot allocation schemes is evaluated. Joint detection techniques are used to decrease intracell-interference [Ver98]. intracell-interference factors are 0.1 and 0.2 respectively in downlink and uplink [AWH02]. The maximum

Table 6.2: Propagation model constants

	$BS - BS$	$BS - MS$	$MS - MS$
k [dB]	-112.7	-127.7	-147.4
γ [dB]	35.5	35.5	40
std[$a_{x,y}$] [dB]	4.24	6	7.34
MCL [dB]	92.32	52.67	38.02

number of codes per slot is reduced to 10 in each cell. Mobility and fast fading are not considered in simulations to reduce the complexity of joint detection techniques.

6.5.2 Simulations and Results

We define CIR_M as the geometric mean value of CIR over two frames, i.e. one Transmission Time Interval (TTI), for a given connection. A low quality connection is defined as a connection where:

$$\text{CIR}_M < \text{CIR}_{target} - 0.5 \text{ dB}, \quad (6.8)$$

in either uplink or downlink.

For each slot allocation technique, the percentage U of unsatisfied codes is estimated:

$$U = \frac{N_u}{N_l} \times 100, \quad (6.9)$$

where N_l is the number of all requested codes and N_u is the number of unsatisfied codes over all frames, mobiles and cells.

All codes of an unsatisfied user are considered as unsatisfied codes. A user is considered as unsatisfied when one of the following events happens:

- ◇ The user call is blocked by the call admission control
- ◇ The user call is dropped after 5 seconds of low quality connection
- ◇ The connection is considered of low quality for more than 5% of the call session

Furthermore, we define the percentage of bad-quality codes as the percentage of dropped codes summed to the percentage of codes that have been considered of low quality for more than 5% of the user call session. The percentage of blocked codes is the percentage of codes blocked by the call admission control.

Each point in the presented plots is the result of 40 simulations. In each simulation, we emulate an active mobile system during 30 minutes. The normalized pathgain is always less than one because each mobile is served by the best server. Hence, when $\vartheta_{\text{SANP},j,l} = 1$, the SANP is reduced to the simple diversified switching point and the sets of high interference-cells are reduced to the null set. In all simulations, we have assumed that all cells have the same normalized pathgain threshold ϑ_{SANP} .

In figure 6.10, the percentage of unsatisfied codes is plotted as a function of the normalized pathgain threshold ϑ_{SANP} when the normalized cell load is 0.65. Moreover, the percentage of bad-quality codes and the percentage of blocked codes are also plotted. The optimal performance is obtained for $\vartheta_{\text{SANP}} = 0.6$ (-2.2 dB). This value is used to compare the SANP to existing slot allocation schemes.

As depicted in figure 6.10, the percentage of bad-quality codes is an increasing function while the percentage of blocked codes is a decreasing function of ϑ_{SANP} as expected. When the value of ϑ_{SANP} increases, the cardinality of sets $\Psi_{i,j}$ decreases, allowing more active mobiles in crossed slots. Therefore, more radio resources are available but the probability of high mobile-to-mobile interference increases. Hence, the percentage of blocked codes decreases while the percentage of bad-quality codes increases. Moreover, we can see that the percentage of bad-quality codes is the limiting factor when the interference avoidance method is used. We can note also that the performance of the SANP method is approximately constant when the normalized pathgain threshold is near to the optimal value.

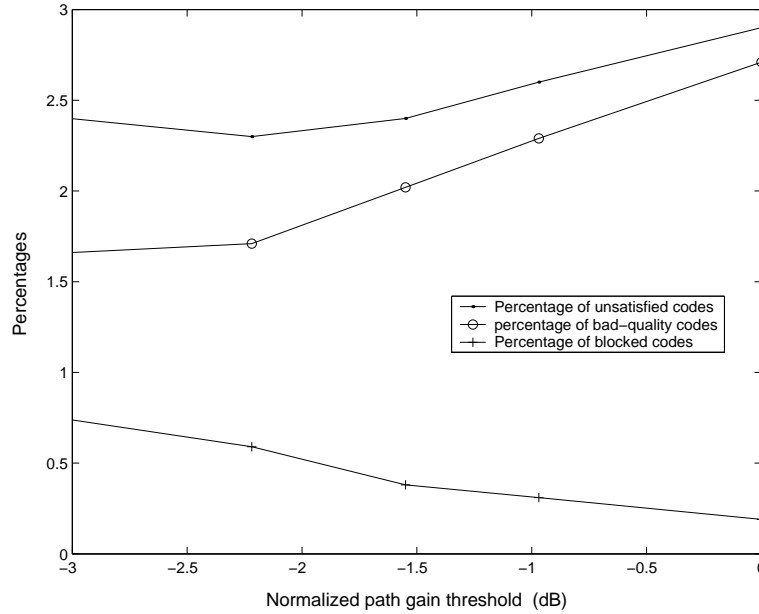


Figure 6.10: The percentage of unsatisfied, bad-quality and blocked codes as a function of ϑ_{SANP} for a normalized cell load of 0.65

In figure 6.11, the percentage of unsatisfied codes is plotted as a function of the normalized cell load for each slot allocation method. The normalized pathgain threshold and the pathgain threshold for the SANP and the SAP are respectively -2.2 and -113 dB. We can note that the common switching point technique gives better results than the diversified switching point technique for low cell loads. However, the percentage of unsatisfied codes in the common switching point technique become higher compared to the one offered by the diversified switching point technique as the cell load increases. This result is due to the fact that the radio resources offered by the common switching point in the downlink of asymmetric cells become scarce when the load exceeds a threshold. Moreover, the uplink slots of symmetric cells suffer from high mobile-to-base station interference due to the limitation in the number of slots.

The percentage of unsatisfied codes offered by the SANP is always less than the percentage of unsatisfied codes offered by the SAP and certainly from the one given by the common switching point and the diversified switching point techniques.

In figure 6.12 and 6.13, the percentages of bad-quality codes and blocked codes are respectively plotted as a function of the normalized cell load.

As expected, these figures show that the common switching point technique is limited by the blocking probability while the diversified switching point technique is limited by the outage probability due to high mobile-to-mobile and base station-to-base station interference. When interference avoidance methods are used, the percentage of blocked codes is higher than the one obtained by the simple diversified switching point technique. This is due to the constraint in the allocation of crossed slots. However, this constraint allows the slot allocation technique to avoid high mobile-to-mobile interference and thus, to decrease the percentage of bad-quality codes.

We can also emphasize that for high cell loads, the percentage of bad-quality and blocked codes are lower when the SAP method is used instead of the SANP method (figure 6.12 and 6.13).

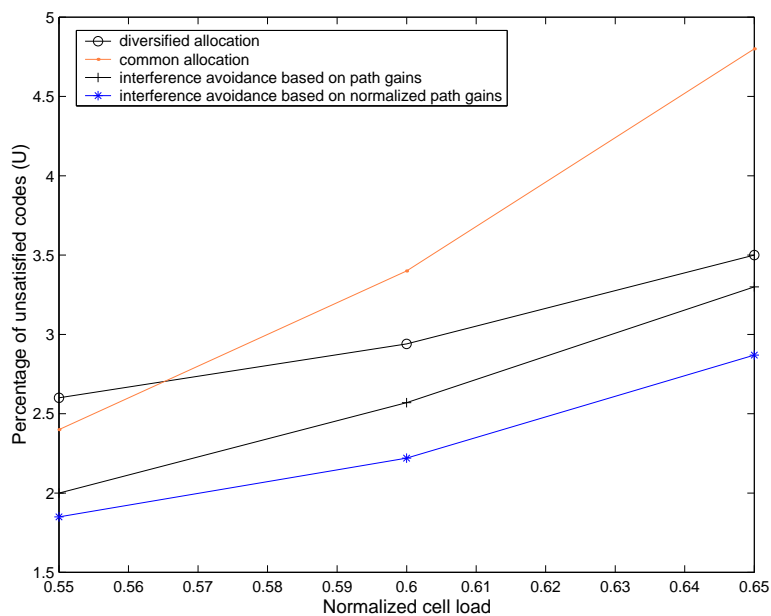


Figure 6.11: The percentage of unsatisfied codes as a function of the normalized cell load

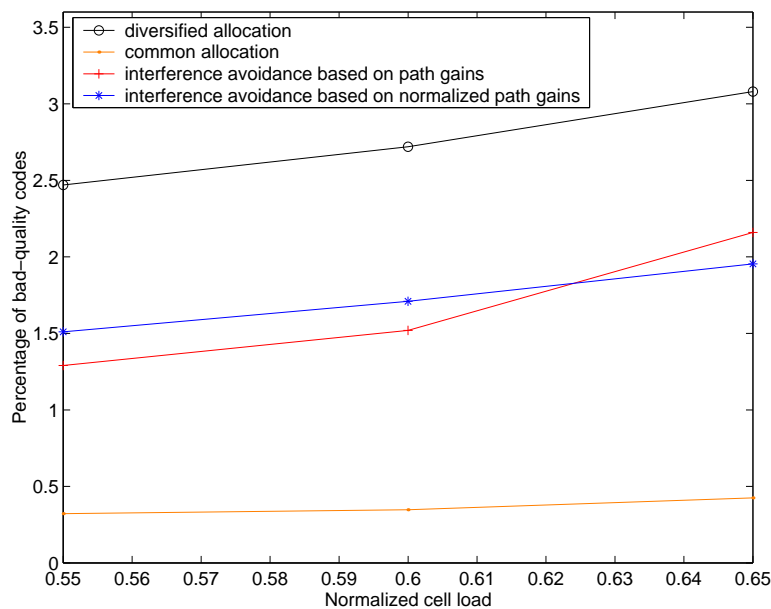


Figure 6.12: The percentage of bad-quality codes as a function of the normalized cell load.

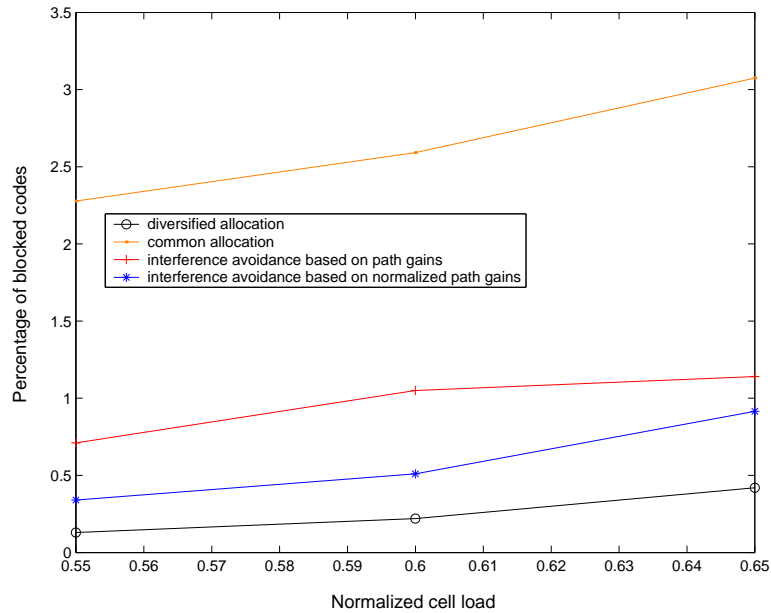


Figure 6.13: The percentage of blocked codes as a function of the normalized cell load.

6.6 Summary

In this chapter, we have proposed two interference avoidance methods that avoid high mobile-to-mobile interference. Like other interference avoidance methods, the proposed methods use the pathgain between mobiles and base stations to avoid high mobile-to-mobile interference. Moreover, the proposed methods use dynamic thresholds and therefore adapt the slot allocation to traffic distribution between uplink and downlink. By using dynamic thresholds, slot allocation can avoid high mobile-to-mobile interference without increasing the blocking probability. Moreover, we integrate the impact of uplink transmitted power by using the normalized pathgain instead of the pathgain toward neighboring base stations. Therefore, high mobile-to-mobile interference are detected with more precision than methods using pathgains.

The proposed methods ameliorate the performance of diversified switching point techniques and give better results than other interference avoidance methods.

It must be noted that the proposed methods do not significantly increase the signaling traffic, i.e. only one new signaling message is added. Therefore, the implementation of these methods is simple and feasible in operational systems.

The optimal threshold is difficult to estimate because it depends on several non constant parameters. Nevertheless, simulation results have shown that the effect of the threshold is not important near to the optimal threshold. Therefore, more suited threshold can be found using planning tools.

Moreover, adaptive versions of the proposed schemes can be used in real systems. In these adaptive schemes, the threshold varies depending on the blocking and bad-quality code percentages, and the cell load of neighboring cells. The SAP and SANP may be used also in the slot reallocation procedure (i.e. inter-slot handover) to reduce high mobile-to-mobile interference generated by the variation in the radio interface.

Chapter 7

Conclusions and Perspectives

Time division duplex is adopted in third generation telecommunications systems due to its high spectral efficiency, low cost and simple device implementation. The flexibility of the TDD mode in handling asymmetric traffic make this mode a promising candidate for 4G wireless systems. However, the flexibility of the TDD mode comes at the expense of increasing the probability of high interference situations. Thus, efficient RRM must be used to alleviate the problem of high interference. In this thesis, we focus on power control and slot allocation techniques. Power control is an important issue to reduce the interference profile, in particular for CDMA systems. Slot allocation techniques offer a new degree of flexibility to CDMA systems. This flexibility can be used to reduce the interference profile, especially when services with high asymmetry between uplink and downlink are required.

7.1 Conclusions

Power control and slot allocation studies have been hot subjects in the last few years. However, these issues have not reach optimal performance in term of simplicity, interference reduction and offering high QoS levels. Therefore, we have proposed RRM procedures that enhance QoS levels with low complexity and small signaling traffic.

A main focus of this thesis is on designing an optimum power control that can be used in all types of slots and situations. Therefore, we have proposed a simplified generic optimum power control algorithm that can be used in uplink, downlink and crossed slots. The proposed optimum power control is a centralized scheme for noiseless systems and requires the knowledge of the pathgains. A variant of the proposed algorithm is also proposed for noisy systems. The simplified feature of the algorithm is reached by using the received powers in uplink and the total transmitted power in downlink instead of the specific transmitted powers of mobiles. This simplification leads to faster convergence to the optimal solution due to the small size of the pathgain matrix. The fast convergence allows the implementation of the optimum algorithm in operational systems and the investigation of complex slot allocation techniques. Using this algorithm, we have compared the upper-bound QoS levels in crossed and uplink slots. The results of this comparison have lead us to a better understanding of the behavior of systems with crossed slots. As expected, crossed slots can offer higher QoS levels if slot allocation techniques can avoid high mobile-to-mobile interference.

A generic mobile-based stepwise removal algorithm based on the simplified optimum power control is proposed also. The stepwise removal algorithm allows the system to disable as few as possible of connections, in order to offer the required QoS level for all remaining connections. Using this algorithm, the outage probability decreases without a significant increase of the blocking

probability. It should be noted that the proposed algorithm is the first stepwise algorithm that takes into account same-entity interferences.

A constrained optimum power control algorithm is proposed also. The proposed constrained power control algorithm takes into account the lower-bound power limitations. The lower-bound constraint is generally omitted by assuming perfect amplifier, which allows all power levels. However, amplifiers have a range of allowed power levels with an acceptable equipment complexity. Therefore, a transmitted power lower-bound is fixed and the optimum solution may not be in the allowed power range. This situation may lead to unnecessary increase in the transmitted power and eventually to a decrease in the QoS level of some connections. These cases are encountered especially in rural environments where the interference level is very close to the background noise and has a high variation across cells. Moreover, the TDD mode and ad-hoc systems are more affected by this situation due to the wide range of interference. The wide range of interference is caused by the presence of high mobile-to-mobile interference which are not taken into account in the design of power control range. Therefore, the investigation of lower-bound constraint is an interesting field. The generic constrained optimum power computes the least-power vector that provides a required QoS level for all connections and takes into account upper and lower-bound power limitations.

Since the radio environment is highly changing, adaptive schemes are suited to better allocate transmitted powers. Moreover, a CIR margin is used to prevent the CIR level from falling below the desired target. However, the CIR margin induces unnecessary power increase and may lead to high outage probability. Therefore, a stabilization zone can replace the CIR margin; if the CIR of a mobile is in the stabilization zone, the transmitted power is stabilized. Thus, the stabilization zone can be considered as adaptive CIR margin. In addition to the outage amelioration, the stabilization zone decreases the transmitted power. Low power transmission leads to a low electromagnetic radiation and to an increase in battery life.

The combination of the TDD mode and the TDMA technique adds a new degree of freedom to UMTS systems. This issue can be exploited by efficient slot allocation techniques. In the literature, we can find a big number of slot allocation strategies: allocating the slot with the highest achievable CIR, the slot with the lowest power budget, the slot with the lowest interference profile, etc. The performances of these strategies are evaluated by comparing their offered QoS levels. A more efficient performance evaluation can be achieved using a slot allocation reference. The most suited slot allocation reference is the optimum technique that find the best mobile distribution of mobiles over slots. However, the optimum technique is not feasible; the slot allocation problem can be defined as a max-min-max problem with mixed-integer nonlinear constraints. This problem is an NP-hard problem and it is very difficult to find the optimum solution when the number of slots, cells or mobiles is slightly high. Therefore, the optimum technique has to be replaced by methods that have always high performance. A possible solution is to divide the total optimization problem into several small problems (e.g. the slot allocation strategy is executed in each cell independently of other cells). Obviously, an allocation where all slots have approximately the same CIR can give high performance. In order to obtain this allocation, we propose two combinatorial methods: find the allocation in each cell with a fair distribution of mobiles over cells or find the allocation that gives directly a fair distribution in the system. In the first method, low-gain mobiles are grouped with high-gain mobiles in each cell. In the second method, on the contrary, high-gain mobiles are grouped with each other in each cell and thereafter high-gain mobile groups are grouped with low-gain groups of other cells. The second method is suited in noiseless systems where the achievable CIR depends only on the normalized pathgain matrix. In noisy systems however, power limitation is an important factor for the slot allocation performance. Therefore, the performance of the second method decreases due to the high variance of the transmitted powers in different cells. On the contrary, having a fair distribution of mobiles over slots in each cell guarantee a fair distribution of

powers during slots also. Therefore, this method is more suited in noisy systems.

We have also proposed iterative heuristic methods that distribute high-gain mobiles at the beginning. Distributing high-gain mobiles at the beginning helps the scheme to estimate the CIR in each slot. This is due to the fact that the pathgains of high-gain mobiles are the main factors for determining the achievable CIR. The proposed iterative heuristic method offers higher performance than the combinatorial methods though it is far faster. Another solution to the optimization problem is to combine a re-allocation scheme with simulated annealing. Simulated annealing is chosen from meta-heuristic methods because it is the oldest method that prevents the convergence to local optima and does not need big memory. The re-allocation method using simulated annealing has shown the best performance. Moreover, the re-allocation method can be used in operational systems by using the transmitted power as performance-index for slots.

In spite of the advantages of the TDD mode, mobile-to-mobile interference are allowed and may dramatically decrease the performance of the system. The difficulty in avoiding mobile-to-mobile interference is that pathgains between mobiles are very difficult to be estimated. Therefore, methods based on pathgains between mobiles and base stations are used to estimate pathgains between mobiles and avoid high mobile-to-mobile interference. In chapter six, we have proposed two methods. The first method uses the pathgains between mobiles and interfering cells, whereas the second method uses the normalized pathgains. Unlike the slot allocation method based on mobile-to-base station pathgains, the slot allocation method based on mobile-to-base station normalized pathgains takes into account the transmitted power levels. Both methods allow dynamic forbidden zones. In forbidden zones, mobiles are prevented from being active with other mobiles active in the opposite link direction. The dynamic feature of these methods conserves the flexibility of the TDMA-CDMA/TDD system though the outage probability is decreased.

We conclude this thesis by emphasizing the crucial importance of RRM to guarantee acceptable levels of QoS. This thesis has suggested power control algorithms and slot allocation techniques that offer high QoS levels with low power consumption. We emphasize also that RRM techniques must be used carefully in order to exploit efficiently the scarce radio units.

7.2 Perspectives

We studied the simplified generic optimal power control in a system where only one QoS level is required (i.e. all mobiles require the same CIR). However, next generation systems must accommodate different services that have different QoS requirements. The simplified generic optimal power control can be easily extended to cover these types of systems. This is left for future works.

In the TDD mode, the interference power in a server is broadcast to all mobiles of the server. Therefore, an uplink decentralized power control based on the proposed optimum power control with the consideration of thermal noise is one of possible future work. Thereafter, a combined power control using the iterative optimum power control in uplink and any downlink power control can be designed for crossed slots.

The generic mobile-based stepwise removal algorithm is the first removal algorithm for crossed slots and may be taken as a basic algorithm for more efficient removal algorithms. Due to the drastic reduction in the computation time and to crossed slots integration, the proposed optimum power control can be used to develop sophisticated channel allocation techniques.

The adaptive power control algorithm has been evaluated in downlink slots only. Further investigation can be made to evaluate the performance of the algorithm in crossed slots, where a perfect power control is used in uplink.

At the end of our work, we have noticed that there is a lack in the study of slot allocation

optimization. The results of our simulations have shown that the random allocation can offer high performance in some situations. We have proposed several methods that offer higher QoS levels. However, we cannot say if the solution of these methods are close or very far from the optimum solution. Further challenges include the introduction of methods that give a good approximation of the optimal solution. This approximation can be used as a reference for slot allocation techniques.

The emerging services in wireless systems require high flexibility in the radio interface. One possibility to insure this flexibility is to combine the advantages of several wireless networks. This can be done by developing control layers able to insure best QoS levels according to available networks and constraints introduced by radio channels. These control layers are intended to perform Common Radio Resource Management (CRRM) procedures to different wireless networks. The meta-heuristic method proposed to the re-allocation scheme can be adapted to take into account several radio interface and perform vertical-handovers. Moreover, the simplified optimum power control and its application can be adapted to all interference-limited systems.

Appendix A

Useful Propositions for Constrained Power Control Algorithms

In this appendix, we introduce the propositions used to design the constrained power control algorithm in chapter three. These propositions can be used also to better understand the behavior of power control algorithms in general and to design new algorithms.

Proposition A.1 Let \mathbf{P}_W be a power vector that satisfies the following matrix equation:

$$\frac{1 + \gamma_0}{\gamma_0} \mathbf{P}_W = \mathbf{Z}_W \mathbf{P}_W + \mathbf{N}_W \quad (\text{A.1})$$

Let X be a power level higher than one element $P_{W,j}$ of \mathbf{P}_W . There exists a power vector \mathbf{P} with $P_j = X$ that satisfy:

$$\frac{1 + \gamma_0}{\gamma_0} \mathbf{P} \geq \mathbf{Z}_W \mathbf{P} + \mathbf{N}_W$$

Proof. We have $X \geq P_{W,j}$, then there exists a constant $c \geq 1$ such as $X = cP_{W,j}$. Let $\mathbf{P} = c\mathbf{P}_W$, therefore $P_j = X$. Moreover, $\mathbf{P}_W = \frac{\gamma_0}{1+\gamma_0} (\mathbf{Z}_W \mathbf{P}_W + \mathbf{N}_W)$; therefore, $\frac{\mathbf{P}}{c} = \frac{\gamma_0}{1+\gamma_0} (\mathbf{Z}_W \frac{\mathbf{P}}{c} + \mathbf{N}_W)$. Thus:

$$\begin{aligned} \mathbf{P} &= c \frac{\gamma_0}{1 + \gamma_0} \left(\frac{1}{c} \mathbf{Z}_W \mathbf{P} + \mathbf{N}_W \right) \\ &= \frac{\gamma_0}{1 + \gamma_0} \mathbf{Z}_W \mathbf{P} + c \frac{\gamma_0}{1 + \gamma_0} \mathbf{N}_W \end{aligned}$$

However, $c \geq 1$; therefore, $c \frac{\gamma_0}{1+\gamma_0} \mathbf{N}_W \geq \frac{\gamma_0}{1+\gamma_0} \mathbf{N}_W$ and hence:

$$\mathbf{P} \geq \frac{\gamma_0}{1 + \gamma_0} (\mathbf{Z}_W \mathbf{P} + \mathbf{N}_W)$$

■

Remark A.1 We can interpret proposition A.1 as follows: In a CDMA system, it is always possible to increase the power of one element of the optimal solution and to find feasible solutions in non upper-bounded constrained problems.

Remark A.2 We consider a CDMA system where the solution of equation (A.1) involves a set U of power elements smaller than P_{\min} . If we set all elements of the set U to P_{\min} , it is possible that we cannot find a set of remaining powers that satisfy inequality $\frac{1+\gamma_0}{\gamma_0} \mathbf{P}_W \geq \mathbf{Z}_W \mathbf{P}_W + \mathbf{N}_W$ ¹.

Proposition A.2 Let \mathbf{P}_W be an $(N \times 1)$ vector that satisfy equation (A.1)¹. All $(N \times 1)$ vectors $\tilde{\mathbf{P}}_W \geq \mathbf{P}_W$ and satisfying at least $(N - 1)$ equations² of the system of linear equations (A.1), satisfies also:

$$\frac{1 + \gamma_0}{\gamma_0} \tilde{\mathbf{P}}_W \geq \mathbf{Z}_W \tilde{\mathbf{P}}_W + \mathbf{N}_W. \quad (\text{A.2})$$

Proof. Let $\tilde{\mathbf{P}}_W$ be an $(N \times 1)$ power vector satisfying $(N - 1)$ equations of linear equations (A.1) with $\tilde{\mathbf{P}}_W \geq \mathbf{P}_W$. Let i be the index of the equation that $\tilde{\mathbf{P}}_W$ does not satisfy by definition. Let \mathbf{Z}_{W_s} , \mathbf{N}_{W_s} be the $((N - 1) \times (N - 1))$ matrix and the $((N - 1) \times 1)$ vector formed by eliminating the i th row from matrix \mathbf{Z}_W and vector \mathbf{N}_W respectively (s stands for subsystem). By definition, $\tilde{\mathbf{P}}_W$ satisfies the conditions of the proposition:

$$\begin{aligned} \frac{1 + \gamma_0}{\gamma_0} \tilde{\mathbf{P}}_W &= \mathbf{Z}_{W_s} \tilde{\mathbf{P}}_W + \mathbf{N}_{W_s} \\ \tilde{P}_{W,k} &\geq P_{W,k} \quad \forall k \in [1 \cdots N]. \end{aligned} \quad (\text{A.3})$$

By definition, equation (A.2) is fulfilled in $(N - 1)$ rows of matrix \mathbf{Z}_W . Therefore, we must only prove the following inequality:

$$\frac{1 + \gamma_0}{\gamma_0} \tilde{P}_{W,i} \geq \sum_{k=1}^N \mathcal{Z}_{W,i,k} \tilde{P}_{W,k} + N_{W,i}.$$

As $\tilde{P}_{W,i} \geq P_{W,i}$ we can apply proposition A.1. Therefore, there exists a power vector \mathbf{P} satisfying:

$$\begin{aligned} P_i &= \tilde{P}_{W,i} \\ &\text{and} \\ \frac{1+\gamma_0}{\gamma_0} \mathbf{P} &\geq \mathbf{Z}_W \mathbf{P} + \mathbf{N}_W. \end{aligned} \quad (\text{A.4})$$

The latter is certainly fulfilled for the subset of matrix inequality:

$$\frac{1 + \gamma_0}{\gamma_0} \mathbf{P} \geq \mathbf{Z}_{W_s} \mathbf{P} + \mathbf{N}_{W_s}$$

As $\tilde{\mathbf{P}}_W$ is the optimal solution of (A.3), we can deduce from remark 3.2 in section 3.2.1 that $\mathbf{P} \geq \tilde{\mathbf{P}}_W$ when P_i is considered as a constant. Hence:

$$\sum_{k=1}^N \mathcal{Z}_{W,i,k} P_k \geq \sum_{k=1}^N \mathcal{Z}_{W,i,k} \tilde{P}_{W,k}. \quad (\text{A.5})$$

Moreover, equation (A.4) gives:

$$\frac{1 + \gamma_0}{\gamma_0} P_i \geq \sum_{k=1}^N \mathcal{Z}_{W,i,k} P_k + N_{W,i}.$$

¹See the demonstration of proposition A.3

¹This matrix equation is equivalent to N linear equations

² \mathbf{P}_W satisfies a system of linear equations if all the **equalities** of the system are satisfied.

We remind that $P_i = \tilde{P}_{W,i}$, therefore:

$$\frac{1 + \gamma_0}{\gamma_0} \tilde{P}_{W,i} \geq \sum_{k=1}^N \mathcal{Z}_{W,i,k} P_k + N_{W,i}.$$

Therefore:

$$\frac{1 + \gamma_0}{\gamma_0} \tilde{P}_{W,i} \geq \sum_{k=1}^N \mathcal{Z}_{W,i,k} \tilde{P}_{W,k} + N_{W,i}.$$

■

Proposition A.3 Let \mathbf{P}_W be the solution of equation (A.1), with at least one power element lower than P_{\min} . Let E_S be the set of indices k for which $P_{W,k} < P_{\min}$ and P_{\min} is a feasible solution. The optimal solution in term of minimizing the total transmitted power that satisfies the inequality (A.2) with a power vector $\mathbf{P} \geq \mathbf{P}_{\min}$ must satisfy the following constraints:

- For *only some* indices $m \in E_S$, $P_m = P_{\min}$
- For all other indices, we must have:

$$\frac{1 + \gamma_0}{\gamma_0} P_{W,i} = \sum_{k=1}^N \mathcal{Z}_{W,i,k} P_{W,k} + N_{W,i} \quad \forall i \neq m$$

Proof. Let U be the set of indices k for which $P_{W,k} < P_{\min}$. In order to prove proposition A.3, we must prove that the set E_S exists, that the set of all indices corresponding to equations for which P_{\min} is not feasible, cannot be in the solution of the optimization problem with the lower-bound power constraint and that only some elements of E_S must be fixed to P_{\min} .

a) Let i be the index of the lowest transmitted power in vector \mathbf{P}_W : $P_{W,i} = \min_{k \in [1 \dots N]} P_{W,k}$. Let $\mathbf{P} = c\mathbf{P}_W$, with $c = \frac{P_{\min}}{P_{W,i}}$. \mathbf{P} is a solution of $\frac{1+\gamma_0}{\gamma_0} \mathbf{P} \geq \mathbf{Z}_{W_s} \mathbf{P} + \mathbf{N}_{W_s}$ (see the demonstration of A.1). Therefore, the inequality i is satisfied:

$$\frac{1 + \gamma_0}{\gamma_0} P_{\min} \geq \sum_{k=1}^N \mathcal{Z}_{W,i,k} P_k + N_{W,i}$$

Nevertheless, $P_k \geq P_{\min}$ for all k . Therefore, $\sum_{k=1}^N \mathcal{Z}_{W,i,k} P_k \geq \sum_{k=1}^N \mathcal{Z}_{W,i,k} P_{\min}$. Therefore, P_{\min} is a feasible power for equation i . Hence, $i \in E_S$ and $E_S \neq \emptyset$.

b) Let i be an equation for which P_{\min} is not feasible (i.e. $i \in U$); therefore,

$$\frac{1 + \gamma_0}{\gamma_0} P_{\min} < \sum_{k=1}^N \mathcal{Z}_{W,i,k} P_{\min} + N_{W,i}.$$

Thus, other powers must be smaller or equal P_{\min} in order to set the element i of an inequality solution¹ \mathbf{P} to P_{\min} . This is impossible, because \mathbf{P} must satisfy $\mathbf{P} \geq \mathbf{P}_W$ (see remark 3.2). Therefore, P_i must be higher than P_{\min} . Furthermore, for all equations k for which $P_{W,k} > P_{\min}$ (i.e. $k \notin U$), then P_{\min} is not a feasible power for equation k (see remark 3.2). Therefore, all elements corresponding to equations for which P_{\min} is not feasible must be strictly higher than P_{\min} .

¹We call a vector \mathbf{P} satisfying $\frac{1+\gamma_0}{\gamma_0} \mathbf{P} \geq \mathbf{Z}_{W_s} \mathbf{P} + \mathbf{N}_{W_s}$ an inequality solution.

c) In order to show that only some elements of E_S (and not all elements) must be fixed to P_{\min} we take an example:

$$\mathbf{Z}_W = \begin{pmatrix} 1 & 0.4 & 0.5 \\ 0.8 & 1 & 0.6 \\ 0.03 & 0.22 & 1 \end{pmatrix} \quad \mathbf{N}_W = \begin{pmatrix} 0.53 \\ 0.52 \\ 0.38 \end{pmatrix}$$

$P_{\min} = 0.8$ and $\gamma_0 = 0.5$. We obtain:

$$\mathbf{P}_W = \begin{pmatrix} 0.55 \\ 0.73 \\ 0.85 \end{pmatrix}$$

This vector does not satisfy the lower-bound power constraint (i.e. $U = \{1, 2\}$). However, P_{\min} is feasible for the two first equations. Therefore $E_S = \{1, 2\}$. For $P_{W,1} = P_{W,2} = 0.8$, we obtain $P_{W,3} = 0.865$. For these values, the CIR of the second user is only 0.48 which is smaller than γ_0 . In order to satisfy all constraints, only the power of the first mobile should be fixed to P_{\min} . In this case, the CIR of the latter is 0.7 while the other mobiles have a CIR of 0.5. ■

The following proposition is intended to determine the subset of indices for which the power must be fixed to P_{\min} in order to obtain the optimal solution.

Proposition A.4 Let E be a nonempty set of indices for which the corresponding powers can be set to P_{\min} . Let $\mathbf{P} = \{P_k : P_k = P_{\min} \text{ if } k \in E \text{ and } \frac{1+\gamma_0}{\gamma_0} P_k = \sum_{m=1}^N \mathcal{Z}_{W,k,m} P_m + N_{W,k} \text{ if } k \notin E\}$ and let i be an index of E for which $\frac{1+\gamma_0}{\gamma_0} P_{\min} < \sum_{m=1}^N \mathcal{Z}_{W,i,m} P_m + N_{W,i}$. Thus, the power element P_i cannot be set to P_{\min} in the power vector \mathbf{P} that satisfies the matrix inequality (A.2) and $\mathbf{P} \geq \mathbf{P}_{\min}$.

Proof. Let $\mathbf{P} = \{P_k : P_k = P_{\min} \text{ if } k \in E \text{ and } \frac{1+\gamma_0}{\gamma_0} P_k = \sum_{m=1}^N \mathcal{Z}_{W,k,m} P_m + N_{W,k} \text{ if } k \notin E\}$. When using \mathbf{P} , a user subset of E is satisfied (i.e. $\frac{1+\gamma_0}{\gamma_0} P_{\min} \geq \sum_{k=m}^N \mathcal{Z}_{W,k,m} P_m + N_{W,k}$) and the remaining users of E are unsatisfied (i.e. $\frac{1+\gamma_0}{\gamma_0} P_{\min} < \sum_{m=1}^N \mathcal{Z}_{W,k,m} P_m + N_{W,k}$) (see proposition A.3). The latter are grouped in subset U . We remind that only mobiles of the set E can be set to P_{\min} with a power vector higher than the lower-bound. Therefore, no other different sets of users can use the power P_{\min} . In order to satisfy the users in set U , we have two choices: 1) increase the powers of mobiles in set U (\bar{P}_k must be higher than P_{\min} for all $k \in U$). Therefore, the only powers to be fixed to P_{\min} must be from the set $E - U$. 2) decrease the powers of mobiles in set $E - U$. In this case, the powers in the set $E - U$ are smaller than P_{\min} . This solution does not satisfy the lower-bound constraint. Therefore, the only powers to be fixed to P_{\min} must be from the set $E - U$. Therefore, mobiles of set U cannot transmit with P_{\min} and satisfy all constraints in the lower-bounded constraint power control problem. ■

Remark A.3 It must be noted that set E is included in set E_s (see proposition A.3).

Appendix B

Number of all Possible Partitions in a CDMA/TDMA System

In this appendix, we compute the number of all possible partitions and the number of partitions that consider only fair mobile distributions into slots in all cells. We consider a TDMA-CDMA/TDD system with T slots, M cells and N_j mobiles in cell j . We denote by \mathcal{N} the total number of investigated partitions in order to find the optimal partition in term of maximizing the minimum CIR. Obviously, a partition with empty slots cannot be the optimal partition; for any partition with empty slots, we can take a mobile i from a nonempty slot n_n and allocate an empty slot n_e to this mobile. In the new partition, the CIRs of mobiles during slot n_n increase and the CIR of mobile i increases also. Therefore, we can always find a partition with nonempty slots better than a partition with empty slots. Moreover, we call \mathcal{N}_j the number of partitions in cell j .

B.1 \mathcal{N} as a function of \mathcal{N}_j

The following equation can be deduced using recurrence method:

$$\mathcal{N} = \frac{\prod_{j=1}^M \mathcal{N}_j}{T!}. \quad (\text{B.1})$$

Proof. The number of partitions in one cell is $\mathcal{N}_j/T!$, that satisfy B.1. The number \mathcal{N}_j is divided by $T!$ to eliminate the number of slot permutations (The slot permutation is considered when \mathcal{N}_j is computed). Assume that $\mathcal{N}^{(M)} = \frac{\prod_{j=1}^M \mathcal{N}_j}{T!}$ for M cells, and prove that $\mathcal{N}^{(M+1)} = \frac{\prod_{j=1}^{M+1} \mathcal{N}_j}{T!}$ for $M+1$ cells. For each partition of cell $M+1$, there is $\mathcal{N}^{(M)}$ possible distributions that give different interference profiles at least in one slot. Moreover, there is \mathcal{N}_{M+1} partitions in cell $M+1$. Hence, the number of possible partitions for $M+1$ cells is given by:

$$\mathcal{N}^{(M+1)} = \mathcal{N}_{M+1} \mathcal{N}^{(M)}.$$

Thus,

$$\mathcal{N}^{(M+1)} = \frac{\prod_{j=1}^{M+1} \mathcal{N}_j}{T!},$$

and the equation is proved by recurrence. ■

B.2 Computation of \mathcal{N}_j

In this section, we compute the number of ways \mathcal{N}_j of partitioning a set of N_j elements into T nonempty subsets that cannot be associated to more than A elements simultaneously. We emphasize that the number of elements N_j must not be higher than $A \times T$ in order to allocate all elements.

B.2.1 All possible Partitions

From combinatory algebra, we know that Stirling number $\mathcal{S}(N_j, T)$ gives the number of ways of partitioning a set of N_j elements into T nonempty subsets without repetition. However, the number $\mathcal{S}(N_j, T)$ does not consider the limitations in the number of elements in a subset. In the following, we denote by $\mathcal{S}_A(N_j, T)$ the number of all possible partitions with nonempty subsets, where each subset can be associated to A elements at maximum.

It must be noted that in $\mathcal{S}_A(N_j, T)$ no repeated combinations are counted. We call a repeated combination a combination that can be obtained by a permutation of an existing combination.

The number $\mathcal{S}_A(N_j, T)$ is computed by recurrence. In order to guarantee that no repetition is performed, we fix the association of the first element to the first subset. Therefore, no other subsets can have the same pattern than the first subset. Hence, we may have 0, 1, ... or $A - 1$ elements other than the first element in the first subset. By fixing the first element in the first slot, we have $\binom{k-1}{N_j-1}$ combinations of k elements in the first subset. For each combination of k elements in the first subset, we have $\mathcal{S}_A(N_j - k, T - 1)$ partitions of $N_j - k$ elements into $T - 1$ subsets. Hence, $\mathcal{S}_A(N_j, T)$ is given by the following recurrence equation:

$$\mathcal{S}_A(N_j, T) = \sum_{k=\varrho}^v \binom{k-1}{N_j-1} \mathcal{S}_A(N_j - k, T - 1), \quad (\text{B.2})$$

where ϱ and v are the minimum and the maximum numbers of elements that can be allocated to the first subset.

The factor ϱ is used to guarantee that at least one element is associated to the first subset and to limit the number of the remaining elements to $A(T - 1)$ at maximum, i.e. the number of remaining elements can be supported by the $T - 1$ slots. Therefore, ϱ is given by:

$$\varrho = \max(1, N_j - A(T - 1)). \quad (\text{B.3})$$

The factor v is used to limit the number of elements in the first subset to A and to guarantee that at least one element is associated to each remaining subset. Therefore, v is given by:

$$v = \min(A, N_j - (T - 1)) \quad (\text{B.4})$$

It must be noted that the number $\mathcal{S}_A(N_j, T)$ is equivalent to $\mathcal{S}(N_j, T)$ if all partitions do not contain subsets with more than A elements; therefore:

$$\mathcal{S}_A(N_j, T) = \mathcal{S}(N_j, T) \quad \text{if } n - A \leq T - 1 \quad (\text{B.5})$$

Furthermore, the total number of partitions into one subset equal to unity:

$$\mathcal{S}_A(N_j, 1) = 1 \quad (\text{B.6})$$

Certainly, there is no partitions if the number of elements exceeds the maximum number of elements that can be accepted in the subsets:

$$\mathcal{S}_A(N_j, T) = 0 \quad \text{if } n > A \times T \quad (\text{B.7})$$

Finally, the number \mathcal{N}_j of all partitions with all possible permutations is given by:

$$\mathcal{N}_j = T! \times \mathcal{S}_A(N_j, T), \quad (\text{B.8})$$

If we consider all partitions with empty subsets, the number \mathcal{N}_j becomes:

$$\mathcal{N}_j = \sum_{n=\varrho_T}^T n! \times \mathcal{S}_A(N_j, n) \quad (\text{B.9})$$

where the minimum number of subsets ϱ_T is the number of subsets that allows the distribution of all the elements. therefore:

$$\varrho_T = \left\lceil \frac{N_j}{A} \right\rceil \quad (\text{B.10})$$

B.2.2 Partitions with only Fair Element Distributions to Subsets

In this section, we compute the number of partitions with only fair element distributions into subsets. The number of partitions \mathcal{N}_j is given by the following equation:

$$\mathcal{N}_j = \prod_{n=0}^{T-1} \mathcal{N}_{j,n},$$

where $\mathcal{N}_{j,n}$ is the number of possible combinations in subset n if the $n - 1$ previous subsets are allocated. $\mathcal{N}_{j,n}$ is the number of ways of picking $N_j^{(n)}$ unordered elements from the set of non-allocated elements $\Omega_{u,n}$. $N_j^{(n)}$ is the number of elements allocated to subset n . In order to have a fair mobile distribution to subsets, the number of elements allocated to subset n must satisfy the following equation:

$$N_j^{(n)} = \begin{cases} \left\lceil \frac{N_j}{T} \right\rceil & \text{if } n \leq \varepsilon - 1 \\ \left\lceil \frac{N_j}{T} \right\rceil - 1 & \text{if } n > \varepsilon - 1 \end{cases},$$

where ε is the remainder of the ratio N_j/T . Hence, the cardinality of $\Omega_{u,n}$ is given by the following equation:

$$\text{card}(\Omega_{u,n}) = \begin{cases} N_j - n \left\lceil \frac{N_j}{T} \right\rceil & \text{if } n \leq \varepsilon \\ N_j - \varepsilon \left\lceil \frac{N_j}{T} \right\rceil - (n - \varepsilon) \left(\left\lceil \frac{N_j}{T} \right\rceil - 1 \right) & \text{if } n > \varepsilon \end{cases},$$

and therefore, $\mathcal{N}_{j,n}$ can be computed using the following equation:

$$\mathcal{N}_{j,n} = \begin{cases} \frac{N_j - n \left\lceil \frac{N_j}{T} \right\rceil !}{\left\lceil \frac{N_j}{T} \right\rceil ! \left[N_j - n \left\lceil \frac{N_j}{T} \right\rceil \right] !} & \text{if } n \leq \varepsilon \\ \frac{N_j - \varepsilon \left\lceil \frac{N_j}{T} \right\rceil - (n - \varepsilon) \left\lceil \frac{N_j}{T} \right\rceil - 1 !}{\left\lceil \frac{N_j}{T} \right\rceil - 1 ! \left[N_j - \varepsilon \left\lceil \frac{N_j}{T} \right\rceil - (n - \varepsilon) \left\lceil \frac{N_j}{T} \right\rceil - 1 \right] !} & \text{if } n > \varepsilon \end{cases},$$

and \mathcal{N}_j can be written as:

$$\begin{aligned} \mathcal{N}_j = & \frac{N_j!}{\left(\left\lceil \frac{N_j}{T} \right\rceil\right)! \left[N_j - \left\lceil \frac{N_j}{T} \right\rceil\right]!} \times \frac{\left(N_j - \left\lceil \frac{N_j}{T} \right\rceil\right)!}{\left(\left\lceil \frac{N_j}{T} \right\rceil\right)! \left[N_j - 2 \left\lceil \frac{N_j}{T} \right\rceil\right]!} \times \cdots \times \\ & \frac{\left(N_j - \varepsilon \left\lceil \frac{N_j}{T} \right\rceil\right)!}{\left(\left\lceil \frac{N_j}{T} \right\rceil - 1\right)! \left(N_j - (\varepsilon + 1) \left\lceil \frac{N_j}{T} \right\rceil + 1\right)!} \times \frac{\left(N_j - (\varepsilon + 1) \left\lceil \frac{N_j}{T} \right\rceil + 1\right)!}{\left(\left\lceil \frac{N_j}{T} \right\rceil - 1\right)! \left(N_j - (\varepsilon + 2) \left\lceil \frac{N_j}{T} \right\rceil + 2\right)!} \times \\ & \cdots \times \frac{\left(N_j - \varepsilon \left\lceil \frac{N_j}{T} \right\rceil - (T - 1 - \varepsilon) \left(\left\lceil \frac{N_j}{T} \right\rceil - 1\right)\right)!}{\left(\left\lceil \frac{N_j}{T} \right\rceil - 1\right)!} \times 1. \end{aligned}$$

By simplifying the denominator of each fraction by the numerator of the following fraction, we obtain the following equation:

$$\mathcal{N}_j = \frac{N_j!}{\left[\left(\left\lceil \frac{N_j}{T} \right\rceil\right)!\right]^\varepsilon \left[\left(\left\lceil \frac{N_j}{T} \right\rceil - 1\right)!\right]^{T-\varepsilon}}.$$

Appendix C

Publications

International Conferences

- J. Nasreddine and X. Lagrange, "A Simplified Generic Optimum Power Control Scheme for CDMA Cellular Systems," in *Proc. of the IEEE Workshop on Adaptive Wireless Networks (in conjunction with GLOBECOM 2004)*, pp. 414 - 418, Dallas, USA 2004
- J. Nasreddine and X. Lagrange, "Performance of TD-CDMA Systems during Crossed Slots", in *Proc. of the 60th IEEE Semiannual Vehicular Technology Conference (VTC Fall 2004)*, vol. 2, pp. 798 - 802, Los angeles, USA, September 2004
- J. Nasreddine, L. Nuaymi and X. Lagrange, "Downlink Adaptive Power Control Algorithm for 3G Cellular CDMA Networks", in *Proc. of the 15th IEEE International Symposium on Personal, Indoor and Mobile Radio communications conference (PIMRC 2004)*, vol. 3, pp. 2192 - 2196, Barcelona, Spain, 2004
- D. Nogu et, J-P. Bouyoud, L. Zaghdoudi, D. Varreau, B. Jechoux, P. LeCorre, X. Lagrange, J. Nasreddine, "A Hardware Testbed for UMTS/TDD Joint Detection Base-Band Receivers", in *Proc. of the IEEE International Symposium on Spread Spectrum Techniques and Applications (ISSSTA 2004)*, pp. 972 - 976, 2004
- J. Nasreddine, L. Nuaymi and X. Lagrange, "Adaptive Power Control Algorithm for 3G Cellular CDMA Networks", in *Proc. of the 59th IEEE Semiannual Vehicular Technology Conference (VTC Spring 2004)*, vol. 2, pp. 984 - 988, Milan, Italy, May 2004
- J. Nasreddine and X. Lagrange, "Time Slot Allocation Based on Normalized Path Gain for TD-CDMA TDD Systems", in *Proc. of the 1st International conference on Information and Communication technologies: From theory to Application (ICTTA 2004)*, pp. 195 - 196, Damascus, Syria, 2004
- J. Nasreddine, X. Lagrange, "Time Slot Allocation Based on a Path Gain Division Scheme for TD-CDMA TDD Systems," in *Proc. of the 57th IEEE Semiannual Vehicular Technology Conference (VTC Spring 2003)*, vol. 2, pp. 880-884 , Jeju, Korea, April 2003
- J. Nasreddine, X. Lagrange, "Comparison of Different Slot Allocation Schemes in a TD-CDMA TDD System," in *Proc. of the second IEEE Workshop on Applications and Services in Wireless Networks (ASWN 2002)*, Paris, France, July 2002

- J. Nasreddine, X. Lagrange, "Power Control and Slot allocation in a TD-CDMA System," in *Proc. of the 55th IEEE Vehicular Technology Conference (VTC Spring 2004)*, vol. 2 , pp. 880-884, Birmingham, Al, USA, May 2002

Technical Reports

- Jad Nasreddine et Xavier Lagrange, "Application pour les démonstrations de service", PETRUS DEL3.3, janvier 2003
- Jad Nasreddine et Xavier Lagrange, "Analyse des résultats et conclusions", PETRUS DEL4.3, Octobre 2002
- Jad Nasreddine, Xavier Lagrange et Khaled Al Jazzar, "Simulateur système pour le mode TDD", PETRUS DEL4.2, Aout 2002
- Jad Nasreddine, Sana Ben Jamaa, Xavier Lagrange et Seba Kayrouz, "Allocation dynamique de ressources radio", PETRUS DEL4.1, janvier 2002

Bibliography

- [Aei73] J. M. Aein, “Power Balancing in Systems Employing Frequency Reuse,” *COMSAT Technical Review*, vol. 3, 1973.
- [AG02] Siemens AG, “TD-SCDMA: the Solution for TDD Bands,” *TD-SCDMA white paper*, 2002.
- [AG03] Siemens AG, “TDD UE-UE Interference Simulations,” *TSG-RAN Working Group 4 (Radio meeting n26)*, 2003.
- [AJK99] Y. Argyropoulos, S. Jordan, and S. P. R. Kumar, “Dynamic Channel Allocation in Interference-limited Cellular Systems with Uneven Traffic Distribution,” *IEEE Transactions on Vehicular Technology*, vol. 48, pp. 224 – 232, 1999.
- [AN82] H. Alavi and R. W. Nettleton, “Downstream Power Control for a Spread Spectrum Cellular Mobile Radio System,” in *Proc. of the IEEE Global Communications Conference (GLOBECOM’82)*, pp. 84 – 88, 1982.
- [ARZ98] M. Andersin, Z. Rosberg, and J. Zander, “Distributed Discrete Power Control in Cellular PCS,” *Wireless Personal Communications*, vol. 6, pp. 211 – 231, 1998.
- [ASPR⁺01] R. Agusti, O. Sallent, J. Pérez-Romero, J. Ruela, and C. Guerrini, “ARROWS Strategies for RRM,” in *Proc. of the IST Mobile and Wireless Communications Summit*, 2001.
- [AW01] S. Ammari and A. Wautier, “Interference Factor Evaluation for CDMA System Capacity Analysis,” in *Proc. of the 53rd IEEE Vehicular Technology Conference (VTC Spring 2001)*, vol. 3, pp. 1573 – 1577, 2001.
- [AWBG02a] S. Ammari, A. Wautier, A. Braik, and L. Gattoufi, “Code Allocation Schemes for the Downlink of a TD-CDMA System,” in *Proc. of the 13th IEEE International Symposium on Personal, Indoor and Mobile Radio Communications (PIMRC 2002)*, vol. 5, pp. 2097 – 2101, 2002.
- [AWBG02b] S. Ammari, A. Wautier, A. Braik, and L. Gattoufi, “Multiple Access Interference Model in a TD-CDMA System for Capacity Evaluation and Throughput Optimization,” in *Proc. of the 56th IEEE Vehicular Technology Conference (VTC Fall 2002)*, vol. 4, pp. 2298 – 2302, 2002.
- [AWH02] S. Ammari, A. Wautier, and W. Hachem, “Modélisation du brouillage entre cellules et impact sur les performances (UL/DL),” *PETRUS DEL2.3*, 2002.

- [AZ98] L. Ahlin and J. Zander, *Principles of Wireless Communications*. Lund, Sweden: Studentlitteratur, 1998.
- [BE64] F. Bock and B. Ebstein, "Assignment of transmitter powers by linear programming," *IEEE Transactions on Electromagnetic Compatibility*, vol. 6, pp. 36 – 44, 1964.
- [Ber03] F. Berggren, *Power Control and Adaptive Resource Allocation in DS-CDMA Systems*. Royal Institute of Technology (KTH), 2003.
- [BPZ97] M. Berg, S. Pettersson, and J. Zander, "A Radio Resource Management Concept for 'Bunched' Personal Communication Systems," Radio Communication Systems, KTH publications, Tech. Rep., 1997.
- [Can96] H. Cancela, *Evaluation de la sûreté de fonctionnement: modèles combinatoires et markoviens*. Thèse de Doctorat, U.F.R. Science pour l'ingénieur, Université de Rennes 1, 1996.
- [CYMH97] L. Chen, S. Yoshida, H. Murata, and S. Hirose, "A dynamic Channel Assignment Algorithm for Asymmetric Traffic in Voice/Data Integrated TDMA/TDD Mobile Radio," in *Proc. of the International Conference on Information, Communications and Signal Processing (ICICS 1997)*, vol. 1, pp. 215 – 219, 1997.
- [DBK⁺98] E. Dahlman, P. Beming, J. Knutsson, F. Ovesjo, M. Persson, and C. Roobol, "WCDMA-the Radio Interface for Future Mobile Multimedia Communications," *IEEE Transactions on Vehicular Technology*, vol. 47, pp. 1105 – 1118, 1998.
- [DGNS98] E. Dahlman, B. Gudmundson, M. Nilsson, and J. Sköld, "UMTS/IMT-2000 Based on Wideband CDMA," *IEEE Communications Magazine*, vol. 36, no. 9, pp. 70 – 80, 1998.
- [ENS97] R. Esmailzadeh, M. Nakagawa, and E. A. Sourour, "Time-division Duplex CDMA Communications," *IEEE Personal Communications*, vol. 4, pp. 51 – 56, 1997.
- [FC02] R. Fraile and N. Cardona, "Resource Allocation Strategies for the TDD Component of UMTS," in *Proc. of the 13th IEEE International Symposium on Personal, Indoor and Mobile Radio Communications (pimrc 2002)*, vol. 1, pp. 21 – 25, 2002.
- [FJ02] I. Forkel and X. Jin, "Performance Comparison between UTRA-TDD High Chip Rate and Low Chip Rate Operation," in *Proc. of The 13th IEEE international symposium on personal, indoor and mobileradio communications (PIMRC 2002)*, vol. 5, pp. 2102 – 2106, 2002.
- [FKWS01] I. Forkel, T. Kriengchaiyapruk, B. Wegmann, and E. Schulz, "Dynamic Channel Allocation in UMTS Terrestrial Radio Access TDD Systems," in *Proc. of 53rd Vehicular Technology Conference (VTC 2001 Spring)*, vol. 2, pp. 1032 – 1036, 2001.
- [FM93] G. J. Foschini and Z. Miljanic, "A Simple Distributed Autonomous Power Control Algorithm and its Convergence," *IEEE Transactions on Vehicular Technology*, vol. 42, pp. 641 – 646, 1993.
- [Gan71] F. R. Gantmacher, *The theory of matrices*. New York: Chelsea publishing company, 1971, vol. 2.

- [GVG94] S. A. Grandhi, R. Vijayan, and D. J. Goodman, "Distributed Power Control in Cellular Radio Systems," *IEEE Transactions on Communications*, vol. 42, pp. 226 – 228, 1994.
- [GVGZ93] S. A. Grandhi, R. Vijayan, D. J. Goodman, and J. Zander, "Centralized Power Control in Cellular Radio Systems," *IEEE Transactions on Vehicular Technology*, vol. 42, pp. 66 – 468, 1993.
- [GVL96] G. H. Golub and C. F. Van Loan, *Matrix Computations*. The Johns Hopkins University Press, 1996.
- [GZ94] S. A. Grandhi and J. Zander, "Constrained Power Control in Cellular Radio Systems," in *Proc. of the 44th IEEE Vehicular Technology Conference (VTC 1994)*, vol. 2, pp. 824 – 828, 1994.
- [GZY95] S. A. Grandhi, J. Zander, and R. Yates, "Constrained Power Control," *International Journal of Wireless Personal Communications*, vol. 1, 1995.
- [Haa00] H. Haas, *Interference Analysis and Dynamic Channel Assignment Algorithms in TD-CDMA/TDD Systems*. The University of Edinbergh, 2000.
- [Han99] S. V. Hanly, "Congestion Measures in DS-CDMA Networks," *IEEE Transactions on Communications*, vol. 47, pp. 426 – 437, 1999.
- [HARW00] W. Hongyu, H. Aiging, H. Rong, and G. Weikang, "Balanced Distributed Power Control," in *Proc. of the 11th IEEE International Symposium on Personal, Indoor and Mobile Radio Communications (PIMRC 2000)*, vol. 2, pp. 1415 – 1419, 2000.
- [Hay94] S. Haykin, *Communication Systems*. John Wiley and sons, inc, 1994.
- [HC00] J. D. Herdtner and E. K. P. Chong, "Analysis of a Class of Distributed Asynchronous Power Control Algorithms for Cellular Wireless Systems," *IEEE Journal on Selected Areas in communications*, vol. 18, pp. 436 – 446, 2000.
- [HKK⁺00] M. Haardt, A. Klein, R. Koehn, S. Oestreich, M. Purat, V. Sommer, and T. Ulrich, "The TD-CDMA Based UTRA TDD Mode," *IEEE Journal on Selected Areas in Communications*, vol. 18, pp. 1375 – 1385, 2000.
- [HM01] H. Haas and S. McLaughlin, "A Dynamic Channel Assignment Algorithm for a Hybrid TDMA/CDMA-TDD Interface Using the Novel TS-Opposing Technique," *IEEE Journal on Selected Areas in Communications*, vol. 19, pp. 1831 – 1846, 2001.
- [Hol03] H. Holma, *A Study of UMTS Terrestrial Radio Access Performance*. Helsinki University of Technology Communications Laboratory Technical Report T49, 2003.
- [HT00] H. Holma and A. Toskala, *WCDMA for UMTS*. Artech House, 2000.
- [HY98] C.-Y. Huang and R. D. Yates, "Rate of Convergence for Minimum Power Assignment Algorithms in Cellular Radio Systems," *Wireless Networks Journal*, vol. 4, pp. 223 – 231, 1998.
- [Ing93] L. Ingber, "Simulated annealing: Practice versus Theory," *Mathl. Comput. Modelling*, vol. 18, pp. 29 – 57, 1993.

- [JFFP01] L. Jorgueski, E. Fledderus, J. Farserotu, and R. Prasad, "Radio Resource Allocation in third Generation Mobile Communication Systems," *IEEE Communications Magazine*, vol. 39, pp. 117 – 123, 2001.
- [JJ00] W. S. Jeon and D. G. Jeong, "Comparison of Time Slot Allocation Strategies for CDMA/TDD Systems," *IEEE Journal on Selected Areas in Communications*, vol. 18, pp. 1271 – 1278, 2000.
- [JK00] R. Jantti and S.-L. Kim, "Second-Order Power Control with Asymptotically Fast Convergence," *IEEE Journal on Selected Areas in Communications*, vol. 18, pp. 447 – 457, 2000.
- [JK03] R. Jantti and S.-L. Kim, "Power Control with Partially Known Link Gain Matrix," *IEEE Transactions on Vehicular Technology*, vol. 52, pp. 1288 – 1296, 2003.
- [KCK00] S.-H. Kim, K.-N. Chang, and S. Kim, "A Channel Allocation for Cellular Mobile Radio Systems Using Simulated Annealing," *Telecommunication Systems*, vol. 14, pp. 95 – 106, 2000.
- [KGV83] S. Kirkpatrick, C. D. J. Gellat, and M. P. Vecchi, "Optimization by Simulated Annealing," *Science*, vol. 220, pp. 671 – 680, 1983.
- [KH00] K. Kim and Y. Han, "A Call Admission Control with Thresholds for Multi-Rate Traffic in CDMA Systems," in *Proc. of the 51st IEEE Vehicular Technology Conference Proceedings (VTC Spring 2000)*, vol. 2, pp. 830 – 834, 2000.
- [Kim99] D. Kim, "A Simple Algorithm for Adjusting Cell-site Transmitter Power in CDMA Cellular Systems," *IEEE Transactions on Vehicular Technology*, vol. 48, pp. 1092 – 1098, 1999.
- [KKB96] A. Klein, G. K. Kaleh, and P. W. Baier, "Zero Forcing and Minimum-Mean-Square-Error Equalization for Multiuser Detection in Code Division Multiple Access Channels," *IEEE Transactions on Vehicular Technology*, vol. 45, pp. 276 – 287, 1996.
- [KLR02] J. Kurjenniemi, O. Lehtinen, and t. Ristaniemi, "Downlink Power Control of Dedicated Channels in UTRA TDD," in *Proc. of 13th IEEE International Symposium on Personal, Indoor and Mobileradio Communications (PIMRC 2002)*, 2002.
- [KLR03] J. Kurjenniemi, O. Lehtinen, and T. Ristaniemi, "Improving UTRA TDD Downlink Power Control with Asymmetrical Steps," in *Proc. of the 57th IEEE Semiannual Vehicular Technology Conference (VTC Spring 2003)*, vol. 4, pp. 2480 – 2484, 2003.
- [KN96] I. Katzela and M. Naghshineh, "Channel Assignment Schemes for Cellular Mobile Telecommunication Systems: a Comprehensive Survey," *IEEE Transactions Personal Communications*, vol. 3, pp. 10 – 31, 1996.
- [KP00] G. V. Kotsakis and S. Papavassiliou, "An Iterative Approach to the Power Control Problem in Wireless Networks for Integrated Services," in *Proc. of the 52nd IEEE Vehicular Technology Conference (VTC Fall 2000)*, vol. 1, pp. 265 – 272, 2000.
- [Kun99] D. Kunz, "Transitions from DCA to FCA Behavior in a Self-Organizing Cellular Radio Network," *IEEE Transactions on Vehicular Technology*, vol. 48, pp. 1850 – 1861, 1999.

- [Lem00] M. Lemmo, "TDD Solves 3G Hotspot Problem," InterDigital, Tech. Rep., 2000, lu.
- [LG02] X. Li and Z. Gajic, "Centralized Power Control in Coordinated CDMA Systems using Krylov Subspace Iterations," in *Proc. of the IASTED International Conference on Communications, Internet and Information Technology*, pp. 305 – 309, 2002.
- [LGT99] X. Lagrange, P. Godlewski, and S. Tabbane, *Réseaux GSM-DCS, 4e édition revue et augmentée*. Hermes, Paris 1999.
- [Lin01] M. Lindström, "Improved TDD Resource Allocation through Inter-Mobile Interference Avoidance," in *Proc. of the 53rd IEEE Vehicular Technology Conference (VTC Spring 2001)*, vol. 2, pp. 1027 – 1031, 2001.
- [LL96] T.-H. Lee and J.-C. Lin, "A Fully Distributed Power Control Algorithm for Cellular Mobile Systems," *IEEE Journal on Selected Areas in Communications*, vol. 14, pp. 692 – 697, 1996.
- [LLS95] T.-H. Lee, J.-C. Lin, and Y. T. Su, "Downlink Power Control Algorithms for Cellular Radio Systems," *IEEE Transactions on Vehicular Technology*, vol. 44, pp. 89 – 94, 1995.
- [LWN02] J. Laiho, A. Wacker, and T. Novosad, *Radio Network Planning and Optimisation for UMTS*. Chichester, GB: John Wiley & sons, 2002.
- [LZ99] M. Lindström and J. Zander, "Dynamic Link Asymmetry in 'Bunched' Wireless Networks," in *Proc. of the 50th IEEE Vehicular Technology Conference (VTC Fall 1999)*, vol. 1, pp. 352 – 356, 1999.
- [MBX93] L. R. Maciel, H. L. Bertoni, and H. H. Xia, "Unified Approach to Prediction of Propagation over Buildings for all Ranges of Base Station Antenna Height," *IEEE Transactions on Vehicular Technology*, vol. 42, pp. 41 – 45, 1993.
- [Mey74] H. J. Meyerho, "Method for Computing the Optimum Power Balance in Multibeam Satellites," *COMSAT Technical Review*, vol. 4, pp. 39 – 147, 1974.
- [MH01] L. Mendo and J. M. Hernando, "On Dimension Reduction for the Power Control Problem," *IEEE Transactions on Communications*, vol. 49, pp. 243 – 248, 2001.
- [Mit93] D. Mitra, "An Asynchronous Distributed Algorithm for Power Control in Cellular Radio Systems," in *Proc. of 4th WINLAB Work-shop of 3rd Generation Wireless Information Networks*, pp. 77 – 186, 1993.
- [MLG99] C. Mihailescu, X. Lagrange, and P. Godlewski, "Radio Resource Management for Packet Transmission in UMTS WCDMA System," in *Proc. of the 50th Vehicular Technology Conference (VTC Fall 1999)*, vol. 1, pp. 573 – 577, 1999.
- [Moh98] W. Mohr, "Investigation of the UMTS Radio Interface in the ACTS FRAMES Project," in *Proc. of the UMTS workshop, IEEE ComSoc Germany, university of Ulm*, vol. 1, pp. 33 – 64, 1998.
- [NA83] R. W. Nettleton and H. Alavi, "Power Control for a Spread Spectrum Cellular Mobile Radio System," in *Proc. of the IEEE Vehicular Technology Conference (VTC 1983)*, pp. 242 – 246, 1983.

- [NL02a] J. Nasreddine and X. Lagrange, “Analyse des résultats et conclusions,” *PETRUS DEL4.3*, 2002.
- [NL02b] J. Nasreddine and X. Lagrange, “Comparison of Different Slot Allocation Schemes in a TD-CDMA TDD System,” in *Proc. of the second IEEE Workshop on Applications and Services in Wireless Networks (ASWN 2002)*, 2002.
- [NL03a] J. Nasreddine and X. Lagrange, “Application pour les démonstrations de service,” *PETRUS DEL3.3*, 2003.
- [NL03b] J. Nasreddine and X. Lagrange, “Time Slot Allocation Based on Path Gain Division Scheme for TD-CDMA TDD Systems,” in *Proc. of the 57th IEEE Semiannual Vehicular Technology Conference (VTC Spring 2003)*, vol. 2, pp. 1410 – 1414, 2003.
- [NL04a] J. Nasreddine and X. Lagrange, “Performance of TD-CDMA Systems during Crossed Slots,” in *Proc. of the 60th IEEE Vehicular Technology Conference (VTC Fall 2004)*, vol. 2, pp. 798 – 802, 2004.
- [NL04b] J. Nasreddine and X. Lagrange, “A Simplified Generic Optimum Power Control Scheme for CDMA Cellular Systems,” in *Proc. of the IEEE Workshop on Adaptive Wireless Networks (in conjunction with GLOBECOM 2004)*, pp. 414 – 418, 2004.
- [NL04c] J. Nasreddine and X. Lagrange, “Time Slot Allocation Based on Normalized Path Gain for TD-CDMA TDD Systems,” in *Proc. of the 1st International conference on Information and Communication technologies: From theory to Application (ICTTA 2004)*, pp. 195 – 196, 2004.
- [NLAJ02] J. Nasreddine, X. Lagrange, and K. Al Jazzar, “Simulateur système pour le mode TDD,” *PETRUS DEL4.2*, 2002.
- [NLBJK02] J. Nasreddine, X. Lagrange, S. Ben Jamaa, and S. Kayrouz, “Allocation dynamique de ressources radio,” *PETRUS DEL4.1*, 2002.
- [NLG02] L. Nuaymi, X. Lagrange, and P. Godlewski, “A Power Control Algorithm for 3G WCDMA System,” in *Proc. of The European Wireless Conference*, 2002.
- [NNL04a] J. Nasreddine, L. Nuaymi, and X. Lagrange, “Adaptive Power Control Algorithm for 3G Cellular CDMA Networks,” in *Proc. of the 59th IEEE Semiannual Vehicular Technology Conference (VTC04)*, 2004.
- [NNL04b] J. Nasreddine, L. Nuaymi, and X. Lagrange, “Downlink Adaptive Power Control Algorithm for 3G Cellular CDMA Networks,” in *Proc. of the 15th IEEE International Symposium on Personal, Indoor and Mobile Radio Communications (PIMRC 2004)*, vol. 3, pp. 2192 – 2196, 2004.
- [NRB02] S. Naghian, M. Rintamaki, and R. Baghaie, “Dynamic Step-Size Power Control in UMTS,” in *Proc. of The 13th IEEE International Symposium on Personal, Indoor and Mobile Radio Communications (PIMRC 2002)*, vol. 4, pp. 1606 – 1610, 2002.
- [Oli99] M. W. Oliphant, “The Mobile Phone Meets the Internet,” *IEEE Spectrum*, vol. 36, pp. 20 – 28, 1999.

- [PHT97] G. J. R. Povey, H. Holma, and A. Toskala, "TDD-CDMA Extension to FDD-CDMA Based Third Generation Cellular System," in *Proc. of the 6th IEEE International Conference on Universal Personal Communications*, vol. 2, pp. 813 – 817, 1997.
- [PN98] G. J. R. Povey and M. Nakagawa, "A Review of Time Division Duplex-CDMA Techniques," in *Proc. of the 5th IEEE International Symposium on Spread Spectrum Techniques and Applications (ISSSTA 1998)*, pp. 630 – 633, 1998.
- [Pov94] G. J. R. Povey, "Frequency and Time Division Duplex Techniques for CDMA Cellular Radio," in *Proc. of the 5th IEEE International Symposium on Spread Spectrum Techniques and Applications (ISSSTA 1994)*, pp. 309 – 313, 1994.
- [Pov97] G. J. R. Povey, "Time Division Duplex-Code Division Multiple Access for Mobile Multimedia Services," in *Proc. of the 8th IEEE International Symposium on Personal, Indoor and Mobile Radio Communications (PIMRC 1997)*, pp. 1034 – 1037, 1997.
- [PW93] U. W. Pooch and J. A. Wall, *Discrete Event Simulation. A Practical Approach*. Boca Raton, Florida: CRC Press, Inc, 1993.
- [PYCW99] Z. Pu, X. You, S. Cheng, and H. Wang, "Transmission and Reception of TDD Multi-carrier CDMA Signals in Mobile Communications System," in *Proc. of the 49th IEEE Vehicular Technology Conference (VTC Spring 1999)*, 1999.
- [RVK01] M. Rintamaki, I. Virteij, and H. Koivo, "Two-Mode Fast Power Control for WCDMA Systems," in *Proc. of The 53rd IEEE Vehicular Technology Conference (VTC Spring 2001)*, vol. 4, pp. 2893 – 2897, 2001.
- [SMG98] ETSI SMG2, "Proposal for a Consensus Decision on UTRA," ETSI SMG TDoc 032/98, 1998.
- [SW99a] C. W. Sung and W. S. Wong, "The Convergence of an Asynchronous Cooperative Algorithm for Distributed Power Control in Cellular Systems," *IEEE Transactions on Vehicular Technology*, vol. 48, pp. 563 – 570, 1999.
- [SW99b] C. W. Sung and W. S. Wong, "A Distributed Fixed-Step Power Control Algorithm with Quantization and Active Link Quality Protection," *IEEE Transactions on Vehicular Technology*, vol. 48, pp. 553 – 562, 1999.
- [TS202a] "MAC Protocol Specification," *Third Generation Partnership Project, Technical Specification Group Radio Access Network*, TS 25.321 (Release 5), December 2002.
- [TS202b] "RLC Protocol Specification," *Third Generation Partnership Project, Technical Specification Group Radio Access Network*, TS 25.322 (Release 5), December 2002.
- [TS202c] "PDCP Protocol Specification," *Third Generation Partnership Project, Technical Specification Group Radio Access Network*, TS 25.323 (Release 5), September 2002.
- [TS202d] "BMC Protocol Specification," *Third Generation Partnership Project, Technical Specification Group Radio Access Network*, TS 25.324 (Release 5), September 2002.
- [TS202e] "Radio Resource Control (RRC)," *Third Generation Partnership Project, Technical Specification Group Radio Access Network*, TS 25.331 (Release 5), September 2002.

- [TS202f] “Physical Channels and Mapping of Transport Channels onto Physical Channels (FDD),” *Third Generation Partnership Project, Technical Specification Group Radio Access Network*, TS25.211 (Release 5), Mars 2002.
- [TS202g] “Physical Channels and Mapping of Transport Channels onto Physical Channels (TDD),” *Third Generation Partnership Project, Technical Specification Group Radio Access Network*, TS25.221 (Release 5), Mars 2002.
- [TS202h] “Radio Interface Protocol Architecture,” *Third Generation Partnership Project, Technical Specification Group Radio Access Network*, TS25.301 (Release 5), September 2002.
- [TS202i] “Radio Resource Management Strategies,” *Third Generation Partnership Project, Technical Specification Group Radio Access Network*, TS25.922 (Release 5), March 2002.
- [TS202j] “RF System Scenarios,” *Third Generation Partnership Project, Technical Specification Group Radio Access Network*, TS25.942 (Release 5), June 2002.
- [TS203a] “Physical Layer Procedures (FDD),” *Third Generation Partnership Project, Technical Specification Group Radio Access Network*, TS25.214 (Release 5), September 2003.
- [TS203b] “Physical Layer Procedures (TDD),” *Third Generation Partnership Project, Technical Specification Group Radio Access Network*, TS25.224 (Release 5), September 2003.
- [TS203c] “(UTRAN) Overall Description,” *Third Generation Partnership Project, Technical Specification Group Radio Access Network*, TS25.401 (Release 5), June 2003.
- [TS204] “Quality of Service (QoS) Concept and Architecture,” *Third Generation Partnership Project, Technical Specification Group Radio Access Network*, TS 23.107 (Release 5), Mars 2004.
- [UMT98] “Universal Mobile Telecommunications System (UMTS); Selection procedures for the choice of radio transmission technologies of the UMTS,” *TR 101 112 (UMTS 30.03)*, April 1998.
- [UMT04] “Universal Mobile Telecommunications System (UMTS); UE Radio Access capabilities definition,” *TS 25.306 V6.1.0 (ETSI TS 125 306 V6.1.0)*, mars 2004.
- [Var62] R. S. Varga, *Matrix Iterative Analysis*. New Jersey: Prentice-Hall, 1962.
- [Ver98] S. Verdu, *Multiuser Detection*. Cambridge University Press, 1998.
- [VKK01] I. Virtej, O. Kansanen, and H. Koivo, “Enhanced Predictive Fast Power Control for 3G Systems,” in *Proc. of the 53rd IEEE Vehicular Technology Conference (VTC Spring 2001)*, vol. 4, pp. 2864 – 2868, 2001.
- [VRK00] I. Virtej, M. Rintamaki, and H. Koivo, “Enhanced Fast Power Control for WCDMA Systems,” in *Proc. of the 11th IEEE International Symposium on Personal, Indoor and Mobile Radio Communications (PIMRC 2000)*, vol. 2, pp. 1435 – 1439, 2000.
- [WAH04] A. Wautier, S. Ammari, and W. Hachem, “Low Complexity Linear Detection for Asynchronous CDMA Signals Over Frequency Selective Channels,” in *Proc. of the 12th European Signal Processing Conference (EUSIPCO’2004)*, 2004.

- [WC01] S.-H. Wie and D.-H. Cho, "Time Slot Allocation Scheme Based on a Region Division in CDMA/TDD Systems," in *Proc. of the 53rd IEEE Vehicular Technology Conference (VTC Spring 2001)*, vol. 4, pp. 2445 – 2449, 2001.
- [WSC01] J.-H. Wen, J.-S. Sheu, and J.-L. Chen, "An optimum downlink power control method for CDMA cellular mobile systems," in *Proc. of IEEE International Conference on Communications (ICC 2001)*, vol. 6, pp. 1738 – 1742, 2001.
- [WSW⁺03] J.-H. Wen, J.-S. Sheu, J.-Y. Wang, J.-L. Chen, and T.-K. Woo, "A Feasible Method to Implement Optimum CIR-Balanced Power Control in CDMA Cellular Mobile Systems," *IEEE Transactions on Vehicular Technology*, vol. 52, pp. 80 – 95, 2003.
- [Wu99] Q. Wu, "Performance of Optimum Transmitter Power Control in CDMA Cellular Mobile Systems," *IEEE Transactions on Vehicular Technology*, vol. 48, pp. 571 – 575, 1999.
- [Zan92a] J. Zander, "Distributed Cochannel Interference Control in Cellular Radio Systems," *IEEE Transactions on Vehicular Technology*, vol. 41, pp. 305 – 311, 1992.
- [Zan92b] J. Zander, "Performance of Optimum Transmitter Power Control in Cellular Radio Systems," *IEEE Transactions on Vehicular Technology*, vol. 41, pp. 57 – 62, 1992.
- [Zan97] J. Zander, "Radio Resource Management in Future Wireless Networks: Requirements and Limitations," *IEEE Communications Magazine*, vol. 35, no. 8, pp. 30 – 36, 1997.
- [ZF94] J. Zander and M. Frodigh, "Comment on 'Performance of Optimum Transmitter Power Control in Cellular Radio Systems'," *IEEE Transactions on Vehicular Technology*, vol. 43, p. 636, 1994.
- [ZKAQ01] J. Zander, S.-L. Kim, M. Almgren, and O. Queseth, *Radio Resource Management for Wireless Networks*. Norwood, USA: Artech house publishers, 2001.

VU :

Le Directeur de Thèse

Xavier LAGRANGE

VU :

Le Responsable de l'Ecole Doctorale

Olivier BONNAUD

VU pour autorisation de soutenance :

Rennes, le 15 février 2005

Le Président de l'Université de Rennes 1

Bertrand FORTIN

VU après soutenance pour autorisation de publication :

Le Président de Jury,